Molecular and functional characterization of the candidate tumor antigens *placenta specific 1* and *claudin 6*

Dissertation

zur Erlangung des Grades

Doktor der Naturwissenschaften

Am Fachbereich Biologie

der Johannes Gutenberg Universität Mainz

Meike Wagner

geboren am 14.06.1983 in Frankfurt am Main

Mainz, 2014

Dekan:

1. Berichterstatter:

2. Berichterstatter:

Tag der mündlichen Prüfung: 18.09.2014

“All truths are easy to understand once they are discovered –
the point is to discover them.”

Galileo Galilei

Summary

Identification of tumor-specific antigens is central to the effectiveness of cancer immunotherapies. Within this study, two candidate tumor antigens, *placenta-specific 1 (PLAC1)* and *claudin 6 (CLDN6)*, were characterized regarding their suitability to serve as antigens for cancer immunotherapeutic approaches.

PLAC1 is a tumor-specific antigen with tumor-promoting functions in breast cancer. The estradiol (E_2)-responsive *PLAC1* gene is known to be regulated by estrogen receptor α (ERα), specificity protein 1 (SP1) and CCAAT/enhancer binding protein β-2 (C/EBPβ-2). However, additional regulators of *PLAC1* were not identified so far. Here, it was investigated whether members of the nuclear receptor co-activator (NCOA)/p160 family are involved in ERα/E_2-mediated trans-activation of *PLAC1* in breast cancer. Using chromatin immunoprecipitation (ChIP), NCOA3 was identified to be selectively recruited to the *PLAC1* promoter upon E_2-stimulation only in ERα-positive MCF-7 breast cancer cells but not in ERα-negative SK-BR-3 cells. RNAi-mediated silencing of NCOA3 revealed diminished PLAC1 mRNA and protein levels in MCF-7 but not in SK-BR-3 cells. Stimulation of MCF-7 cells with E_2 resulted in decreased up-regulation of *PLAC1* compared to control transfected cells. Moreover, a significant correlation of *PLAC1* and *NCOA3* expression was found in ERα-positive human breast cancer tissues only. Collectively, these data show that PLAC1 is a downstream target of NCOA3 and provides a relationship between NCOA3 and PLAC1 that could be important for future immunotherapies targeting hormone-responsive breast cancer.

The tight junction molecule CLDN6 is an embryonic antigen that plays a major role during epithelial differentiation. In this study, expression, function and regulation of CLDN6 in cancer was characterized. Analysis of *CLDN6* expression by quantitative *real-time* RT-PCR showed that *CLDN6* is absent in adult normal tissues but frequently overexpressed in many cancers, especially in ovarian, testicular and lung cancer. RNAi-mediated silencing of *CLDN6* did not reveal any function for CLDN6 in proliferation, apoptosis, cell cycle, migration and adhesion in three different cancer cell lines. However, colony formation was decreased in CLDN6-negative compared to CLDN6-positive PA-1 teratocarcinoma cells. The capacity to form colonies at distant sites is a key feature of tumor cells with tumor-initiating potential suggesting a role for CLDN6 in cancer stem cells (CSC). This

was further supported by the significant correlation of *CLDN6* expression with several CSC-specific markers in ovarian cancer detected in this study. Moreover, CLDN6 was found here to be specifically detected on the surface of induced pluripotent (iPS) cells and up-regulated throughout the course of reprogramming. Thus, CLDN6 could be confirmed as a specific marker for iPS cells. Bisulfite sequencing and methylation-specific qPCR (MsqPCR) revealed that *CLDN6* expression in tumors is associated with promoter hypomethylation. However, it is likely that promoter demethylation is not sufficient for up-regulation of *CLDN6* in cancer. Accordingly, promoter analysis using deletion constructs, ChIP and RNAi-mediated silencing suggests that CCCTC-binding factor (CTCF) and brother of regulator of imprinted sites (BORIS) are possible transcription factors regulating *CLDN6* in cancer. In summary, this work introduces CLDN6 as highly specific tumor antigen with a possible role in CSC that could be used for cancer immunotherapy in particular to target CSC.

Zusammenfassung

Die Identifizierung tumorspezifischer Antigene ist das Herzstück in der Entwicklung effektiver Krebsimmuntherapien. In dieser Arbeit wurden zwei verschiedene Kandidaten-Antigene, *placenta-specific 1 (PLAC1)* und *claudin 6 (CLDN6)*, in Hinblick auf ihre potentielle Verwendung in der Krebsimmuntherapie analysiert.

PLAC1 ist ein tumorspezifisches Antigen mit tumorfördernden Funktionen in Brustkrebs. Das östradiol (E_2)-responsive *PLAC1* wird durch *estrogen receptor α* (ERα), *specificity protein 1* (SP1) und *CCAAT/enhancer binding protein β-2* (C/EBPβ-2) reguliert. Weitere Regulatoren von *PLAC1* wurden bisher nicht identifiziert. Daher wurde in dieser Arbeit untersucht, ob Mitglieder der *nuclear receptor co-activator* (NCOA)/p160 Familie in der ERα/E_2-vermittelten Trans-Aktivierung von *PLAC1* in Brustkrebs involviert sind. Mittels Chromatin Immunopräzipitation (ChIP) wurde herausgefunden, dass NCOA3 nach E_2-Stimulation selektiv an den Promoter von *PLAC1* in ERα-positiven MCF-7 jedoch nicht in ERα-negativen SK-BR-3 Brustkrebszellen rekrutiert wird. Der RNAi-vermittelte *knock down* von NCOA3 führte wiederum nur in MCF-7, nicht in SK-BR-3 Zellen zu vermindertet Expression von PLAC1 und weitere Stimulation von MCF-7 Zellen mit E_2 führte zu einer verminderten Hochregulation von *PLAC1* im Vergleich zu den Kontrollzellen. Darüber hinaus wurde eine signifikante Korrelation zwischen der Expression von *PLAC1* und der Überexpression von *NCOA3* nur in ERα-positiven humanen Brustkrebsproben entdeckt. Zusammenfassend weisen die Daten darauf hin, dass PLAC1 ein Zielgen von NCOA3 ist. Der Zusammenhang zwischen NCOA3 und PLAC1 könnte von Relevanz für zukünftige immuntherapeutische Ansätze zur Bekämpfung von hormon-responsivem Brustkrebs sein.

Das *tight-junction* Molekül CLDN6 ist ein embryonales Antigen, das eine wichtige Rolle in der epithelialen Differenzierung spielt. In dieser Arbeit wurde die Expression, Funktion und Regulation von CLDN6 in Krebs charakterisiert. Mittels quantitativer *real-time* RT-PCR wurde gezeigt, dass *CLDN6* in adulten Normalgeweben nicht exprimiert ist, jedoch in verschiedenen Krebsarten, besonders Ovarial-, Hoden- und Lungenkrebs überexprimiert ist. Durch RNAi-vermittelten *knock down* von *CLDN6* in drei verschiedenen Tumorzelllinien konnte

keine Funktion für CLDN6 in Proliferation, Zellzyklus, Apoptose, Adhäsion oder Migration gefunden werden. Jedoch wurde eine verminderte Koloniebildung von CLDN6-negativen im Vergleich zu CLDN6-positiven PA-1 Teratokarzinomzellen gefunden. Die Fähigkeit zur Koloniebildung ist eine Haupteigenschaft von Tumorzellen mit tumor-initiierendem Potential. Dies deutet auf eine Rolle von CLDN6 in Krebsstammzellen hin, was durch die signifikante Korrelation von *CLDN6* mit verschiedenen Krebsstammzellmarkern in Ovarialtumorgeweben gestützt wird. Darüber hinaus konnte CLDN6 als spezifischer Marker für humane induzierte pluripotente Stammzellen (iPS) identifiziert werden, da CLDN6 spezifisch auf der Oberfläche von iPS Zellen exprimiert ist und im Verlauf der Reprogrammierung hochreguliert wird. Mittels Bisulfit-Sequenzierung und methylierungs-spezifischer qPCR konnte gezeigt werden, dass die Expression von *CLDN6* in Tumoren mit einer Hypomethylierung des Promoters einhergeht. Diese reicht aber nicht aus, um die Expression von *CLDN6* im Tumor zu aktivieren. Promoteranalysen mittels Deletionkonstrukten und ChIP sowie RNAi-Experimente konnten zeigen, dass *CCCTC-binding factor* (CTCF) und *brother of regulator of imprinted sites* (BORIS) an der Regulation von *CLDN6* in Krebs beteiligt sind. Zusammenfassend wird in dieser Arbeit gezeigt, dass CLDN6 ein hochspezifisches Tumorantigen mit einer möglichen Rolle in Krebsstammzellen ist. Es stellt daher ein vielversprechendes Zielmolekül für die Krebsimmuntherapie dar, insbesondere bei Ansätzen, die gegen Krebsstammzellen gerichtet sind.

Table of contents

Abbreviations

°C	degree centigrade
SDS	sodium dodecyl sulfate
5-aza-dC	5-aza-2'-deoxycytidine
7-AAD	7-Amino-Actinomycin D
aa	amino acid
bp	base pair
bcDNA	bisulfite converted DNA
BSA	Bovine serum albumin (Fraction V)
CDH1	Cadherin 1 (E-Cadherin)
C/EBPβ-2	CCAAT/enhancer binding proteinβ isoform 2
CTCF	CCCTC-binding factor
ChIP	chromatin immunoprecipitation
CLDN6	Claudin 6
cDNA	complementary DNA
CGI	CpG islands
CTCFL / BORIS	CTCF-like / Brother Of Regulator Of Imprinted Sites
CXCR4	CXC motif chemokine receptor 4
Ct	cycle treshold
CpG	cytosine-phosphate-guanine
Da	Dalton
DNA	deoxyribonucleic acid
DMSO	dimethyl sulfoxide
dNTP	dinucleotide triphosphate
ddH2O	distilled water
DTT	dithiothreitol
ds	double-stranded
DMEM	Dulbecco's Modified Eagles medium
ESC	embryonic stem cells
ECL	enhanced chemoluminescence
eGFP	enhanced green fluorescence protein
EPCAM	epithelial cell adhesion molecule
E.coli	*Escherichia coli*
ERα	estrogen receptor α
EGTA	Ethylene glycol tetraacetic acid
EDTA	ethylenediaminetetraacetic acid
FCS	fetal calf serum
FACS	florescent activated cell sorting
gDNA	genomic DNA
GNL3	Guanine nucleotide-binding protein-like 3 / nucleostemin
HA	hemagglutinin
HRP	horeradish peroxidase
ERBB2	human epidermal growth factor receptor 2 / HER2/neu
HFF	human foreskin fibroblasts
hTERT	human telomerase reverse transcriptase
HMS	hypermethylated standard
HPRT1	hypoxanthine phosphoribosyltransferase 1
ICI	ICI 182 780, Fulvestrant
IVT-RNA	in vitro transcribed RNA
iPSC	induced pluripotent stem cells
KLF4	Kruppel-like factor 4
L1CAM	L1 cell adhesion molecule
LMO2	LIM domain only 2
LIN28B	lin-homolog 28b
LB	Luria-Bertani-medium
MAGE	melanoma antigen
mRNA	messenger RNA
MsqPCR	methylation-specific quantitative real-time PCR
MEM	minimal essential medium
MMLV-RT	Moloney Murine Leukemia Virus Reverse Transcriptase
MSI1	musashi 1
NGS	Next generation sequencing
ns	non silencing
NEAA	non-essential aminoacids
NP-40	Nonidet P-40
NCOA	Nuclear receptor coactivator
ORF	open reading frame
ON	overnight
pCAF	p300/CBP-associated factor
PE	paired-end
Pen/Strep	Penicillin/Streptomycin
PBL	peripheral blood lymphocyte
PPAR	peroxisome proliferator-activated receptor
PBS	phosphate buffered saline
Triton X-100	p-isooctylphenylpolyoxyethylen
PLAC1	Placenta-specific 1
PAGE	polyacrylamid gel electrophorese
PCR	polymerase chain reaction
Tween-20	polyoxyethylene (20) sorbitan monolaurate
POU2F1/OCT1	POU class 2 homeobox 1 / octamer binding transcription factor 1
POU5F1/OCT3/4	POU class 5 homeobox 1 /Octamer binding transcription factor 3/4
PROM1	prominin 1 / CD133
qRT-PCR	quantitative real-time RT-PCR analysis
RNA	Ribonucleic acid
Pol II	RNA polymerase II
RT	room temperature
RPMI	Roswell Park Memorial Institute
SALL4	sal-like protein 4
ss	single stranded
shRNA	small hairpin RNA
siRNA	small interfering RNA
NaOAc	sodium acetate
DOC	Sodium deoxycholate
SDS	sodium dodecyl sulfate
SP1	specificity protein 1
SOX2	SRY (sex determining region Y)-box 2
ST8SIA1	ST8 alpha-N-acetyl-neuraminide alpha-2,8-sialyltransferase 1
SSEA-4	Stage specific embryonic antigen 4
SOC	Super Optimal broth with Catabolite repression
TSP50	testes-specific protease 50
Taq	Thermus aquaticus
TFIIB	Transcription factor II B
TSS	transcription start site
tRNA	transfer RNA
Tris	tris-(hydroxymethyl)-aminomethane
v/v	volume per volume

1 Introduction

1.1 Origin of cancer

The Edwin Smith papyrus, an ancient Egyptian medical textbook on surgery which dates back to around 3000 BC is the oldest known document which reports cancer. It describes eight tumors of the breast treated by cauterization. The unknown author states that no treatment exists for this disease [1]. Now, in 2014, cancer remains one of the leading causes of death worldwide. In 2008, 12.7 million new cases and 7.6 million deaths from cancer were denoted in a study by the International Agency for Cancer Research (IARC) of the World Health Organization (WHO) (Figure 1) [2].

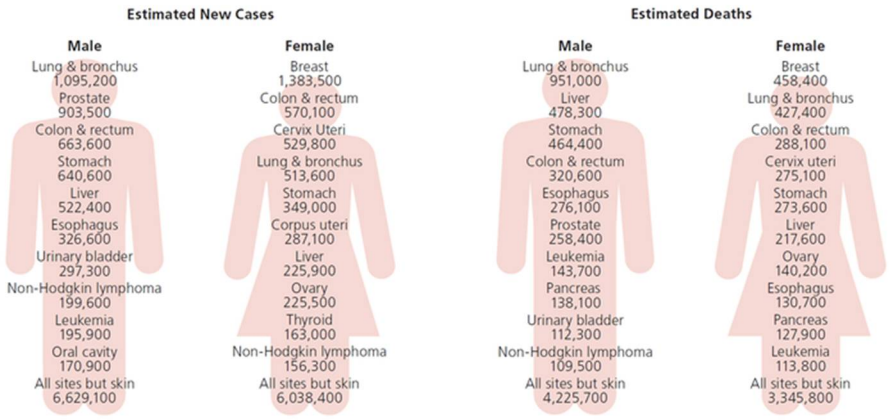

Figure 1 Estimated new cancer cases and deaths for leading cancer sites, source GLOBOCAN 2008. About 12.7 million new cases and 7.6 million deaths from cancer are estimated to have occurred in 2008 worldwide, with 56% of the cases and 64% of the deaths in the economically developing world. The most commonly diagnosed cancer and the leading cause of death are breast cancer in women and lung and bronchus cancer in men. [2]

Cancer is a group of diseases origin from normal cells of the body in which cell growth and division is out of control. The human body has more than 200 cell types thus more than 200 types of cancer exist. Tumorigenesis, the transformation of a normal cell into a cancer cell, is the result of a multi-step process. Cellular changes, genetic and epigenetic mutations in genes which regulate cell growth, differentiation, apoptosis, angiogenesis, metabolism and tissue invasion accumulate and result in breaching of anticancer defense mechanisms programmed in normal cells. Moreover, tumors are capable of evading immune destruction [3,4]. Some of the cancer cells can enter the lymph vessels or

bloodstream and invade in distant organs, a process called metastasis. Notably, metastases are the major cause of death from cancer.

1.1.1 Epigenetic mechanisms are involved in tumorigenesis

Cancer is not only driven by genetic mutations, also by changes in the epigenetic landscape. The term “epigenetics” describes heritable changes in gene expression that do not involve a change in the DNA sequence and happen “on the top” of the genome [5]. Our entire genome is densely packed in a complex of DNA wrapped around histones, called nucleosomes, the basic unit of chromatin. In principle, the density of the chromatin defines the level of gene expression. Heterochromatin defines highly condensed regions with inactive genes whereas euchromatic regions, that contain active genes, are relatively open and hence, transcription factors can bind to DNA. Epigenetic regulation includes two major mechanisms: DNA methylation and covalent histone modifications, both resulting in alteration of chromatin. DNA methylation occurs primarily at cytosines within CpG dinucleotides and is mediated by DNA methyltransferases (DNMTs). The CpG dinucleotides are largely depleted from the genome except at short regions called CpG islands (CGIs), which are ~500-4000 bp in length and occur at proximal promoter regions of about 50 % of mammalian genes. CGIs are predominantly not methylated in normal cells. However a remarkable difference exists in CGI methylation between germline and somatic cells [6]. Genes that are developmentally active in the germline, during gametogenesis or embryogenesis are silenced in normal somatic cells. DNA methylation of CGIs is associated with silencing of the corresponding gene and necessary to maintain the silenced state [6–8]. The second major epigenetic regulation occurs at the N-terminal tails of histones that can be posttranslationally modified by methylation, acetylation, phosphorylation and others. The so-called histone code, various combinations of modifications at certain positions, defines if a more open or closed state of chromatin is present hence leading to activation or repression of gene expression [9].

Epigenetic processes have fundamental roles during normal development, differentiation and adult cell renewal in controlling the emergence of defined cellular phenotypes [10]. Two major epigenetic changes occur during tumorigenesis. First, very early events include a global loss of DNA methylation throughout the entire genome, found in virtually every cancer type. Loss of DNA

methylation in regions that are methylated in normal cells is associated with abnormal transcription. Many oncogenes that are not or only low expressed in normal cells have been reported to be upregulated in association with cancer-specific decrease in promoter DNA methylation [11]. Loss of global DNA methylation, especially in periocentric regions is probably a major cause of genomic instability in cancer cells [11,12]. Second, a localized increase in DNA methylation at CGIs in promoter regions is detected in cancer cells resulting in tight transcriptional repression of mainly tumor suppressor genes. This results, as an alternative to gene mutation, in loss of function of the corresponding gene [11,13,14].

1.1.2 Cancer stem cells are an important subpopulation in tumors

Tumors are highly heterogeneous; the tumor bulk consists of rapidly proliferating cells as well as postmeiotic, differentiated cells [15]. There is increasing evidence that a subpopulation of cancer cells exists within tumors which retain stem-like properties [16,17]. This subpopulation is termed cancer stem cells (CSCs) or tumor-initiating cells (TICs). These cells share many features with normal stem cells: they can undergo self-renewal and differentiation and are capable to form all heterogeneous cell types of a tumor. Furthermore, CSCs appear to be highly tumorigenic and are able to initiate tumor formation, maintain tumor growth and play critical roles in tumor metastasis. Moreover, CSCs grow slower and are more chemoresistant as the remaining cells of the tumor, a fact that could explain tumor recurrence and metastasis. The slowly proliferating CSCs are ineffectively targeted by conventional cancer therapies which mainly target the rapid proliferating tumor bulk [18–20]. Resistance of CSCs to chemo- and radiotherapy can be explained by proliferating quiescence, activation of DNA damage response and other anti-apoptotic signaling pathways, aldehyde hydrogenase (ALDH) activity and expression of efflux pumps like ATP-binding cassette (ABC) transporters. In particular, these efflux pumps provide protection from xenobiotic drugs and can lead to multi-drug resistance [21,22]. ALDH activity is another detoxifying mechanism to protect CSCs from cytotoxic aldehyds [23]. Thus, it is suggested that elimination of CSCs is highly necessary for long-time cure of patients. Tumor antigens which are expressed on CSCs could be used to target CSCs and eradicate the entire tumor in combination with classical therapies.

1.2 Therapy of cancer

Treatments for cancer exist – current classical cancer therapies include chemotherapy, radiation therapy and surgery. Even in the ancient literature, early detection and complete removal of the neoplasms was recommended as the only effective therapy [24]. In the late 19th century, with the discovery of X-rays by Wilhelm Röntgen, radiation therapy was introduced in cancer treatment. In the 1920s it was recognized that nitrogen mustard effectively kills cancer cells [25,26]. This was the birth of chemotherapeutic agents – cytotoxic substances which kill either rapidly growing cells by damaging their DNA or blocking functions in cell growth and replication – to treat cancer. However, surgery, radio- and chemotherapy often only lead to a temporary remission but cannot always prevent cancer recurrence mainly because disseminated cells resulting in metastatic spread are not efficiently destroyed. Furthermore, these classical therapies often harm also the surrounding normal tissues. Therefore, more effective therapies were developed which can be combined with chemo- and radiation therapy to improve activity and reduce side effects. Increasing knowledge of the immune system and tumor cell biology has led to the development of cancer immunotherapies and targeted therapies. These therapies use molecular targets which are specifically altered in cancer cells (mainly involved in growth and survival of cancer cells) rather than by simply interfering with all rapidly dividing cells of the body like chemotherapy does [27]. Immunotherapeutic approaches to attack cancer have achieved successful results in the last years and will be introduced briefly in the next chapter.

1.2.1 Cancer immunotherapy

The idea to use the immune system to combat cancer is rather old. In the late 19th century, William B. Coley injected a mixture of live or inactivated bacteria directly into tumors of cancer patients leading to successful recovery by unspecific stimulation of the immune system [28]. Based on the immune surveillance theory, the host's immune system has a homeostatic role in controlling cancer [29]. Today it is known that cancers have the ability to escape a functional immune system because of the high similarity between tumor and normal cells or because tumor cells are capable to suppress the immune system. Moreover, a complex cross-talk

between tumor and host exists during cancer development (theory of cancer immunoediting) [30–32]. To date, cancer immunotherapy is one of the most promising strategies in cancer therapy and was selected by Science magazine as the breakthrough of the year 2013 because of encouraging results from cancer immunotherapy clinical trials [33]. The increased knowledge that tumor cells are significantly altered compared to normal cells and that immune cells can be engineered to attack cancer cells has led to numerous immunotherapeutic approaches. Cancer immunotherapies can be divided into two subtypes: active immunotherapy in which the patient's immune system is trained to attack the tumor cells (cancer vaccines and adjuvants) and passive immunotherapy in which the patient's immune system is recruited to target tumor cells by administration of therapeutic monoclonal antibodies, adoptive T-cell transfer or cytokines [34]. Cancer immunotherapies specifically target cancer cells without harming normal viable cells. A key feature of a highly specific and effective cancer immunotherapy is thus the target itself and therefore many efforts have been made over the past decades to find highly specific tumor antigens.

1.2.2 Ideal tumor antigens suitable for cancer immunotherapy

The key to effective cancer immunotherapies is the selectivity of the drug and its capability to induce an immune response. The identification of tumor antigens is a continuous challenge in tumor immunology. An ideal tumor antigen for cancer immunotherapy should be specific and stably expressed in the primary tumor and metastasis but absent from or highly restricted in normal tissues to prevent autoimmunity and harming of healthy cells. Ideal tumor antigens often exert crucial functions for survival and/or proliferation of the tumor cell. To be accessible for antibodies, the tumor antigen should be stably expressed on the surface of cancer cells whereas cell-based immunotherapies can also use tumor antigens which are located inside the cells [35].

Primarily tumor antigens that are important in characterized cellular processes or signaling pathways relevant for the malignant phenotype and survival of tumor cells are attractive targets for cancer immunotherapeutic approaches. Key molecules in these processes can be potential targets for therapeutic antibodies, for example receptor tyrosine kinases or growth factors such as vascular endothelial growth factor (VEGF) that exerts an essential role in tumor

angiogenesis and can be targeted by neutralizing antibodies (Bevacizumab / Avastin®, Roche) [34]. Knowledge about how tumor-specific antigens are regulated, allows conclusion about mechanisms that are deregulated in cancer and can be targeted by therapies. For example, oncogenes can be targeted by interfering with the signaling pathways in which they are involved e.g. Cetuximab/Erbitux (EGFR inhibitor), Sorafenib/Nexavar (BRAF inhibitor) or Trastuzumab/Herceptin (targeting HER2) [36].

A large number of tumor antigens have been characterized so far. General categories based on molecular criteria and examples for each group are listed in Table 1. Notably, some tumor antigens may fall in more than one category.

Table 1 General categories of tumor antigens, explanations and examples thereof. [37–39]

Category	Explanation	Example
oncofetal/embryonic	typically only expressed in fetal tissues and cancerous somatic cells	CEA , TAG-72
oncoviral	encoded by tumorigenic transforming viruses	HPV E6, E7
overexpressed	highly elevated expression in neoplasia compared to expression in normal tissue	Ep-CAM, Her2/neu
cancer-germline	expressed only by cancer cells and adult reproductive tissues (testis, ovary, placenta)	MAGE family , NY-ESO-1
lineage-restricted/ differentiation	Tissue or cell-type specific, expressed largely by a single cancer histotype	Tyrosinase, Melan-A/MART-1
mutated	only expressed by cancer as a result of genetic mutation or alteration in transcription	p53, Ras
splice variants	specific splice variants from a gene are expressed in tumors	Lactate dehydrogenase C, CLDN18.2
Posttranslationally altered	tumor-associated alteration in glycosylation etc.	MUC1
idiotypic	highly polymorphic genes where a tumor cell expresses a specific “clonotype”	Ig, TCR in B-/T-cell leukemia, lymphoma, myeloma

CEA = carcinog-embryogenic antigen; TAG-72 = tumor antigen-72; HPV = human papilloma virus; Ep-CAM = epithelial cell adhesion molecule; Her2/neu = human epidermal growth factor receptor 2; MAGE = melanoma-associated antigen; NY-ESO-1 = New York esophageal squamous carcinoma 1; Melan-A/MART-1 = melanoma antigen recognized by T cells-1; MUC1 = mucin1; Ig = Immunoglobulin; TCR = T cell receptor

A distinguished class of tumor antigens are cancer germline antigens (CGA) also known as cancer testis antigens (CTA). These antigens were originally identified because of their immunogenicity in cancer patients and their recognition by $CD8^+$ T-cells [40,41] and antibodies [42,43]. So far, more than 130 CGAs have been identified [44–46]. The expression pattern of CGAs in normal tissues is highly restricted to testis, ovary and placenta while they are aberrantly expressed in a

wide range of human cancers [45–48]. In testis, CGAs are mainly expressed in spermatogonia, the self-renewing stem cell population of testicular germ cells but they are also found in spermatocytes. In ovary, CGAs are expressed in primary oocytes. In placenta, CGAs are found in trophoblastic cells which give rise to placenta and chorion [49–51].

CGAs tend to be expressed coordinately in tumors, suggesting that a common regulatory mechanism exists [46,52,53]. Interestingly, a majority of CGA promoters are located within CGIs, suggesting that epigenetic mechanisms are involved in coordinated upregulation of CGAs in certain type of cancers [54–57]. Moreover, as CGAs are expressed only in the germline but repressed in somatic tissues, re-activation of gametogenic programs in cancer may result in activation of CGAs in cancer [46,47]. Only recently, some CGAs have been found to be expressed also in cancer stem cells such as *BORIS/CTCFL*, *MAGE-A2*, *-A3* and *-A4* [58].

Cancer/placenta antigens (CPA) represent a subgroup of CGAs which are highly expressed in trophoblastic cells and low expressed in testis but show no expression in spermatogonia. CPAs are frequently expressed in cancers [51]. Indeed, many characteristics are shared by cancer cells and cells of the trophoblast, described by John Beard in his “trophoblastic theory of cancer” in 1902 [59] and restated by Lloyd Old in 2007 with “cancer is a somatic cell pregnancy” [51]. The shared features which occur both during pregnancy and cancer are invasion in surrounding tissues [60], neovascularization [61], immunological escape [62], telomerase activity [63], aneuploidy [64] and epigenetic changes [65]. Possibly, cancer cells acquire these features by reactivation of genes normally expressed in embryonic and fetal life.

Another eminent class of tumor antigens represents the oncofetal or embryonic antigens that are exclusively expressed in embryonic tissues but transcriptionally silenced after birth. Oncofetal antigens are overexpressed in tumors while the corresponding normal tissue remains negative [35,66]. As causative for re-expression of oncofetal antigens in cancer the activation of ESC signaling pathways in cancers are assumed.

In this thesis, two candidate tumor antigens were characterized. The following chapters will describe the current knowledge about both targets.

1.3 Placenta-specific 1 (PLAC1)

PLAC1 (placenta-specific 1) was introduced as a novel member of cancer-associated placental genes in 2007 [67,68]. PLAC1 is a potent candidate for antibody-based immunotherapeutic approaches because a) it is specifically expressed in various cancer types but not in human normal tissues except placenta and b) it is localized in or near the plasma membrane.

1.3.1 Structure and regulation of *PLAC1*

PLAC1 is a placenta-specific gene which is essentially involved in normal placental and embryonic development [69]. *PLAC1* is an X-linked gene, mapping to Xq26 (human) and X A5 (mouse), identified in 2000 by direct cDNA sequence analysis of a X-chromosomal locus around the *HPRT* gene [70], a locus found to be important for fetal and placental development [71–73].

The *PLAC1* gene structure is conserved between mouse and human with ~ 75% homology at the DNA level and ~ 60% at the protein level [70]. The first sequence analysis of *PLAC1* in 2000 by Cocchia and coworkers revealed three exons downstream of a predicted promoter which is now referred to be promoter P2 with exons 4 to 6, the same is true for murine *Plac1*. Today it is known that the *PLAC1* gene is regulated by two distinct promoters, named P1 and P2, separated by 100 kb. The *PLAC1* gene encodes six exons; exons 1 to 5 are rather small whereas exon 6 is the largest one containing the complete open reading frame (ORF). The transcription starts either from promoter P1 and P2 leading to five isoforms for human *PLAC1* or four isoforms for murine *Plac1*. In all cases, the terminal exon 6 with the protein coding sequence is completely included (Figure 2).

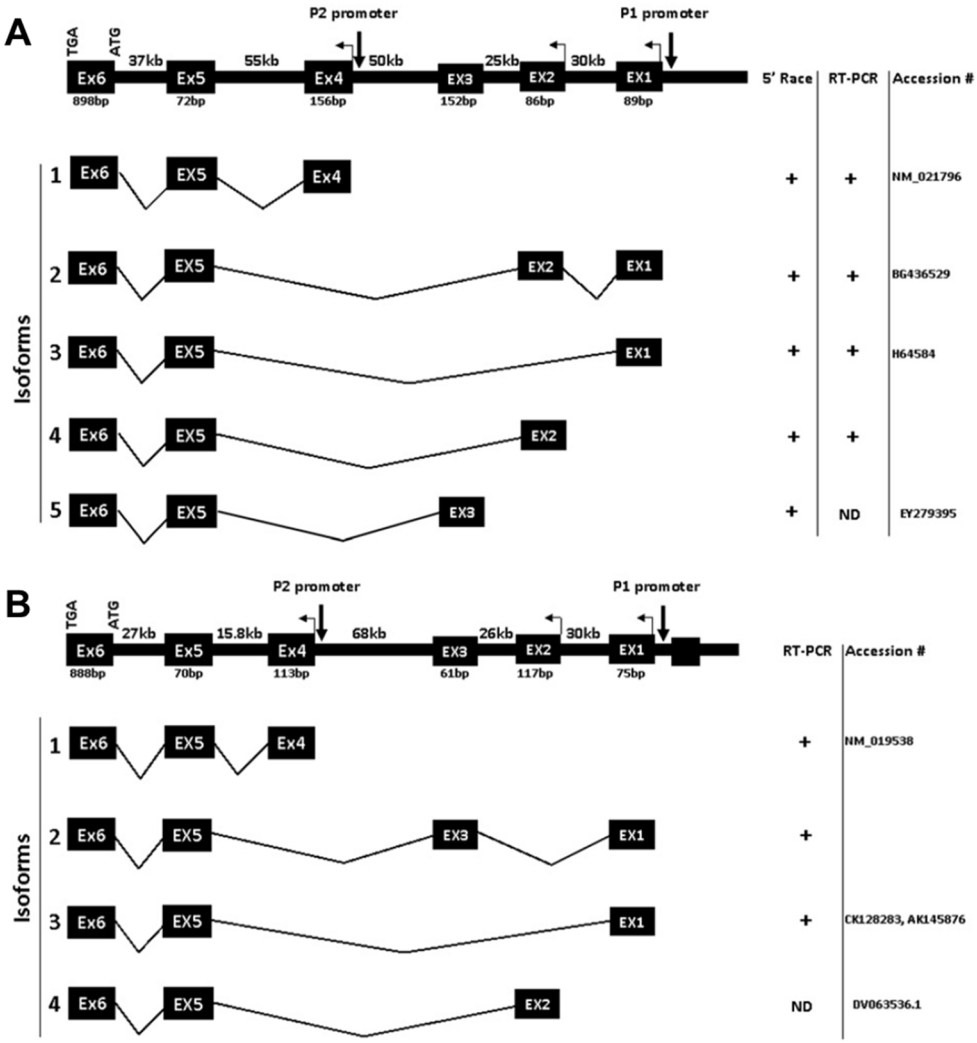

Figure 2 Schematic representation of the human (A) and mouse (B) *PLAC1* gene structures with dual promoters. The top line in (A) and (B) positions promoters P1 and P2 in relation to six exons, introns and their sizes. Five human and four mouse splice transcript isoforms detected by RACE and RT-PCR are diagrammed below. For both human and mouse only transcripts starting at P2 promoter include exons 4-6; transcripts originating at P1 promoter include various other exons but always skip exon 4. The columns at right indicate isoforms detected from a human placental RNA library or in BeWo cells by 5' RACE experiments or RT-PCR. For mouse, splice isoforms confirmed by RT-PCR are indicated. Available Genbank database accession numbers supporting isoforms are also indicated. [Exon 3 was identified as a potential exon by its homology to an EST, EY27935 derived, from a monkey cDNA library]. ND means not detected. [74]

The human PLAC1 protein consists of 212 amino acids (aa), whereas murine Plac1 is 173 aa in length. PLAC1 is suggested to be extracellular, contains a cleavable signal peptide of 23 aa at the N-Terminus and a transmembrane domain (aa 23 to 40) downstream of the signal peptide [75]. Furthermore a significant sequence homology to zona pellucida 3 protein (ZP3) is found. ZP3 motifs are found in extracellular receptor-like glycoproteins, e.g. transforming growth factor beta (TGF-β) receptor type III (betaglycan) or uromodulin [76]. As ZP3 motifs are important to form filamentous structures it is suggested that PLAC1 polymerizes or has a functional role in interaction with protein partners [77–79]. The PLAC1

protein is membrane-associated and speculated to have a receptor-like function modulating specific cell-cell or ligand-receptor interactions unique to the maternal-placental interface [80].

The regulation of *PLAC1* appears to be very complex and up to now it is only partially understood how *PLAC1* is differentially expressed in placenta and certain cancer types but repressed in normal tissues. Both promoters are active to some extend in placenta and cancer cell lines but the promoter usage differs. For example, in human placenta and the human breast cancer cell line MCF-7, P2 is the preferred promoter, whereas P1 is preferentially used in the human choriocarcinoma cell lines BeWo and JAR [74]. So far, several transcription factors were discussed to regulate *PLAC1* either at promoter P1, P2 or both. Chen and coworkers found that nuclear receptor retinoid X receptor α (RXRα) in combination with liver X receptor α or β (LXRα / LXRβ) can activate *PLAC1* expression from both promoters in placenta and different cancer cell lines [74]. Furthermore, involvement of tumor protein 53 (TP53), retinoblastoma protein (RB) and nuclear receptor co-activator 2 (NCOA2) was demonstrated at promoter P1 in SV40-transduced primary fibroblasts. While expression of TP53 repressed PLAC1 promoter P1, RB potentiated *PLAC1* transcription in conjunction with NCOA2, particularly when RXRα and LXR agonists were present [81]. Moreover, PPARδ was suggested as an additional regulator for *Plac1*, as activation of PPARδ in the mouse mammary epithelium results in the appearance of ER- and PR-positive and ErbB2-negative infiltrating ductal carcinomas which are associated with an up-regulation of *Plac1* [82] .

Our group analyzed in previous studies exclusively promoter P2 and discovered that basal expression of *PLAC1* is governed by the concerted action of the transcription factors SP1 and isoform 2 of CCAAT/enhancer binding protein β (C/EBPβ) in three different breast cancer cell lines [83]. Furthermore, we showed that *PLAC1* is an estrogen-responsive gene as ERα-signaling in MCF-7 cells further transactivates *PLAC1* expression. Interestingly, the *PLAC1* promoter region (P2) exhibits no estrogen-response elements (ERE), thus the estradiol-mediated transactivation of *PLAC1* acts via a non-classical pathway. Activated ERα tethers DNA-bound SP1 and C/EBPβ-2 which results in enhanced expression of *PLAC1*. Accordingly, ERα-positive breast tumors display significantly higher *PLAC1* expression levels compared with ERα-negative tumors [83]. In summary, these

first results lead us to an early model of the *PLAC1* transactivation complex at promoter P2 (Figure 3).

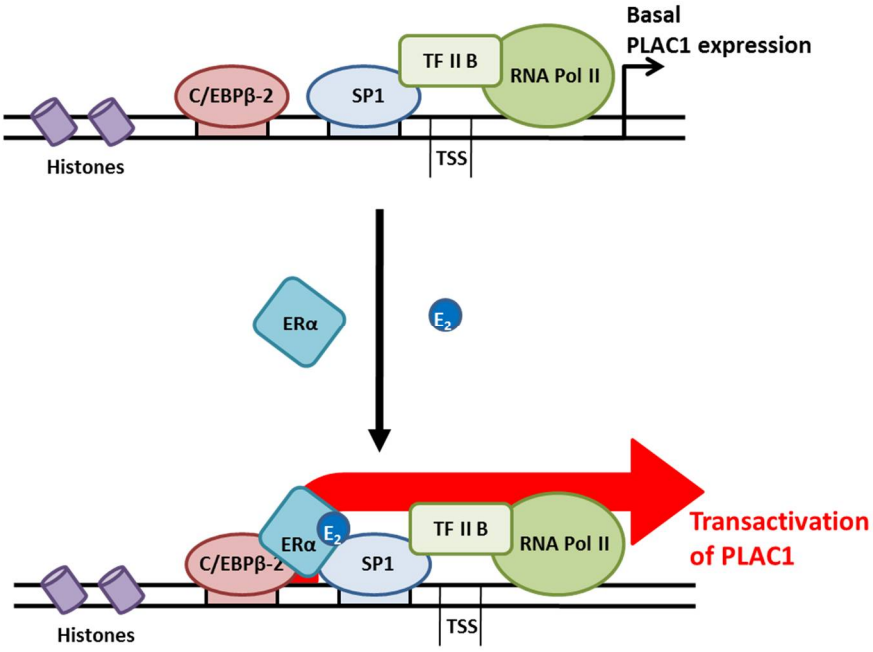

Figure 3 Early model of the *PLAC1* transactivation complex at promoter P2. Basal expression of *PLAC1* is maintained upon binding of C/EBPβ-2 and SP1 as well as general transcription factor II B (TF II B) and RNA polymerase II (RNA Pol II) to the *PLAC1* promoter adjacent to the transcription start site (TSS). Stimulation of cells with estradiol (E_2) leads to activation and binding of ERα to C/EBPβ-2 and SP1 which enhances the expression of *PLAC1*.

1.3.1.1 The role of nuclear receptor co-activators (NCOA) in gene regulation

The p160/NCOA family of nuclear co-activators is a key family involved in steroid-receptor-mediated gene regulation. Three family members are known so far, NCOA1 [84], NCOA2 [85] and NCOA3, also known as amplified in breast cancer 1 (AIB1) and steroid receptor co-activator 3 (SRC-3) [86,87]. NCOAs mediate transcriptional activation of nuclear receptors by bridging the nuclear receptor with co-activators and the basal transcription machinery. NCOAs have been shown to interact with a panel of nuclear receptors for examples estrogen receptor (ER) [88], progesterone receptor (PR) [88] and androgen receptor (AR) [89] but also other transcription factors, e.g. activator protein-1 (AP-1) [90], nuclear factor-κB (NFκB) [91] or E2F transcription factor 1 (E2F1) [92]. Interaction of the receptor with a co-activator is crucial for assembly and stabilization of a preinitiation complex at the target gene promoter [93]. NCOAs possess molecular structures necessary to recruit other co-regulators and general transcription factors, which leads to chromatin remodelling and transcriptional activation by recruitment of RNA polymerase II [94,95]. For example, NCOA1 and 3 contain a histone

acetyltransferase (HAT) activity domain suggesting a direct role for these co-activators in chromatin remodeling during initation of transcription of certain target genes [96,97]. Moreover, activation domains of NCOAs are responsible for interaction with general transcription cointegrators like cyclic AMP response element-binding protein (CBP) and the histone acetyltransferase p300 [98] as well as histone methyltransferases [99,100].

NCOA genes are amplified and overexpressed in various human cancers, in particular in hormone-promoted breast cancers whereas if at all low expression is found in normal breast tissue [101]. NCOAs increase the function of steroid receptors like ER, PR and AR which in turn facilitates the hormonal promotion of breast, prostate and ovarian cancer. Interestingly, NCOAs display unique, non-redundant functions in breast tumorigenesis [94,102]. However, NCOAs promote carcinogenesis through several pathways (Xu et al 2009). For example, NCOA1 can promote migration, invasion and metastasis of breast cancer cells by activating colony stimulating factor 1 (CSF1), TWIST1 or Akt [103,104]. The overexpressed NCOA3 can act through various signaling pathways to increase proliferation, survival and growth as well as migration, invasion and metastasis of cancer cells such as increasing the function of E2F1, the activity of the insulin-like growth factor 1(IGF1) signaling pathway, epidermal growth factor receptor (EGFR) and ERBB2, and the expression of matrix metalloproteinases (MMPs) [101]. The *in vivo* role of NCOA3 was analyzed in multiple mouse models which either are deficient for NCOA3 or overexpress NCOA3 in mammary epithelia using the *mouse mammary tumor virus (MMTV)* promoter. MMTV is a milk-transmitted retrovirus that causes mammary tumors in mice and is used to study the role of genes in mammary tumorigenesis in mouse models [105,106]. The most important results were taken from a study with *MMTV-Ncoa3* transgenic mice which developed mammary hyperplasia and spontaneous malignant mammary tumors indicating that overexpressed NCOA3 is oncogenic [107].

In this study, it was examined if NCOA1, 2 or 3 are involved in ERα-mediated trans-activation of PLAC1 especially because these proteins have been shown to be crucial in breast cancer.

1.3.2 The role of PLAC1 in placenta and fetal development

In humans, *PLAC1* is detectable upon week 8 and throughout pregnancy in trophoblastic cells, in contrast murine *Plac1* diminishes after 14.5 days post coitus (dpc) of gestation [70,80]. *PLAC1* expression is strictly confined to the differentiated cells of the placental syncytiotrophoblast and increasing during gestation and is positively regulated by the growth factors FGF-7 and EGF which are essential for trophoblast development [108]. During embryonic development, murine *Plac1* is expressed in several murine tissues including lung, heart, brain, kidney, liver and intestine [109].

Since the discovery of *PLAC1* in 2000 it was strongly suggested that it plays an essential role in placental development but evidences were missing. Finally, very recently this was proven by Jackman and co-workers who disclosed *Plac1* as an essential factor for murine normal placental and embryonic development using a *Plac1* mutant mouse model. Ablation of Plac1 is associated with placentomegaly and intrauterine growth retardation [69]. Further analysis of the *Plac1* knock-out (KO) phenotype revealed that *Plac1* is associated with development of a lethal hydrocephalus indicating that *Plac1* is expressed in the fetal brain and directly influences brain development [109]. However, a functional and molecular role of Plac1 in brain as well as placental development remains to be analyzed.

1.3.3 PLAC1 and cancer

As mentioned before, PLAC1 underlies tight transcriptional repression in any human normal tissue, except testis and differentiated cells of the placental syncytiotrophoblast, in which *PLAC1* is expressed throughout human gestation. In contrast, PLAC1 is frequently activated and highly expressed in a variety of human cancers, in particular breast cancer, and cancer cell lines of different origin [67].

Our group found previously that PLAC1 exhibits important biological functions in cancer. PLAC1 is a critical factor for cancer cell proliferation, as silencing of PLAC1 results in a pronounced G1 cell cycle arrest accompanied by decreased cyclin D1 expression and hypophosphorylation of AKT kinase. Moreover, cell motility, migration and invasion of breast cancer cells are decreased by silencing of PLAC1. Tumor-promoting functions of PLAC1 can be antagonized by specific

antibodies, thereby qualifying PLAC1 as promising candidate for targeted therapies of cancer [67].

1.4 The tight junction molecule claudin 6 (CLDN6)

Claudin 6 (*CLDN6*) is a member of the claudin multigene family of tight junction proteins which includes 27 known members [110]. Cell-cell adhesion in epithelial and endothelial cells is mediated by the apical junctional complex which consists of three major components, tight junctions, adherens junctions and desmosomes. Tight junctions serve two major functions: first, they are essential in regulating the paracellular barrier and second, maintain the polarity of the epithelial and endothelial cells [111]. In the last few years it became more and more convincing that tight junctions play a role in proliferation, transformation and metastasis of cancer cells [112]. Dysregulation of claudins leads to disruption of tight junctions in epithelial cells which in turn results in loss of cell polarity and impairment of the epithelial integrity. Decreased cell-cell adhesion and increased mobility of cancer cells are suggested to be main events of epithelial to mesenchymal transition (EMT), an important step in cancer progression and metastasis [113,114].

1.4.1 Structure and regulation of *CLDN6*

The human *CLDN6* gene is located on the reverse strand of chromosome 16p13.3 in close proximity to *CLDN9* that is located on the forward strand (Figure 4). Three transcript isoforms are known so far; *CLDN6-001* encodes for three exons whereas *CLDN6-201* encodes for two exons, in both isoforms the last exon contains the complete ORF of 660 bp encoding for the same protein sequence, 220 aa in length. In contrast, *CLDN6-002* has three exons, the last two exons encode for an N-terminal truncated variant of 39 aa in length (Figure 4).

The *Claudin 6* gene is highly conserved among different species. For example, mice and men exhibit 88% homology at DNA and protein level. Murine *Cldn6* is located on the forward strand of chromosome 17 A3.3 while only one splice isoform is known so far (source: ensemble.org).

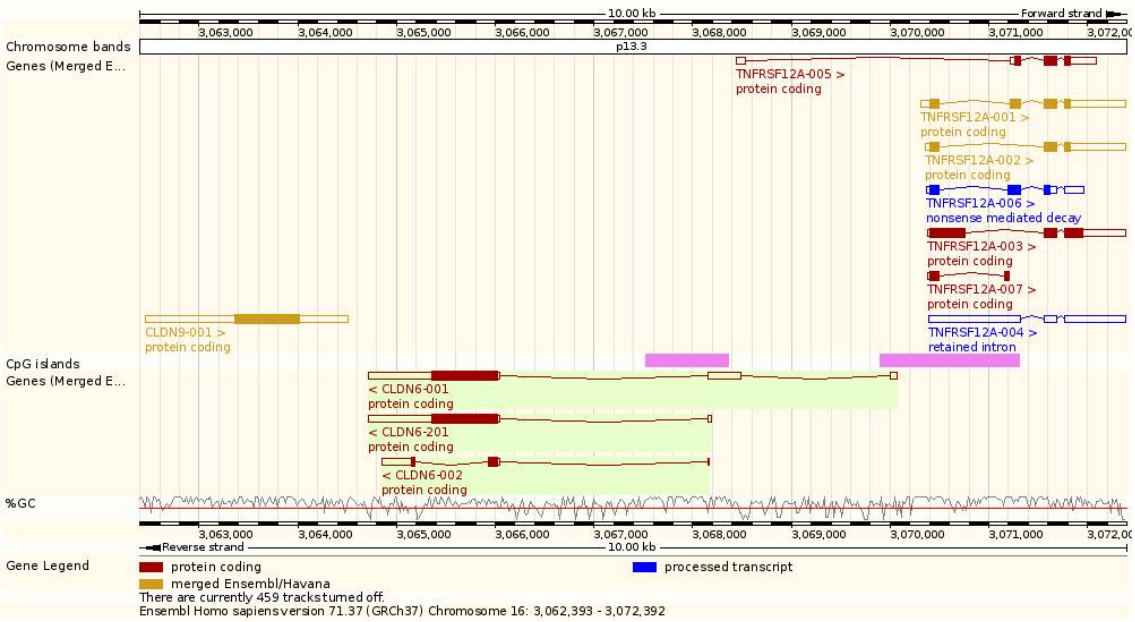

Figure 4 Chromosomal location of *CLDN6* (16p13.3). Violet boxes mark the CpG islands in front of *CLDN6*. Red boxes mark protein coding regions of the transcript sequences. From: ensemble.org, ensemble Homo sapiens version 71.37 (GRCh37), downloaded on 12.6.2013.

Claudins are between 205 and 305 aa in length and have a molecular weight of 21 to 34 kDa. CLDN6 comprises 220 aa and is 23 kDa in size [115]. CLDN6 shows the highest similarity in sequence to CLDN9 but also CLDN3 and 4 [116]. The claudin protein structure is highly conserved among the different family members, thus CLDN6 exhibits a claudin-typical protein-sequence and structure (Figure 5). Claudins are major integral membrane proteins of tight junctions with four membrane-spanning domains and two extracellular loops (Figure 5). The first extracellular loop (EL1) contains two conserved cysteines which are suggested to increase protein stability by formation of an intramolecular disulfide bond [117]. Charged amino acids in EL1 indicate that this loop is important for paracellular ion selectivity [118]. The second extracellular loop, EL2, is considered to be important for oligomerization of claudins through hydrophobic interactions between conserved aromatic residues [119]. The amino- (NH_2) and carboxyl- (COOH) terminal tails of claudins both end in the cytoplasm. The C-terminal end is the most diverse region in a claudin molecule, its length varies between 21 and 63 aa (106 aa in CLDN23), it contains a PDZ-binding motif that can be posttranscriptional modified which is important for signal transduction. For example, claudins can be phosphorylated by protein kinases A or C (PKA or PKC) influencing their localization and function [120,121]. Furthermore, claudins can interact via their PDZ-domain directly with cytoplasmic proteins like zona occludens (ZO) -1,-2 and

-3 [122]. Other posttranslational modifications, like palmitoylation, are important for oligomerization and incorporation of claudins into tight junctions [123].

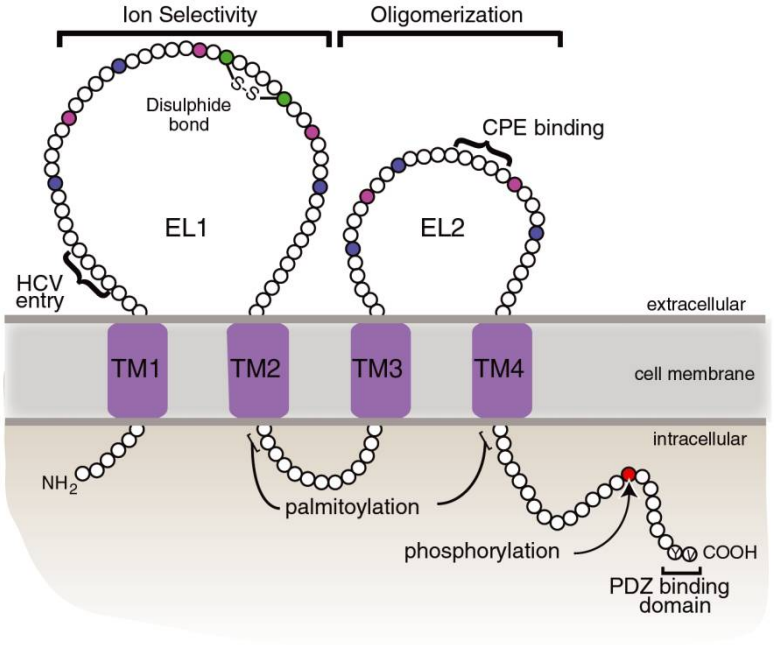

Figure 5 Schematic structure of a claudin molecule. Claudins have four transmembrane domains (TMD 1-4) and two extracellular loops (EL1 and 2) which mediate paracellular ion selectivity and oligomerization. The intracellular carboxyl (-COOH) terminus harbors a PDZ binding domain which undergoes posttranscriptional modification important for signal transduction. Phosphorylation and palmitoylation sites as well as regions important for HCV entry and CPE binding are depicted. Adopted from 124.

CLDN6 serves as a co-receptor for Hepatitis C virus entry, which has also been shown for CLDN1 and 9 [125,126]. Moreover, CLDN6 is a receptor for *Clostridium perfringens* enterotoxin (CPE) as well, which has also been disclosed for CLDN3, -4 and -7 [127–129].

For a long period of time, *CLDN6* regulation was analyzed only in regard to epithelial differentiation during embryogenesis. There are hints that murine *Cldn6* is regulated by the bone morphogenetic protein (BMP) signaling pathway in embryogenesis [130] but clear evidences are missing so far. BMP-4 silencing does not result in any changes of Cldn6 expression in mouse embryos [131]. Retinoid X and acid receptors RXRα and RARγ as well as hepatocyte nuclear factor 4α (HNF-4α) have been shown to induce Cldn6 expression and *de novo* formation of functional tight junctions and epithelial cell polarity upon retinoid acid treatment in murine F9 embryonal carcinoma cells [132,133].

In cancer, epigenetic mechanisms such as DNA methylation are suggested to be involved in deregulation of *CLDN6* [134–136]. Indeed, *CLDN6* has two CpG islands in its promoter region (Figure 4). Furthermore, CLDN6 can be induced by treatment with 17-β-estradiol in MCF-7 cells suggesting that ERα-related pathways

are involved in *CLDN6* regulation in breast cancer [137]. Overexpression of miRNAs 7 and 218 can also up-regulate CLDN6 in breast cancer cell lines by changing the epigenetic landscape of the promoter region [138]. Moreover, a recent report showed that the p38 MAPK pathway is activated in MCF-7 and HBL-100 cells overexpressing CLDN6 [139,140]. Interestingly, p38 MAP kinases and Src are involved in the upregulation of CLDN6 during dedifferentiation resulting in dysfunction of salivary gland cells [141]. Remarkably, CLDN6 is upregulated in a breast cancer 1 (BRCA1)-null ovarian cancer cell line suggesting a role for the breast and ovarian cancer susceptibility gene in the regulation of *CLDN6* [142].

In summary, the regulation of *CLDN6* appears to vary between cancer types and a general mechanism of *CLDN6* regulation in cancer is not identified so far.

1.4.1.1 **The role of CTCF and BORIS (CTCFL) in cancer**

CTCF (CCCTC-binding factor) and BORIS (Brother of regulator of imprinted sites) also known as CTCFL (CTCF-like) are transcription factors involved in the epigenetic regulation during normal development and cancer. CTCF is suggested to exert tumor suppressive functions as its target genes are mainly involved in proliferation and cell growth and overexpression of CTCF results in a senescent-like state with a cell cycle arrest. Moreover, CTCF is a multivalent factor and can act also as transcriptional activator and is implicated in insulation, imprinting and X-inactivation [143–146].

BORIS is a paralog of CTCF and evolved by a gene duplication event [147,148]. *BORIS* maps to a region on chromosome 20q13 that is frequently amplified in several types of cancer. Interestingly, the same types of tumors show loss of heterozygosity (LOH) at 16q22 where *CTCF* is located [143,149]. A comparison of the exon-intron structures of human *CTCF* and *BORIS* reveals a remarkable homology between all exons coding for 11 zink fingers (ZF), which mediate DNA binding (Figure 6). Thus, BORIS and CTCF can bind to the same DNA motifs. Many different DNA sequences can be bound because the ZFs are used combinatorial. In contrast, the exons coding for N- and C-terminal regions differ substantially suggesting that BORIS and CTCF exert different functions upon DNA binding [143]. Notably, 23 alternative spliced transcript variants encoding 17

isoforms have been found for *BORIS* while only three transcript variants and two isoforms are known for *CTCF* [150].

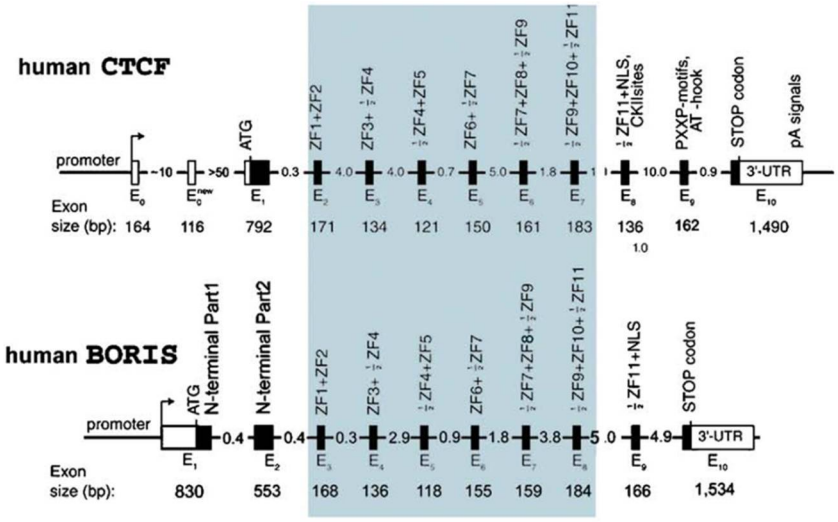

Figure 6 Comparison of the exon-intron structures of human *CTCF* and *BORIS* genes. A blue box shows the region of homology over the exons encoding the 11 ZF domain. Modified from 143.

BORIS and CTCF are mutually exclusive expressed during male germ cell development where they are responsible for erasure and re-establishment of methylation marks during male germ cell development (Figure 7) [143,147]. Recently, it has been shown that BORIS is expressed in oocytes where it coincides with global DNA demethylation as well as in ESC while disappearing upon ES cell differentiation [150–152]. The cancer-germline antigen BORIS is frequently up-regulated in a variety of cancer types including ovarian and lung cancer as well as leukemia [153,154]. The sibling rivalry between CTCF and BORIS for DNA binding sites caused by aberrant activation of BORIS in somatic cells results in dysregulation of target gene expression and proliferation of cancer cells (Figure 7). Activation of BORIS coincides with global hypomethylation during tumorigenesis [147]. BORIS is suggested to be directly involved in epigenetic dysregulation of global or specific sites in cancer because it can interact with methyltransferases [143]. BORIS activates many testis-specific target genes during spermatogenesis, for example CGAs such as NY-ESO-1 [155], MAGE-A1 [156] and CST [157]. These genes are normally repressed by CTCF in somatic cells but up-regulated in cancer, likely by BORIS. As binding of BORIS or CTCF results in different gene expression of the target genes it is likely that their protein partners are substantially involved in the outcome of gene regulation. Notably, CTCF binds preferentially methylated genomic regions whereas BORIS preferentially binds to unmethylated DNA sequences. This does not exclude

binding of CTCF to unmethylated or BORIS to methylated DNA sequences [150,156,158–161].

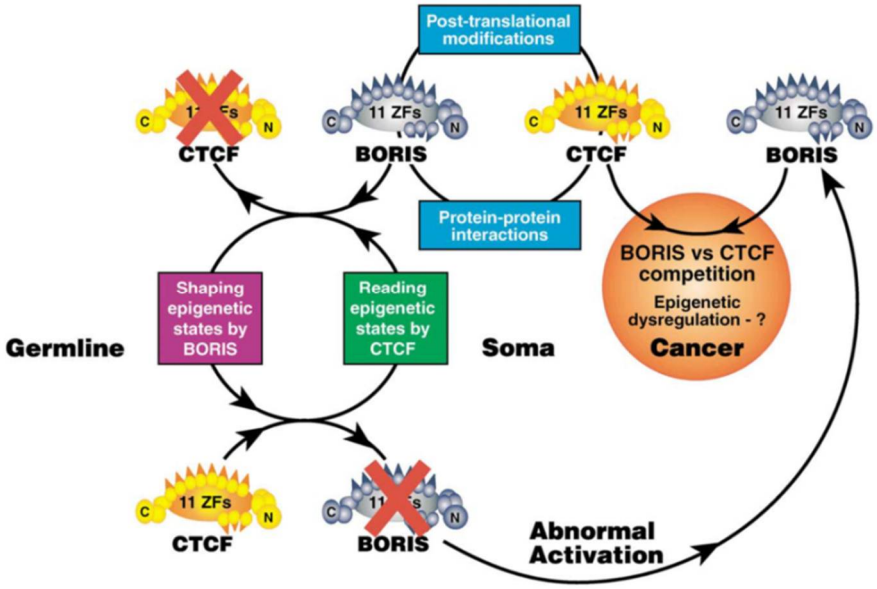

Figure 7 A model for CTCF and BORIS functions in normal cells and cancer. Adopted from 143.

In this study it was analyzed, if BORIS and/or CTCF exert any regulative effect on CLDN6 expression in cancer because the CLDN6 promoter features several CTCF/BORIS binding sites.

1.4.2 The role of claudin 6 in embryogenesis and fetal development

Claudin 6 was discovered in 1999 by similarity searches of mouse expressed sequence tag (EST) clones to the previous identified claudin 1 and -2 sequences [162]. Two years later, Cldn6 was found to be expressed in murine embryonal stem cells (ESC) committed to the epithelial cell fate and to be important for tight junction formation in epithelial cells. Studies with embryoid bodies (EB), which mimic very early development, uncovered that Cldn6 expression arises with the onset of epithelialization and is coexpressed with Keratin 8 (K8), a very early epithelial marker. Noteworthy, Cldn6 expression increases with differentiation of EBs while remaining restricted to the epithelial zone [130]. In the embryo, Cldn6 expression is found to be broadly expressed throughout the epiblast until day 8.5 when Cldn6 becomes restricted to definitive endoderm and from day 9.5 on, Cldn6 is found to be expressed in the entire gut, otic vesicles, a small region of the forebrain and mesonephros [163].

Moreover, Cldn6 is specifically expressed in undifferentiated mouse pluripotent stem cells whereas its expression continuously decreases throughout the course of stem cell differentiation and can be used as a specific marker to isolate stem cells from mixed cellular populations [164]. Indeed, a meta-analysis of human ESC transcriptome data from 38 different studies disclosed also human CLDN6 as one of 40 genes specifically expressed in hESC but not in any adult tissue [165]. Moreover, CLDN6 was recently detected as a specific marker for human induced pluripotent stem cells (iPSC) [166].

In vivo studies with transgenic mice overexpressing *Cldn6* in the suprabasal layer of the epidermis via the *Involucrin* (*Inv*) promoter revealed that Cldn6 is essential for the epidermal permeability barrier function of the skin. *Inv-Cldn6* mice die within 2 days of birth because of increased water loss through a defective epidermal barrier (Turksen and Troy, 2002). Furthermore, overexpression of Cldn6 affects the epidermal differentiation program as epidermal differentiation markers, several claudins as well as components of the Klf4 signaling pathway were deregulated. The severity of the phenotype increases with the level of Cldn6 overexpression [167–170]. Interestingly, *Cldn6* null mice appear viable and fertile without any phenotypic abnormalities [163].

Noteworthy, Cldn6, together with Cldn4, is essential for normal blastocyst formation as removal of Cldn6 and Cldn4 from tight junctions in the trophoectoderm of mouse embryos, which is the first epithelial structure emerging during mammalian development, results in a defective permeability barrier of the trophoectoderm and subsequent inhibition of blastocyst formation [129].

Thus, claudin 6 serves major functions during embryogenesis, especially in epithelial differentiation.

1.4.3 The role of claudin 6 in cancer and other diseases

Among the claudin family of proteins, *claudin 6* is unique because of its expression pattern that is restricted to ESC and embryonal tissues (epithelial structures of fetal lung, gastrointestinal tract, liver, kidney, heart and brain) [116,166,171,172]. In mice, Cldn6 is expressed also in neonatal tissues and adult kidney [173]. However, CLDN6 is absent in human adult organs [116,171,172]. In cancer, CLDN6 expression was found in germ cell tumors, ovarian cancer and lung

adenocarcinoma and cancers with a primitive phenotype [164,172,174] as well as gastric adenocarcinomas [175]. Moreover, CLDN6 is highly overexpressed in pediatric tumors of the brain (atypical teratoid/rhabdoid tumors) and kidney, liver and soft tissue (malignant rhabdoid tumors) [171,176]. At least for a gastric adenocarcinoma cell line, AGS, it was shown that, amongst other claudins, CLDN6 overexpression resulted in an increase in cell migration, proliferation and invasiveness of tumor cells [177]. On the other hand, silencing of CLDN6 in breast cancer been shown to promote anchorage-independent growth and correlate with a more aggressive phenotype of the tumors, the so-called claudin-low phenotype [135,178,179].

CLDN6 plays a role in other diseases as well. For example, up-regulation of Cldn6 is associated with adipogenesis [180] and it has been shown to act as a co-receptor for HCV entry in cells [126,181,182] as well as for CPE-mediated cytotoxicity in ovarian cancer cells [128].

As mentioned before, CLDN6 is found to be specifically expressed in murine and human iPSC [164,166]. In particular, it is possible to isolate tumorigenic stem cells from mixed populations using specific antibodies against CLDN6, indicating that CLDN6 could be important in cancer stem cells. However, the role of CLDN6 in cancer stem cells and tumor progression is not identified so far.

1.5 Aims of the thesis

The present study is subdivided into two parts, both aiming to characterize tumor-specific antigens as potential targets for cellular or antibody-based cancer immunotherapy.

The first part is focused on the analysis of the regulation of PLAC1 in cancer. Our group provided intriguing evidence that *PLAC1* is regulated by estradiol-dependent mechanisms but the complete complex of transcription factors was not known so far. To this end, it should be investigated which other factors in addition to ERα, SP1 and C/EBPβ are involved in estradiol-dependent transactivation of *PLAC1*. Focus of this study was the p160/NCOA co-activator family.

The second part concentrates on the molecular and functional characterization of CLDN6 in cancer. At the beginning of this study, very little was known about the expression, function and regulation of CLDN6 in cancer. Thereto, a comprehensive study of the function as well as regulation of CLDN6 was conducted.

The specific aims included a comprehensive analysis of the expression of *CLDN6* transcripts in human normal adult tissues as well as a variety of cancer tissues by quantitative RT-PCR. In functional cellular assays, it should be studied if CLDN6 exerts a function in proliferation, apoptosis, cell cycle, migration, and adhesion or colony formation of cancer cells, particularly in cancer stem cells. Concerning the regulation of CLDN6, the aim was to elucidate if epigenetic mechanisms, particularly DNA methylation, is involved in regulation of *CLDN6* and moreover, which transcription factors are involved in the up-regulation of *CLDN6* in cancer.

In summary, the study should add understanding how *PLAC1* and *CLDN6* are regulated in cancer and thus open new ways for therapeutic strategies. Moreover, to know the function of CLDN6 in cancer can add to its use as a diagnostic or therapeutic target for cancer immunotherapy.

2 Material

2.1 Cell lines und culture media

All cell lines used for this study were kindly provided by Ganymed Pharmaceuticals AG.

Table 2 Human cell lines and culture media used for this study.

Cell line	(Tumor) Type	Culture medium
MCF-7	Breast carcinoma	DMEM, 10% FCS, 0.5% Pen/Strep
SK-BR-3	Breast carcinoma	DMEM, 10% FCS, 0.5% Pen/Strep
NEC-8	Testicular carcinoma	RPMI, 10% FCS, 0.5% Pen/Strep
NIH-OVCAR3	Ovarian adenocarcinoma	RPMI, 20% FCS, 0.01 mg/mL human insulin, 0.5% Pen/Strep
PA-1	Ovarian teratocarcinoma	MEM, 10% FCS, 0,1 mM MEM NEAA, 1 mM sodium pyruvate, 1,5 g/L sodium bicarbonate, 0.5% Pen/Strep
PA-1 SC12 LVTS2 50 and 54	Ovarian teratocarcinoma with stable lentiviral shRNA-mediated knockdown of CLDN6	Refer to medium for PA-1 cells
PA-1 SC12 LVTS2 76	Ovarian teratocarcinoma, stably transfected with control shRNA vector	Refer to medium for PA-1 cells
DAN-G	Pancreatic carcinoma	RPMI, 10% FCS, 0.5% Pen/Strep
HEK293	Human embryonic kidney	DMEM/F12, 10% FCS, 0.5% Pen/Strep

2.2 Tissues

Normal and tumor tissues were obtained as human surplus materials during routine diagnostic or therapeutic procedures and stored at -80°C until use.

2.3 siRNA duplexes

A pool of four different siRNA duplexes targeting *NCOA-3* (NM_006534), *CLDN6* (NM_021195), *BORIS* (NM_080618, NR_072975; NM_001269040–NM_001269052; NM_001269054; NM_001269055) or *CTCF* mRNA sequence (NM_006565 and NM_001191022) or a mixture of two different siRNA duplexes targeting *PLAC1* mRNA sequence (NM_021796) was used. As control, a pool of four non-silencing (ns) siRNA duplexes (D-001810-10-05, Dharmacon) was used. Catalog numbers and sequences can be found in the appendix (see chapter 7.2).

2.4 Antibodies

2.4.1 Primary antibodies

Table 3 Primary antibodies used for Western Blot analyses in this study.

Antibody	Dilution / Concentration	Manufacturer
Monoclonal mouse anti-PLAC1; clone 22-3A-1	5 µg/mL	Ganymed Pharmaceuticals AG
Monoclonal rabbit anti-NCOA1; clone 128E7	1:1000	Cell Signaling
Polyclonal rabbit anti-NCOA2; ab10491	1:1000	Abcam
Monoclonal rabbit anti-NCOA3; clone 5E11	1:1000	Cell Signaling
Monoclonal rabbit anti-Claudin 6; 18865	1:1000	IBL
Polyclonal rabbit anti-BORIS; ab126766	1:300	Abcam
Monoclonal mouse anti-β-Actin; clone AC15	1:50000	Sigma Aldrich

Table 4 Primary antibodies used for ChIP analyses in this study.

Antibody	Manufacturer
Monoclonal mouse anti-NCOA1; clone 1135/H4	Abcam
Polyclonal rabbit anti-NCOA2; ab9261	Abcam
Monoclonal mouse anti-NCOA3; clone AX15.3	Abcam
Polyclonal rabbit anti-SP1; ab13370	Abcam
Monoclonal rabbit anti-CEBPβ; clone E299	Abcam
Monoclonal mouse anti-ERα; clone 33	Abcam
Monoclonal mouse anti-p300; clone 3G230 / NM-11	Abcam
Polyclonal rabbit anti-pCAF; ab12188	Abcam
Monoclonal mouse anti-Histone H3 (acetyl K9); clone AH3-120	Abcam
Polyclonal rabbit anti-Histone H4 (acetyl K8); ab15823	Abcam
Monoclonal mouse anti-TFIIB; clone IIB1	Abcam
Polyclonal rabbit anti-RNA polymerase II; ab5131	Abcam
Polyclonal rabbit anti-HA tag ChIP grade; ab9110	Abcam
Monoclonal mouse anti-p53; clone DO-1	Santa Cruz
Monoclonal mouse anti-BORIS; clone F-1	Santa Cruz
Polyclonal goat anti-CTCF; sc-15914X	Santa Cruz

2.4.2 Secondary antibodies

Table 5 Secondary antibodies used for Western Blot analyses in this study.

Antibody	Dilution	Manufacturer
HRP-conjugated goat anti-mouse IgG	1:5000	Jackson Immuno Research
HRP-conjugated goat-anti-rabbit IgG	1:5000	Jackson Immuno Research

2.4.3 Antibodies for FACS analysis

Table 6 Primary antibodies used for FACS analysis in this study.

Antibody	Dilution/ Concentration	Manufacturer
Human anti-CLDN6 IMAB027-AlexaFluor647	1:400	Ganymed Pharmaceuticals AG
Mouse anti-SSEA-4-V450	2 µl / test	BD Horizon, BD Biosciences

2.5 Reagents

2.5.1 Chemicals

17-β-estradiol (E2758)	Sigma Aldrich
5-aza-2'-deoxycytidine	Sigma Aldrich
7-AAD	Sigma Aldrich
Accutase	PAA Laboratories GmbH
Acetic acid	AppliChem
Agarose	AppliChem
Ampicillin	Sigma Aldrich
Bacto-Agar	Difco
Bacto-Tryptone	Difco
Bacto-Yeast Extract	Difco
Bovine serum albumin (BSA) fraction V pH 7.0	Serva Electrophoresis GmbH
Bromphenol blue	AppliChem
Calcein AM	Life Technologies
Chloroform / isoamyl alcohol 24:1	Sigma Aldrich
Collagen R solution 0.2 %	Serva Electrophoresis GmbH
Coomassie Brilliant-Blue R-250	AppliChem
Crystal Violet	AppliChem
Dimethylsulfoxide (DMSO)	AppliChem
DNA loading buffer (6X)	Fermentas
dNTP Set, 100 mM solutions	GE Healthcare
Dulbecco's phosphate buffered saline (D-PBS), w/o calcium and magnesium; pH 7.2	Life Technologies
Dulbeccos modified eagle medium (DMEM)	Life Technologies
Dulbeccos modified eagle medium (DMEM), phenol-red free	Life Technologies
Endotoxin-free water	Sigma Aldrich
Ethanol absolute 96 %	Roth
Ethidiumbromide, 1% solution	AppliChem

Ethylendiamintetraacetate (EDTA) 0.5 M pH 8.0	Sigma Aldrich
Ethylene glycol tetraacetic acid (EGTA)	Sigma Aldrich
FACS Clean/Flow/Rinse	BD Biosciences
Fetal bovine serum, charcoal stripped	Sigma Aldrich
Fetal calf serum (FCS)	PAA Laboratories GmbH
Formaldehyde solution, min. 36.5 % puriss.	Sigma Aldrich
Formaldehyde, 37 %	Roth
Glycerin, anhydrous	Merck
Glycine	Roth
Glycogen	Sigma Aldrich
Hoechst	Sigma Aldrich
Human cDNA clone CTCFL, NM_080618.2; SC311151	Origene (amsbio biotechnology)
Human insulin	Sigma Aldrich
Human recombinant laminin-111	BioLamina
ICI 182,780	Sigma Aldrich
Isopropanol	Roth
Kanamycin	Sigma Aldrich
Lithium Chloride	Sigma Aldrich
Lumi-Light western blotting substrate	Roche
Methanol	Merck
Milk powder	Gabler Saliter
Minimum Essential Medium (MEM)	Life Technologies
Minimum Essential Medium (MEM), phenol-red free	Life Technologies
Non-essential amino acids (NEAA)	Life Technologies
NP-40	Ambion
Nuclease-free water	Qiagen
Penicillin (10 000 U/mL) / Streptomycin (10 mg/mL)	Life Technologies
Phenol solution (equilibrated with 10 mM Tris HCl pH 8.0, 1 mM EDTA)	Sigma Aldrich
Ponceau S, practical grade	AppliChem
Pro Gel 10/12/14 and 4-20 % Tris/Glycine Gels	Anamed Elektrophorese GmbH
Protein A or G Agarose beads	Millipore
RPMI 1640, GlutaMAX	Life Technologies
RPMI 1640, phenol-red free	Life Technologies
Sodium acetate	Roth
SOC medium	Life Technologies
Sodium bicarbonate	Life Technologies
Sodium chloride	Roth
Sodium deoxycholate (DOC)	Sigma Aldrich
Sodium dodecyl sulfate (SDS)	Sigma Aldrich
Sodium pyruvate	Life Technologies
Trishydroxymethylaminomethan (TRIS)	Roth
Triton X 100	Merck
tRNA	Sigma Aldrich
Trypan blue, 0.4 % solution	Gibco
TrypLE Express	Life Technologies
Tween 20	Sigma Aldrich
Universal Methylated Human DNA Standard	Zymo Research
β-mercapto-ethanol	Appli Chem

2.5.2 Oligonucleotides

Oligonucleotides used for this study were purchased from Eurofins MWG Operon and are listed in the appendix in chapter 7.3.

2.5.3 TaqMan® Gene Expression Assays

TaqMan® Gene Expression Assays used in this study for qRT-PCR analysis on a Fluidigm instrument were purchased by Life technologies. Catalog numbers can be found in the appendix (7.4).

2.5.4 DNA and protein ladders

DNA ladders Gene Ruler 1 kB and 50 bp	Fermentas
Protein ladder Precision Plus Protein Dual Color Standard	BioRad
Protein ladder Magic Mark XP Western Protein Standard	Life Technologies

2.5.5 Enzymes

Hot Star *Taq* DNA Polymerase	Qiagen
PfuUltra Hotstart DNA Polymerase	Stratagene
Phusion HotStart II High Fidelity DNA Polymerase	Thermo Scientific
Proteinase K	Sigma Aldrich
Restriction enzymes (*BamHI, NheI, HindIII, EcoRI*)	Fermentas
RNase A	Sigma Aldrich
SuperScript™ II Reverse Transcriptase	Life Technologies
T4 DNA Ligase	Fermentas

2.5.6 Kits

CYQUANT® GR Cell Proliferation Assay Kit	Molecular Probes
EndoFree Plasmid Maxi Kit	Qiagen
EpiTect Bisulfite Kit	Qiagen
NucleoSpin Plasmid Mini Kit	Macherey-Nagel
PE Annexin V Apoptosis Detection Kit	BD Biosciences
PerfeCta® qPCR FastMix®	Quanta Biosciences
PrimeScrit RT Reagent Kit	Takara Bio Inc.
QIAamp DNA Mini Kit	Qiagen
QIAquick (MinElute) Gel Extraction Kit	Qiagen
QIAquick (MinElute) PCR Purification Kit	Qiagen
QuantiTect SYBR Green PCR Kit	Qiagen
RNeasy Mini Kit	Qiagen
SuperSignal West Dura Extended Duration Subtrate Kit	Pierce Biotechnology
SuperSignal West Femto Extended Duration Subtrate Kit	Pierce Biotechnology
TaqMan® PreAmp Master Mix	Life Technologies
TOPO® TA cloning® kit	Life Technologies

2.5.7 Buffers and solutions

Buffers and solutions for molecular biology methods

TAE buffer (50X), pH 8	2 M Tris, 1 M glacial acetic acid, 0.5 M EDTA
Ethidium bromide stock solution	0.05 % ethidium bromide in H_2O
Luria-Bertani (LB)-medium	10 g/L Bacto-Trypton, 5 g/L Bacto- yeast extract, 5 g/L NaCl
LB-Agar-plates	15 g Bacto-Agar, 1 L LB-medium

Buffers and solutions for biochemical methods

SDS loading buffer Laemmli (4X), pH 6.8	250 mM Tris-HCl, pH 7.5, 34 % (w/v) Glycerol, 8,2 % (w/v) SDS, 0,008 % bromphenol blue, 5 % β-mercaptoethanol
SDS running buffer (10X)	250 mM Tris, 192 mM Glycine, 10 % SDS
Transfer buffer (10X), pH 8.3	250 mM Tris, 192 mM Glycine, 20 % Methanol
PBS (10X)	1.37 M NaCl, 27 mM KCl, 100 mM Na_2HPO_4, 18 mM KH_2PO_4
Wash buffer PBS-T (1X)	1X PBS, 0.1 % Tween 20
Coomassie staining solution (aqueous)	0.25 g Coomassie Brilliant Blue (0.1%), 40 % ethanol, 10 % acetic acid
Coomassie destaining solution	40 % ethanol, 10 % acetic acid
Ponceau S solution	0.1 % (w/v) Ponceau S, 5 % acetic acid
Blocking solution	5 % milk in 1X PBS/T (0.1 %)
Antibody dilution	1 % milk in 1X PBS/T (0.1 %)
Paro Fix (ChIP)	50 mM Hepes/NaOH pH 8.0, 1 mM EDTA, 0.5 mM EGTA, 100 mM NaCl, 11 % Formaldehyde
Paro Rinse 1 (ChIP)	10mM Tris pH 8.0, 10 mM EDTA pH 8.0, 0.5 mM EGTA, 0.25 % Triton X-100
Paro Rinse 2 (ChIP)	10 mM Tris pH 8.0, 1 mM EDTA, 0.5 mM EGTA, 100 mM NaCl
Lysis buffer (ChIP)	50 mM Hepes/KOH pH 7.5, 500 mM NaCl, 1 mM EDTA, 1 % Triton X-100, 0.1 % DOC, 0.1 % SDS, Add fresh protease inhibitor cocktail (1X)
DOC buffer (ChIP)	10 mM Tris pH 8.0, 0.25 M LiCl, 0.5 % NP-40, 0.5 % DOC, 1 mM EDTA
Elution buffer (ChIP)	1 % SDS, 0.1 M $NaHCO_3$
TE buffer	10 mM Tris, pH 8.0, 1 mM EDTA

Buffers and solutions for cell biology methods

FACS buffer	1X PBS, 5 % FCS, 5 mM EDTA
7-AAD staining solution	1X PBS, 100 µg/mL RNase A, 25 µg/mL 7-AAD, 0.1 % Triton-X
10X Annexin V binding buffer	0.1 M Hepes/NaOH (pH 7.4), 1.4 M NaCl, 25 mM $CaCl_2$
Annexin V / 7-AAD staining solution	100 µL 1X Annexin V binding buffer diluted in H_2O, 5 µL 7-AAD, 5 µL Annexin V
Fixation-staining solution for colony forming assay	10 % EtOH, crystal violet 0.5 % (w/v)

Fixation-staining solution for adhesion assay	10 % EtOH, crystal violet 0.2 % (w/v)
CyQUANT® GR dye/cell-lysis buffer for proliferation assay	1 mL cell lysis buffer (20X), 19 mL nuclease-free water, 50 µL CyQUANT® GR dye (400X)
Luciferase Assay Reagent II (LAR II) for Dual-Luciferase Reporter assay	1 mL LAR II, 1 mL dd H_2O
Stop & Glo Reagent for Dual Luciferase Reporter assay	1 mL Stop & Glo buffer, 1 mL dd H_2O, 20 µL Stop & Glo Substrate

2.5.8 Consumables

15 and 50 ml PP tubes	Greiner
24-well plates	Costar
6-well plates	BD Biosciences
8-strip PCR tubes, 0.2 mL	Molecular Bio Products
96-well plates F-bottom	Costar
96-well plates F-bottom, white / black	Thermo Scientific
BD Falcon round bottom tubes, 14 mL	BD Biosciences
Cell scrapers	BD Biosciences
Cell strainer, 40 µm, Nylon	BD Biosciences
Cryo tubes, 2 mL	Greiner
Eppendorf tubes, 0,5 / 1,5 / 2 mL	Eppendorf
Filter tips 1-10 µL	Eppendorf
Filter tips, 100-1250 µL / 3-300 µL /1-100 µL	Sarstedt
Microtiterplates Immuno Plate Maxisorp Surface (96-well)	Nunc
Sterican needle (size 1 and 18)	B. Braun
Nitrocellulose membrane 0.2 µm	GE Healthcare
Pasteur pipettes	Roth
Poly-L-Lysin coated 96-well plates	Greiner
RNase-free tubes 0,5 mL	Molecular Bio Products
RNase-free tubes 1,5 / 2 mL	Eppendorf
Round bottom 5 mL FACS tubes	BD Biosciences
Serological Pipette, 5 / 10 / 25 / 50 mL	Greiner
Surgical disposable scalpels	B. Braun
BD Discardit II Syringes, 2 / 5 / 10 mL	BD Biosciences
Injekt-F 1 mL Syringe	B. Braun
Tips	Sarstedt
Tissue culture dishes, 10 cm^2	Greiner
Tissue culture flasks, T25 / T75 / T175	Greiner
Vitronectin-coated 96-well plates	R&D Systems
Whatman Paper	GE Healthcare
Etched grid cover slips (23x23mm)	Bellco Glass

2.6 Devices

Abiprism Taqman 7300 Real Time PCR	Applied Biosystems
Agarose gel electrophoresis cells	BioRad
Bag sealer	Futura Jr
BioMark™ HD Real Time PCR	Fluidigm
Cell culture incubator	Binder
Centrifuge Heraeus Multifuge X3R	Thermo Scientific
Centrifuges bench top, Heraeus Pico and Fresco 21	Thermo Scientific
Clean bench Golden Line	Kojair

Electrophoresis power supply	Invitrogen
FACS Canto II and FACS Aria	BD Biosciences
Fluorescence plate reader Wallac Victor^2	Perkin Elmer
Gel documentation system Gel Jet Imager	Intas
HiSeq (Next Generation Sequencer)	Illumina
IFX Controller HX	Fluidigm
ImageQuant LAS 4000 Chemiluminescence detection	GE Healthcare
Inverse fluorescence microscope eclipse T*i*	Nikon
Inverse microscope eclipse TS100	Nikon
Magnetic stirrer	IKA
Microbiological incubator	VWR
Overhead shaker (wheel)	Kisker Biotech GmbH
Plate reader infinite M200	Tecan
QIAcube	Qiagen
QIAxcel capillary electrophoresis	Qiagen
Roller mixer SRT6	Stuart
Semi dry blotting apparatus	BioRad
Shaker Infors HT	Infors AG
Sonicator Bioruptor Plus	Diagenode
Spectrophotometer Nanodrop 2000	Thermo Scientific
ST5 Cat rocking shaker	NeoLab
Thermocycler T3	Biometra
Thermomixer compact / comfort	Eppendorf
Tissue Lyser II	Qiagen
Vortex2 genie	Scientific industries
Water bath	GFL
X-cell SureLock™ Mini Cell Electrophoresis	Invitrogen

3 Methods

3.1 Molecular biology methods

3.1.1 Purification of genomic DNA from cell lines and tissues

Genomic DNA (gDNA) was purified from cell lines and tissues with the silica-membrane-based QIAamp DNA Mini Kit (Qiagen) according to the manufacturer's instructions. Up to 5 x 10^6 cells grown in 6-well plates were lysed enzymatically with a chaotropic salt-containing buffer for 10 min at 56°C. Proteinase K was added to the cellular lysate for inactivation of nucleases and digestion of proteins. For fresh frozen tissues, up to 25 mg of tissue were homogenized using a TissueRuptor (Qiagen) prior lysis and incubated at 56°C until tissues were completely lysed. 96 % EtOH was added to the lysate prior loading to the QIAamp Mini spin-columns to provide appropriate binding conditions. To get rid of protein and other contaminants, two washing steps were performed with provided wash buffers. gDNA was eluted in 200 µL nuclease-free water and stored at -20°C. gDNA concentration and purity was determined by spectrophotometric measurement (Nanodrop 2000, Thermo Scientific).

3.1.2 Purification of total RNA from cell lines and tissues

Isolation of total RNA from cell lines and tissues was done with RNeasy Mini Kit (Qiagen) according to the manufacturer's instructions and automated on QIAcube. Briefly, up to 1x10^7 cells grown in a 6-well plate were lysed and homogenized using the provided highly denaturating guanidine-thiocyanate-containing buffer to inactivate RNases ensuring isolation of intact RNA. Up to 30 mg of fresh frozen tissue samples were homogenized using a TissueRuptor (Qiagen) and lysed. Prior to adding the samples to the RNeasy Mini spin-columns with silica-based membranes, 70 % EtOH was added to provide appropriate binding conditions of the RNA to the silica-membrane. Several washing steps provide efficient eradication of contaminants. Finally, the RNA was eluted in 30 µL RNase-free water and subsequently used for cDNA synthesis. RNA concentration and purity was analyzed using a Nanodrop 2000 photometer. For long term storage, RNA was preserved at -80°C.

3.1.3 First strand cDNA synthesis

2 µg total RNA was converted to cDNA using SuperScript™ II Reverse Transcriptase (Life Technologies) which is an engineered version of the Moloney Murine Leukemia Virus Reverse Transcriptase (MMLV-RT). The reaction mix containing 2 µg RNA, 1 µL of dT18 or dT18-tag primer (50 µM) and 1 µL dNTP mix (10 mM of each) was incubated at 70°C for 3 min, cooled down to 42°C and kept on ice. 4 µL 5X First strand buffer, 2 µL DTT (0.1 M), 3 µL RNase-free water and 1 µL SuperScript™ II Reverse Transcriptase (200 units) were added to a final reaction volume of 20 µL and incubated for 1 h at 42°C. The reaction was inactivated by heating at 70°C for 15 min. The obtained cDNA was diluted 1:10 to a final volume of 200 µL for subsequent quantitative real-time RT-PCR analysis (qRT-PCR).

3.1.4 Polymerase chain reaction

Polymerase chain reaction (PCR) is a method to amplify a specific region of DNA across several orders of magnitude. In this study different PCR methods were used depending on the question.

3.1.4.1 **Standard end-point PCR**

50-100 ng gDNA or 2.5 µL of cDNA (1:10 dilution from 3.1.3) were used as templates for standard end-point PCR. 1 µL of sense and antisense primer (10 µM), 3 µL 10x PCR buffer (Qiagen), 0.5 µL dNTP-mix (10 mM), 0.2 µL HotStar *Taq* (*Thermus aquaticus*) DNA polymerase (250 units) (Qiagen) and 22.8 µL nuclease-free water were mixed. Reactions were performed in a 25-35 cycles PCR, the annealing temperature varied depending on the used primers.

Themal Cycler profile for standard end-point PCR:

Initial activation step:	95 °C	15 min
3-step cycling (25 to 35 cycles):		
Denaturation:	94 °C	30 sec
Annealing:	56-64 °C	30 sec
Extension:	72 °C	1 min per kb DNA
Final extension:	72 °C	10 min

To obtain PCR product with a very low error-rate usable for cloning, PCR was perfomed using the *Pyrococcus*-like proofreading enzyme Phusion Hot Start II High Fidelity DNA Polymerase (Thermo Scientific). 100 ng genomic DNA or plasmid DNA were used as template and mixed with 1 µL dNTP-mix (10 mM), 10 µL 5X Phusion HF buffer, 1.5 µL of sense and antisense primer (10 µM), 0.5 µl Phusion Hot Start II DNA Polymerase (2 U/µL) and 34.5 µL nuclease-free water. Reactions were performed in a 30 cycles PCR, the annealing temperature varied depending on the used primers.

Themal Cycler profile for Phusion PCR:

Initial activation step:	98 °C	30 sec
3-step cycling (30 cycles):		
Denaturation:	98 °C	10 sec
Annealing:	56-64 °C	30 sec
Extension:	72 °C	30 sec per kb DNA
Final extension:	72 °C	10 min

3.1.4.2 Quantitative real-time RT-PCR

3.1.4.2.1 SYBR green

Quantitative real-time RT-PCR (qRT-PCR) was performed using the ABI PRISM 7300 sequence detection system and software (Applied Biosystems with QuantiTect SYBR green Kit (Qiagen)). SYBR green binds to dsDNA of PCR products and emits green fluorescence upon excitation. The intensity of fluorescence increases during amplification, fluorescence is measured after each cycle. 5 µL cDNA from 3.1.3 was mixed with 1 µL of sense and antisense primer (10 µM) respectively, 8 µl RNase-free water and 15 µl of SYBR green PCR mix. Reactions were performed in duplicates in a 40 cycle PCR. Annealing temperatures varied between 58°C and 62°C depending on primers used.

Thermal Cycler Profile qPCR

Stage	Repetitions	Temperature	Time (MM:SS)
1	1	95 °C	15:00
2	40	95 °C	00:30
		58 - 62 °C	00:30
		72 °C	00:30
3 (Dissociation)	1	95 °C	00:15
		60 °C	01:00

95 °C 00:15

Relative quantification by the $2^{-\Delta\Delta Ct}$ method was used to determine gene expression levels (mRNA). C_t (threshold cycle) indicates cycle number at which the amount of amplified target reaches a fixed threshold. C_t of target gene is normalized to C_t of a reference gene, in this study *Hypoxanthin-Phosphoribosyl-Transferase 1* (*HPRT1*) was used, which is measured in the same sample (ΔC_t value). As calibrator, untreated cells or an internal calibrator (40 – average of *HPRT1* Ct values of all samples) were used ($\Delta\Delta C_t$ value). It is assumed that primer efficiency is close to one, therefore the amount of target is given by $2^{-\Delta\Delta Ct}$ which indicates fold change in gene expression in treated sample compared to untreated control, which is 1.

3.1.4.2.2 qRT-PCR using TaqMan® gene expression assays

For a larger cohort of samples, qRT-PCR analysis was performed with TaqMan® gene expression assays (Life technologies) using a Fluidigm BioMark™ HD (Fluidigm). To exclude that the TaqMan® probes bind gDNA, cDNA was synthesized using PrimeScript RT Reagent Kit with gDNA Eraser (Takara Bio Inc.) according to the manufacturer's instructions. Samples were prepared and analyzed according to the Fluidigm® Advanced Development Protocol 28 - Fast Gene Expression Analysis using TaqMan® GE Assays rev A2. Loading onto 96.96 Gene Expression Dynamic Array IFCs was accomplished by the IFC Controller HX. Chip arrays were analyzed via a Fluidigm BioMark HD system. Data sets were evaluated according to the $2^{-\Delta\Delta Ct}$ -method.

3.1.4.3 Methylation-specific quantitative real-time PCR

Methylation-specific quantitative real-time PCR (MsqPCR) was performed using the ABI PRISM 7300 sequence detection system and software (Applied Biosystems with QuantiTect SYBR green Kit (Qiagen)) to detect DNA methylation in tumor cell lines, normal and tumor tissues. Different oligonucleotides specific for methylated or unmethylated DNA covering 3-5 CpGs (10 µM) were mixed with 50 ng bisulfite converted DNA, 15 µL SYBR green PCR mix and 8 µL nuclease-free water. The reactions were performed in duplicates in a 40 cycles PCR.

Thermal Cycler Profile MSq-PCR

Stage	Repetitions	Temperature	Time (MM:SS)
1	1	95 °C	15:00
2	40	95 °C	00:30
		56 - 62 °C	00:30
3 (Dissociation)	1	95 °C	00:15
		60 °C	01:00
		95 °C	00:15
		60 °C	00:15

3.1.5 Bisulfite sequencing

Bisulfite sequencing is a method to determine cytosine methylation at sequence levels. EpiTect Kit (Qiagen) was used for bisulfite treatment of gDNA to ssDNA. For bisulfite reactions, 2 µg gDNA in a volume of 20 µL was mixed with 85 µL Bisulfite Mix and 35 µL DNA Protect Buffer. Conversion of gDNA to ssDNA was performed in a thermal cycler using the following program:

Denaturation	5 min	95 °C
Incubation	25 min	60 °C
Denaturation	5 min	95 °C
Incubation	85 min	60 °C
Denaturation	5 min	95 °C
Incubation	175 min	60 °C
Hold	indefinite	20 °C

High bisulfite salt conditions, high temperature and low pH result in a complete conversion of unmethylated cytosines. The DNA Protect Buffer provides effective DNA denaturation and prevents fragmentation of DNA at these high temperatures and low pH. Resulting bisulfite converted ssDNA was purified using a spin-protocol, washed with optimized buffers to remove bisulfite salts and chemicals which could inhibit the sequencing procedures. All centrifugation steps were carried out at 13000 rpm, 1 min, RT. Purified ssDNA was eluted in 20 µL nuclease-free water by centrifugation for 1 min at 12000 rpm and subsequently stored at -20°C. ssDNA was amplified by PCR using primers specific for bisulfite converted DNA (listed at 7.3.2). PCR products were cloned into a TA-vector for subsequent Sanger Sequencing (MWG Eurofins Operon).

3.1.6 Next generation sequencing (NGS)

For NGS analysis, PCR products with different barcodes were purified using the QIAquick MinElute PCR Purification Kit (Qiagen) according to the manufacturer's instructions and DNA concentration was measured using a Qubit spectrophotometer (Invitrogen). All fragments from one sample were pooled to a concentration of 1 µg in 26 µL. DNA was phosphorylated using 2 µL T4 Polynucleotide Kinase (10 U), 4 µL 10X Phosphorylation buffer, 4 µL ATP (10 mM) and 4 µL nuclease-free water for 20 min at 37°C following 10 min at 75°C. Afterwards, the reaction was purified again. For PE-adapter ligation purified DNA was incubated with 1 µL of PE-adapters mix for 10 min at 30°C. Then, ligation was stopped and purified using magnetic Agencourt AMPure Beads and eluted in 20 µL of nuclease-free water. To ensure that fragments between 200 and 250 bp were used only, a size selection using a 2 % E-Gel-System (Invitrogen) was performed. Size selected DNA fragments were enriched by PCR. 40 µL DNA was mixed with 20 µL 5X Phusion HF buffer, 2 µL PE-primer 1 and 2 (25 µM each), 3 µL dNTP-Mix, 32 µL nuclease-free water and 1 µL Phusion DNA Polymerase. A 12 cycle PCR was performed at 65°C annealing temperature for 30 sec. PCR products were purified with magnetic beads again and eluted in 30 µL of nuclease-free water. Finally, DNA concentration and purity was analyzed using a BioAnalyzer.

3.1.7 Agarose gel electrophoresis

Agarose gel electrophoresis is a method to analyze, quantify and purify nucleid acids. An electric field is used to separate the nucleic acid molecules by their length. Negatively charged nucleic acid molecules migrate through the agarose matrix to the positively charged anode, whereas larger fragments migrate slower through the gel pores. Depending on fragment size, 1 % or 2 % (w/v) agarose was dissolved in 1X TAE buffer and 0.005 % Ethidium bromide was added to visualize DNA on the gel. Samples were diluted in 6X loading dye (Fermentas) and applied to the gel. Gels were run at 100 V (preparative gels) or 130 V (analytical gels) and analyzed by exposure to UV light (254 nm for analytical gels, 366 nm for preparative gels).

3.1.8 Purification of nucleic acids after gel electrophoresis

PCR products or DNA fragments were excised from agarose gels after electrophoresis and purified using the QIAqick Gel Extraction Kit (Qiagen) according to manufacturer's protocol. Agarose was solubilized by incubation at 56°C for 10 min in an appropriate buffer and DNA was selectively bound to a silica-membrane. Isopropanol was added to the dissolved gel and applied onto the spin-column. Washing steps were performed to remove agarose contaminant, ethidium bromide and salts. Purified DNA was eluted in 30-50 µL nuclease-free water. To purify enzymatically modified or amplified DNA fragments after PCR, QIAquick PCR purification Kit (Qiagen) or for purification of fragments < 100 bp MinElute PCR purification kit (Qiagen) was used according to the manufacturer's protocol.

3.1.9 Restriction endonuclease digest

Plasmid DNA or PCR products were double digested with 3-5 U / µg DNA of appropriate restriction endonucleases using recommended buffers at specified conditions in a total volume of 50-80 µL. Digestion of PCR products was performed ON at 37°C and subsequently purified using QIAquick PCR purification Kit (Qiagen) and analyzed by gel electrophoresis. For double digestion of vector backbones, digestion with the first restriction endonuclease was incubated for ~ 9 h and then purified using QIAquick PCR purification Kit (Qiagen). The second restriction endonuclease was added and incubated ON at 37°C and subsequently gel purified and analyzed by gel electrophoresis.

3.1.10 Ligation of DNA fragments

Ligation of linearized vector with insert (PCR product or restriction endonuclease digest) was prepared with 20-100 ng plasmid DNA and 3- to 5-fold excess of insert. Reaction was performed using 1 µL T4-DNA Ligase (10 U/µL) (Fermentas) and 2 µL 10X T4-DNA Ligase Buffer (Fermentas) in a final volume of 20 µL and incubated at RT for 3 h.

3.1.11 Transformation of chemically competent *E.coli* cells

Chemically competent One Shot® TOP10 *E.coli* cells (life technologies) were thawed on ice, mixed with 1 - 100 ng of plasmid DNA and kept on ice for 30 min. Cells were transformed by heat-shock for 30 s at 42°C in a water bath and chilled for 2 min on ice. 250 µL pre-warmed SOC medium was added and cells were incubated at 37°C under vigorous shaking for 1 h. To propagate transformed cells, up to 250 µL of the bacterial suspension was plated on LB-agar plates containing 100 mg/mL ampicillin or 25 µg/mL kanamycin, depending on antibiotic resistance gene of the used plasmid and incubated ON at 37°C.

3.1.12 Purification of plasmid DNA from bacterial cultures

Isolation of plasmid DNA was performed with Nucleo Spin Plasmid DNA Purification Kit (Macherey-Nagel) according to the manufacturer's instructions. 4 mL LB-medium containing the appropriate antibiotics were inoculated with a single colony picked from the LB-agar-plate and grown ON at 37°C on an orbital shaker. Prior to purification of the plasmid DNA, colony PCRs with appropriate primers were performed to control for presence of desired inserts. Cultures were harvested by centrifugation for 30 sec at 11000 x g. Optimal cell lysis was achieved by addition of the appropriate buffers provided in the kit, which lead to release of the plasmid DNA from the *E.coli* host cells and neutralization of the lysate. Precipitated protein, genomic DNA and cell debris were pelleted by centrifugation for 10 min at 11000 x g and clear supernatant with solved plasmid DNA was loaded onto the spin-columns. Two washing steps were performed to remove contaminants and plasmid DNA was eluted in 50 µL of nuclease-free water by centrifugation for 1 min at 11000 x g. Purified plasmid DNA was stored at -20 °C. For long-term storage, cell suspensions were stored at -80 °C in 50 % glycerol.

For purification of endotoxin-free, transfection-grade plasmid DNA, EndoFree Plasmid Maxi Kit (Qiagen) was used according to manufacturer's protocol. Endotoxins or Lipopolysaccharids (LPS) are cell-membrane components of Gram-negative bacteria which can highly reduce transfection efficiencies of DNA into cells. Using standard plasmid DNA purification, often endotoxins are not removed properly. Endotoxin-removal was ensured by incubation with a specific entotoxin-removal buffer provided in the kit. This buffer prevents binding of LPS molecules

from binding to the resin in the Qiagen-tips. Plasmid DNA was eluted in 400 µL of endotoxin-free water and subsequently stored at -20 °C. The DNA concentration and purity was measured using the NanoDrop 2000 spectrometer (Thermo Scientific).

3.2 Cell biology methods

3.2.1 Propagation of cell lines

All cell lines used in this study were cultured in specified medium containing 0.5 % penicillin/streptomycin (for respective medium formation, refer to 2.1) in an incubator at 37°C, 95 % humidity and 5 % CO_2. Adherent cells were split upon 80 to 95 % confluence with TrypLE express (or Accutase for flow cytometry) and transferred into a fresh culture flask. Medium was changed every 2 to 3 days. To determine cell numbers and viability, cells were diluted 1:2 in Trypan Blue (0.1 %) and counted using a standard Neubauer chamber. Trypan Blue stains only dead cells because it cannot pass the intact cell membrane of living cells. Therefore, dead cells appear blue and can be distinguished from living cells.

3.2.2 Treatment of cells with different fine chemicals

Prior to estradiol-treatment studies, MCF-7 cells were cultured in phenol-red free DMEM supplemented with 10% charcoal stripped FCS for 72 h. Cells were treated with 100 nM 17-β-estradiol (E_2) and/or with 5 µM of the complete estrogen receptor blocker ICI 182,780 (ICI) for 12 h.

For analysis of DNA-methylation, SK-BR-3, DAN-G, PA-1 and NIH-OVCAR3 cells were treated with 2 µM or 10 µM 5-aza-2'-deoxycytidine (5-aza-dC) diluted in respective culture medium for 72 h.

3.2.3 Freezing/thawing of cell lines

For cryopreservation, cells were harvested, counted and centrifuged (311 x g, 4°C, 5 min). 2-5 x 10^6 cells were resuspended in freezing medium (90 % FCS, 10 % DMSO) and stored ON at -80°C in liquid isopropanol before long term storage at -196 °C in liquid nitrogen.

Cells were thawed in a 37°C water bath. Cell suspension was collected in 9 mL prewarmed culture medium and centrifuged immediately at 311 g for 5 min. Cell pellet was resuspended in fresh medium and cells were maintained at 37°C, 95 % humidity and 5 % CO_2.

3.2.4 Transfection of cells with siRNA

Prior to several functional assays, the cells were transfected with different siRNAs (refer to chapter 7.2) to generate a transient knockdown of different genes. siRNAs and transfection medium was diluted in serum-free medium prior to adding the transfection complexes onto the cells.

24 h prior transfection, the indicated cell numbers (refer to Table 7) were seeded in antibiotic-free culture medium and incubated at 37°C, 5 % CO_2 ON. Before addition of the transfection complexes, culture medium was changed. Cells were harvested at different time points as indicated.

Table 7 Conditions for transfection of siRNA in 6-well format

Cell line and used cell number / 6-well	Concentration of siRNA (nM)	Volume of transfection reagent	Incubation time
3 x 10^5 MCF-7	5 nM diluted in 100 µL serum-free (sf) medium	12 µl HiPerFect (Qiagen) diluted in 100 µL sf medium	10 min, RT
5 x 10^5 SK-BR-3	80 nM diluted in 200 µl sf medium	4 µl DharmaFect (Dharmacon) diluted in 200 µl sf medium	5 min, RT, then mix both tubes, 20 min, RT
3 x 10^5 PA-1	5 nM diluted in 100 µL sf medium	12 µl HiPerFect (Qiagen) diluted in 100 µL sf medium	10 min, RT
5 x 10^5 NIH-OVCAR3	5 nM diluted in 100 µL sf medium	12 µl HiPerFect (Qiagen) diluted in 100 µL sf medium	10 min, RT
8 x 10^5 NEC-8	10 nM diluted in 250 µL sf medium	5 µL Lipofectamine RNAiMAX (life technologies) diluted in 250 µL sf medium	20 min, RT
3 x 10^5 DAN-G	5 nM diluted in 100 µL sf medium	12 µl HiPerFect (Qiagen) diluted in 100 µL sf medium	10 min, RT

3.2.5 Transfection of cells with plasmid DNA

Transfection of cells with plasmid DNA was performed using Lipofectamine 2000 or Lipofectamine LTX (Life Technologies) according to the manufacturer's protocol. 24 h prior transfection, 1x10^6 cells per well of a 6-well plate or depending on cell line used, 5-8x10^6 cells per 10 cm dish were seeded in antibiotic-free medium and incubated at 37°C, 5 % CO_2 ON. Transfection-sensitive cell lines

were transfected with Lipofectamine LTX that exerts lower toxicity as Lipofectamine 2000. Cells were harvested at different time points as indicated.

Table 8 Conditions for transfections with plasmid DNA

Culture vessel	Volume of plating medium	Volume of dilution medium	DNA	Lipofectamine 2000	Lipofectamine LTX
6-well	2 mL	0,25 mL	4 µg	10 µL	8 µL (4 µL Plus Reagent added to DNA)
10 cm	15 mL	1 mL	20 µg	60 µL	47 µL (20 µL Plus Reagent added to DNA)

3.2.6 Dual-Luciferase reporter assay

For reporter assays, CLDN6 promoter fragments of different lengths were cloned into the promoter less *Renilla* luciferase vector pGL4.76 [*hRluc*/Hygro]. As an internal control, the firefly luciferase vector pGL4.13 [*luc2*/SV40] was used. The activity of the experimental reporter is normalized to the activity of firefly luciferase to compensate experimental variability in transfection efficiency. The ratio of pGL4.76 to pGL4.13 for co-transfection was 50:1. 24 h after transfection, cells were rinsed in 1X PBS, lysed in 1X passive lysis buffer (PLB) buffer and stored at -20 °C until measurement. First, the luminescent signal from firefly luciferase was measured by adding 50 µL Luciferase Assay Reagent II to 30 µL lysate. The firefly luciferase luminescence was quenched by adding 50 µL of Stop & Glo Reagent to the lysate and the *Renilla* luciferase luminescence can be measured immediately.

3.2.7 Proliferation assay

To analyze the proliferation of tumor cells after knockdown of CLDN6, the fluorescent-based CYQUANT® GR cell proliferation assay kit (Molecular Probes, life technologies) was used. As phenol-red may interfere with fluorescence of CyQUANT® GR dye, all steps were performed with phenol-red free culture media.

PA-1, NIH-OVCAR3 and NEC-8 cells were transfected with siRNA according to 3.2.4. 24 h after transfection, cells were detached with TrypLE express, counted and centrifuged. 5000 cells per well were seeded in 96-well microplates and proliferation of cells was assayed 24 h / 48 h / 96 h after reseeding. At the desired time points, cells were washed very carefully with 1X PBS and microplates were freezed at -80°C ON. The freezing step is important to assure efficient cellular lysis. The plates were thawed at RT and 200 µL of freshly prepared CyQUANT®

GR dye/cell-lysis buffer mixture was added to each sample well and incubated for 5 min at RT. Fluorescence was measured using the fluorescence microplate reader Victor^2 (Wallac Coulter) with filters appropriate for ~480 nm excitation and ~520 nm emission maxima.

3.2.8 Wound healing assay

For analysis of wound healing, etched grid cover slips, 23x23mm (Bellco Glass) were added to sample wells of a 6-well plate. Cover slips were washed twice with 1X PBS and coated with collagen R (20 mg/mL in 1X PBS) for 30 min at 37°C to assure that cells can adhere to the glass surface. Wells were washed with 1X PBS and 6 x 10^5 PA-1 cells were added per well and allowed to adhere ON at 37°C, 5 % CO_2. 24 h after seeding, PA-1 cells were transfected with *CLDN6*-siRNA or *non-silencing*-siRNA according to 3.2.4. Cells were grown to monolayers of 100 % confluence in complete culture medium for 48 h. 12 h prior wounding, cells were serum starved in starvation medium (MEM, 1% FCS) to induce higher migration of cells after wounding. Confluent monolayers were wounded using a disposable 200 µL pipette tip and washed twice with complete growth medium to remove floating cells. Wound closure was analyzed at different time points (0, 4, 8, 12 and 24 h) and pictures were taken at 10 different fields per samples with a microscope. Wound closure was analyzed with Image J using the polygon selection tool to analyze cell-free area between both cell boundaries. Cell-free area at time point 0 h was taken as 0 % wound healing and percentages of wound healing at different time points were calculated with regard to measured cell-free area at 0 h.

3.2.9 Adhesion assay

3.2.9.1 Cell-cell adhesion assay

Adhesion of tumor cells to a confluent cell monolayer of the same or other origin was analyzed using the cell-cell adhesion assay. PA-1, NIH-OVCAR3 and DAN-G cells were transfected with *CLDN6*-siRNA or *non-silencing*-siRNA according to 3.2.4. 72 h after transfection, cells were harvested with Accutase, counted and adjusted to 5 x 10^5 cells / mL in complete growth medium. Cells were allowed to recover from harvesting for 30 min at 37°C, 5 % CO_2. After recovery, cells were washed once with 1X PBS and resuspended in serum-free culture medium and

stained with 1 µM Calcein AM in serum-free culture medium for 30 min at 37°C. Cells were washed once with 1X PBS to remove excessive Calcein AM and resuspended in serum-free culture medium. 24 h prior the start of the assay, $5x10^4$ PA-1 or NIH-OVCAR3 cells were seeded in sample wells of a 96-well microplate to ensure that cells are grown to 100 % confluence. The monolayers in the 96-well plate were washed once with 1X PBS and 100 µL of siRNA-treated PA-1 / NIH-OVCAR3 / DAN-G cell suspensions were added. Six replicates per sample were performed. Cells were allowed to adhere for 1.5 to 3 h at 37°C, 5 % CO_2. Non-adherent cells were removed by washing cells twice with 1X PBS. Fluorescence of adherent cells was measured using a Victor^2 microplate reader (Wallac coulter) with filters appropriate for ~480 nm excitation and ~520 nm emission maxima. To calculate the percentage of adherent cells with regard to the starting population ($5x10^4$ cells), fluorescence measurement of 5 x 10^4 cells of each cell line was included. Furthermore, wells with 1X PBS only and unstained cells were included as background controls.

3.2.9.2 **Cell-matrix adhesion assay**

This assay was performed to analyze efficiency of tumor cells to adhere to the extracellular matrix molecules vitronectin, laminin-111 and poly-L-lysine. 96-well microplates with maxisorp surface were coated ON at 4°C with 60 µL laminin-111 (30 mg/mL in 1X PBS). Laminin-111 solution was aspirated and wells were washed with 1X PBS. Laminin-111 and poly-L-lysine coated plates (Greiner) were blocked with 1 % BSA (Sigma Aldrich) for 30 min at RT to avoid unspecific binding. Wells were washed with 1X PBS and pre-warmed culture medium was added until cells were ready for seeding. Vitronection-coated plates (R&D) were ready-to-use.

PA-1, NIH-OVCAR3 and DAN-G cells were transfected with *CLDN6*-siRNA or *non-silencing*-siRNA according to 3.2.4. 72 h after transfection, cells were harvested with Accutase, counted and adjusted to $5x10^5$ cells / mL in complete growth medium. Cells were allowed to recover from harvesting for 30 min at 37°C, 5 % CO_2. After recovery, cells were washed once with 1X PBS, resuspended in serum-free culture medium and 100 µL of siRNA-treated PA-1 / NIH-OVCAR3 / DAN-G cell suspensions were added to the sample wells of 96-well microplates coated with different matrix compounds. Cells were allowed to adhere for 1.5-3 h at 37°C,

5% CO_2. Non-adherent cells were removed by washing cells twice with 1X PBS and 150 µL fixation-staining solution (0.2 % crystal violet in 10 % EtOH) was added per sample well and incubated at RT for 30 min. Wells were washed with dH_2O to remove excessive stain and fixed cells were allowed to dry ON. 100 µL 10 % acetic acid was added per well and incubated for 20 min at RT with shaking. Solution was resuspended and absorbance was measured at 595 nm using a microplate reader infinite M200 (Tecan).

3.2.10 Colony formation assay

The colony formation assay is used to analyze the ability of a single cell to grow into a colony. 500-700 CLDN6+ and CLDN6- PA-1 cells were sorted using a FACSAria cell sorter (BD) directly into 6-well plates containing complete growth medium. The cells were incubates for 10 days at 37°C, 5% CO2 and medium was changed every 3-4 days. At day 10, cells were washed with 1X PBS and subsequently fixed and stained by adding 1 mL of 0.5 % crystal violet in 10 % EtOH for 30 min at RT. Wells were washed with water to remove excessive dye and allowed to dry ON. Pictures were taken and colonies were counted manually. At least 50 cells were considered to be a colony.

3.3 Flow cytometry

Flow cytometry is a laser based method for cell counting, cell sorting and detection of biomarkers. Flow cytometry was performed using a FACS Canto II (BD) with Diva software and data was analyzed using Flow Jo software.

3.3.1 Staining of cell surface proteins

Cells were harvested with Accutase to reduce damage of cell-surface proteins and counted. $1x10^6$ cells per tube were centrifuged (460 x g, 5 min, 4°C), washed in FACS-buffer and stained with appropriate antibody concentrations diluted in 100 µL FACS-buffer 30 min at 4°C in the dark. Cells were washed twice prior measurement. To determine cell viability, 7-Amino-Actinomycin (7-AAD) staining was included. Therefore, cells were incubated for 15 min at RT with diluted 7-AAD (5 µL 7-AAD in 100 µL FACS buffer per test). Cell were washed once and resuspended in 150 µL FACS-buffer for measurement.

3.3.2 Cell cycle analysis by DNA-content

Cell cycle analysis was performed using 7-AAD. 7-AAD intercalates in dsDNA and undergoes a spectral shift upon DNA binding. Cells have to be permeabilized and fixed prior to 7-AAD staining. 72 h after siRNA-treatment, cells were harvested with Accutase and counted. $1x10^6$ cells per tube were centrifuged (460 x g, 5 min, 4°C), resuspended in 400 µL ice-cold 1X PBS and chilled on ice. 3.6 mL ice-cold 70 % EtOH was added to a new tube and cell suspension was added drop-wise onto the EtOH while vortexing. Cells were fixed ON at 4°C. Fixed cells were centrifuged and resuspended in 5 mL 1X PBS, incubated for 2 min at RT and centrifuged. Cells were resuspended in 300-500 µL 7-AAD staining solution (RNase A (100 µg/mL), 7-AAD (25 µg/mL), 0.1 % Triton-X in 1X PBS) and incubated for 30 min at RT in the dark. RNase A and Triton X are used to get rid of RNA and proteins which could falsify DNA content measurement. Cells were measured using a low flow rate under 400 events/second and linear scale to gain optimal separation of different cell cycle phases.

3.3.3 Apoptosis assay

Apoptosis was analyzed using PE-AnnexinV/7-AAD Apoptosis Detection Kit (BD) according to manufacturer's instructions. 72 h after treatment with siRNA, NIH-OVCAR3 cells were harvested with Accutase and counted. $1x10^6$ cells per tube were centrifuged (460 x g, 5 min, 4 °C) and resuspended in 1 mL pre-warmed complete growth medium and allowed to recover for 30 min at 37°C. Cells were centrifuged and washed twice with cold 1X PBS, resuspended in 100 µL 1X binding buffer with 5 µL PE-Annexin V and 5 µL 7-AAD and incubated for 15 min at RT in the dark. Finally, 200 µL 1X binding buffer were added prior to measurement.

3.4 Biochemical methods

3.4.1 Preparation of whole cell lysates

For preparation of whole cell lysates, 250 µL 4 X Laemmli sample buffer were added to cells grown in a 6-well plate, harvested with a cell scraper and immediately kept on ice. After freezing ON at -80°C, lysates were homogenized

with syringe and needle. For Western blot analyses except detection of CLDN6, cell lysates were boiled to 95 °C for 5 min prior to loading to the gel.

3.4.2 SDS-Polyacrylamide gel electrophoresis

SDS-PAGE (Sodium dodecyl sulfate – polyacrylamide gel electrophoresis) is a standard biochemical method to separate proteins according to their electrophoretic mobility. SDS is an anionic detergent used to denature secondary and tertiary structures of proteins by conferring a negative charge to linearized proteins which is evenly distributed per unit mass of the protein resulting in a separation by size during electrophoresis. Protein denaturation is further supported by usage of reducing agents like β-mercaptoethanol in the sample loading buffer which lead to cleavage of inter- and intramolecular disulfide bonds. In this study, tris-glycine-SDS gels (Anamed Gelelektrophorese) with different concentrations of acrylamide-bisacrylamide in the resolving gel were used depending on molecular weight of separated proteins. The higher the concentration of acrylamide-bisacrylamide, the lower is the gel pore size resulting in separation of smaller proteins. Gels were adjusted in the electrophoresis chamber (Invitrogen) and 5 – 30 µL of whole cell lysates from 3.4.1 were loaded on the gel. Gels were run at 125 V, 60 mA for approximately 90 min.

3.4.3 Western blot

Western blot is a technique for detection of specific proteins in cell or tissue lysates [183,184]. Proteins in whole cell lysates were separated by SDS-PAGE (see 3.4.2) and transferred to nitrocellulose membrane (Whatman) using semi-dry blotting technique. Gels were blotted 90 min with 1.5 A / cm^2 of gel (Semi Dry Blotting apparatus, BioRad). Gels were stained immediately after blotting with Coomassie to analyze transfer efficiency. Unspecific binding sites of the membrane were blocked with 5 % milk powder in PBS/T for 1 h on RT. Immunostaining was performed using mouse or rabbit monoclonal antibodies reactive to several proteins listed in chapter 2.4.1 by incubation ON at 4 °C. Membranes were washed three times in 1 X PBS/T for 10 min. Detection of primary antibodies was performed with horseradish peroxidase-conjugated goat-anti-mouse or goat-anti-rabbit secondary antibodies (Jackson ImmunoReseach Laboratories). Membranes were incubated 1 h on RT with secondary antibodies

and subsequently washed three times prior to detection of chemiluminescence. Detection of housekeeping protein β-actin was used as loading control.

3.4.4 Chromatin Immunoprecipitation

Chromatin immunoprecipitation (ChIP) is a method to study interactions between specific proteins (i.e. transcription factors or histones) and a genomic DNA region. For ChIP analysis, cells were seeded in 10 cm dishes, treated and harvested to time points as indicated in the results part. Cross-linking of the proteins and genomic DNA was performed by addition of 1 % formaldehyde (diluted in Paro Fix) to cells and incubated 10 min at RT. Crosslinking was stopped by addition of 315 µl glycine (2.5 M) and incubation for 10 min at 4°C. For preparation of chromatin, dishes were washed twice with 1X PBS, cells were scraped off in 3 mL 1X PBS and centrifuged at 600 g for 7 min at 4°C. For removal of cytoplasm, pellets were resuspended in 10-30 mL of Paro Rinse 1, incubated 5 min on ice and centrifuged again. Subsequently, a washing step with Paro Rinse 2, incubation for 15 min on ice and centrifugation followed. Pellets were resuspended in 900 µl / plate of lysis buffer and incubated for efficient cell lysis for 3 h on ice. A crucial step in ChIP is shearing of gDNA into fragments of 200 to 700 bp. Here, sonication was performed using a Biorupter Plus sonicator (Diagenode) using 15 cycles with 30 sec ON and 45 sec OFF at high amplitude. This resulted usually in fragments of 250-300 bp. After sonication, samples were centrifuged for 10 min at 14000 g at 4°C to get rid of any cell debris. The chromatin concentration was measured using Hoechst (200 ng/mL) in a fluorometer.

To ensure successful sonication, a chromatin size checkup prior ChIP was performed. 20 µg sonicated chromatin was subjected to RNase A (0.2 mg/mL final concentration) digestion at 37°C for 30 min and proteinase K digestion (200 µg/mL proteinase K, 1 % SDS, 100 mM NaCl) for 2.5 h at 55°C and cross linking was reversed ON at 65°C. DNA was precipitated with EtOH (100 % EtOH, 1/10 volume 3 M NaOAc (pH 5.2), 1 µL glycogen) by centrifugation for 2 h at 14000 x g at 4°C. Pellets were washed with 70 % EtOH, air-dried for 30 min and resuspended in 40 µL TE buffer. 1 µg and 2 µg DNA were loaded on a 1.2 % agarose gel for analysis of fragment sizes.

ChIP was performed with 70 µg chromatin and 5 µg of respective antibodies. Prior to addition of antibody, pre-clearing of chromatin with salmon-sperm saturated protein A or G agarose beads (depending on the antibody subtype used for ChIP) was performed for 1 h at 4°C with overhead shaking. The pre-clearing reduces nonspecific immunoprecipitation by removal of proteins which bind unspecifically to the beads. 1 % of the chromatin after pre-clearing was taken as input for later quantification and stored at -20°C. Pre-cleared chromatin and antibody were incubated for ChIP 16 h at 4°C with overhead shaking. To bind the immunoprecipitated antibody-protein-DNA complexes, salmon-sperm saturated protein A or G agarose beads were added and incubated for 3 h at 4°C with overhead shaking. Washing steps with lysis buffer, DOC buffer and TE buffer were performed to remove non-specifically bound chromatin. Afterwards IP was eluted from beads twice with elution buffer for 20 min at RT with overhead shaking. Next, crosslinking had to be reversed to purify bound DNA fragments. First, IP fraction was incubated with RNase A for 3 min at 37°C followed by proteinase K digestion (50 µg/mL proteinase K, 10 mM EDTA, 40 mM Tris pH 6.5) for 2.5 h at 55°C and reversal of crosslinking ON at 65°C. Reversal of crosslinking of the input was performed as described before for size checkup.

DNA was purified by phenol-chloroform extraction. First, phenol was added, centrifuged at 13000 rpm for 10 min at RT and upper aequeous phase was transferred into a new tube. Second, chloroform/IAA was added, centrifuged and upper aequeous phase was taken again. EtOH precipitation was done as described earlier in this chapter. DNA pellets were resuspended in 40 µL TE buffer.

Purified DNA was analyzed by conventional PCR (only for PLAC1 promoter) and quantitative real time PCR for presence of respective promoter fragments (refer to chapter 7.3.4 for primer list).

3.5 Statistics

Depending on the question, different statistical tests (paired t-test, ANOVA, Spearman or Pearson correlation) were performed. For statistical analysis, Graph Pad Prism Software was used. *P*-values < 0.05 were considered statistically significant.

4 Results

In the presented work, two different candidate tumor antigens, PLAC1 and CLDN6, were characterized. Therefore, part I deals with the analysis of the regulation of *PLAC1* whereas part II concentrates on the analysis of regulation and function of CLDN6 in cancer.

4.1 Analysis of the Estradiol (E_2)-dependent regulation of *PLAC1* in breast cancer

In the first part of this study, the transcriptional regulation of *PLAC1* is examined in further detail. As described in the introduction of this thesis (refer to chapter 1.3.1), a large part of the transcriptional complex at the *PLAC1* promoter was recently elucidated by our group [83]. However, the complete transcriptional complex is not clarified up to now. The aim of this study was to shed further light on the E_2-dependent activation of *PLAC1* in breast cancer cells. This was analyzed using two different PLAC1-expressing breast cancer cell lines: ERα-positive MCF-7 and ERα-negative SK-BR-3 cells. The results of this chapter have been published in [185].

4.1.1 Expression of p160/NCOA family and PLAC1 in breast cancer cell lines

The p160/NCOA family of co-activators has a prominent role in nuclear receptor mediated activation of gene expression especially in hormone-related cancers [101]. To study the regulation of *PLAC1* with regard to E_2-mediated signaling in breast cancer, two different breast cancer cell lines were chosen: the ERα-positive MCF-7 and ERα-negative SK-BR-3 breast cancer cells. MCF-7 cells have been shown to up-regulate PLAC1 upon treatment with E_2 [83]. SK-BR-3 cells are not E_2-responsive because these cells lack expression of ER [186]. First, the expression of NCOA1, NCOA2 and NCOA3 as well as PLAC1 in both cell lines was analyzed on transcript level by quantitative real-time RT-PCR (qRT-PCR) and on protein level by Western blot analysis in MCF-7 and SK-BR-3 cells (Figure 8 A, B). Both cell lines express all three co-activators and PLAC1 while slightly different

expression levels are detected: NCOA3 is higher expressed in MCF-7 cells compared to NCOA1 and NCOA2, whereas in SK-BR-3 cells expression of NCOA3 was reduced compared to the other family members. Interestingly, PLAC1 expression is higher in SK-BR-3 cells compared to MCF-7 cells.

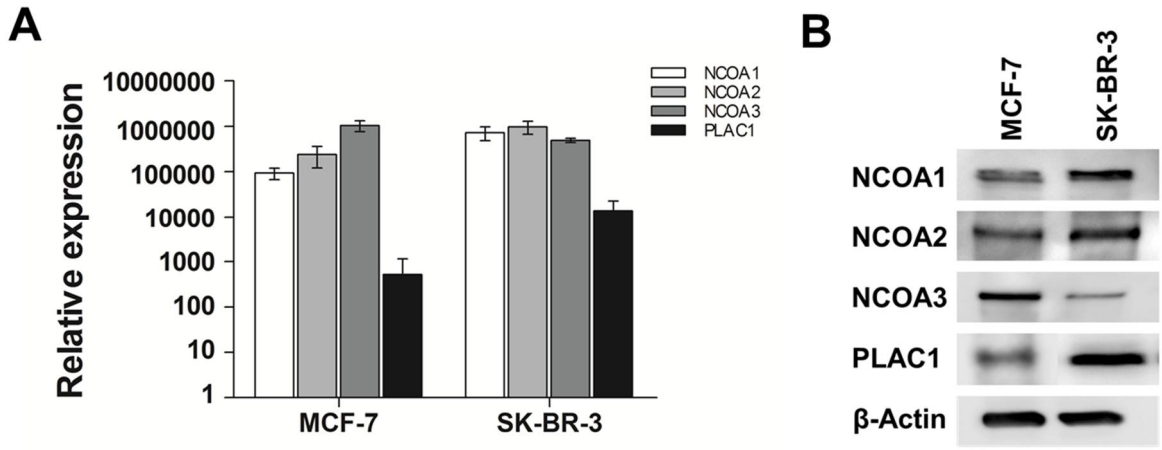

Figure 8 Expression of NCOA1, 2, 3 and PLAC1 in ERα-positive MCF-7 and ERα-negative SK-BR-3 breast cancer cells. (A) Real-time RT-PCR quantification of *NCOA1, 2, 3* and *PLAC1* mRNA expression in MCF-7 and SK-BR-3 breast cancer cells. Shown are mean and standard deviation of a minimum of three individual experiments. (B) Protein expression of NCOA1, 2, 3 and PLAC1 in MCF-7 and SK-BR-3 breast cancer cells were analyzed by Western blot. β-actin was used as a loading control.

4.1.2 NCOA3 is selectively recruited to the endogenous *PLAC1* promoter in estrogen-responsive MCF-7 cells

The next question to address was if NCOA1, 2 or 3 participate in the formation of an E_2-dependent pre-initiation complex on the endogenous *PLAC1* promoter. It is known that these co-activators are recruited to promoters of estrogen-responsive genes [101]. An elegant method to analyze if certain factors are bound to a specific promoter region is ChIP. Because it should be analyzed if the members of the p160/NCOA family are involved in E_2-mediated regulation of *PLAC1*, ChIP assays were performed with nuclear extracts from untreated MCF-7 and SK-BR-3 cells or cells treated for 12 h with 100 nM E_2 in presence or absence of the ERα-antagonist ICI, which is known to efficiently inhibit the actions of endogenous and exogenous E_2, or with ICI alone. The *PLAC1* promoter region analyzed here harbors the C/EBPβ-2 and SP-1 binding site (-348 to -198 bp) for which it has been demonstrated previously that these binding sites are a prerequisite for the formation of a functional transactivation complex [83]. To ensure that specific enrichment of the different factors is detected by ChIP, a negative control locus upstream of the *PLAC1* promoter (-1219 to -1064) was included. After ChIP with

specific antibodies the enrichment of SP1, C/EBPβ-2, ERα, NCOA1, 2 and 3, p300, pCAF, acetylated histones H3 and H4 (AcH3 and AcH4), general transcription factor IIB (TFIIB) and RNA polymerase II (Pol II) was analyzed by end-point PCR as well as quantitative PCR to determine the relative occupancy. First, our previous results could be confirmed as recruitment of C/EBPβ-2 and ERα to the *PLAC1* promoter was strongly and specifically induced by E_2 in MCF-7 cells, whereas no apparent differences in the recruitment of SP1 in the presence or absence of E_2 were observed (Figure 9 A, B). Specific enrichment of NCOA3 but not NCOA1 and NCOA2 was detected in MCF-7 cells upon treatment with E_2. Full NCOA3 co-activator function also requires the recruitment of the histone acetyl transferases p300 and pCAF. Acetylation of histones by these factors modifies chromatin structure and provides a more accessible promoter environment for recruitment of components of the general transcriptional machinery [93]. Accordingly, specific recruitment of histone acetyl transferases p300 and pCAF, acetylated histones H3 and H4, TFIIB and Pol II to the *PLAC1* promoter upon E_2-treatment was detected in MCF-7 cells. In contrast, in ERα-negative SK-BR-3 cells, formation of this pre-initiation complex by treatment with E_2 could not be observed. These results indicate a selective involvement of NCOA3 in the assembly of an active E_2/ERα-induced pre-initiation complex at the *PLAC1* promoter in ERα-positive MCF-7 cells.

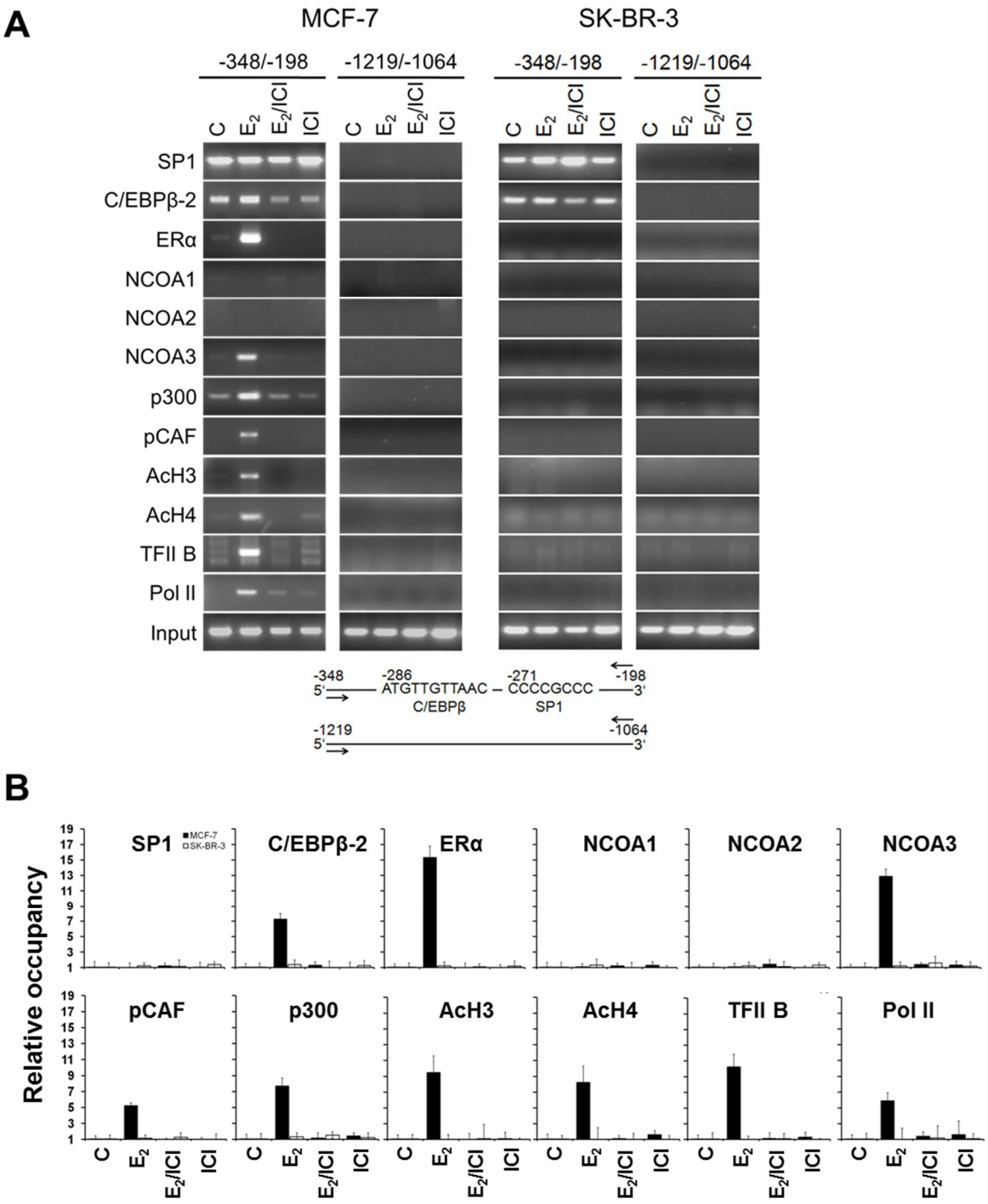

Figure 9 Selective E_2-dependent recruitment of NCOA3 to the endogenous *PLAC1* promoter in ERα positive MCF-7 cells. (A) Chromatin immunoprecipitation (ChIP) was performed with chromatin prepared from MCF-7 and SK-BR-3 cells which were either untreated (C), treated with 17-β-estradiol (E_2) alone, with ICI alone or with both compounds (E_2/ICI) for 12 h. The promoter region of PLAC1 containing the C/EBPβ and SP1 elements (-348/-198) and a region upstream of the promoter (-1219/-1064) as negative control were analyzed by PCR following immunoprecipitation with the indicated antibodies. Amplification products from soluble chromatin prior to precipitation are shown as control (Input). (B) Quantitative analysis of the recruitment and occupancy shown in (A) determined by real-time RT-PCR. The results corrected by input are shown as fold increase compared to unstimulated cells used as a reference.

4.1.3 E_2-mediated transactivation of PLAC1 is dependent on NCOA3

To directly assess the impact of NCOA3 on PLAC1 transcript and protein expression, NCOA3 was silenced by transient transfection with a pool of four NCOA3-specific siRNA duplexes in MCF-7 and SK-BR-3 cells. 48h after transfection, cells were harvested and PLAC1 as well as NCOA3 expression were analyzed by qRT-PCR and Western blot. Transcript levels of NCOA3 were specifically reduced by 80 % compared to non-transfected cells and cells transfected with non-silencing control siRNA duplexes in both cell lines (Figure 10 A). Strikingly, silencing of NCOA3 resulted in a concomitant loss of PLAC1 expression only in ERα-positive MCF-7 cells but not in ERα-negative SK-BR-3 cells. These findings could be confirmed on protein level by Western blot analysis (Figure 10 B).

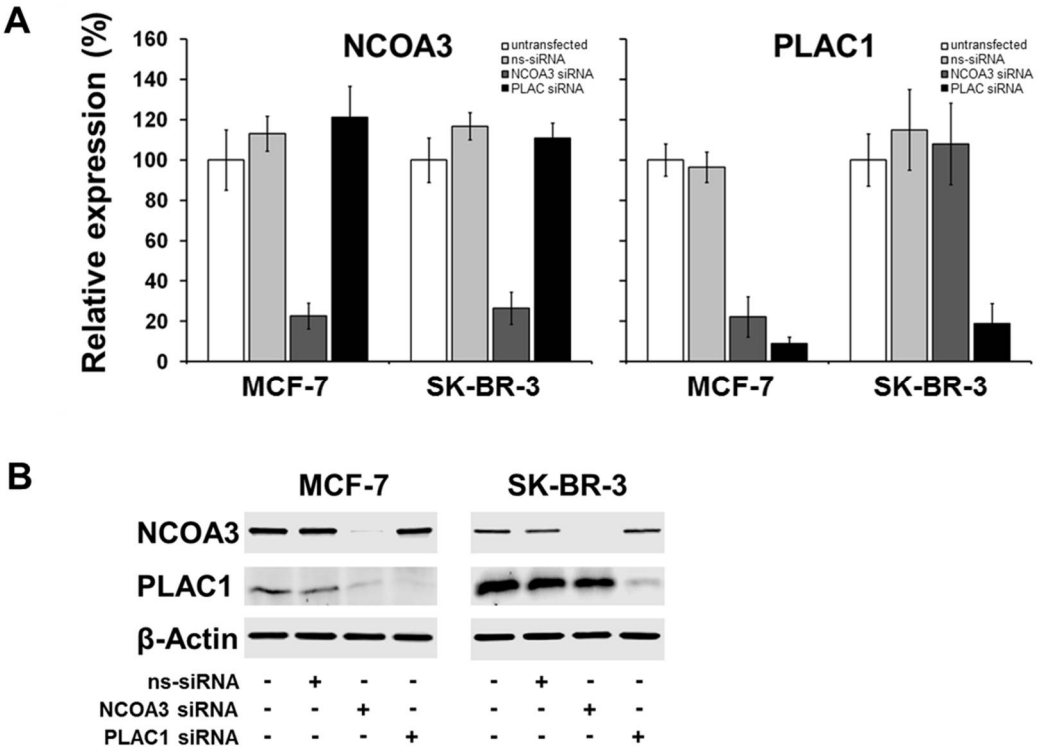

Figure 10 Silencing of NCOA3 diminishes PLAC1 expression only in ERα-positive MCF-7 cells. (A) Quantitative real-time RT-PCR expression analysis of NCOA3 and PLAC1 in MCF-7 and SK-BR-3 cells 48 h after transfection with NCOA3- or PLAC1-specific siRNA duplexes or a non-silencing (ns) siRNA-pool. The results are shown as fold increase compared to untransfected cells used as a reference. (B) Protein expression of NCOA3 in MCF-7 and SK-BR3 cells 48 h after transfection with siRNA duplexes targeting NCOA3 or PLAC1 mRNA.

Noteworthy, silencing of NCOA3 in MCF-7 cells did not result in complete loss of PLAC1 expression, as basal expression of PLAC1 in breast cancer is not dependent on ERα-signaling [83]. Transfection of MCF-7 and SK-BR-3 cells with a

mixture of two *PLAC1*-specific siRNAs was conducted to verify that knockdown of NCOA3 specifically affects PLAC1 mRNA and protein level (Figure 10 A, B).

As ChIP analysis revealed that NCOA3 is only present at the PLAC1 promoter in MCF-7 cells when treated with E_2, the next step was to further verify the importance of NCOA3 for E_2-mediated transactivation of PLAC1. For this purpose, MCF-7 cells were E_2-depleted by culturing in phenol-red free DMEM with 10% charcoal-stripped FCS for 72 h and subsequently transfected with *NCOA3*-targeting siRNA duplexes or control siRNA (*ns*-siRNA). 48 h after transfection, MCF-7 cells were exposed to 100 nM E_2, 5 µM ICI or both (E_2/ICI) and analyzed by qRT-PCR on *PLAC1* expression. E_2-treatment induced *PLAC1* expression only in non-transfected cells and cells transfected with *ns*-siRNA duplexes (Figure 11). In contrast, *PLAC1* transactivation was nearly abolished in cells lacking NCOA3, further confirming the important function of NCOA3 for E_2/ERα-induced transactivation of *PLAC1* in breast cancer cells.

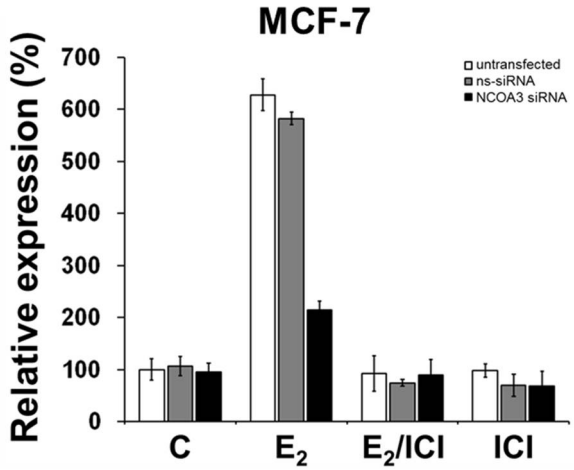

Figure 11 ERα-mediated transactivation of *PLAC1* is dependent on NCOA3. Quantitative real-time RT-PCR analysis of *PLAC1* expression in E_2-depleted (72 h) MCF-7 cells in response to no E_2 (C), treatment with 100 nM E_2, or E_2 and 5 µM ICI, or ICI alone for 12 h. 48 h prior to treatment, cells were transfected with siRNA duplexes targeting *NCOA3* or a *non-silencing* (*ns*) siRNA. Shown are mean and standard deviation of two independent experiments.

4.1.4 *PLAC1* expression is increased in NCOA3 overexpressing and ERα-positive breast cancer samples

The previous experiments were performed exclusively in tumor cell lines. To get insight in a broader range of patients, the relationship between *PLAC1* and *NCOA3* was investigated by qRT-PCR *in vivo* in 48 human primary breast cancer tissue samples including both ERα-positive as well as ERα-negative samples. Since overexpression of NCOA3 in breast cancer has been shown to be associated with clinical parameters [187–189], it was of interest if high *PLAC1* expression is associated with *NCOA3* overexpression and moreover, if any

differences are observed between ERα-positive and –negative breast cancer samples. For this purpose, we subdivided the 48 breast cancer samples into two groups depending on *NCOA3* expression levels. Relative expression of *NCOA3* below 100000 were considered to be '*NCOA3* low' (N = 25), whereas relative expression of *NCOA3* over 100000 were considered to be 'N*COA3* high' (N = 23). In contrast, relative expression of *NCOA3* in human normal breast tissue is about 10000. While no difference in *PLAC1* expression was found between '*NCOA3* low' and '*NCOA3* high' expressing breast cancer tissues regardless of the ER-status (Figure 12A) or in the ERα-negative samples (Figure 12C), a significant higher expression of *PLAC1* in the '*NCOA3* high' expressing breast cancer samples was detected exclusively in ERα-positive breast cancer samples (Figure 12B). Interestingly, a slight but not significant difference in *PLAC1* transcript expression levels between '*NCOA3* high' and '*NCOA3* low' expressing samples is also observed in the ERα-negative samples. If *NCOA3* expression has also in ERα-negative breast cancer tissues an influence on *PLAC1* expression levels has to be further investigated in a larger setting to draw a final conclusion.

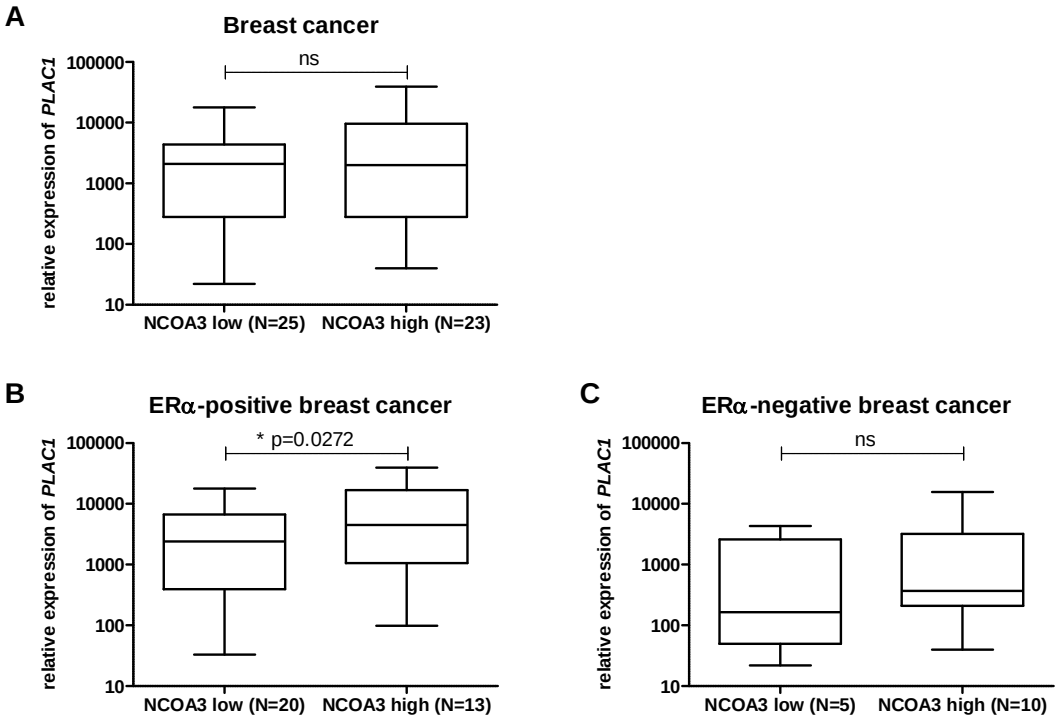

Figure 12 mRNA expression of *PLAC1* is elevated in *NCOA3* overexpressing and ERα-positive human breast cancer samples. (A) *NCOA3* and *PLAC1* mRNA expression was examined by quantitative real-time RT-PCR in 48 human breast cancer samples. '*NCOA3* low' (N = 25) are samples with a relative expression of *NCOA3* below 100000, whereas be '*NCOA3* high' (N = 23) samples have a relative expression of *NCOA3* over 100 000. (B) Evaluation of PLAC1 expression in ERα-positive breast cancer samples with '*NCOA3* low' (N=20) or '*NCOA3* high' (N=13) status. (C) Evaluation of PLAC1 expression in ERα-negative breast cancer samples with '*NCOA3* low' (N=5) or '*NCOA3* high' (N=10) status. Statistical analysis was performed using two-tailed paired Student's t-test. $P \leq 0.05$ was considered statistically significant.

4.2 Analysis of CLDN6 in cancer – expression, function and regulation

The second part of the present study deals with the elucidation of expression, function and regulation of the tight junction molecule CLDN6 in cancer.

4.2.1 *CLDN6* is frequently expressed in cancer but absent in normal adult tissues

In a first experiment, *CLDN6* expression was analyzed in various human normal tissues, cancer cell lines as well as cancer types by qRT-PCR. *CLDN6* was not expressed in any normal tissues except at minor levels in placenta (Figure 13 A). In contrast, *CLDN6* was found to be frequently overexpressed in various cancer cell lines, as shown in Figure 13 B. Cancer cell lines with a relative expression of *CLDN6* above 500 are shown. Tumor tissues, especially ovarian, lung (with a higher prevalence in adenocarcinoma compared to squamous cell carcinoma) and testicular cancer were found to frequently overexpress *CLDN6* (Figure 13 C). Furthermore, sporadic expression of *CLDN6* was observed also in a variety of other cancer types, for example breast cancer and gastric cancer (data not shown).

These data present *CLDN6* as a highly specific tumor antigen and qualifies it as a potent candidate target for *CLDN6*-specific cancer immunotherapies.

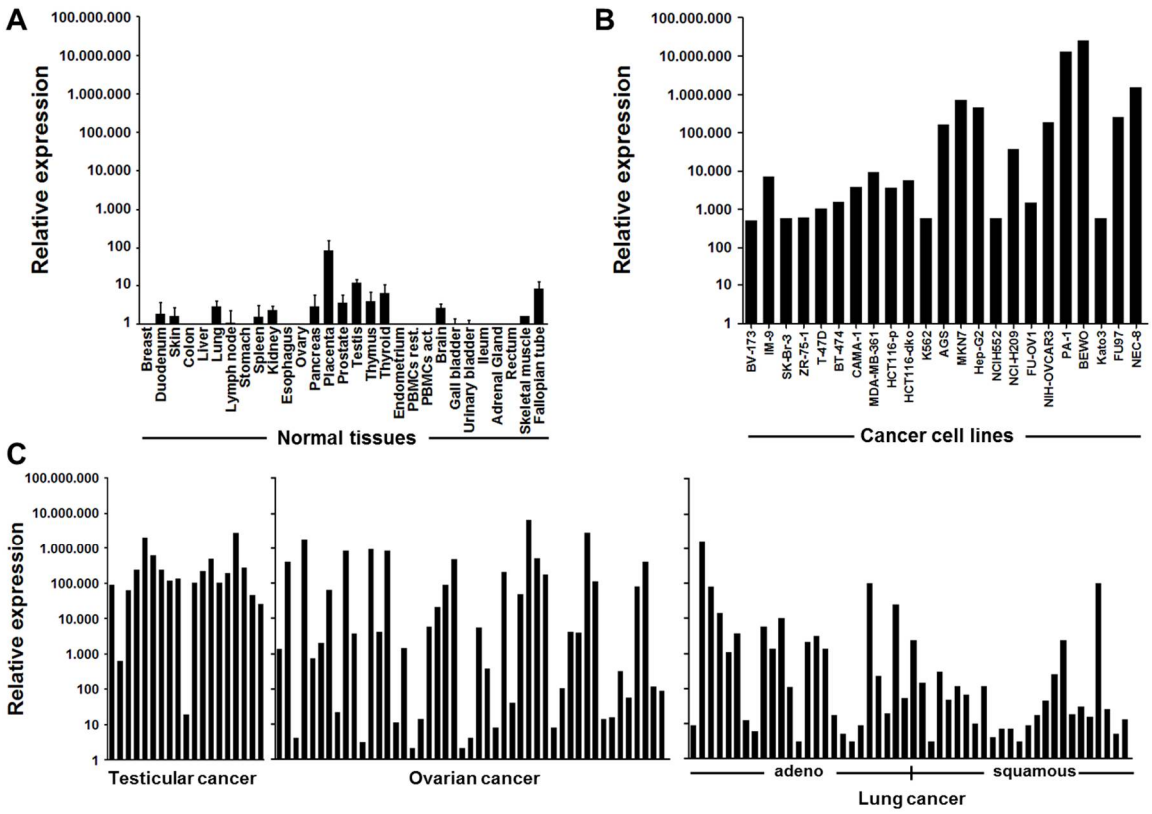

Figure 13 *CLDN6* is overexpressed in cancer cell lines and tissues while not expressed in adult normal tissues. Quantitative 40 cycles real-time RT-PCR in (A) human normal tissues: breast, duodenum, skin, colon, liver, lung, lymph node, stomach, spleen, kidney, esophagus, ovary, pancreas, placenta, prostate, testis, thymus, thyroid, endometrium, peripheral blood mononuclear cells (PBMCs) resting and proliferating, cerebellum, gall bladder, urinary bladder, ileum, adrenal gland, rectum, skeletal muscle and fallopian tube, (B) cancer cell lines BV-173, IM-9, SK-BR-3, ZR-75-1, T47-D, BT-474, CAMA-1, MDA-MB-361, HCT116-p (parental) and HCT116-dko (DNMT double knock out), K562, AGS, MKN7, Hep-G2, NCI-H552, NCI-H209, FU-OV1, NIH-OVCAR3, PA-1, BEWO, Kato3, FU97 and NEC-8 and (C) testicular, ovarian and adeno- and squamous lung cancer tissues. (B) Cancer cell lines with a relative expression level >500 are shown only. Relative expression of *CLDN6* was normalized to relative expression of housekeeping gene *HPRT1*.

4.2.2 Establishment of a transient CLDN6 knockdown system

To analyze the function of CLDN6 in cancer cells, siRNA-mediated silencing of CLDN6 was established in three different tumor cell lines. In this study, the human ovarian teratocarcinoma cell line PA-1, the human ovarian adenocarcinoma cell line NIH-OVCAR3 and the human testicular carcinoma cell line NEC-8 were used for functional analysis of CLDN6 because these cell lines have been show to express high levels of CLDN6 (Figure 13 B).

All three cell lines were transfected with either a pool of four *non-silencing* (*ns*) siRNAs or *CLDN6*-targeting siRNAs (in the following referred to as *ns*-siRNA or *CLDN6*-siRNA) and analyzed 48 h after transfection by qRT-PCR and Western Blot. Knockdown of CLDN6 was highly efficient in all three cell lines both on mRNA as well as on protein level (Figure 14 A, B). Residual mRNA expression in

CLDN6-siRNA treated cells was below 5 % in NEC-8 and NIH-OVCAR3 cells and below 15 % in PA-1 cells compared to untransfected control cells.

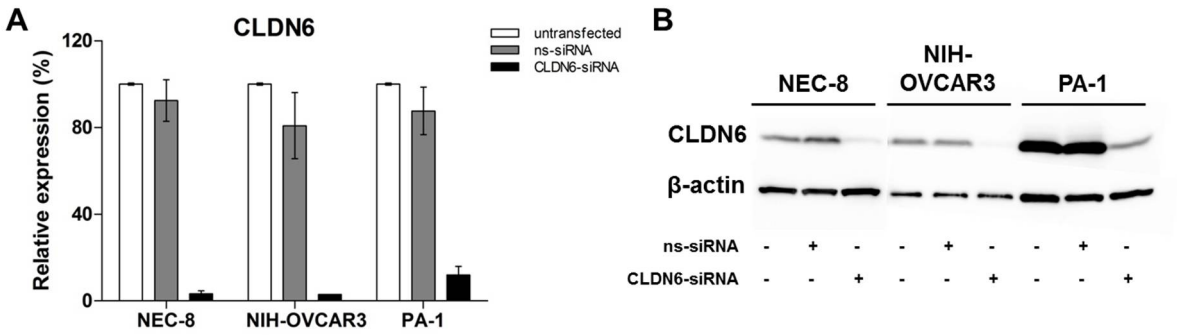

Figure 14 RNAi-mediated silencing of CLDN6 is highly efficient in NEC-8, NIH-OVCAR3 and PA-1 tumor cells. (A) Quantitative real-time RT-PCR expression analysis of *CLDN6* 48 h after transfection with *CLDN6*-specific siRNA duplexes. ns-siRNA, *non-silencing* siRNA. Results are shown as fold increase compared to untransfected cells used as reference. (B) Protein expression of CLDN6 48 h after transfection with siRNA duplexes targeting *CLDN6* mRNA. β-Actin was used as loading control.

CLDN6 knockdowns of these three cell lines were used to further analyze the function of CLDN6 in several cellular *in vitro* assays which are described in the following chapters (4.2.3 and 4.2.4).

4.2.3 Silencing of CLDN6 does not alter proliferation, apoptosis or cell cycle distribution of tumor cell lines

In this study, the effect of siRNA-mediated silencing of CLDN6 on key features of tumorigenesis was assessed. Deregulation of proliferation, cell cycle and apoptosis can lead to uncontrolled expansion of tumor cells.

First, it was investigated if CLDN6 knockdown influences proliferation of tumor cells. For this purpose, PA-1, NIH-OVCAR3 and NEC-8 cells were transfected either with *ns*- siRNA or *CLDN6*-siRNA. Proliferation of tumor cells was analyzed 48 h, 72 h and 96 h after knockdown of CLDN6 using a fluorescence based method. The green fluorescent dye CyQUANT binds to nucleic acids, thus fluorescence is equivalent to DNA content. The higher the fluorescent counts the more cells are present in the well. It is assumed that the fluorescent signal accounts for the cell number.

Results of proliferation assay are depicted in Figure 15 A-C. Neither in NEC-8, PA-1 nor NIH-OVCAR3 remarkable changes in proliferation could be observed 48 h, 72 h or 96 h after transfection with *CLDN6*-targeting siRNA compared to untransfected or *ns*-siRNA transfected cells. Knockdown of CLDN6 was analyzed

at the beginning (24 h after transfection) and at the end of the experiment (96 h after transfection) by qRT-PCR. Knockdown of CLDN6 was efficient during the entire proliferation assay (Figure 15 D).

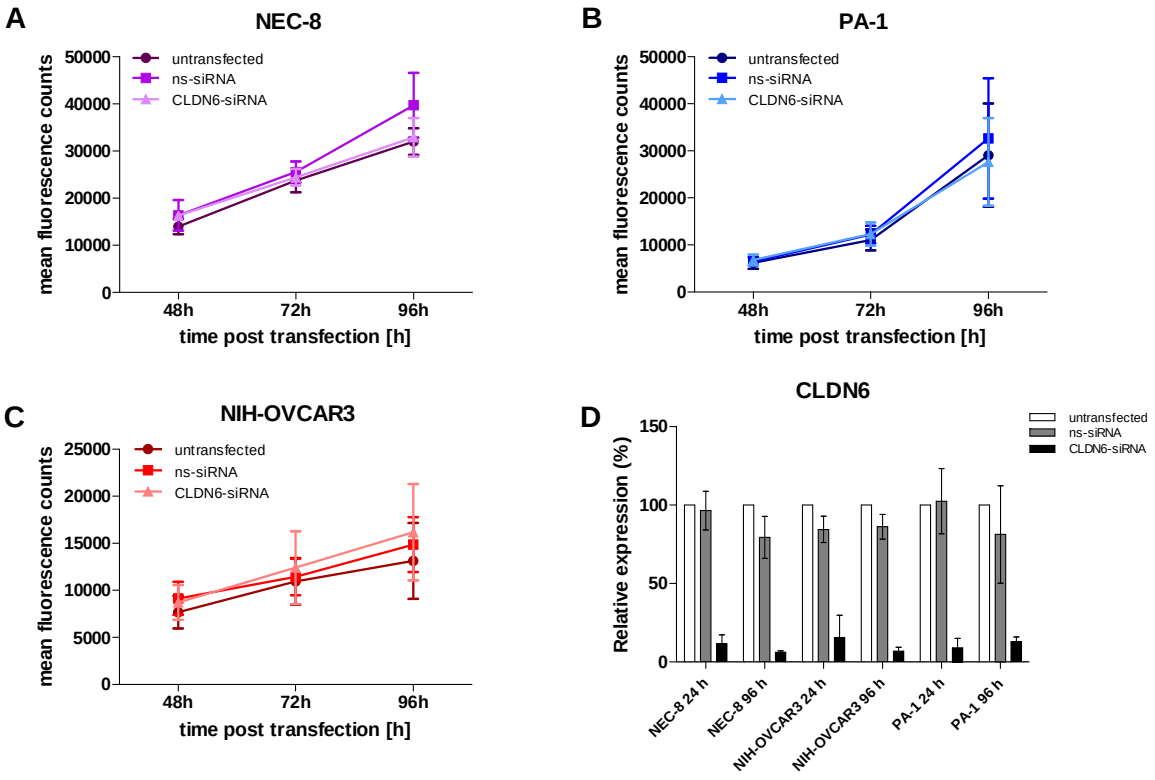

Figure 15 Silencing of *CLDN6* does not alter proliferation of NEC-8, PA-1 and NIH-OVCAR3 cells. (A) NEC-8 (B) PA-1 and (C) NIH-OVCAR3 cells were either transfected with *non-silencing* (ns) siRNA or *CLDN6*-targeting siRNA or left untransfected and fluorescence intensity of incorporated CyQUANT was assayed 48 h, 72 h or 96 h after transfection. (D) Analysis of *CLDN6* knockdown efficiency during proliferation assay. qRT-PCR expression analysis of *CLDN6* 24 h and 96 h after transfection with *CLDN6*-specific siRNA or ns-siRNA duplexes in NEC-8, NIH-OVCAR3 and PA-1 cells. Results are shown as fold increase compared to untransfected cells used as a reference.

Cell cycle progression is often deregulated in tumor cells and proportions of cells which are in active cell division are significantly increased in tumors compared to that of normal tissues. Hence, in this study, changes in cell cycle distribution were analyzed in *CLDN6*-siRNA transfected PA-1, NEC-8 and NIH-OVCAR3 cells compared to untransfected or *ns*-siRNA treated cells 72 h after transfection. This time point was chosen because on the one hand all three cell lines used exhibited a stable knockdown of CLDN6 72 h after transfection (Figure 17 E) and on the other hand it is possible that silencing of CLDN6 needs a little time to display provoked effects on protein level in terms of mRNA half-lives and protein stability. Changes in cell cycle were analyzed using 7-AAD that is excluded from live cells with intact cell membranes whereas damaged membranes of dying or dead cells are penetrated. During cell cycle, DNA content of cells changes. Using 7-AAD, a

characteristic cellular DNA content profile is generated in which fluorescence intensity of 7-AAD is proportional to DNA content. Cells in G1- or G0-phase are diploid (2n), cells in G2/M phase have a double set of chromosomes (4n) and cells in S-phase show an intermediate DNA-content. Dead or damaged cells have fragmented DNA and can be visualized by sub G1 frequency that accounts for apoptotic cell fraction and cell debris.

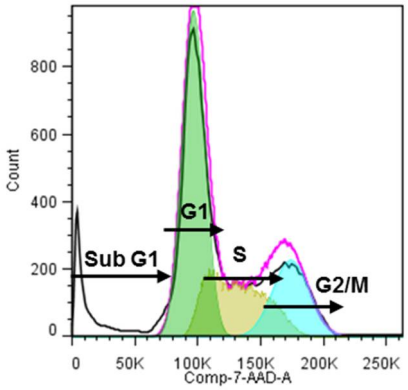

Figure 16 Histogram showing DNA content measurement. Counted events are plotted against 7-AAD fluorescence profile. Sub G1 (black), G1 (green), S (yellow) and G2/M (blue) phases are indicated by colored areas and arrows.

To account for unspecific effects of siRNA treatment, a CLDN6-negative cell line, the pancreatic cancer cell line DAN-G, was included in the analysis.

As shown in Figure 17 A - D no changes in cell cycle distribution of G1, S or G2/M phase were observed in the four tested cell lines. This result indicates that CLDN6 has no effect on cell cycle distribution of the tested tumor cell lines.

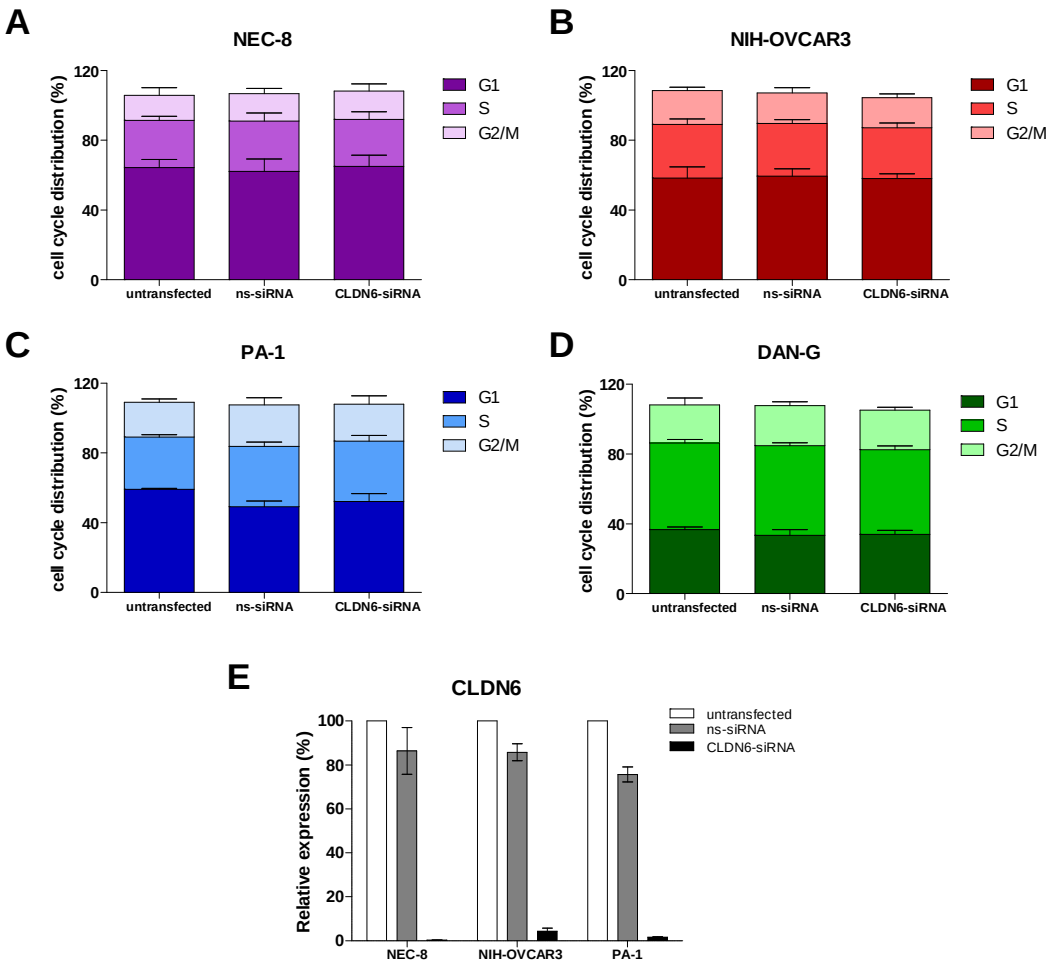

Figure 17 Silencing of *CLDN6* has no effect on cell cycle distribution in cancer cells. (A) NEC-8, (B) NIH-OVCAR3, (C) PA-1 and (D) DAN-G cells were analyzed 72 h after transfection with *non-silencing* (ns) siRNA or *CLDN6*-targeting siRNA or were left untransfected by Flow Cytometry regarding their DNA content. Percentages of each cell cycle phase (G1, S or G2/M-phase) are indicated. (E) qRT-PCR expression analysis of *CLDN6* 72 h after transfection with *CLDN6*-specific siRNA or ns-siRNA duplexes in NEC-8, NIH-OVCAR3 and PA-1 cells. Results are shown as fold increase compared to untransfected cells used as reference. Shown are mean and standard deviation of at least two independent experiments.

In Figure 18, results of sub G1 measurements are depicted. In NEC-8 and PA-1 cells no significant changes in the sub G1 frequency could be detected 72 h after knockdown of *CLDN6* compared to untransfected and *ns*-siRNA transfected cells. Interestingly, a highly significant increase of apoptotic cells is observed in NIH-OVCAR3 cell treated with CLDN6-siRNA 72 h after transfection, compared to untransfected and ns-siRNA treated cells. Unexpectedly, *CLDN6*-siRNA treated DAN-G cells show also an increase in the frequency of apoptotic cells which is only significant compared to the untransfected cells but not to the *ns*-siRNA treated group. Therefore, this might be a general unspecific effect of siRNA treatment in DAN-G cells.

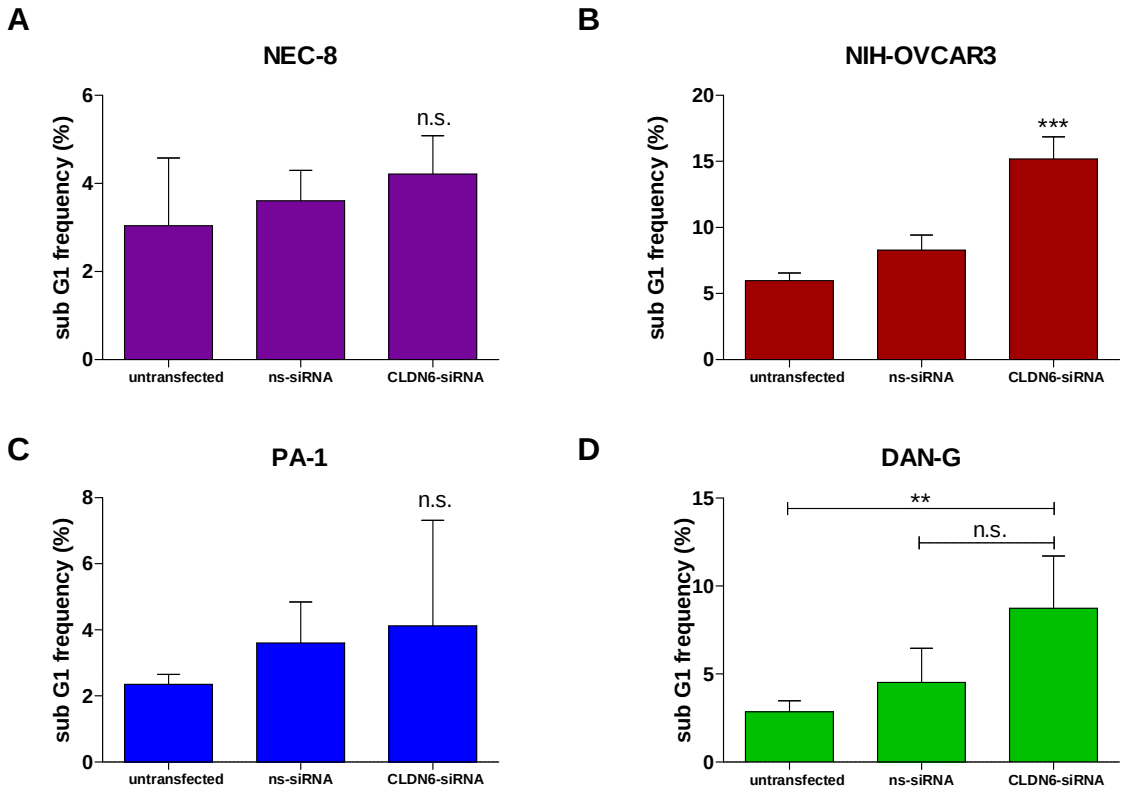

Figure 18 *CLDN6* silencing changes sub G1 frequency during cell cycle analysis in NIH-OVCAR3 and DAN-G cells. (A) NEC-8, (B) NIH-OVCAR3, (C) PA-1 and (D) DAN-G cells were analyzed 72 h after transfection with *non-silencing* (ns) siRNA or *CLDN6*-targeting siRNA or were left untransfected by Flow Cytometry regarding their DNA content. Shown are mean and standard deviation of a minimum of two independent experiments. One-way ANOVA was used for statistical analysis. P-*values* < 0.05 were considered statistically significant. n.s. = not significant.

To analyze in further detail if detected increase in apoptosis after *CLDN6*-siRNA treatment in NIH-OVCAR3 cells accounts for a specific effect caused by knockdown of *CLDN6*, another more specific assay, the AnnexinV/7-AAD staining was used to analyze apoptosis of cancer cells. Using this assay, it can be distinguished between early and late apoptotic and / or necrotic cells. Apoptotic processes include major changes in cell membrane integrity, condensation of cytoplasm and nucleus and internucleosomal cleavage of DNA. The earliest apoptotic event is the membrane flip in which the membrane phospholipid phosphatidylserine (PS) is translocated to the outer leaflet of the plasma membrane. The calcium-dependent phospholipid binding protein Annexin V binds to cells with exposed PS designating early apoptotic cells. In this study, PE-conjugated AnnexinV was used in combination with 7-AAD to distinguish between early and late apoptotic cells. PE-Annexin V^+/7-AAD^- cells are early apoptotic whereas PE-Annexin V^+/7-AAD^+ cells showing highly damaged cell membranes

and DNA cleavage are either late apoptotic or necrotic cells. PE-Annexin V$^-$/7-AAD$^-$ cells are viable cells with intact membranes.

Only NIH-OVCAR3 cells were analyzed because in this cell line a significant effect of *CLDN6*-siRNA treated compared to *ns*-siRNA treated cells was observed (Figure 18 B). As shown in Figure 19, treatment of NIH-OVCAR3 cells with *CLDN6*-siRNA for 72 h results in minor changes of apoptosis. The Annexin V positive (Annexin V+) fraction is slightly but not significant increased compared to the ns-siRNA transfected and untransfected cells (Figure 19 A-C). Furthermore, the other fractions do not display any remarkable changes upon silencing of *CLDN6* (Figure 19 C). Knockdown of *CLDN6* was analyzed 72 h after transfection and at the beginning of the apoptosis assay (Figure 19 D).

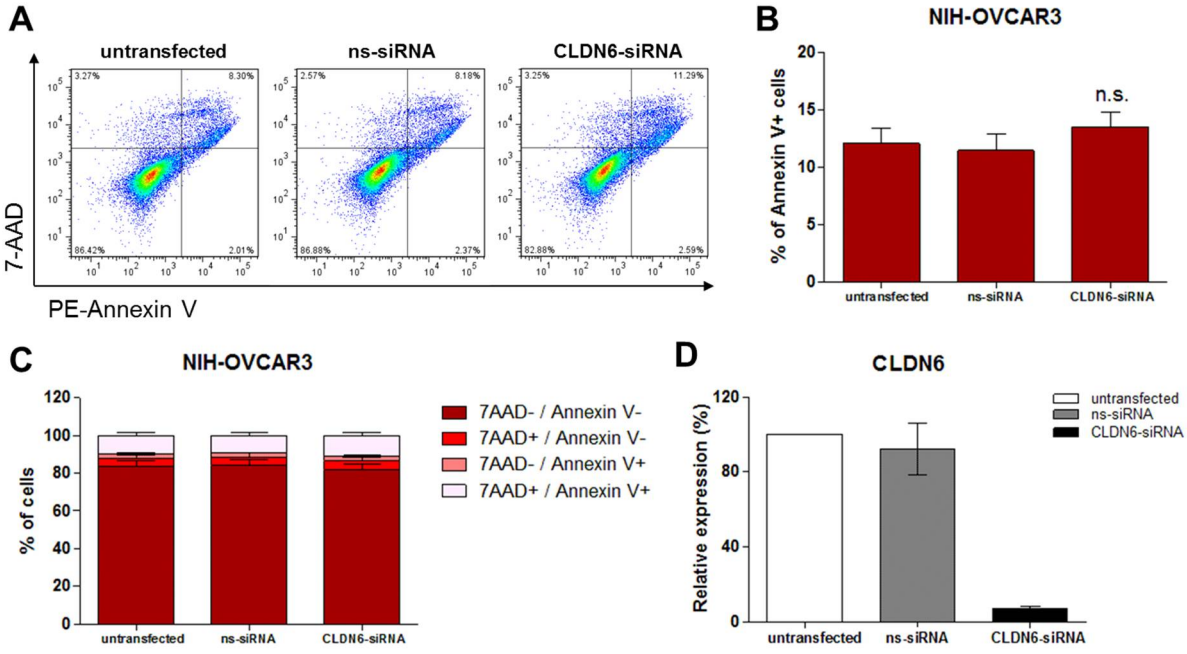

Figure 19 Frequency of apoptotic cells is not significantly changed by silencing of *CLDN6* in NIH-OVCAR3 cells. NIH-OVCAR3 cells were stained with 7AAD and Annexin V 72 h after transfection with ns-siRNA or CLDN6-siRNA and analyzed by flow cytometry. (A) Dot Plots of untransfected, *ns*-siRNA or *CLDN6*-siRNA transfected NIH-OVCAR3 cells. (B) Percentages of Annexin V+ cells (early and late apoptotic cells). One-way ANOVA was used for statistical analysis. *P*-values < 0.05 were considered statistically significant. (C) Distribution of the quadrants shown in (A) in percentages: live cells (7AAD- / Annexin V-), early apoptotic cells (7AAD- / Annexin V+), late apoptotic or necrotic cells (7AAD+ / Annexin V+) or damaged cells (7AAD+ / Annexin V-). (D) qRT-PCR expression analysis of *CLDN6* 72 h after transfection with *CLDN6*-specific siRNA or ns-siRNA duplexes in NIH-OVCAR3 cells. Results are shown as fold increase compared to untransfected cells used as reference. Shown are mean and standard deviation of at least two independent experiments.

These results suggest that *CLDN*6 silencing has no significant effect on induction of apoptosis in NIH-OVCAR3 cells.

In summary, CLDN6 seems to be not important for proliferation, cell cycle distribution or induction of apoptosis in NEC-8, NIH-OVCAR3 and PA-1 cells.

4.2.4 Silencing of CLDN6 has no effect on migration, cell-cell or cell-matrix adhesion of tumor cells

Another set of experiments was performed to address the question if silencing of *CLDN6* has an influence on migration or adhesion of tumor cells. Migration and loss of cell-cell or cell-matrix adhesion are key events during metastatic processes when tumor cells. Metastatic tumor cells loose attachment to other tumor cells as well as cells of the tumor stroma which is followed by invasion in surrounding tissues and migration through the bloodstream to different organs. As claudins are tight-junction molecules it is likely that these molecules take part in cell-cell or cell matrix adhesion processes.

To analyze if CLDN6 plays a functional role in migration, a wound healing assay was performed. For this assay it is crucial that the cells used adhere well and can grow to 100 % confluency. As NEC-8 and NIH-OVCAR3 cells do not grow to 100 % confluency, only PA-1 cells were used for this assay.

PA-1 cells were either not transfected or transfected with *ns*-siRNA or *CLDN6*-siRNA. 48 h after transfection, confluent monolayers were wounded using a disposable 200 µL pipette tip. The wound closure was analyzed at different time points (0-24h). A representative experiment is shown in Figure 20.

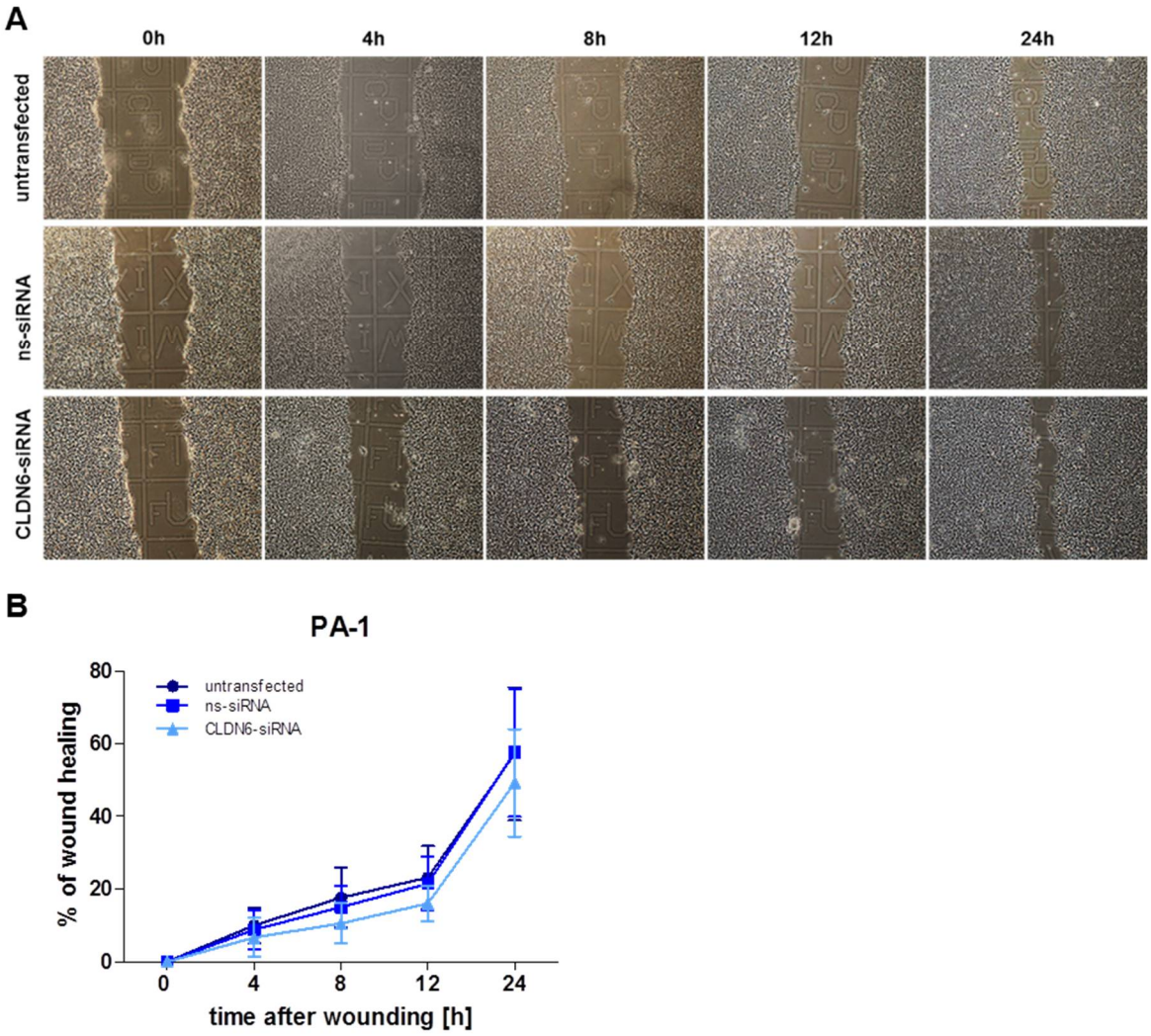

Figure 20 Wound Healing is not affected after CLDN6 knockdown in PA-1 cells. 48 h after transfection with ns- or CLDN6-siRNA, wounding was performed using a 200 µL pipette tip. (A) To analyze wound healing, pictures were taken at different time points after wounding (0, 4, 8, 12 and 24 h) and cell-free area was measured using polygon selection tool of Image J. (B) Percentages of wound healing were calculated respective to cell-free area at 0 h for every sample. 10 fields per sample were analyzed. Mean and standard deviation of two experiments are shown.

The next question was if CLDN6 is important for cell-cell or cell-matrix adhesion of tumor cells. For cell-cell adhesion, NIH-OVCAR3, PA-1 and DAN-G cells were transfected with *ns*-siRNA or *CLDN6*-siRNA. 72h after transfection, cells were stained with calcein AM and seeded onto an unstained confluent monolayer of either PA-1 or NIH-OVCAR3 cells. Non-fluorescent calcein AM is a cell-permanent dye that is converted to the green-fluorescent calcein in live cells by intracellular esterases. Cells were allowed to adhere for either 1 h or 3 h. NIH-OVCAR3 cells show overall stronger adhesion to PA-1 or NIH-OVCAR3 layers than PA-1 or DAN-G cells. However, in comparison to untreated or *ns*-siRNA treated cells, *CLDN6*-siRNA treated cells show in none of the cell lines used any significant effect in adhesion to PA-1 or NIH-OVCAR3 monolayers (Figure 21).

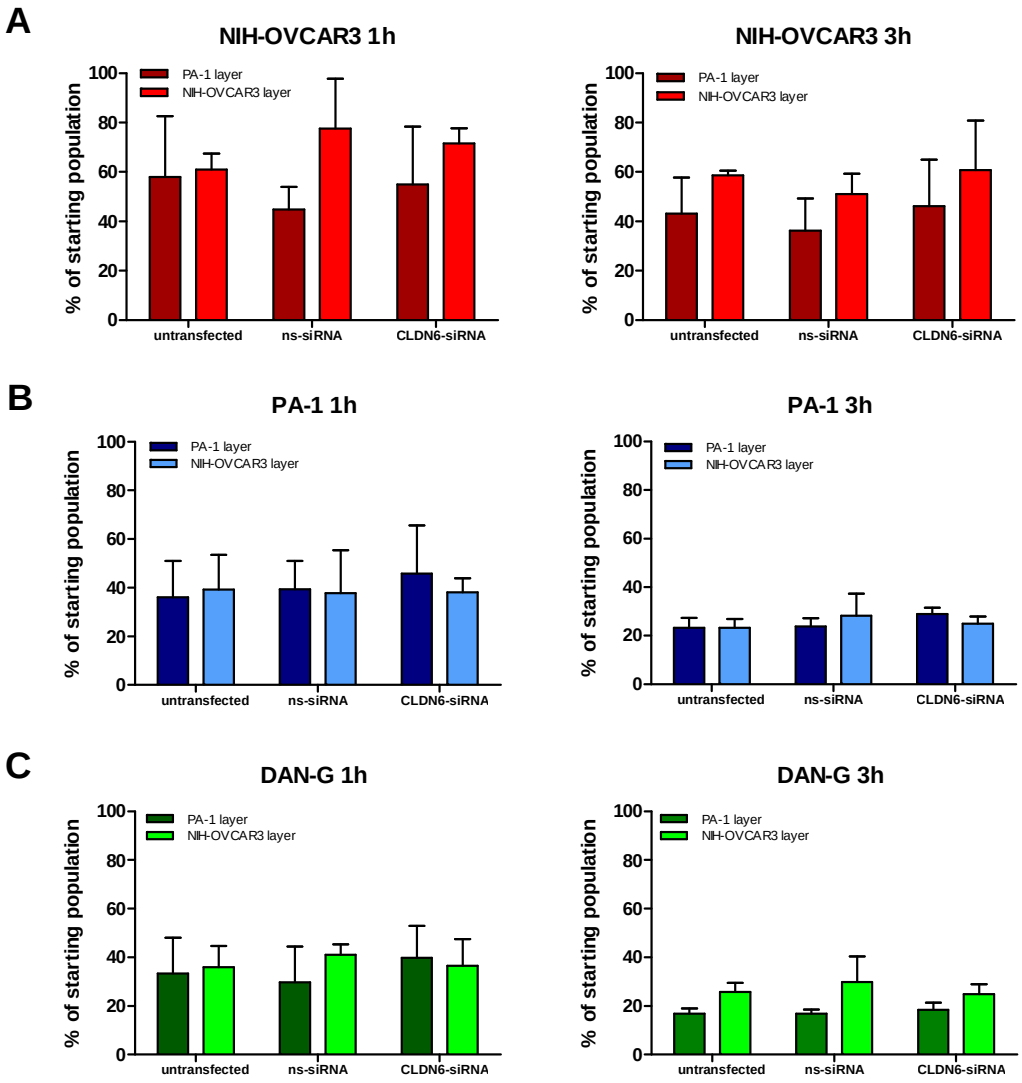

Figure 21 Silencing of *CLDN6* does not alter cell-cell adhesion of tumor cells. (A) NIH-OVCAR3, (B) PA-1 or (C) DAN-G cells were either not transfected or transfected with *ns*- or *CLDN6*-siRNA. 72 h after transfection, cells were stained with 1 µM calcein AM and seeded onto confluent monolayers of either PA-1 or NIH-OVCAR3 cells (PA-1 layer, NIH-OVCAR3 layer) and allowed to adhere for 1 and 3 h. Non-adherent cells were washed away and fluorescence of adherent cells was measured using a fluorometer (Wallac Victor2, Perkin Elmer). Percentages of adherent cells regarding to the starting population (5 x 10^4 cells) are shown. Mean and standard deviation of at least two independent experiments are shown.

Next, the effect of *CLDN6* silencing on cell-matrix adhesion of tumor cells was analyzed. For this purpose, different matrix molecules were chosen: Laminin-111 and vitronectin are both known to be matrix molecules important for embryonic stem cells (ESC) and cancer [190–193]. As CLDN6 is known to have a functional role during epithelial development and is expressed only in ESC, embryonic tissues and cancer [116,130,165,194], vitronectin and laminin-111 were considered to be suitable for analysis of CLDN6-dependent cell-matrix adhesion. Poly-L-lysine enhances independently of receptors the electrostatic interaction of the negatively-charged cell membranes and the positively charged attachment factors on the culture surface and therefore served as a very good positive control.

NIH-OVCAR3, PA-1 and DAN-G cells were transfected with *ns*-siRNA or *CLDN6*-targeting siRNA. After 72 h cells were seeded onto vitronectin, laminin-111 or poly-L-lysine coated plates and were allowed to adhere for 3 h. Non-adherent cells were washed away and remaining adherent cells were stained with crystal violet. In Figure 22 results of the cell-matrix adhesion assay are shown. No influence of *CLDN6*-knockdown was observed on adhesion to vitronectin, laminin-111 or poly-L-lysine in the different cell lines (Figure 22).

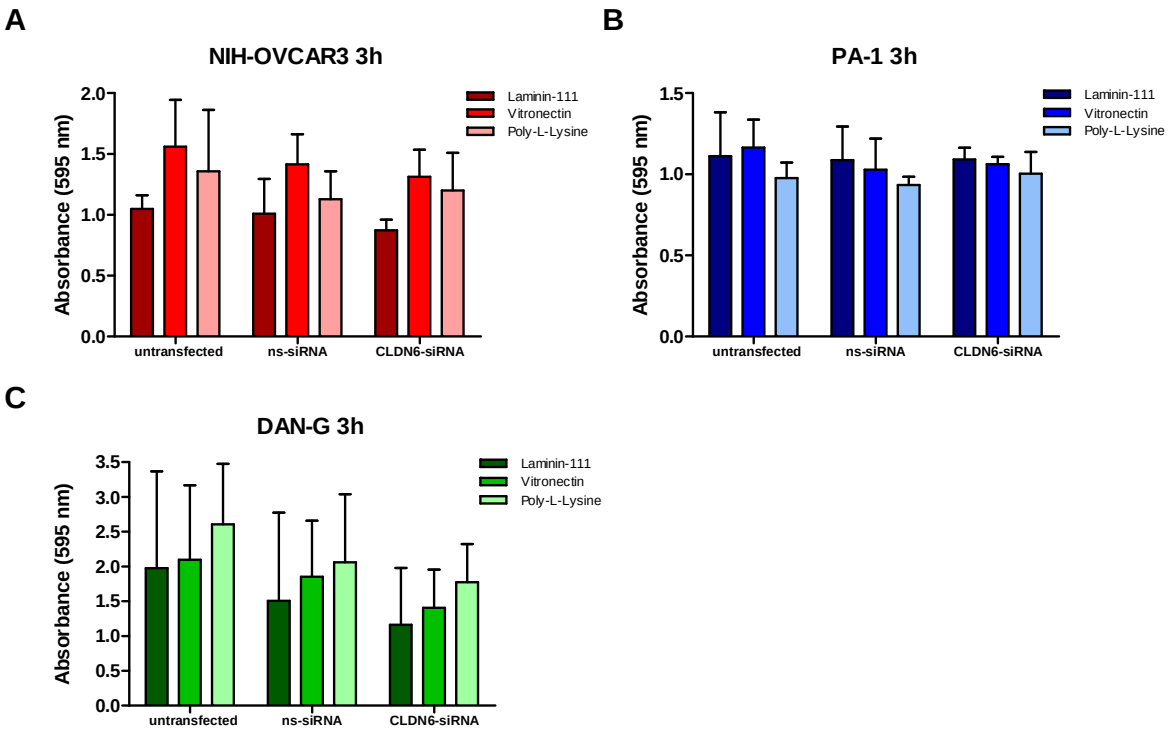

Figure 22 Cell-matrix adhesion of tumor cells is not affected by silencing of *CLDN6*. (A) NIH-OVCAR3, (B) PA-1 or (C) DAN-G cells were either not transfected or transfected with *ns*- or *CLDN6*-siRNA. 72 h after transfection, cells were seeded on 96-well plates coated with the respective matrix molecule (5E4 cells per well) and allowed to adhere for 3 h. During the adhesion assay, cells were maintained in serum-free media to prevent that proteins contained in the serum interfere with the adhesion process. Non-adherent cells were washed away and adherent cells were fixed and stained with crystal violet (0.2 % crystal violet in 10 % EtOH). Stained cells were dissolved in acetic acid and absorbance was measured in a spectrometer (Tecan). Mean and standard deviation of at least two experiments are shown.

These results suggest that CLDN6 has no effect on cell-cell or cell-matrix adhesion to vitronectin, laminin 111 or poly-L-lysine in the tested tumor cell lines.

To conclude this chapter, in this study no remarkable effect on cell migration, cell-cell adhesion or cell-matrix adhesion was found by silencing of *CLDN6* in PA-1 and NIH-OVCAR3 tumor cells. Additionally, in the CLDN6-negative control cell line DAN-G no specific effects were observed.

4.2.5 CLDN6-positive tumor cells show increased colony formation potential compared to CLDN6-negative tumor cells

Recent data from literature indicated that CLDN6 could have a function in embryonic stem cells and/or cancer stem cells [164–166].

Therefore, it was highly interesting to analyze if CLDN6 is important for colony formation of tumor cells. Colony formation is a key feature of tumor cells. This allows the tumor cells to grow at the primary as well as metastatic or distant sites.

The colony formation assay is a long-term assay lasting over 14 days. For that reason, transient siRNA-mediated knockdown of *CLDN6* was not useful and PA-1 cell lines carrying a stable lentiviral small hairpin RNA (shRNA) mediated knockdown of *CLDN6* were used. These were generated by Ganymed pharmaceuticals and kindly provided for this study. Two PA-1 *CLDN6*-knockdown clones, named PA-1 50 and 54 were used. As control, a PA-1 clone was used which carries a stable lentiviral non-targeting control shRNA (PA-1 76). The surface expression of CLDN6 was analyzed by flow cytometry and revealed that PA-1 50 and 54 cells display a moderate knockdown of CLDN6 compared to the control clone PA-1 76 with ~99% CLDN6-expressing cells (Figure 23 A). In PA-1 50, 13% of the cell population displays a medium CLDN6-level whereas only 0.345% are CLDN6-low. In contrast, 58% of the PA-1 54 cell population displays a medium CLDN6 expression whereas 8.61% are CLDN6-low. The knockdown is more efficient in PA-1 54 compared to PA-1 50 cells. For subsequent colony forming assays, 500 cells were sorted based on their CLDN6 expression as CLDN6-negative and CLDN6-positive cells directly into 6-well plates and allowed to grow for up to 14 days.

Regardless of the knockdown efficiency, CLDN6-negative cells show a remarkable decrease in colony formation compared to CLDN6-positive cells in both cell lines (Figure 23 B). This result indicates that CLDN6 is important for colony formation in PA-1 cells.

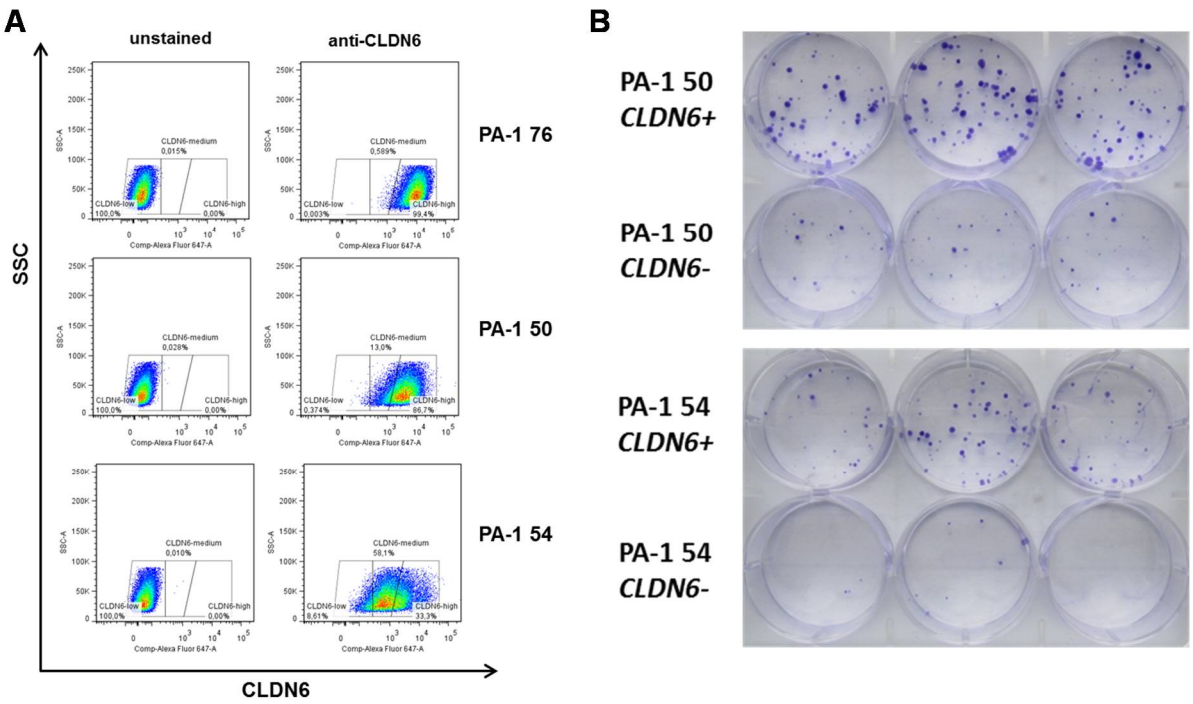

Figure 23 CLDN6 plays a role in colony formation of PA-1 cells. (A) Flow cytometry analysis of CLDN6 expression in the control cell line PA-1 76 (empty vector control) as well as CLDN6-knockdown cell lines PA-1 50 and PA-1 54. Anti-CLDN6 antibody: IMAB027-AlexaFluor647 (Ganymed Pharmaceuticals). The depicted gates were used for sorting of CLDN6-low or CLDN6-high cells for colony formation assay. (B) Colony formation assay of CLDN6-positive (+) and CLDN6-negative (-) PA-1 50 and 54 cells. 500 cells per well were sorted directly in 6-well plates and allowed to grow for up to 14 days. For fixation and staining of colonies, 0.2 % crystal violet in 10 % EtOH was used. A representative experiment from three independently performed experiments is shown here.

4.2.6 CLDN6 is in part regulated via epigenetic mechanisms

There are evidences from the literature, that CLDN6 could be regulated by epigenetic mechanisms. Mostly, it is described that CLDN6 is down regulated by promoter methylation in breast and esophageal cancer [134–136]. As described in more detail in chapter 1.1.1, DNA methylation occurs mainly at the cytosines in the CpG context and high methylation frequency at gene promoters is associated with genomic silencing.

To date, three transcript isoforms of *CLDN6* are known (source: ensemble.org) and indeed, two independent CpG islands are found in the promoter region of *CLDN6* (see Figure 4 in chapter 1.4.1). The first CpG island is located in front of the transcription start site (TSS) of *CLDN6-001* and 1402 bp long whereas the second CpG island is in front of *CLDN6-201/-002* and 836 bp in length.

To get a first insight into the DNA methylation status of the promoter region of CLDN6, experiments with the demethylating agent 5-aza-2'-deoxycytidine (5-aza-dC) were performed. The cytidine analog 5-aza-dC is incorporated into DNA upon

replication and inhibits DNA methyltransferases resulting in hypomethylation of DNA. PA-1 and NIH-OVCAR3 (CLDN6-positive) as well as SK-BR-3 and DAN-G cells (CLDN6-negative) were treated with 2 µM and 10 µM 5-aza-dC for 72 h respectively and CLDN6 mRNA as well as protein level were detected by qRT-PCR and Western Blot (Figure 24). 5-aza-dC treatment resulted in an up-regulation of CLDN6 at the mRNA and protein level only in SK-BR-3 and DAN-G cells at both concentrations. SK-BR-3 and DAN-G cells do not express CLDN6 endogenously. In contrast, PA-1 and NIH-OVCAR3 cells with endogenously high expression of CLDN6 showed no induction of CLDN6 expression by treatment with 5-aza-dC.

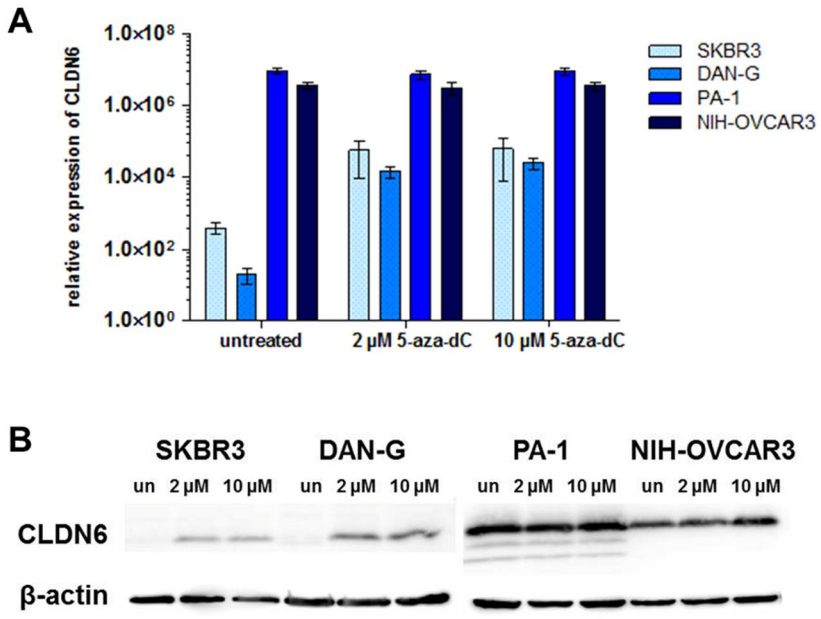

Figure 24 Treatment of tumor cell lines with 5-aza-dC results in up-regulation of CLDN6. (A) mRNA level of *CLDN6* analyzed by qRT-PCR in SK-BR-3, DAN-G, PA-1 and NIH-OVCAR3 cells either untreated or treated with 2 µM or 10 µM 5-aza-dC for 72 h. Mean and standard deviation of at least two independent experiments are shown. (B) Western Blot analysis of CLDN6 protein in SK-BR-3, DAN-G, PA-1 and NIH-OVCAR3 cells either untreated or treated with 2 µM or 10 µM 5-aza-dC for 72 h. β-actin was used as loading control.

These results suggest that the promoter of CLDN6 is methylated in SK-BR-3 and DAN-G cells whereas in PA-1 and NIH-OVCAR3 cells an unmethylated promoter region is present and disclose that CLDN6 could be regulated by DNA methylation.

To confirm CpG methylation of the CLDN6 promoter at sequence levels, the promoter regions upstream of the transcription start site (TSS) of *CLDN6-001* and *CLDN6-201/-002* covering both CpG islands were examined by bisulfite sequencing in different tumor cell lines. Bisulfite sequencing is a method to determine the DNA methylation pattern at sequence levels. Treatment of gDNA with sodium bisulfite results in conversion of unmethylated cytosine (C) residues into uracil (U) by deamination whereas methylated cytosines remain unchanged

because the methyl group protects against cleavage (Figure 25). Thus, bisulfite treatment results in specific changes in the DNA sequence which can be compared to a genomic reference DNA in order to determine the methylation pattern.

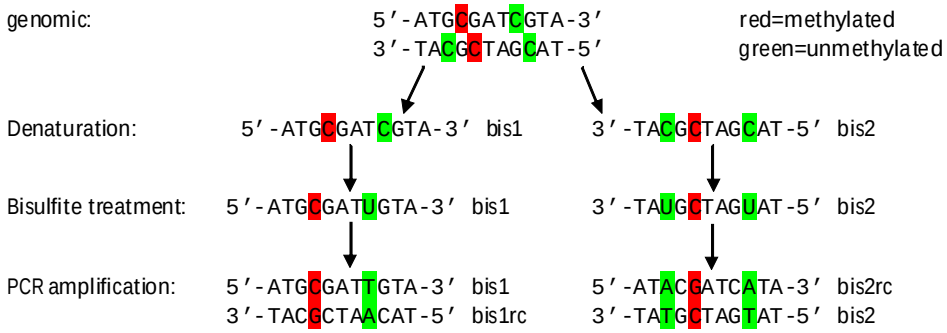

Figure 25 Bisulfite treatment of gDNA results in conversion of unmethylated cytosines. Denaturation of gDNA results in DNA strand separation, sense-strand is named bis1, antisense strand is named bis2. Bisulfite treatment results in conversion of unmethylated C to U. Amplification by PCR is necessary to obtain dsDNA. rc = reverse complement.

Genomic DNA from tumor cells was bisulfite converted and specific promoter regions covering both CpG islands were amplified by PCR with bisulfite-specific primers and subsequently sequenced by Sanger-Sequencing. It is important that the PCR-amplicons are not longer than 500 bp because the bisulfite leads to an enormous fragmentation of DNA during conversion and it is problematic to amplify longer fragments from bisulfite converted DNA. Therefore, four to five overlapping fragments of both promoter regions were amplified by PCR, cloned and 10 clones per fragment were analyzed for every cell line. Comparison of the bisulfite converted DNA to the genomic reference DNA uncovers methylated and unmethylated cytosines.

The promoter region -1181 to +25 bp in front of *CLDN6-001* harboring the first CpG island was analyzed in DAN-G and PA-1 cells. Interestingly, in both cell lines regardless of the CLDN6 expression status, the promoter region was nearly completely demethylated (Figure 26). This either implicates that this region is not important for the regulation of CLDN6-001 or that methylation is not an important factor for the regulation of CLDN6-001 in DAN-G and PA-1 cells. Furthermore it is possible that this CpG island is primarily important for the regulation of genes which are located on the forward strand of chromosome 16 (Figure 4 in chapter 1.4.1). Thus, all further studies were concentrated on the regulation of *CLDN6* on the promoter region of *CLDN6-201/-002*.

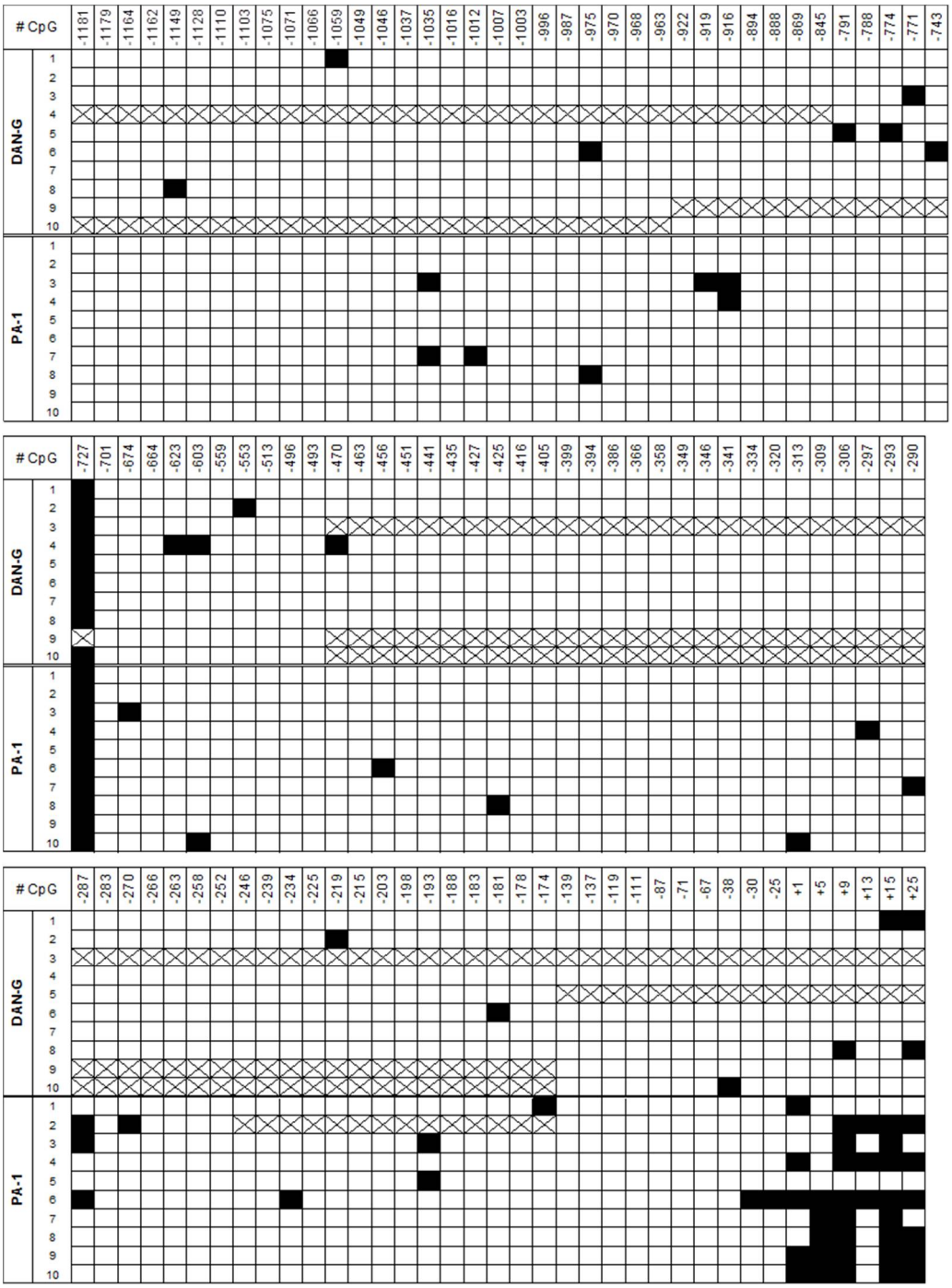

Figure 26 *CLDN6-001* promoter region (-1181 to +25 bp) is highly demethylated in DAN-G and PA-1 tumor cells. gDNA from DAN-G and PA-1 cells was treated with bisulfite for conversion. PCR was performed on bisulfite-converted DNA to amplify promoter fragments. The PCR-products were cloned into TOPO-TA-vectors and purified plasmid DNA was sent for sequencing. 10 clones per cell line were analyzed by bisulfite sequencing. Black boxes represent methylated cytosines and white boxes unmethylated cytosines. X designates failed sequencing of the corresponding clone.

Next, the promoter region upstream of *CLDN6-201/-002* harboring the second CpG island was analyzed by bisulfite sequencing in DAN-G, PA-1 and NEC-8 cells. In contrast to CLDN6-001 promoter region, a remarkable difference in CpG methylation was found between CLDN6-negative DAN-G cells and CLDN6-positive PA-1 and NEC-8 cells (Figure 27). Nearly the entire analyzed region from

-480 to +230 bp respective to the TSS of *CLDN6-201/-002* was found to be methylated in DAN-G cells whereas in PA-1 and NEC-8 cells almost no methylated cytosines were present. Interestingly, the CpG at position +8 bp was methylated in all tested clones by Sanger Sequencing. Furthermore, CpG/+8 bp is the last CpG of the amplified fragment in close proximity to the primer, suggesting that the methylated CpG could be due to an error during primer elongation. However, this could not be confirmed by NGS using other primers (Figure 30), thus it is proposed to be an artifact of Sanger-sequencing without regulative importance.

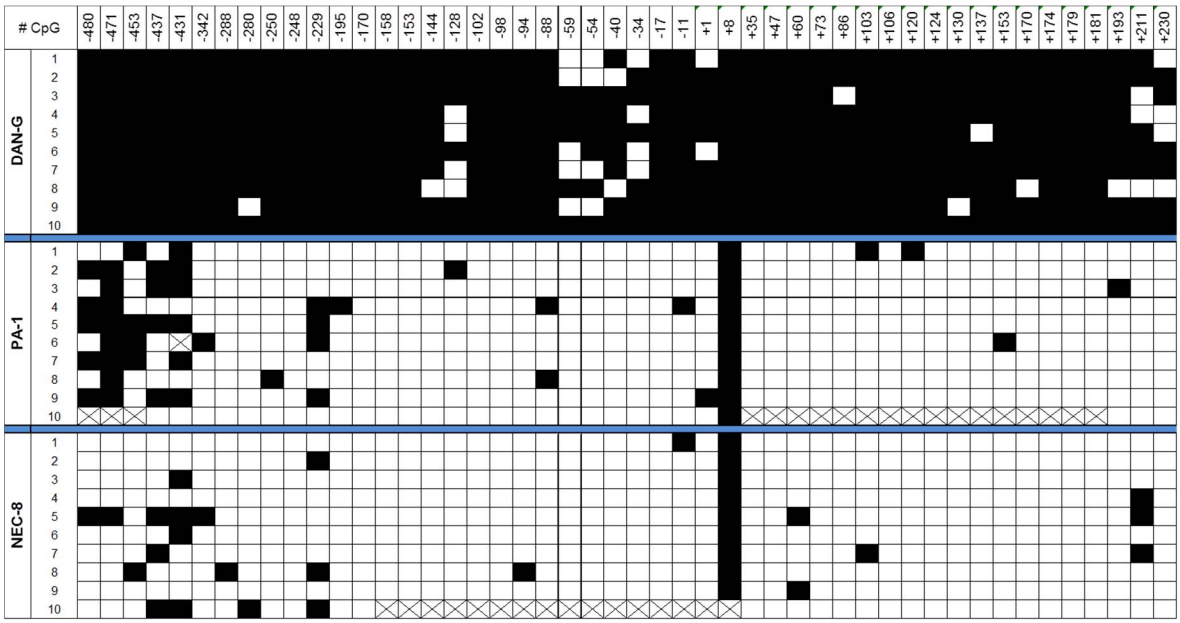

Figure 27 *CLDN6-201/-002* promoter region (-480 to +230 bp) displays differences in methylation between DAN-G and PA-1 or NEC-8 tumor cells. gDNA from DAN-G, PA-1 and NEC-8 cells was treated with bisulfite for conversion. PCR was performed on bisulfite-converted DNA to amplify promoter fragments. The PCR-products were cloned into TOPO-TA-vectors and purified plasmid DNA was sent for sequencing. 10 clones per cell line were analyzed by bisulfite sequencing. Black boxes represent methylated cytosines, white boxes unmethylated cytosines. X designates failed sequencing of the corresponding clone.

Because the promoter region -480 to +230 bp at the TSS of *CLDN6-201/-002* showed these intriguing differences in methylation frequency between CLDN6-positive and - negative cell lines, it was examined if this is also valid for human ovarian and lung tumor samples. To confirm the results obtained from bisulfite sequencing and to test a larger cohort of samples, a method to analyze the DNA methylation pattern via next generation sequencing (NGS) was established in this study. A proof of concept with targeted sequencing of 12 samples per flow cell lane was established using an ultraplexing approach in which sample-specific barcodes were introduced by PCR (Figure 28). The barcodes allow to map the sequence reads to the different reference sequences of every single sample

during bioinformatics analysis of the results. Primers for six overlapping fragments covering region -545 to +230 of the *CLDN6-201/-002* promoter were generated. Amplicon sizes were chosen to be shorter than 200 bp to ensure that no information gets lost, because when using paired end sequencing the read lengths are around 200 bp. As six different overlapping fragments were generated, all six fragments from one sample shared the sample-specific barcode.

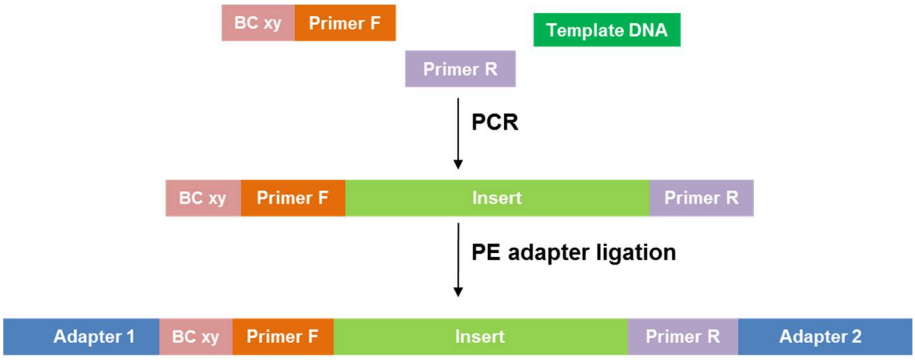

Figure 28 Assembly of *CLDN6* promoter fragments for NGS. Forward primer (Primer F) with sample-specific barcodes (BC xy), reverse primer (Primer R) and template DNA (bisulfite converted DNA from normal ovary or lung, ovarian or lung tumor samples or tumor cell lines) were amplified by PCR. Subsequently, paired end (PE) adaptors (Illumina) for paired-end sequencing by NGS were ligated to the PCR products.

Results of NGS analysis are depicted in Figure 29. Bioinformatic analysis was performed by the Computational Medicine Department of TRON gGmbH. Shortly, gained sequence reads were assigned to every single sample by the sample-specific barcode. The bisulfite converted sequences were compared to the genomic sequence of the analyzed *CLDN6* promoter region and percentages of methylation were calculated for every CpG position. As several million clones can be analyzed by NGS, a more distinguished picture of the methylation frequencies for every single CpG dinucleotide was obtained. Results from bisulfite sequencing (Sanger) could be confirmed, as DAN-G cells show a high level of methylation (100 % methylation is indicated by red color, 0 % methylation is indicated by green color) whereas NEC-8 cells appear to be almost completely demethylated. Unexpectedly, both normal ovary and lung showed a very high degree of demethylation of the *CLDN6* promoter region. This was surprising because CLDN6 is not expressed in adult normal tissues and if DNA-methylation of the promoter region has a main impact on gene expression, the promoter region would be expected to be methylated in normal tissues.

Intriguing differences between CLDN6-positive and –negative lung and ovarian tumors were found. In lung cancer samples, both CLDN6-positive samples are

overall less methylated compared to CLDN6-negative samples. It is apparent that in all tumor samples the region downstream of the TSS (+8 to +193) is higher methylated compared to the remaining tested promoter region. Remarkable differences were found in the methylation of certain regions within the *CLDN6* promoter between different patients, for example, sample #1337 (CLDN6-negative ovarian cancer) was highly demethylated in region -342 to +8 bp but highly methylated in region +103 to +193 bp, whereas #184 (CLDN6-negative ovarian cancer) was in the entire tested region methylated at high levels. Moreover, #1337 displayed a comparable methylation pattern to #1325, a CLDN6-positive ovarian cancer sample.

	Tumor cell lines		Normal tissues		Lung cancer				Ovarian cancer			
					CLDN6 positive		CLDN6 negative		CLDN6 positive		CLDN6 negative	
# CpG	DAN-G	NEC-8	ovary # 426	lung # 817	# 562	# 4404	# 743	# 810	# 779	# 1325	# 184	# 1337
-480	70,46	24,13	54,04	59,27	56,63	52,20	77,82	71,70	25,54	40,67	79,39	55,97
-471	68,13	28,18	53,33	60,53	54,77	45,51	75,88	69,06	24,51	36,01	80,53	60,72
-453	39,08	20,84	42,95	38,39	33,65	26,91	50,51	46,34	14,52	24,57	58,80	39,45
-437	36,75	32,25	32,30	31,45	34,49	29,61	50,17	48,22	15,29	25,33	61,42	28,42
-431	47,78	32,21	56,91	45,85	45,17	37,32	62,28	59,57	22,91	33,38	70,24	47,19
-342	81,60	9,20	25,99	13,48	13,19	20,18	29,59	29,10	6,93	11,86	55,84	11,72
-288	77,44	10,41	13,57	15,34	16,28	13,72	26,77	32,19	10,65	13,83	53,99	19,86
-280	77,37	15,40	23,26	15,94	16,36	12,81	24,72	32,93	10,13	14,38	53,44	18,85
-250	77,19	10,04	25,14	11,79	11,55	10,64	20,06	32,88	8,64	12,39	51,54	17,17
-248	78,02	10,28	16,72	10,51	10,47	10,04	18,29	32,10	7,85	11,75	51,01	24,16
-229	77,42	12,14	15,73	15,51	16,87	17,21	30,34	37,88	10,38	13,20	51,89	26,88
-195	75,95	9,49	10,30	10,81	10,77	12,32	22,18	30,09	8,97	13,65	43,16	13,40
-170	70,61	8,46	7,08	8,09	8,13	9,36	16,62	23,86	7,38	11,83	39,86	11,06
-158	71,59	8,75	7,07	8,27	8,59	8,76	15,61	25,60	7,04	12,05	40,44	10,68
-153	74,96	9,29	12,88	13,25	14,04	14,25	25,50	31,13	10,29	15,79	44,65	34,86
-144	61,35	6,78	7,23	8,26	8,18	7,65	13,76	22,21	7,13	11,24	38,71	14,84
-128	60,10	8,92	8,95	9,84	9,74	9,48	17,75	26,59	8,90	13,15	38,55	12,25
-102	71,88	9,08	8,97	10,32	10,79	10,54	18,66	30,30	9,16	13,16	40,78	11,08
-98	72,86	8,78	9,59	10,92	11,59	11,95	22,69	29,68	9,48	14,15	41,54	12,26
-94	71,39	8,04	8,50	9,71	10,25	9,58	15,54	28,82	8,54	12,72	40,64	10,64
-88	59,87	7,31	6,69	7,57	7,92	7,50	10,08	21,07	6,71	10,77	34,79	8,37
-59	60,11	5,32	5,47	7,75	7,80	6,00	22,00	62,68	5,78	27,15	72,52	11,91
-54	61,38	5,60	5,19	7,18	8,52	6,35	27,15	59,26	5,87	27,25	71,31	11,57
-40	65,90	6,16	5,11	6,98	6,97	5,85	29,27	57,17	4,90	25,92	69,44	8,44
-34	71,73	6,67	6,38	8,01	8,62	7,31	39,45	60,14	6,74	28,82	74,26	16,32
-17	79,72	7,02	7,76	9,63	11,09	10,64	43,63	66,84	7,64	29,66	74,95	16,70
-11	79,87	7,48	8,06	11,09	13,49	10,86	45,84	65,77	8,27	29,88	74,99	14,85
+1 (TSS)	76,05	7,68	8,48	10,16	12,42	12,05	45,03	62,70	8,44	29,49	73,57	15,33
+8	73,37	7,23	7,28	8,78	9,93	9,61	36,17	58,92	7,40	24,23	71,17	12,24
+35	87,11	7,98	10,00	7,72	19,71	22,39	49,83	64,29	6,99	67,29	83,32	44,56
+47	87,88	5,27	3,80	8,99	17,18	14,25	38,70	60,52	4,84	61,86	85,74	16,72
+60	89,31	5,53	5,98	11,69	22,48	30,18	62,09	66,67	15,60	66,10	86,79	38,72
+73	86,12	4,50	9,57	13,38	28,95	27,97	63,01	66,78	16,94	65,57	82,76	23,51
+86	88,72	8,27	22,84	13,89	25,86	32,97	56,04	67,02	13,83	66,83	86,63	44,02
+103	95,34	5,22	25,16	44,83	63,42	62,15	87,16	82,67	28,03	71,55	94,45	87,40
+106	93,85	4,91	12,53	25,79	51,15	43,59	75,07	74,12	26,26	70,87	92,10	49,10
+120	93,60	4,04	19,49	28,94	42,99	43,87	76,45	70,60	26,05	69,21	92,01	76,76
+124	94,78	5,99	9,43	33,01	48,86	48,47	82,28	75,94	19,96	71,53	92,35	85,26
+130	89,51	4,22	6,26	13,33	19,02	16,55	45,02	57,68	8,86	61,14	87,59	72,33
+137	94,13	5,92	9,29	32,93	48,54	47,74	81,53	75,70	19,68	71,43	91,64	85,06
+153	86,28	9,87	9,98	36,78	44,04	43,45	77,52	79,94	38,10	78,58	86,67	80,69
+170	53,29	7,15	9,49	25,40	38,65	24,95	63,12	67,93	25,81	61,44	65,50	60,25
+174	72,27	7,73	13,70	30,08	35,45	27,58	76,56	64,73	32,69	75,89	59,52	77,97
+179	73,06	11,15	14,31	36,65	48,93	48,09	70,57	70,01	31,86	67,96	73,12	69,78
+181	74,89	12,30	20,55	41,95	57,69	51,72	73,55	70,98	32,05	68,93	74,52	71,75
+193	67,07	10,37	14,28	33,55	39,03	34,54	65,92	63,16	21,00	63,82	69,36	66,90
+211	42,68	9,57	8,15	20,66	24,95	25,81	49,17	44,06	20,66	46,46	47,26	24,98
+230	35,85	9,45	8,33	16,81	21,81	19,99	33,84	36,04	16,57	48,01	26,88	23,01

100% → 0%
methylated

Figure 29 NGS analysis of CpG methylation of the *CLDN6-201/-002* promoter region (-480 to +230 bp) reveals differences in methylation between tumor cell lines, primary normal and tumor tissues. gDNA of tumor cell lines DAN-G and NEC-8, normal ovarian and lung tissue samples as well as lung and ovarian cancer samples were bisulfite converted, bisulfite converted DNA was amplified and sample-specific barcodes were introduced by PCR and subsequently prepared for paired-end NGS on an Illumina HiSeq instrument. The sample-specific barcodes allowed running of 12 samples in one single lane (ultraplexing) and were used

in following bioinformatics analysis to define which reads belong to which sample. Percentages of methylation are shown. 100 % methylation of the corresponding CpG is marked red, 50 % is marked white and 0 % is marked green. Bioinformatic analysis of NGS results were performed by the Computational Medicine Department of TRON gGmbH.

To validate the results from primary materials, three samples were chosen and sequenced by normal Sanger-Sequencing (Figure 30). All analyzed samples, normal ovary (#426), ovary-cancer CLDN6-positive (#779) and ovary-cancer CLDN6-negative (#1337) show the same methylation patterns as obtained by NGS analysis. Interestingly, only by Sanger sequencing the CpG at position +8 is methylated in every sample. Using NGS, a difference in methylation frequency is observed between the samples. This indicated that the detected methylated CpG at position +8 by Sanger Sequencing is the result of a systematical error or an artifact of sequencing, either Sanger or NGS.

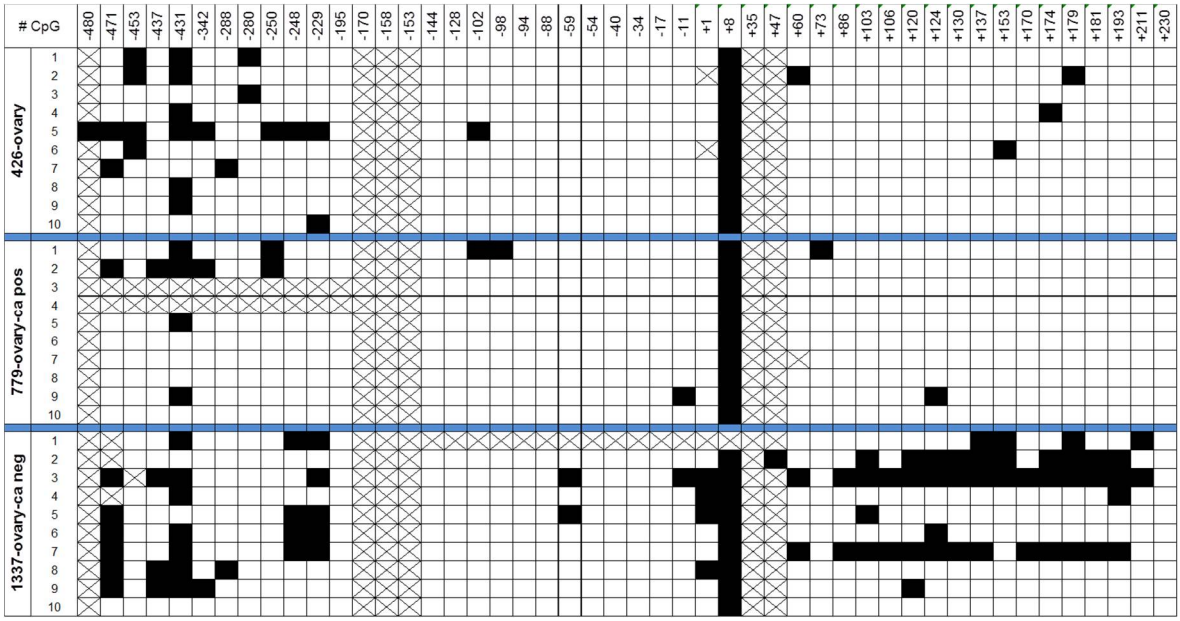

Figure 30 Sanger Sequencing of *CLDN6-201/-002* promoter region (-480 to +230 bp) of an ovary sample (#426) and two tumor samples (#779 and #1337) confirms NGS results. gDNA of the indicated samples was treated with bisulfite for conversion. PCR was performed on bisulfite-converted DNA to amplify promoter fragments. The PCR-products were cloned into TOPO-TA-vectors and purified plasmid DNA was sent for sequencing. 10 clones per sample were analyzed by bisulfite sequencing. Black boxes mark methylated cytosines, white boxes mark unmethylated cytosines. X designates failed sequencing of the corresponding clone.

To analyze the methylation level of the *CLDN6* promoter in a larger cohort of samples, a methylation-specific qPCR (MSqPCR) was established. MSqPCR is a more rapid and cost-effective method to assess the methylation status of groups of CpG sites within a CpG island. MSqPCR is performed on bisulfite converted DNA with primers specific for methylated versus unmethylated DNA [195]. Quantitative PCR allows determination of the amount of target sequence present in the sample. The lower the Ct value (threshold cycle), the more amount of target sequence is

present. Here, primers specific for two regions of the *CLDN6* promoter were designed, both specific either for unmethylated or methylated DNA, designated assay 1 and 2. Assay 1 covers a region upstream of the TSS of *CLDN6-201/-002*, from -220 to -101 bp, assay 2 a region downstream of the TSS, from -40 to +80 bp.

First, the assays were tested in tumor cell lines with different CLDN6 expression (Figure 31). The CLDN6-negative cell lines DAN-G and SK-BR-3 appeared in both assays to be highly methylated because low Ct values were obtained in PCR with primers specific for methylated DNA. As mentioned before, low Ct values indicate the presence of high amount of target sequence in the sample. In contrast, primers specific for unmethylated DNA lead to high Ct values in DAN-G and SK-BR-3 cells indicating that low amount of the target sequence is present. CLDN6 high expressing cell lines NEC-8, PA-1 and NIH-OVCAR3 exhibited low Ct values in the assays with primers specific for unmethylated DNA but very high Ct values in the assays with primers specific for methylated DNA. This result shows that NEC-8, PA-1 and NIH-OVCAR3 cells display unmethylated CpG sites in the analyzed regions. Interestingly, the only cell line which has no tumorigenic origin, HEK-293 cells, appeared to be unmethylated in the analyzed *CLDN6* promoter region but shows only very low endogenous expression of CLDN6. Indeed, later Western blot analysis revealed that HEK293 cells are slightly positive for CLDN6 (Figure 40). The source of the cell line is human embryonic kidney and CLDN6 is known to be expressed in embryonic tissues. However, as HEK293 is an immortalized cell line, CLDN6 expression can also account for aberrant up-regulation in these cells. Several controls were included to validate MSqPCR. Human methylated standard DNA (HMS) is enzymatically methylated. It served as negative control for unmethylated assays but as positive control for methylated assays. Indeed, Ct values of 40 are obtained in the unmethylated assays 1 and 2 whereas Ct values of ~25 are obtained in the methylated assays indicating specific detection of methylated DNA using primers specific for methylated DNA of both assays. DNA from peripheral blood lymphocytes (PBL) and sperm were used either as positive control for unmethylated assays or negative control for methylated assays. Sperm DNA is completely demethylated whereas PBL shows a high degree of demethylation. This is reflected in MSqPCR as sperm DNA shows Ct values of 40 in the methylated assays but ~25 in the unmethylated assay. In the unmethylated

assays, high Ct values for PBL DNA indicate a high degree of demethylation whereas the methylated assays reveal that PBL DNA is indeed not completely demethylated. Furthermore, gDNA was used to ensure that primers bind specifically bisulfite converted DNA which indeed was the case for every single assay. A no template control was included to detect contaminations or primer dimers.

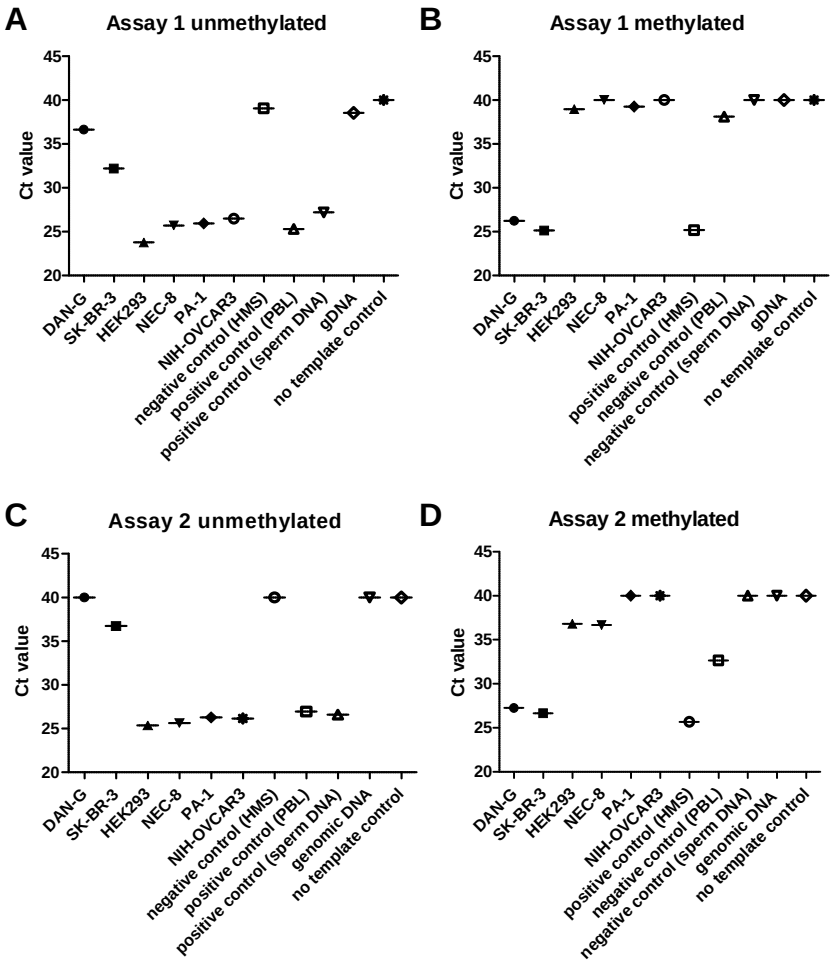

Figure 31 *CLDN6* promoter is methylated in CLDN6-negative cell lines but unmethylated in CLDN6-positive cell lines. (A and B) Methylation-specific qPCR assay 1 in region -220 to -101 bp and (C and D) assay 2 in region -40 to +80 bp of the CLDN6-201 and CLDN6-002 promoter. PCR was performed with either primers specific for unmethylated (A, C) or methylated (B, D) DNA on bisulfite converted DNA from tumor cell lines DAN-G, SK-BR-3, HEK-293, NEC-8, PA-1 and NIH-OVCAR3. As controls, a bisulfite converted human methylated standard DNA (HMS), bisulfite converted DNA from peripheral blood lymphocytes (PBL), bisulfite converted DNA from sperm or genomic sperm DNA was used.

Furthermore, the MSqPCR assays 1 and 2 were used to analyze a larger cohort of normal tissues as well as lung and ovarian cancer samples which are positive or negative for CLDN6 expression. For the analysis, two samples of each of the following normal tissues were tested: colon, liver, lung, kidney, ovary, pancreas, placenta and testis. Moreover, ten lung and ovarian tumor tissues, five CLDN6 positive and five CLDN6 negative respectively were included in the analysis.

Results of these assays are depicted in Figure 32. In normal tissues, both assays displayed high Ct values using primers specific for unmethylated DNA. However, primers specific for methylated DNA revealed a more distinguished picture. In assay 1, placenta appeared to be the only tissue that shows a high grade of methylation and was validated also in assay 2 (Figure 32 A, C). The other normal tissues were found to be unmethylated in the region of assay 1 whereas in assay 2 slight discrepancies were observed. These results indicate that the CLDN6 promoter is virtually not methylated in normal tissues except placenta. To be sure that placenta is methylated, the used samples have to be sequenced.

In tumor tissues, it was also observed that the assays specific for unmethylated DNA exhibit a higher amplification (Ct values ~25) in all samples. Minor differences were observed between CLDN6-positive and -negative tumor samples in both assays. CLDN6-negative tumor samples showed in the unmethylated assays a low decrease in Ct values compared to CLDN6-positive tumor samples. Accordingly, it was observed that CLDN6-positive tumors are lower methylated as CLDN6-negative tumors because the assays specific for methylated DNA exhibited a lower amplification in CLDN6-positive tumor samples, both of lung and ovary (Figure 32 B, D). This indicates that the *CLDN6* promoter region is higher methylated in CLDN6-negative lung and ovarian tumor samples compared to CLDN6-positive samples and confirms hereby the results obtained by NGS (Figure 29).

However, MSqPCR has several disadvantages. To avoid these, the following was considered: first, two assays were designed in different regions of the *CLDN6* promoter (up- as well as downstream of the TSS), second, a minimum of three CpGs were included per primer (methylated and unmethylated) to span a larger section of the promoter and have a higher validity per assay and third, the primers for methylated and unmethylated DNA were designed in the same regions. The two latter points are challenging and not always possible due to sequence-related availability of CpGs, possible primer lengths and minimal or maximal possible annealing temperatures of the used primers. Noteworthy, a problem in MSqPCR is that methylation specific primers also often bind to unmethylated DNA with mismatches at the 3’ end of the primer during annealing. The *Taq* DNA polymerase can efficiently elongate these primers regardless of primer mismatch. Vice versa, primers specific for unmethylated DNA have a high frequency of

mismatch if only few CpGs are covered by the primer. For this reason primers that cover a minimum of three CpG sites were designed. For a final conclusion it is important that methylated and unmethylated assays are considered in conjunction.

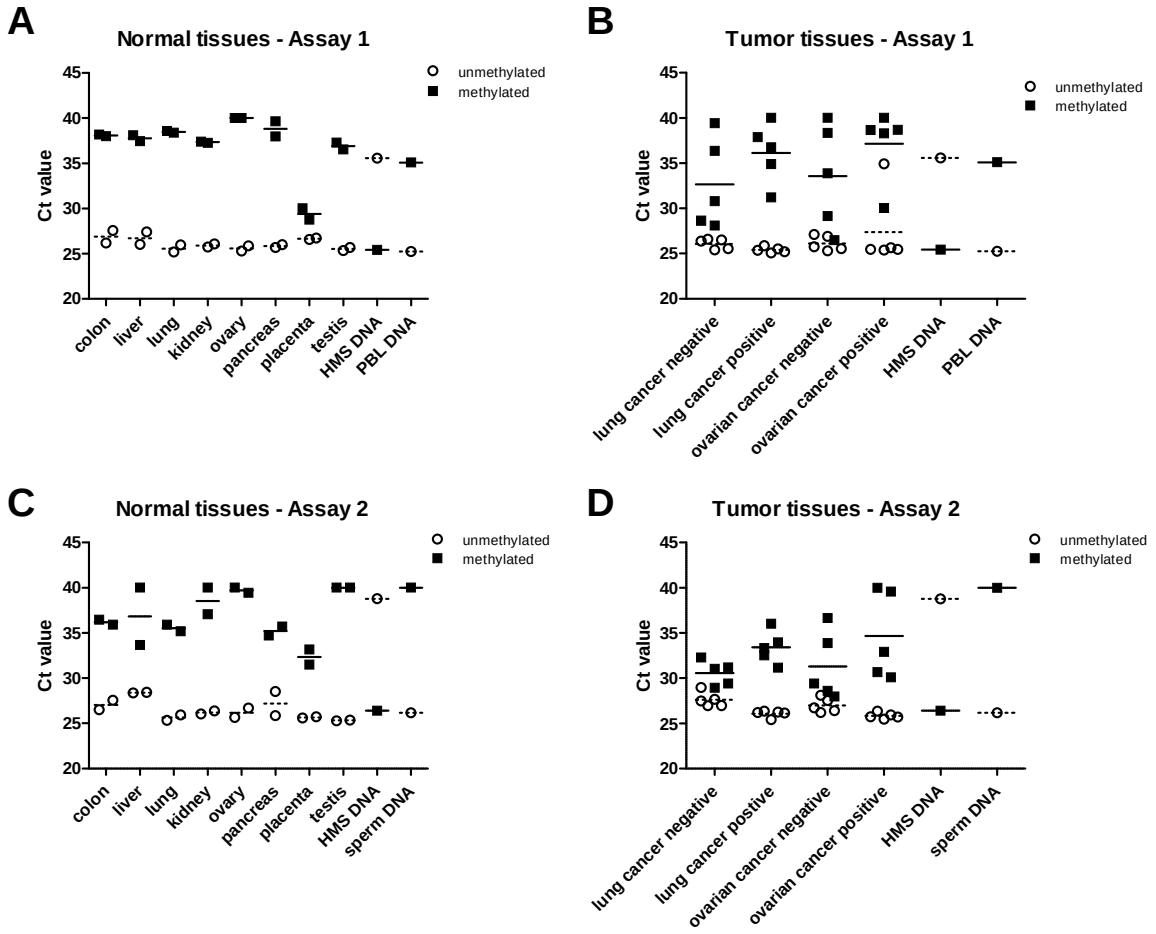

Figure 32 Methylation-specific qPCR in various normal tissues and tumor tissues (lung and ovarian cancer, positive or negative for CLDN6) displays differences in promoter methylation frequencies. (A and B) Assay 1 in region -220 to -101 bp and (C and D) assay 2 in region -40 to +80 bp of the CLDN6-201 and CLDN6-002 promoter on normal or tumor tissues. PCR was performed with either primers specific for unmethylated or methylated DNA on bisulfite converted DNA from normal or tumor tissues. As controls, a bisulfite converted human methylated standard DNA (HMS), bisulfite converted DNA from peripheral blood lymphocytes (PBL) or bisulfite converted DNA from sperm was used.

To conclude, CpG methylation is an important factor in the regulation of *CLDN6* but it seems to be not sufficient to induce CLDN6 expression. If so, the *CLDN6* promoter would be also methylated in normal tissues in which CLDN6 is not expressed endogenously. Therefore, other factors, like tumor-specific transcription factors have to be responsible for the differential regulation of CLDN6 in cancer.

4.2.7 The transcription factors BORIS/CTCFL and CTCF are possible regulators of CLDN6 in cancer

To gain more insight into the regulation of CLDN6 beyond DNA methylation and which transcription factors may be involved, the *CLDN6* promoter region was analyzed in more detail for existing transcription factor binding sites. Several databases exist in which shared ChIP-sequencing (ChIP-Seq) data from different groups are available for a particular genomic location. ChIP-sequencing combines ChIP in which protein-DNA interactions are analyzed and high-throughput sequencing using genome sequencers. ChIP is performed with an antibody against a specific transcription factor and the purified DNA is subsequently sequenced by NGS. Here, it was searched for published transcription factor ChIP-sequencing results at the *CLDN6* promoter in UCSC genome browser and Encyclopedia of DNA elements (ENCODE) database of the University of California Santa Cruz (http://genome-euro.ucsc.edu/). Indeed, ChIP-seq results are available for different tumor cell lines and the human embryonic stem cell line H1-hESC indicating binding of the transcription factor CTCF in the *CLDN6* promoter region (Figure 33).

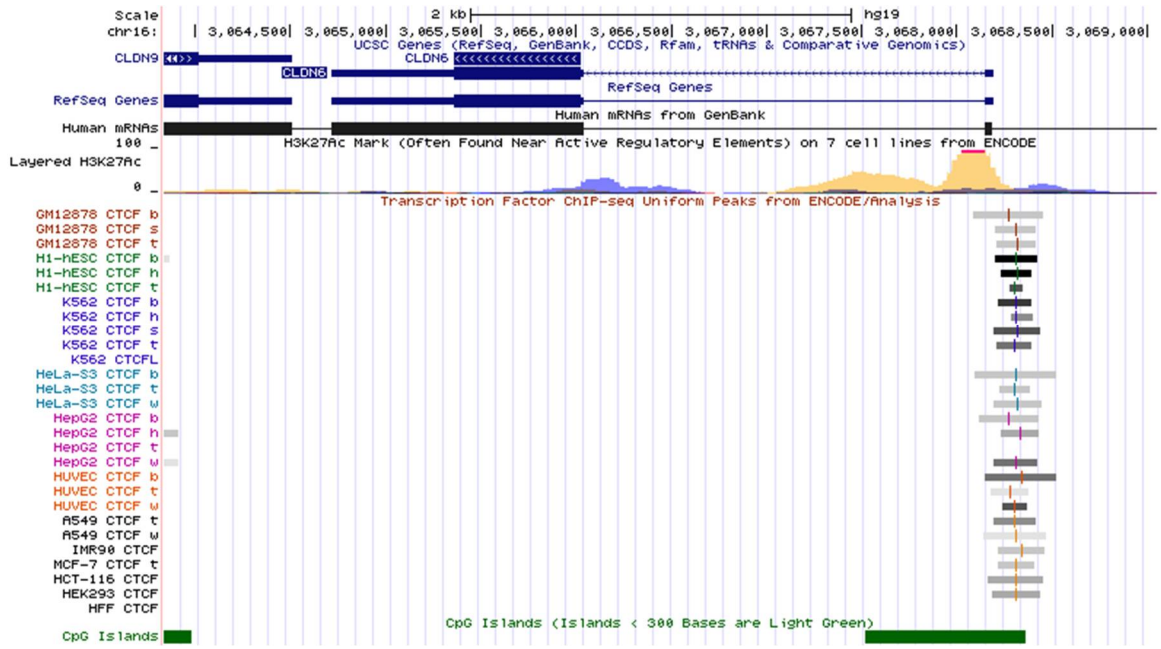

Figure 33 ChIP-Seq data available in UCSC genome browser / ENCODE database indicate binding sites for CTCF and BORIS/CTCFL at the *CLDN6* promoter. In the upper part, the chromosomal location, UCSC and Ref-Seq genes (here CLDN6) are shown in blue and the human mRNA (GenBank) is shown in black. Acetylation of histone H3K27 which is often found near active regulatory elements is highly enriched at the CLDN6 promoter. Transcription factor ChIP-Seq peaks for CTCF can be found in various cell lines at the

CLDN6 promoter. In green, location of CpG islands at CLDN6 promoter is shown. Graphic was downloaded from http://genome-euro.ucsc.edu/ on 4/9/2013; assembly to human genome GRCh37/hg19.

As CTCF and its paralog BORIS/CTCFL (named BORIS in the following parts) share the same DNA binding motif, it is possible that BORIS binds to the *CLDN6* promoter as well. The only BORIS-ChIP-Seq data which can be found in the ENCODE database is in the leukemia cell line K562, where no binding of BORIS was observed at the *CLDN6* promoter. Accordingly, CLDN6 is only very weakly expressed in K562 cells (Figure 13 B). Moreover, ChIP-Seq data for other transcription factors as CTCF and BORIS are available (e.g. Nanog, GATA, ATF) but no enrichment was observed for these factors at the *CLDN6* promoter. Indeed, BORIS and CTCF are expressed at high levels in NIH-OVCAR3 and NEC-8 cells (Figure 38). To analyze if BORIS or CTCF are crucial for CLDN6 expression, siRNA mediated silencing of both factors was performed in NIH-OVCAR3 and NEC-8 cells. Interestingly, silencing of *BORIS* resulted in both cell lines in a down-regulation of *CLDN6* 96 h after transfection whereas silencing of *CTCF* resulted in an up-regulation of *CLDN6* already 48 h after transfection (Figure 34). This indicates that CTCF might serve as a repressor and BORIS as an activator of CLDN6 expression in NEC-8 and NIH-OVCAR3 cells.

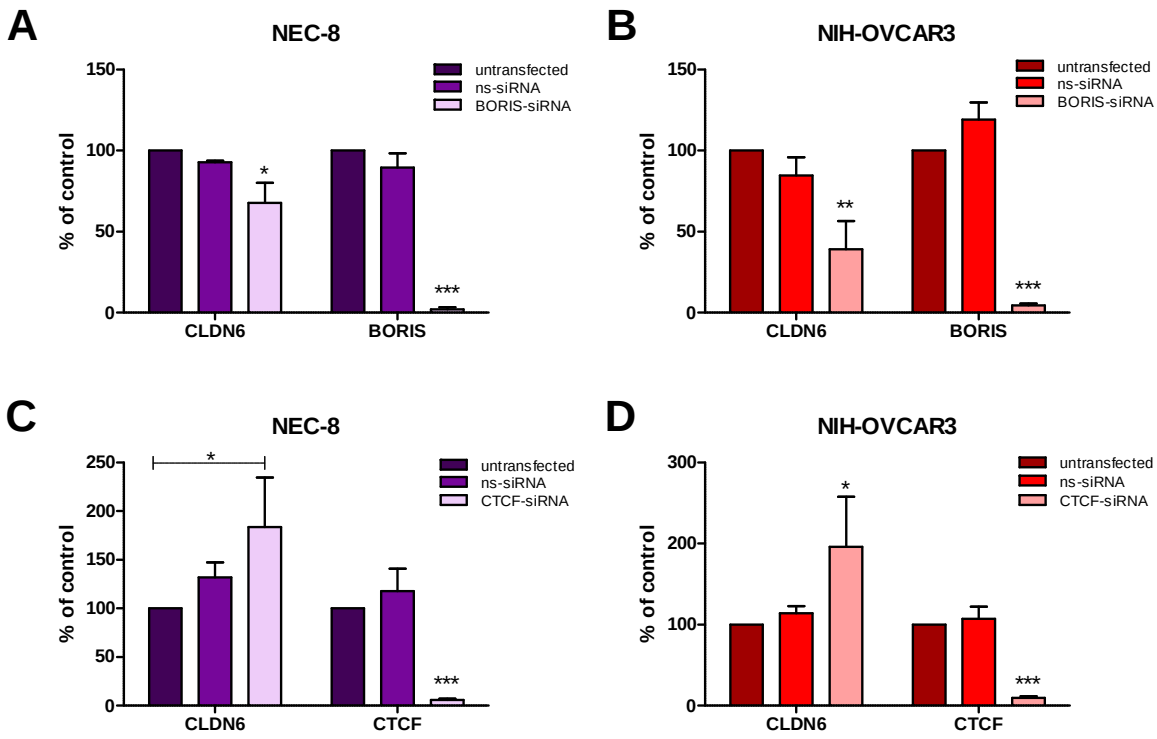

Figure 34 RNAi-mediated silencing of *BORIS* and *CTCF* results in deregulation of *CLDN6* in NEC-8 and NIH-OVCAR3 cells. NEC-8 and NIH-OVCAR3 cells were either not transfected or transfected with *non-silencing (ns)* -siRNA, *BORIS*-siRNA (A, B) or *CTCF*-siRNA (C, D). *CLDN6* mRNA expression was analyzed 48 h after transfection in *CTCF*-silenced cells and 96 h after transfection in *BORIS*-silenced cells by qRT-PCR.

Relative expression levels of *CLDN6*, *CTCF* and *BORIS* were normalized to *HPRT1* and are shown as percent (%) of the respective expression in untransfected control cells.

The next step was to analyze which regions in the *CLDN6* promoter are crucial for its expression. For this purpose, a dual luciferase reporter assay was performed. Using this assay, simultaneous expression of two individual luciferase reporter enzymes, firefly (*Photinus pyralis*) and *Renilla* (*Renilla reniformis*) luciferase, can be measured. Both luciferases do not require post-translational modifications and function as genetic reporters immediately following translation. Firefly luciferase catalyzes the oxidation of beetle luciferin to oxyluciferin in an ATP / Mg^{2+} and O_2 – dependent manner. *Renilla* luciferase catalyzes the oxidation of coelenterazine to coelenteramide. In both biolumniscent reactions, emitted light corresponds to promoter activity.

A fragment of the *CLDN6* promoter located 1483 bp upstream of the CLDN6 transcription start site to +74 bp was analyzed using MatInspector (Genomatix) to identify potential transcription factor binding sites (Figure 35). For this study interesting transcription factors were CTCF/BORIS because of the aforementioned results, SP/GC-Box binding factors because it is known that SP1 is involved in the regulation of CLDN3 and 4 [196,197], cAMP-responsive element binding proteins (CREB) and E2F transcription factors which are known to be involved in EGFR-signaling that is involved in regulation of many claudins [198,199] and any factors that are involved in embryonic signaling pathways which are known to be deregulated in cancer. To get a first insight which region of the *CLDN6* promoter is important for its expression, six deletion constructs (deletion 1 to 6) were generated in ~200 bp steps and cloned into the multiple cloning site (MCS) between *NheI* and *HindIII* restriction sites of the promoter-less luciferase reporter vector pGL4.76 [*hRluc/Hygro*] which encodes for *Renilla* luciferase (Figure 35, Figure 36 A, B).

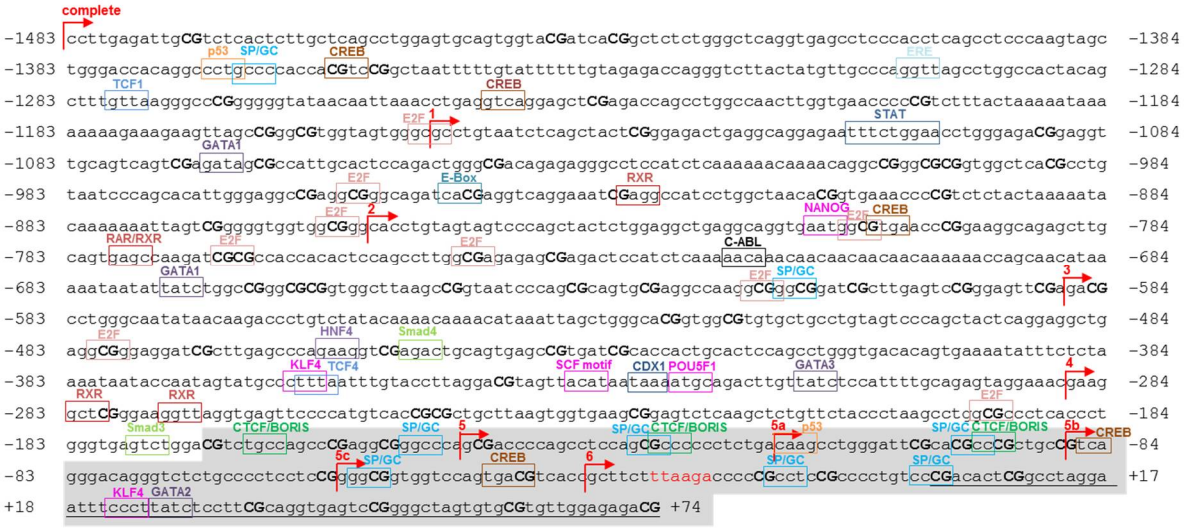

Figure 35 Transcription factor binding sites found in the *CLDN6* promoter (-1483 to +74 bp) used for promoter analysis. The transcription start (+1) is underlined, the CpG island is highlighted in grey, TATA-Box is in red letters, constructs are marked with arrows (complete = -1483 to +74 bp, deletion 1 = -1148 to +74 bp, deletion 2 = -854 to +74 bp, deletion 3 = -587 to +74 bp, deletion 4 = -287 to +74 bp, deletion 5 = -145 to +74 bp, deletion 5a = -115 to +74 bp, deletion 5b = -87 to +74 bp, deletion 5c = -57 to +74 bp, deletion 6 = -33 to +74 bp). The core transcription factor binding sites are boxed. Transcription factor binding site prediction was done using MatInspector (Genomatix). SCF = stem cell factor.

The *CLDN6* promoter sequence from -1483 bp to +74 bp was amplified from human genomic DNA from sperm. To normalize variations in transfection efficiency between different experiments the internal control vector pGL4.13 [*luc2/SV40*] was included. This plasmid encodes for firefly luciferase under the control of a SV40 promoter and was co-transfected in every single experiment. The luciferase activity from the control plasmid is used to standardize variations in the luciferase activity from the reporter constructs.

As shown in Figure 36 C, deletion variants 1 to 4 did not result in significant changes of *CLDN6* promoter activity. Deletion 5 resulted in about 50 % decrease of *CLDN6* promoter activity whereas deletion 6 resulted in a nearly complete abrogation of the *CLDN6* promoter activity indicating that this sequence represents the core promoter of *CLDN6*. Subsequently, to further characterize the core promoter region, shorter deletion variants between deletion 5 and 6 of around 30 bp less per construct were generated to analyze which region between deletion 5 and 6 is crucial for *CLDN6* promoter activity.

Deletion 5a resulted in all tested cell lines in a remarkable decrease of *CLDN6* promoter activity which was further reduced in deletion 5 b and 5 c (Figure 36 D). In particular, the only binding sites located in the critical region of deletion 5 and 5 a are binding sites for the transcription factors CTCF or BORIS and p53 indicating that these factors could be involved in regulation of *CLDN6* (Figure 35). Moreover,

binding sites for SP/GC factors are overlapping with the CTCF/BORIS binding sites indicating that these factors bind concerted to the *CLDN6* promoter.

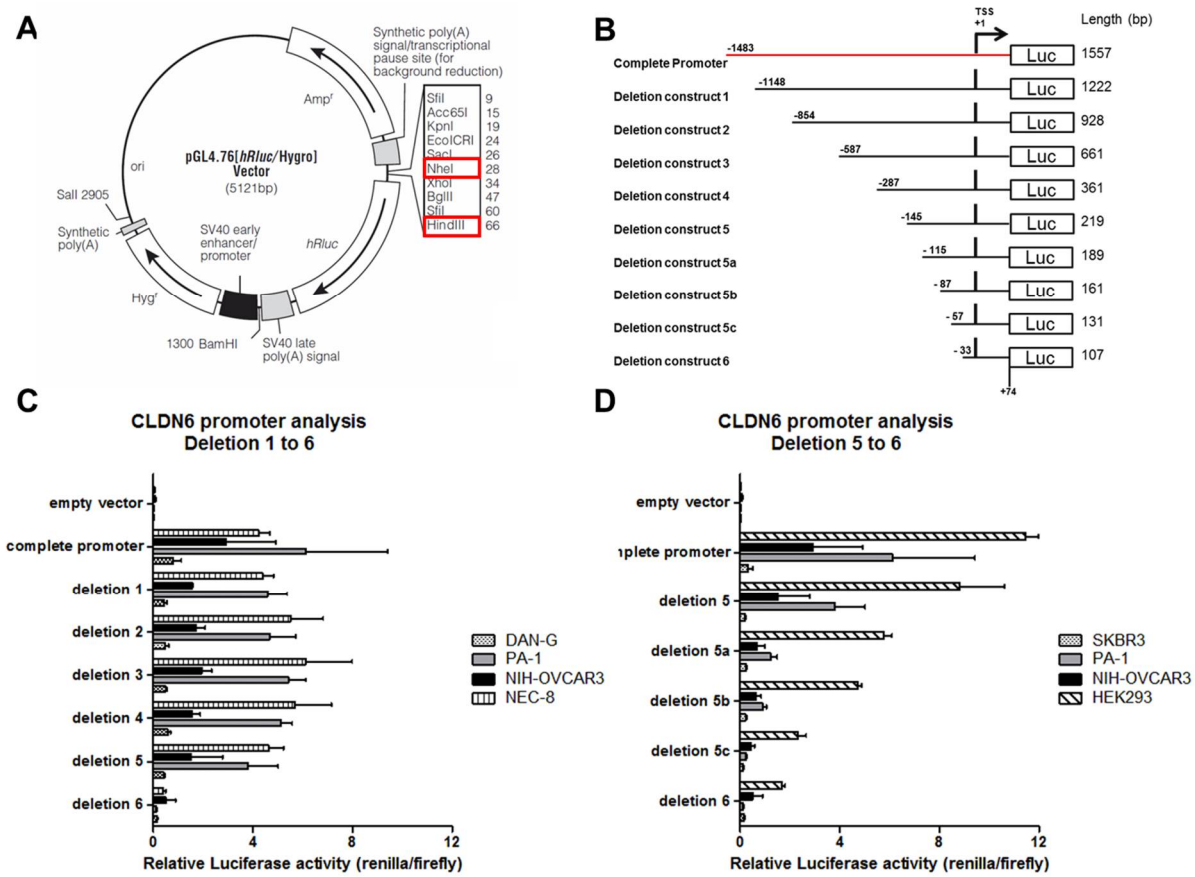

Figure 36 Analysis of the *CLDN6* promoter. (A) For construction of reporter plasmids pGL4.76 with the CLDN6 promoter region or the different promoter deletion variants, PCR products were inserted into the multiple cloning region between NheI and HindIII sites of pGL4.76 basic vector. Vector map is adapted from Promega. (B) Deletion vaiants of the CLDN6 promoter were derived from the complete promoter construct (-1483 bp). +1 means the transcriptional start site (TSS). (C) Dual luciferase reporter gene assay of pGL4.76-complete promoter and deletion variants 1 to 6. DAN-G, PA-1, NIH-OVCAR3 and NEC-8 cells were transfected with the different CLDN6 promoter constructs in pGL4.76 vector and pGL4.13 in a ratio of 50:1. (D) Dual luciferase reporter gene assay of pGL4.76-complete promoter and deletion variants 5, 5a-c and 6. SK-BR-3, PA-1, NIH-OVCAR3 and HEK293 cells were transfected with the different CLDN6 promoter constructs in pGL4.76 vector and pGL4.13 in a ratio of 50:1.

Results from BORIS- and CTCF-silencing as well as the promoter analysis were encouraging that both factors are involved in the regulation of *CLDN6*. The next reasonable step was to analyze if these factors are bound to the *CLDN6* promoter which was examined using ChIP. As mentioned above, besides CTCF and BORIS, p53 could be a possible factor in regulating *CLDN6*. As shown in Figure 35, two binding sites for p53 and three binding sites for CTCF/BORIS exist in the explored *CLDN6* promoter region. Moreover, two further CTCF/BORIS binding sites are found downstream of the TSS and were included in ChIP analysis. Primers spanning the p53 and CTCF/BORIS binding sites were generated for qPCR analysis of ChiP-ed fragments (Figure 37).

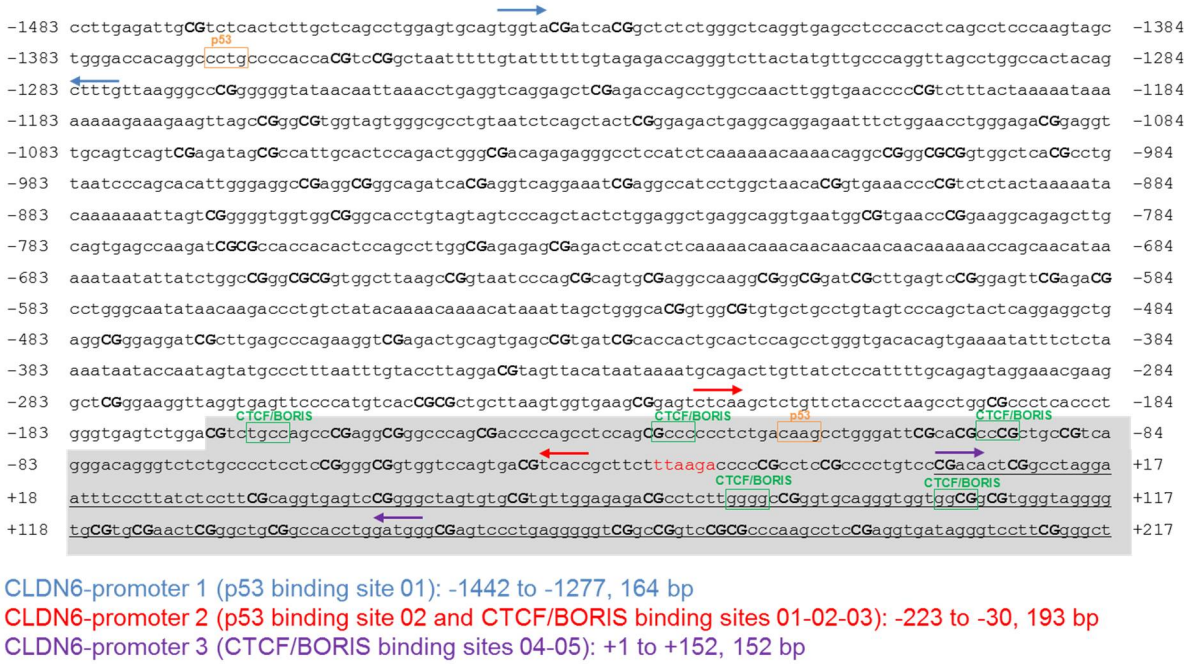

Figure 37 Binding sites for CTCF/BORIS in the *CLDN6* promoter and p53 and primer design for ChIP-qPCR. CLDN6 promoter region from -1483 bp to +217 bp is shown with TATA-Box is indicated in red letters, p53 core binding sites are boxed in orange, CTCF / BORIS core binding sites are boxed in green. CpG island is highlighted in grey. Primers (forward and reverse) are indicated by arrows. Transcription factor binding site prediction was done using MatInspector (Genomatix).

Four different cell lines were chosen for ChIP because of their expression patterns of *BORIS*, *CTCF*, *CLDN6* and *p53* (Figure 38): NIH-OVCAR3 and NEC-8 cells are positive for *BORIS* and *CLDN6* transcript expression whereas SK-BR-3 cells are negative for *BORIS* and *CLDN6*. HEK293 cells are slightly positive for *CLDN6*, negative for *BORIS* and are of non-tumorigenic origin. As CTCF is a unique transcription factor expressed in nearly all tissues, it was conceivable that all cell lines used express *CTCF* mRNA at high levels. SK-BR-3 and NIH-OVCAR3 are known to have mutated p53 whereas HEK293 and NEC-8 contain wild type p53 [200,201]. Interestingly, expression levels of *TP53* are not altered if p53 is mutated or wild type (Figure 38). Thus, four cell lines with different compositions of the distinct factors were analyzed.

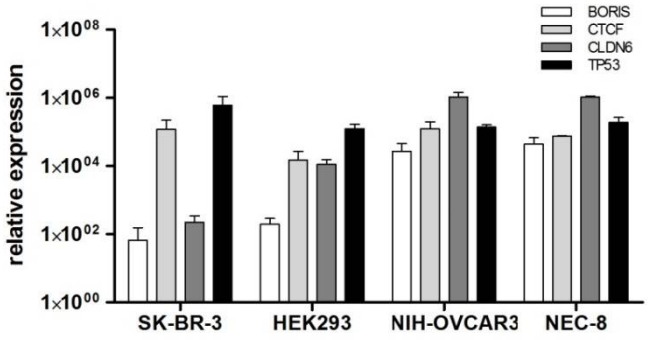

Figure 38 Endogenous expression of *BORIS, CTCF, CLDN6* and *TP53* in SK-BR-3, HEK293, NIH-OVCAR3 and NEC-8 cells. qRT-PCR analysis of *BORIS, CTCF, CLDN6* and *TP53* mRNA expression in the cell lines used for ChIP assay. Relative expression of *BORIS, CTCF, CLDN6* and *TP53* was calculated according to the ΔΔCt method with normalization to expression of the reference gene *HPRT1* and an internal calibrator (40 - average of HPRT1 values of all samples).

Crucial for an efficient ChIP assay is the antibody. For CTCF and p53 very good antibodies are described in the literature [161,202,203]. However, no ChIP-grade anti-BORIS antibody exists. Therefore, an HA-tag was introduced by PCR at the N-terminus of BORIS and cloned into the expression vector pcDNA3.1 and ChIP was performed with an anti-HA antibody to analyze enrichment of BORIS at the *CLDN6* promoter. Transfection efficiency was assessed by control transfection with a vector encoding pEGFP by fluorescence microscopy (Figure 39). SK-BR-3 and HEK293 cells showed well transfection efficiency (estimated 50 % and 95 % respectively) whereas NIH-OVCAR3 were moderate (approx. 25 %) and NEC-8 cells (approx. 5 %) were even after optimization only poorly transfectable. Thus, NEC-8 cells were excluded from subsequent HA-ChIP analysis. BORIS, HA and CLDN6 expression was examined by Western blot analysis (Figure 40). Accordingly to the transfection efficiency analyzed by pEGFP expression, HA and BORIS overexpression was higher in HEK293 and SK-BR-3 cells compared to NIH-OVCAR3. Noteworthy, only overexpressed BORIS protein but not endogenous BORIS could be detected in control-transfected NIH-OVCAR3 cells by Western Blot analysis. This might be due to differential expression of the 17 known isoform from which the used antibody does not detect all. Moreover, also other groups describe problems in detection of endogenous BORIS [150,204]. CLDN6 was highly overexpressed in NIH-OVCAR3 cells while SK-BR-3 cells were negative for CLDN6. Interestingly, HEK293 showed a slight expression of CLDN6. However, overexpression of BORIS was not sufficient to induce CLDN6 expression in any of the cell lines used.

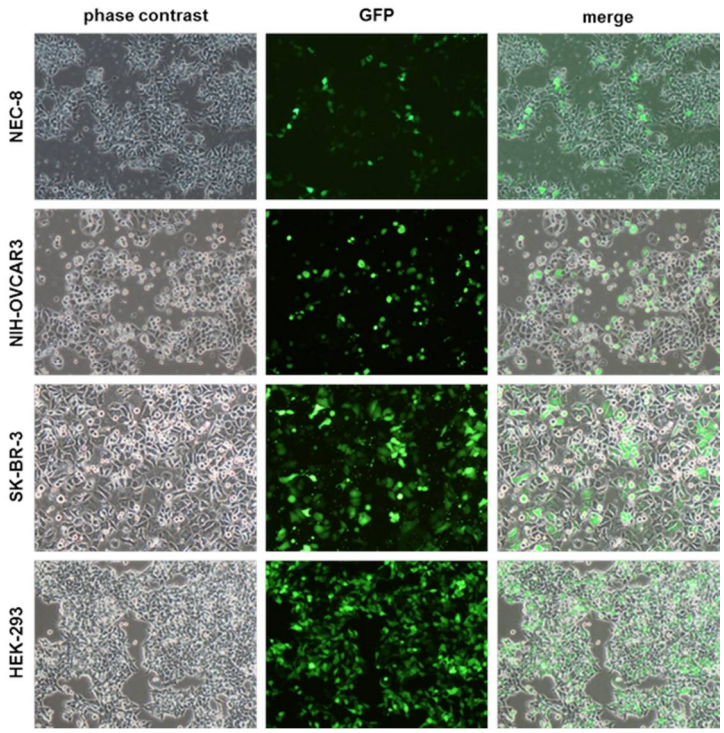

Figure 39 Transfection of plasmid DNA is efficient in NIH-OVCAR3, SK-BR-3 and HEK-293 cells. Cells were transfected with pEGFP-C1 and transfection efficiency was analyzed 48 h after transfection. Pictures were taken in phase contrast and green fluorescence with 10X original magnification. Merged pictures were generated using Nikon software.

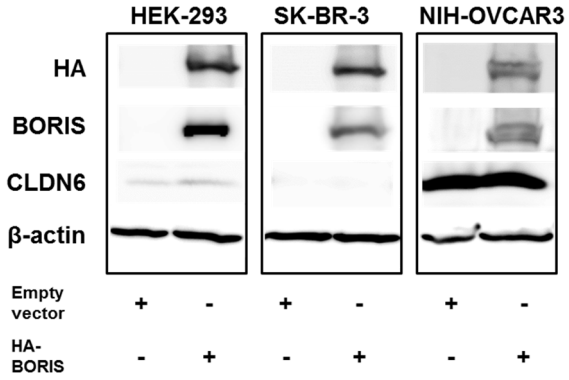

Figure 40 HA-BORIS is efficiently overexpressed in HEK293, SK-BR-3 and NIH-OVCAR3 cells. Cells were transfected either with empty vector control (pcDNA3.1 basic) or HA-BORIS-pcDNA3.1. Western Blot analysis was performed 48 h after transfection with antibodies specific for BORIS and CLDN6. β-actin was used as a loading control.

The result from ChIP analyses are depicted in FFigure 41. CTCF was found to be enriched at the *CLDN6* promoter in region 2 (including CTCF/BORIS binding sites 01-02-03) and region 3 (including CTCF/BORIS binding sites 04-05) in NIH-OVCAR3, NEC-8 and HEK293 but not in SK-BR-3 cells (FFigure 41A). TSP50 served as a positive control gene and showed enrichment for CTCF in all cell lines whereas the negative target hMYC or the non-binding regions in the *CLDN6* promoter (CL6-upstream 1 and 2) showed only weak enrichment. As expected, no enrichment was observed for CTCF in all cell lines used at CL6-promoter 1

because this locus contains a p53 binding site only. The absence of enrichment of CTCF to the *CLDN6* promoter in SK-BR-3 cells was surprising because it was suggested that CTCF acts as a repressor when bound to the *CLDN6* promoter. However, CTCF was detected at the *CLDN6* promoter also in CLDN6-positive NEC-8 and NIH-OVCAR3 cells as well as the slightly positive HEK293 cells indicating that CTCF does not act as a repressor of *CLDN6*. CHIP for p53 revealed that p53 is slightly higher enriched at *CLDN6* promoter only in NIH-OVCAR3 cells. However, compared to the positive control target p21 and negative controls CL6-upstream 1 and 2 as well as TSP50, p53 is not significant enriched at the *CLDN6* promoter (FFigure 41 B). Interestingly, in NIH-OVCAR3 and SK-BR-3 cells, both harboring mutated p53, low enrichment was observed at the p21 promoter. In contrast, HEK293 and NEC-8 cells, both harboring wild-type p53 showed high enrichment of p53 at p21 promoter. This indicates that the ChIP procedure worked well and detection of p53 was specific. Analysis of HA-ChIP indicating BORIS enrichment of the *CLDN6* promoter was compared between control transfected (empty pcDNA3.1 vector) and HA-BORIS-pcDNA3.1 transfected cells 48 h after transfection. Interestingly, BORIS was found to be enriched in both SK-BR-3 and NIH-OVCAR3 cells indicating that BORIS and CTCF are bound in both cells at the *CLDN6* promoter (FFigure 41 C). In HEK293, no considerable enrichment was found at the *CLDN6* promoter compared to the negative as well as positive control targets suggesting that BORIS is not bound to the promoter. NIH-OVCAR3, the only cell line with endogenous BORIS expression also showed binding of overexpressed HA-BORIS. These results indicate that both BORIS and CTCF are bound to the promoter of *CLDN6* and BORIS might compete with CTCF for DNA binding. To test this hypothesis, a CTCF-ChIP was performed in BORIS-silenced NIH-OVCAR3 cells. RNAi-mediated silencing of BORIS was performed as previously described and ChIP was done 96 h after transfection. Indeed, binding of CTCF to the *CLDN6* promoter is slightly increased when BORIS is silenced (FFigure 41 D).

In summary, these results introduce BORIS and CTCF to be important for regulation of *CLDN6* whereas p53 turned out to be not involved in up-regulation of CLDN6 in cancer. Moreover, BORIS and CTCF seem to be not sufficient for *CLDN6* regulation indicating that other transcription factors might be involved in regulation of *CLDN6* as well.

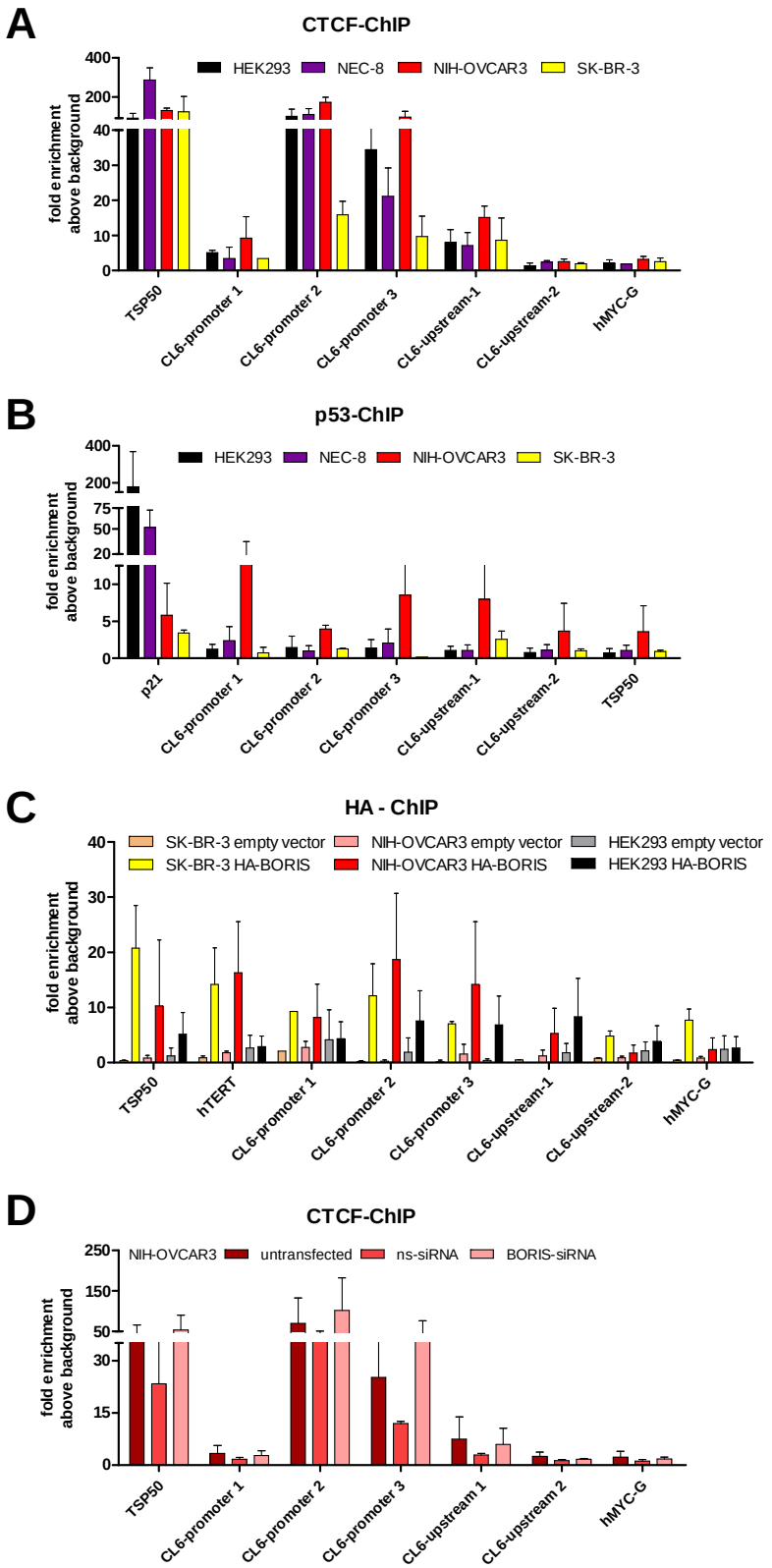

Figure 41 CTCF, p53 and BORIS are bound to the *CLDN6* promoter in different tumor cell lines. (A-C) ChIP was performed with chromatin prepared from HEK293, SK-BR-3, NIH-OVCAR3 and NEC-8 cells either transfected with an empty control vector (pcDNA3.1(+) basic) or HA-BORIS-pcDNA3.1(+). Chromatin was prepared 48h after transfection. The promoter region of CLDN6 containing the p53 elements (CL6-promoter 1 (-1442 to -1277 bp) and 2 (-223 to -30 bp)) and CTCF/BORIS elements (CL6-promoter 2 (-223 to -30 bp) and 3 (+1 to +152 bp)), two regions upstream of the promoter (CL6-upstream 1 (-2510 to -2391 bp) and 2 (-1870 to -1762 bp)) as negative controls as well as target or non-target genes for CTCF/BORIS and p53 (TSP50, hTERT, p21, h-MYC-G) were analyzed by quantitative real-time PCR following immunoprecipitation with antibodies specific for CTCF, p53 or HA. Results corrected by input are shown as fold increase compared to input and an intergenic region (background) used as a reference. (A) CTCF-ChIP. TSP50 was used as a positive control, h-MYC-G as a negative control gene. (B) p53-ChIP. p21 was used as a positive control, TSP50 as a negative control gene. (C) HA-ChIP. The HA antibody was used to detect occupancy of HA-BORIS at the indicated loci. TSP50 and hTERT are known target genes of BORIS and served as positive controls, h-MYC-G was used as negative control gene. (D) CTCF-ChIP in NIH-OVCAR3 was performed 96 h after transfection with ns-siRNA, BORIS-siRNA or with untransfected cells.

4.2.8 CLDN6 correlates with certain (cancer) stem cell specific factors in ovarian cancer

As stated in chapter 4.2.5, CLDN6 could have a function in cancer stem cells. Thus, it was interesting if *CLDN6* gene expression correlates with certain (cancer) stem cell specific factors particularly in ovarian cancer. For this purpose, 42 human ovarian cancer samples were analyzed by qRT-PCR using a Bio Mark™ HD System (Fluidigm). A variety of genes described to be markers for CSC in diverse cancer types or known pluripotency markers of stem cells that can be deregulated in cancer were chosen for this experiment. To examine if expression of *CLDN6* is associated with certain (cancer) stem cell markers, a correlation analysis using Spearman's rho (ρ) was performed [205] (Table 9). Significance of correlation values was assessed by a test on the correlation coefficients. *P*-values were adjusted for multiple testing using the method of Benjamini and Hochberg, and adjusted *p*-values ≤ 0.05 were considered statistically significant [206]. Positive correlation was found for *CLDN6* with *BORIS (CTCFL), musashi 1 (MSI1), lin-homolog 28b (LIN28B), sal-like protein 4 (SALL4), CD24, nucleostemin (GNL3), human epidermal growth factor receptor 2 / HER2/neu (ERBB2), OCT1 (POU2F1), epithelial cell adhesion molecule (EPCAM), L1 cell adhesion molecule (L1CAM)* and *telomerase reverse transcriptase (TERT)* whereas *CD44* were found to correlate negatively with *CLDN6* in the analyzed ovarian cancer samples (Figure 42). Interestingly, the highest correlation of *CLDN6* was found with *CTCFL* (*BORIS*) while no correlation with *CTCF* was present. Whether the correlation of CLDN6 with these markers has a functional or regulative role, remains to be analyzed and will be addressed in future studies in our group.

Table 9 Overview of the results from Spearman correlation analysis of *CLDN6* and different (cancer) stem cell specific factors in ovarian cancer. Shown are Spearman's rho and adjusted p-values for all markers analyzed.

positive correlation			**no correlation**		
marker	*spearman rho*	*p-value*	*marker*	*spearman rho*	*p-value*
CTCFL	0,7801	1,39E-06	Endoglin/CD105	-0,0878	0,746107
MSI1	0,6444	0,00019986	FCGB1A/B/C	-0,1237	0,615194
LIN28B	0,6326	0,0002	FLT3	-0,0978	0,712542
SALL4	0,5475	0,00375998	FUT4	-0,1412	0,596802
CD24	0,5354	0,00441744	GLI1	-0,1153	0,649068
GNL3	0,531	0,00441744	GLI2	0,1367	0,598512
ERBB2	0,4853	0,0111707	HIF-2A/EPAS1	-0,3294	0,168385
POU2F1	0,4843	0,0111707	HAVCR2	-0,3018	0,201801
EPCAM	0,4738	0,0132667	IL1A	-0,091	0,739298
L1CAM	0,4566	0,018498	IL6RA	0,2195	0,415685
TERT	0,4258	0,0320478	ITGA1	-0,3129	0,189975
			ITGA2	-0,312	0,189975
negative correlation			ITGA6	-0,1628	0,532406
marker	*spearman rho*	*p-value*	ITGA9	-0,0669	0,818222
CD44	-0,5135	0,00638357	ITGB1BP1	0,191	0,477832
			ITGB2	-0,2125	0,415685
no correlation			KIT	0,0511	0,877142
marker	*spearman rho*	*p-value*	LMO2	-0,1365	0,598512
ABCB1	-0,2884	0,218737	MET	-0,1745	0,503021
ABCB5	0,1591	0,532406	MS4A1	-0,2566	0,306398
ABCG2	-0,1924	0,477832	MYC	-0,0158	0,960523
AFP	-0,173	0,503021	MYD88	-0,0667	0,818222
ALCAM/CD166	-0,0017	0,991836	NANOG	-0,0978	0,712542
ALDH1A1	-0,1792	0,499984	NCAM1	0,044	0,885672
AMACR	0,0101	0,972292	NF2/Merlin	0,2142	0,415685
ANPEP/CD13	0,1783	0,499984	NGFR	-0,0147	0,960523
ATXN1	0,1244	0,615194	NOTCH1	0,3172	0,189975
BMI1	0,2806	0,235788	PDPN	0,168	0,518238
BMP4	-0,0826	0,763766	PIWIL1	-0,0498	0,877142
BRCA1	0,3903	0,0587986	PLAUR	0,0699	0,818222
CD151	0,2992	0,201801	POU5F1	-0,1236	0,615194
CD19	-0,0343	0,903427	PROM1/CD133	-0,133	0,606964
CD2	-0,291	0,218737	PTEN	0,0194	0,959521
CD27/TNFRSF7	-0,2125	0,415685	SDC1	0,2777	0,236837
CD34	-0,1255	0,615194	SHH	-0,0502	0,877142
CD38	-0,0978	0,712542	SNAI1	0,0058	0,982996
CD47	0,1884	0,479547	SOX2	0,2472	0,335274
CTCF	0,3015	0,201801	SOX4	0,1779	0,499984
CX3CR1	-0,2416	0,348916	ST8SIA1	0,0352	0,903427
CXCL1/Fractalkine	-0,0199	0,959521	STAT3	0,2334	0,374356
CXCR1	-0,1597	0,532406	TNFAIP3	0,0472	0,879625
DLL4	0,0357	0,903427	TFRC/CD71	0,2075	0,428856
DPP4	-0,2216	0,415685	THY1	0,1409	0,596802
EGFR	-0,1438	0,596802	TRRAP	0,3916	0,0587986

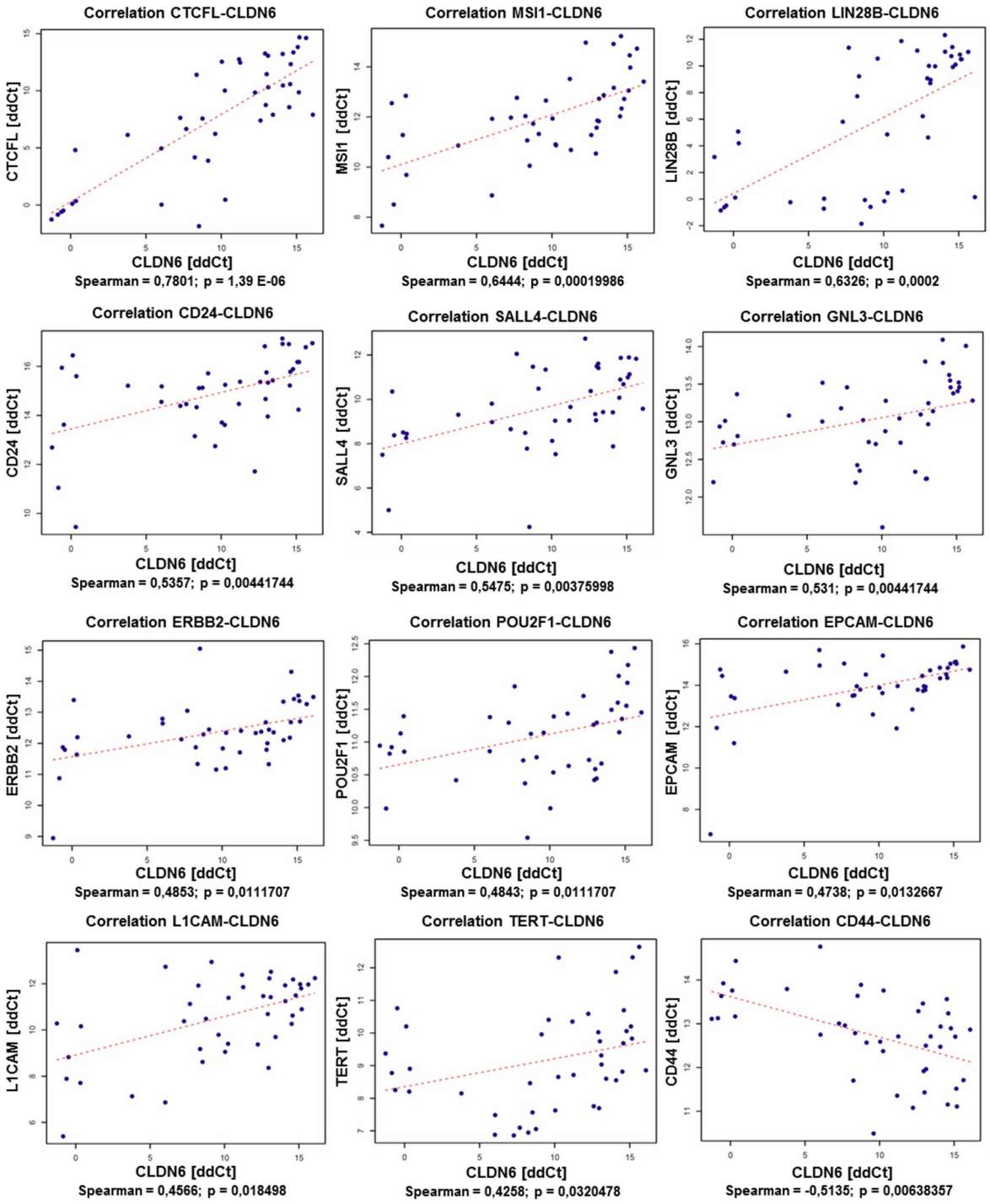

Figure 42 *CLDN6* correlates significantly with several (cancer) stem cell specific factors in ovarian cancer. Scatterplots of delta delta Ct (ddCt) values of *CLDN6* and *CTCFL, MSI1, LIN28B, CD24, SALL4, GNL3, ERBB2, POU2F1, EPCAM, L1CAM, TERT* and *CD44* are shown. Correlation analysis was performed using Spearman's rho (ρ), adjusted *p*-values of ≤ 0.05 were considered statistically significant. Ovarian cancer samples: N = 42.

4.2.9 CLDN6 is a specific marker for human induced pluripotent stem cells

Claudin 6 is expressed in human and mouse ESC as well as during embryogenesis which was extensively studied in mice [116,130,165]. To confirm expression of *Cldn6* in murine ESC, the murine ESC lines E14 and W9.5 were analyzed for mRNA levels and indeed, *Cldn6* was highly expressed in these cell lines (Figure 43 A). Moreover, mRNA levels of *CLDN6* were analyzed in human induced pluripotent stem cells (iPSC) which were generously provided by TRON gGmbH. iPSC were reprogrammed from human neonatal foreskin fibroblasts (HFF) using a specific RNA cocktail (containing IVT-RNA encoding transcription factors *OCT4, SOX2, KLF4, cMYC, NANOG, LIN28* and IFN-escape proteins E3, K3 und B18R and a miR-mix = miRNA-302a/b/c/d and 367). On day 5, 12 and 19 of reprogramming, mock transfected HFFs (transfection without RNA) were compared to HFFs transfected with the RNA cocktail on *CLDN6* by qRT-PCR and flow cytometry. Remarkably, *CLDN6* is up-regulated almost 6000-fold in HFFs treated with the reprogramming cocktail compared to untreated HFF at day 19 of treatment, even at day 12 of treatment an approximately 2000-fold up-regulation of *CLDN6* was observed (Figure 43 B). This result indicates that CLDN6 is expressed in human iPSC.

Flow cytometry was used to examine if CLDN6 is also expressed on the surface of iPSC. As iPSC are grown on HFF feeder cells, co-staining of CLDN6 and stage specific embryonic antigen 4 (SSEA-4), a well-known stem cell marker, was performed to ensure specific detection of iPSCs. For this purpose, HFF cells treated with the reprogramming cocktail or without RNA were collected at day 5, 12 and 19 of treatment and stained with CLDN6- and SSEA-4- specific antibodies analyzed by flow cytometry (Figure 43 C).

On day 5, CLDN6 was not detected on the surface of HFF cells independent of treatment with the reprogramming cocktail. Unexpectedly, SSEA-4 was found to be expressed at 15 % of HFFs, irrespective of treatment with the reprogramming cocktail. This could be explained by the fact that HFFs used are neonatal fibroblasts and possibly these cells retain certain positivity for SSEA-4. On day 12 of treatment, about 63 % of the treated HFFs were positive for SSEA-4 and a CLDN6-SSEA-4 double positive fraction of about 15 % was observed. On day 19

of treatment, 15 % of the treated HFFs were positive for CLDN6 and SSEA-4, representing a distinct subpopulation. It is assumed that the CLDN6-SSEA-4 double-positive subpopulation marks iPSC specifically whereas the CLDN6-SSEA-4 double-negative subpopulation is regarded to be HFF feeder cells or not reprogrammed cells and SSEA-4 single positive cells represent cells which are at the beginning of reprogramming.

As 15 % of the HFF cells were positive for SSEA-4 but not for CLDN6, it is assumed that CLDN6 represents a more specific marker for human iPSC than SSEA-4. SSEA-4 is also expressed in neonatal HFF whereas CLDN6 seems to be specifically expressed only in fully reprogrammed HFF cells which represent the iPSC fraction.

These results indicate that CLDN6 is specifically expressed on the surface of human iPSC.

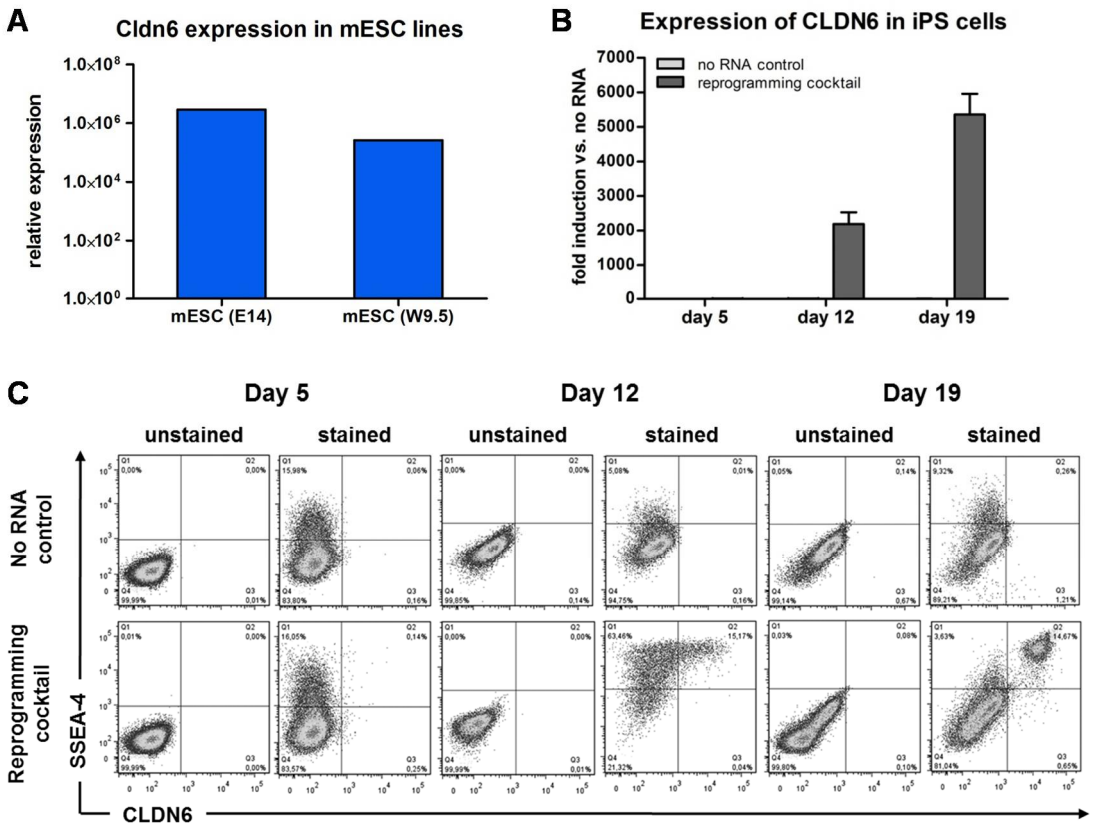

Figure 43 Claudin 6 is expressed in mESC and human iPS cells. (A) mRNA expression of murine *Cldn6* was analyzed in mESC lines E14 and W9.5 by qRT-PCR relative to the housekeeping gene *Hprt1*. (B and C) HFF cells were transfected without RNA (no RNA control) or with a reprogramming cocktail and cells were collected at day 5, 12 and 19 post treatment. Reprogramming cocktail contains IVT-RNA encoding transcription factors OCT4, SOX2, KLF4, cMYC, NANOG, LIN28, EBK= IFN-escape proteins E3, K3 and B18R, miR-mix = miRNA-302a/b/c/d and 367. (B) *CLDN6* mRNA level was analyzed by qRT-PCR. Shown is fold induction of CLDN6 expression of cells treated with the reprogramming cocktail relative to HFF cells from day one of treatment. CLDN6 mRNA expression was normalized to mRNA expression of the housekeeping gene HPRT1. (C) CLDN6 and SSEA-4 surface expression was analyzed by flow cytometry using specific

antibodies for CLDN6 (IMAB027-Alexa Fluor®647, Ganymed Pharmaceuticals) and SSEA-4 (SSEA-4-V450, BD). The experiment was performed in duplicates and representative dot plots are shown.

Additionally, mock treated HFFs as well as iPSC collected on day 5, 12 and 19 of treatment were analyzed for expression of (cancer) stem cell markers by qRT-PCR using a Bio Mark™ HD System (Fluidigm) (for markers, please see Table 9). Thus, it is possible to analyze if *CLDN6* arises with other specific (cancer) stem cell markers during the course of reprogramming. The heat map in Figure 44 shows up- or downregulation of different cancer stem cell markers in HFFs transfected without RNA (no RNA control) versus iPSC (reprogramming cocktail) relative to untreated HFFs on day 0 of treatment. The results are consistent with qRT-PCR and flow cytometry results shown in Figure 43. *CLDN6* expression was found to arise on day 12 of treatment and was further up-regulated on day 19. The up-regulation of *CLDN6* on day 12 and 19 was comparable to other markers such as *EPCAM, E-Cadherin (CDH1), OCT3/4 (POU5F1), CXC motif chemokine receptor 4 (CXCR4), TERT, LIN28B, CD24, NANOG, prominin1 (PROM1/CD133), ST8SIA1, MSI1, SALL4, Lim domain only 2 (LMO2) and SRY (sex determining region Y)-box 2 (SOX2).* Moreover, *ST8SIA1, NANOG* and *PROM1* were highly expressed even on day 5 of treatment while *CLDN6* is not up-regulated at this time point. Whether this has a functional relationship was not analyzed in this study but will be subject of further studies.

Collectively, these results show that CLDN6 is specifically upregulated during course of reprogramming comparable to know stem cell markers and indicates that CLDN6 is a specific marker for iPSC.

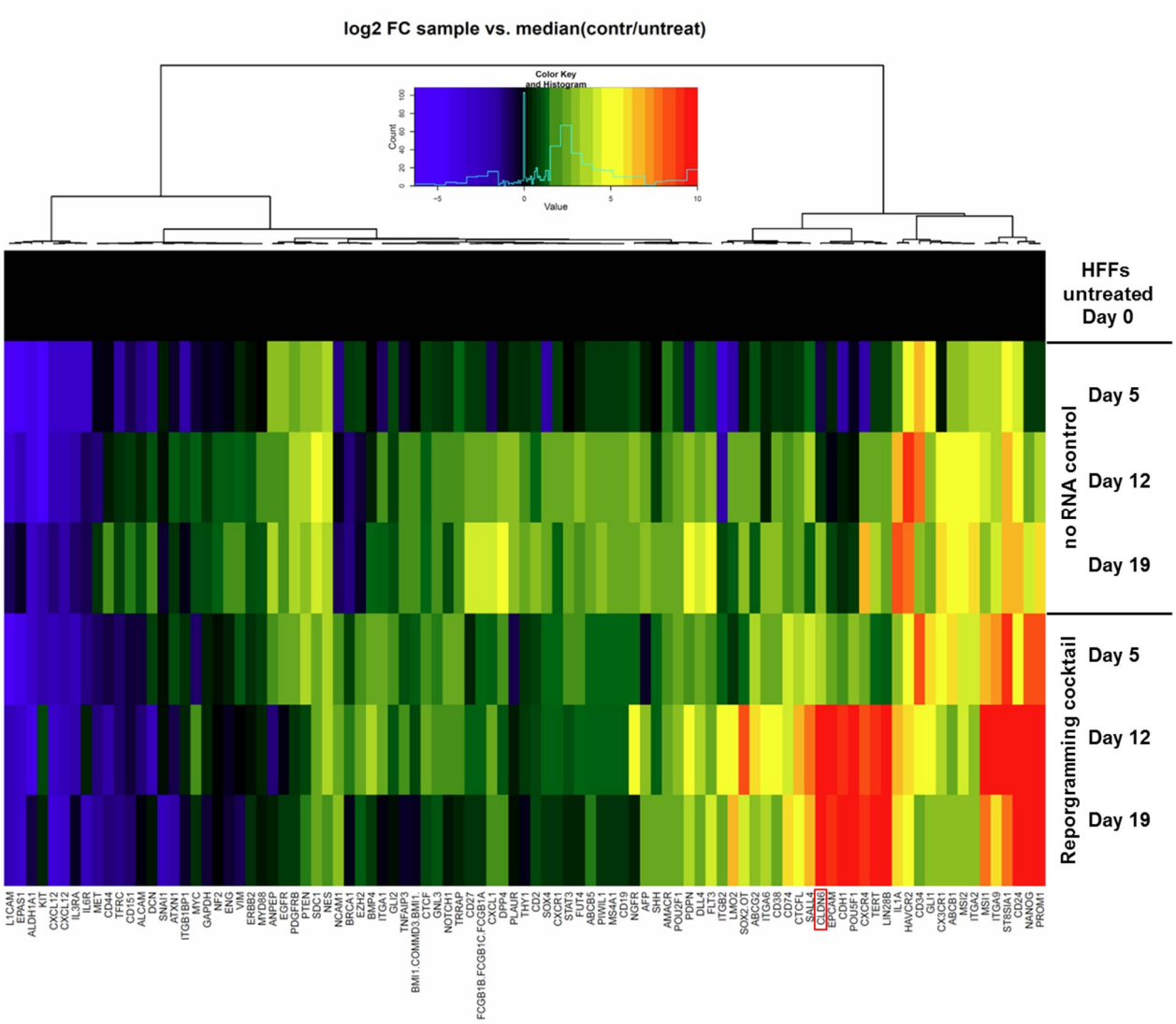

Figure 44 Expression analysis of stem-cell specific factors in human iPSC compared to HFFs. Heat map of expression values (log 2 fold change (FC)) of HFFs untreated at day 0, HFF cells control treated (no RNA control) and HFF cells treated with the reprogramming cocktail (iPSC) at day 5, 12 and 19. Expression values of HFF cells control treated or treated with the reprogramming cocktail depicted as log2 of fold changes compared to untreated HFF cells from day 0.

5 Discussion

5.1 The high need for tumor-specific molecular targets in cancer immunotherapy

The purpose of this study was to examine the previously identified candidate tumor antigens *PLAC1* and *CLDN6* regarding their potential to serve as highly specific targets for cancer immunotherapy. Owing to the success of the first monoclonal antibodies trastuzumab (Herceptin; Genentech) targeting HER2/neu overexpression in breast cancer or rituximab (Rituxan; Genentech) against CD20 in B-cell lymphoma and leukemia, over the past decades, development of therapies to specifically target tumor cells is a major goal in cancer therapy [207,208]. A bottleneck in targeted therapies, immunotherapy or others, is to find highly specific targets and thus avoid harming of healthy tissues. Noteworthy, not only the tumor-specificity of a target is a prerequisite to serve as a potent tumor antigen. Another major point is to elucidate the function and regulation of a target in the tumor cells. Most of the previously identified tumor antigens serve major biological functions in tumor cells and take part in signaling pathways controlling growth and survival [34]. Understanding in which molecular functions and mechanisms the target is involved and how it is regulated, defines its suitability for diagnostic or therapeutic approaches.

5.2 PLAC1

At the beginning of this study, the functional analysis of PLAC1 in breast cancer was already completed. RNAi-mediated silencing of PLAC1 has revealed that it plays a role in proliferation, cell cycle, migration, motility and invasion of breast cancer cells. Furthermore, it was shown that PLAC1 is localized on the surface of cancer cells and can be targeted by monoclonal antibodies. Anti-PLAC1 antibodies are capable to antagonize the tumor-biological function of PLAC1 thus serving as a possible treatment strategy of PLAC1-positive breast cancer [67]. In contrast, the regulation of *PLAC1* is more complex and not fully understood. As mentioned in the beginning of this thesis (refer to chapter 1.3.1), two distinct

promoters (P1 and P2) are responsible for the expression of *PLAC1* in placenta and cancer [74]. Because P2 is predominantly used in breast cancer cells, this study focuses on the regulation of *PLAC1* at promoter P2. Although previous studies showed that basal expression of *PLAC1* is regulated by SP1 and C/EBP-β and ERα-signaling further augments transcription of *PLAC1*, the entire trans-activation complex at the *PLAC1* promoter remained elusive [83].

5.2.1 NCOA3 is a selective co-activator of ERα-dependent trans-activation of PLAC1

In this study, the role of the p160/NCOA family of co-activators in regulation of *PLAC1* in breast cancer cells was analyzed. The key results presented here are: first, explicit involvement of NCOA3 but not NCOA1 or NCOA2 at the E_2-mediated trans-activating complex at *PLAC1* promoter P2 as ChIP assays provided evidence for enrichment of NCOA3 but not the other co-factors at the relevant binding site. Second, silencing of NCOA3 resulted in loss of *PLAC1* trans-activation after E_2-stimulation only in ERα-positive MCF-7 but not in ERα-negative SK-BR-3 cells and third, a significant correlation of *PLAC1* expression and *NCOA3* overexpression was observed in a cohort of ERα-positive breast cancer patients.

NCOA1, NCOA2 and NCOA3 display high homology in structure and sequence thus activating nuclear receptor target genes in a similar fashion. Nevertheless, they serve unique, non-redundant functions in different cell types and tissues [94,101,102]. Aberrant expression of co-activators is suggested to be sufficient for breast cancer initiation. Especially NCOA3 is interesting in this context, as mice overexpressing NCOA3 in mammary epithelial cells develop spontaneous mammary tumors [107]. NCOA3 overexpression is associated with resistance to tamoxifen in patients with ERα-positive tumors. Moreover, NCOA3 significantly correlates with several disease markers such as larger tumor size, higher tumor grade and expression of ERBB2 [101,188,189,209,210]. Thus, NCOA3 is a very attractive target for breast cancer therapy and downstream targets of NCOA3 that may contribute to disease progression are of high interest for development of new therapeutic strategies as well.

NCOA3 is involved in multiple signaling pathways that promote cancer such as proliferation, tumor growth, invasion, metastasis and chemoresistance [211]. In

ER-positive breast cancers, NCOA3 is required for maximal activity of ERα and other hormone receptors [212,213]. Thus, changes in NCOA3 gene expression influence ERα-dependent gene expression and consequently modulate the aforementioned cellular processes [211,214,215]. Indeed, silencing of NCOA3 in MCF-7 cells results in decreased E_2-stimulated proliferation *in vitro.* The inhibition of proliferation is accompanied by changes in cell cycle distribution and is mediated through NCOA3 downstream effectors like cyclin D1, which plays a pivotal role in estrogen-dependent proliferation [102,216]. Most interestingly, NCOA3 is crucial for the activation of cyclin D1 as ectopic overexpression of ER alone is not sufficient for estrogen-dependent cyclin D1 expression and mitogenesis in ER-negative cells [216]. Our group demonstrated previously that PLAC1 is a critical factor for breast cancer progression, as RNAi-mediated silencing of PLAC1 in MCF-7 and BT-549 breast cancer cells results in decreased cyclin D1 levels and induces a G1-S cell cycle block with nearly complete abrogation of proliferation [67]. The here presented findings introduce PLAC1 as a possible downstream effector of NCOA3 that may mediate NCOA3 actions in ERα-positive breast cancer cells.

The specific expression pattern of *PLAC1* in placenta and cancer is regulated by two distinct promoters [74]. Here, explicit involvement of NCOA3 in the formation of an E_2-dependent pre-initiation complex at the *PLAC1* P2 promoter was demonstrated. Noteworthy, very recently, NCOA2 was disclosed in regulation of *PLAC1* at promoter P1 in SV40 transduced primary fibroblasts [81]. Intriguingly, NCOA2 and NCOA3 appear to act under different circumstances as activators of *PLAC1* from different promoters. The regulation of *PLAC1* constitutes to be highly complex and a plethora of different transcription factors seem to be involved in up-regulation of PLAC1 in placenta and cancer. In which extend NCOA3 can act at the promoter P1 for example in placenta remains to be analyzed. Noteworthy, NCOA3 can act as a co-activator also of PPARs [217] and was found to inhibit TP53 in breast cancer cells [218], both factors suggested to be involved in regulation of *PLAC1* [81,82]. This implicates a broader involvement of NCOA3 in the regulation of *PLAC1*. Thus, additional studies are required to dissect the complex regulation of *PLAC1* in placenta and cancer tissues.

5.2.2 Conclusion and future outlook - Improved model of the PLAC1 trans-activation complex

In conclusion, the data provided in this thesis contribute to the knowledge of the E_2/ERα-mediated trans-activation complex formed at the *PLAC1* promoter P2 in breast cancer cells and lead to an improved model of the *PLAC1* trans-activation complex (Figure 45). Basal expression of *PLAC1* is mediated by the concerted action of SP1 and C/EBPβ-2 bound to their cognate elements at the *PLAC1* promoter. Stimulation of estradiol-responsive cells with E_2 results in recruitment of not only ERα but also NCOA3, p300 and pCAF. Concomitantly, acetylation of histones H3 and H4 are induced which accounts for open chromatin. The E_2-ERα induced association of co-activators as well as the chromatin changes favor recruitment of RNA polymerase II and TFIIB resulting in further enhancement of *PLAC1* transcription (Figure 45).

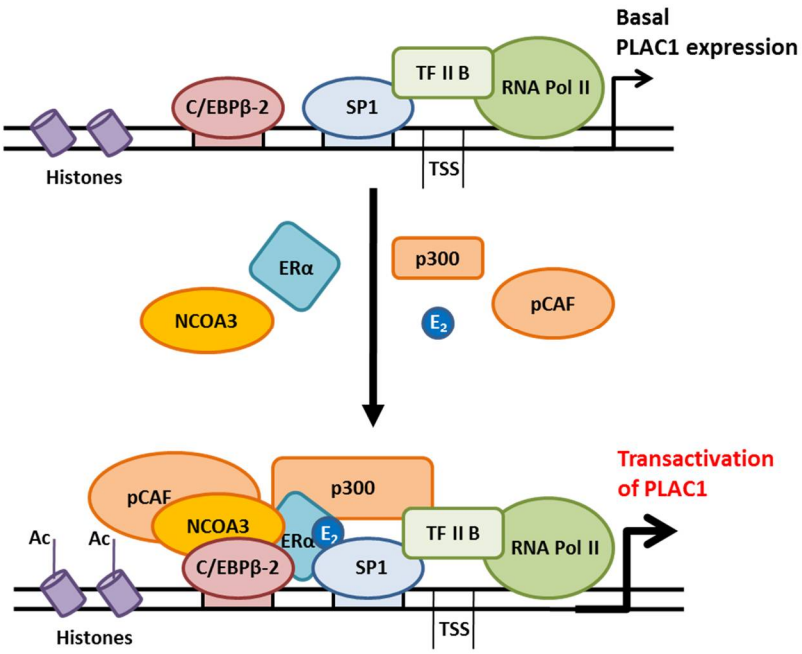

Figure 45 Improved model of the PLAC1 transactivation complex at promoter P2. Basal expression of PLAC1 is maintained upon binding of C/EBPβ-2 and SP1 as well as general transcription factor II B (TF II B) and RNA polymerase II (RNA Pol II) to the PLAC1 promoter adjacent to the transcription start site (TSS). Stimulation of cells with estradiol (E_2) leads to activation and binding of ERα to C/EBPβ-2 and SP1 as well as recruitment of NCOA3, pCAF and p300 as well as acetylation of histones H3 and H4 which further enhances the expression of PLAC1.

The observation that NCOA3 is necessary for E_2-dependent transactivation of *PLAC1* in an ERα-dependent manner suggests PLAC1 as a novel target gene of NCOA3 in ERα-positive breast cancer. The functional relationship between PLAC1 and NCOA3 as well as the correlation analysis of *PLAC1* expression with various clinical parameters like tumor size, overall and disease-free survival as well as resistance to therapy will be subjects of further studies. The presented data add further knowledge to the attractiveness of PLAC1 as a target for immunotherapy of

ERα-positive breast cancer. Noteworthy, PLAC1 is recognized by the National Cancer Institute (NCI) as a candidate target that could serve for vaccine development to treat breast cancer [219].

5.3 CLDN6

CLDN6 offers an exceptional position among members of the claudin family as it is an embryonic antigen not expressed in adult tissues while frequently overexpressed in several types of cancer [116,130,166,171,175–177,220]. This preeminent tumor cell specificity qualifies it as a potent candidate target for cancer immunotherapies. At the beginning of this study, neither the biological role of CLDN6 nor its regulation in cancer was known. Thus, the elucidation of function and regulation of CLDN6 was urgently needed.

5.3.1 CLDN6 is a highly tumor-specific antigen

In this study, *CLDN6* was found to be overexpressed in several cancer types, particularly in ovarian, lung and testicular cancer while not expressed in any normal adult tissue. Furthermore, sporadic expression of *CLDN6* was observed also in a variety of other cancer types such as breast, gastric and skin cancer (data not shown). These findings are in line with several recent reports presenting evidence that CLDN6 is overexpressed in the aforementioned cancer types [164,172,174,175,220]. Moreover, CLDN6 is described as a diagnostic marker for pediatric tumors (atypical teratoid/rhabdoid and malignant rhabdoid tumors) [171,176]. In contrast to the findings presented here, two reports state that CLDN6 is down-regulated in gastric and breast adenocarcinomas compared to normal adjacent tissues [179,221]. However, these findings are disputable because CLDN6 positive staining of normal tissues was not found in any other study.

The distinct expression pattern of CLDN6 in cancer but not in adult normal tissues qualifies it as a highly specific target for diagnostic as well as immunotherapeutic approaches in a wide variety of cancer types.

5.3.2 CLDN6 has no major biological role in proliferation, apoptosis, cell cycle distribution, migration or adhesion of PA-1, NIH-OVCAR3 and NEC-8 tumor cells

Claudins are deregulated in several cancer types and are described to have a function in adhesion, migration, invasion and proliferation of tumor cells. In normal physiology, claudins are important for integrity of tight junctions that are involved in cell-cell adhesion, cell polarity and paracellular passage of molecules and ions in epithelial cells [115,194,222]. Tight junctions are frequently disrupted in cancer resulting in decreased polarity and differentiation that can facilitate metastatic processes [223]. As part of tight junctions, claudins might be involved in this process. Indeed, it has been shown that claudins are often delocalized from tight junctions in cancer cells and even can be present in the nucleus or cytoplasm [224–226]. Moreover, both overexpression as well as down-regulation of claudins was reported to have a positive effect on proliferation, migration, invasion and metastasis depending of the cancer type [194,227–230].

In this study, RNAi-mediated silencing of CLDN6 did not reveal any function of CLDN6 in migration or adhesion of PA-1, NIH-OVCAR3 or NEC-8 tumor cells. Moreover, no major role of CLDN6 could be disclosed in proliferation, apoptosis or cell cycle of tumor cells. Indeed, very sparse literature is found regarding a functional role of CLDN6 in cancer. Zavala-Zendejas and co-workers showed that overexpression of CLDN6 in the gastric adenocarcinoma cell line AGS increases cell migration, proliferation and invasiveness [177]. In contrast, several reports suggest a tumor suppressive role for CLDN6 in breast cancer. Studies in MCF-7 breast cancer cells demonstrate that CLDN6 is epigenetically silenced and stable overexpression of CLDN6 results in down-regulation of invasion and migration of the tumor cells [135,178,179]. Osanai *et al.* further describe promoted invasiveness and transendothelial migration when CLDN6 is silenced in MCF-7 cells [135]. Indeed, the claudin-low subtype of triple-negative breast cancers (TNBC) has been shown to be more aggressive compared to other breast cancer types [231–233]. Interestingly, RNAi-mediated silencing of CLDN6 does not induce apoptosis or alter the cell cycle profile of hESC lines [166] suggesting the CLDN6 serves no major biological role in apoptosis or cell cycle also in hESC.

The fact that no remarkable effect was found by silencing of CLDN6 in this study could be explained in different ways. First, as numerous claudins are overexpressed in cancers it is reasonable to assume that loss of CLDN6 function is compensated by synergistic effects of other claudins. Indeed, the cell lines used express other claudins which have also been shown to play a role in invasion and migration such as CLDN3, 4 and 7 in NIH-OVCAR3 cells [227,234–238]. Unpublished data from our group shows that CLDN7 is expressed in NEC-8 cells in a level comparable to CLDN6 and PA-1 cells slightly express CLDN12.

Second, RNAi-mediated silencing may not completely abolish expression of the corresponding gene. Thus, residual CLDN6 transcript or protein levels could be sufficient to sustain the function of CLDN6 in cancer. Often, higher functional impact is observed when overexpressing a protein. Overexpression of a protein at non-physiological levels carries a high risk to induce artifacts and could end in misleading results. If a stable overexpression rather as an inducible overexpression is used, global cellular changes can induce changes in the phenotype or clonal artifacts arise. Thus, in this study the preferred method was RNAi-mediated silencing. The published reports presenting a functional relevance of CLDN6 in MCF-7 and AGS cells used stably overexpressing clones [135,177]. In line with these ideas, Cldn6 null mice are phenotypically normal while mice overexpressing Cldn6 show a rather severe phenotype and die within 48 h after birth due to skin barrier defects [163,167]. Notably, the authors suggest that other claudins expressed in the endoderm of Cldn6 null mice may compensate for Cldn6 supporting the first idea stated above [163].

In summary, the results of the functional assays presented here indicate that CLDN6 has no major biological effect in proliferation, apoptosis, cell cycle distribution, migration or adhesion of the analyzed cancer cell lines PA-1, NIH-OVCAR3 and NEC-8. To check whether RNAi-mediated knockdown of CLDN6 was not sufficient to exert major effect in functional assays, it would be important to analyze CLDN6 in cells with knock out of entire CLDN6 mRNA and protein for example using zinc finger nuclease (ZNF) technology. Moreover, double knockdown studies would be useful to examine if other claudins can compensate the function of CLDN6 in tumor cells.

5.3.3 CLDN6 might have an important role in cancer stem cells

In this study, CLDN6 was disclosed as a specific marker for human iPSC and was found to be up-regulated throughout the course of reprogramming comparable to several stem cell markers. Moreover, CLDN6 was identified here to be specifically expressed in mESC lines. Several hints are found in the literature that CLDN6 is associated with stem cells: A meta-analysis of hESC transcriptome data of 38 original studies revealed CLDN6 to be one of 40 genes specifically detected in hESC [165]. Among these 40 genes, the authors detected CD24, POU5F1/OCT3/4, NANOG and LIN28 as well. Consistently, CLDN6 was found to be up-regulated in comparable levels to these markers in the present study. In agreement with the findings presented here, only recently, two reports provided evidence that Claudin 6 is a surface marker for murine pluripotent stem cells (mPSC) [164] as well as human pluripotent stem cells (hPSC) [166]. Interestingly, CLDN6+ but not CLDN6- hPSC are capable to form teratomas *in vivo* suggesting a tumorigenic potential of CLDN6+ hPSC [166]. Consistently, the data presented here indicate that CLDN6 might have a role in CSCs as colony formation was impaired in CLDN6- compared to CLDN6+ cells. The efficiency of cells to form colonies is regarded to account for self-renewal capacity that is a key feature of CSCs. CSCs are supposed to generate tumors through the stem cell processes of self-renewal and differentiation. Further supporting evidence is provided by the significant correlation of *CLDN6* with several CSC-markers in human ovarian cancer demonstrated in this work.

Of course, expression of a gene in embryonic or induced pluripotent stem cells is not a prerequisite that this gene is also expressed in CSCs. Though, many stem-cell specific genes are activated in certain cancers contributing to the malignant growth of the tumor [239]. Furthermore, somatic reprogramming using pluripotency factors (OCT4, SOX2, KLF4, C-MYC, NANOG, LIN28) from which many are oncogenes, offers an explanation how CSCs may arise [240,241]. Indeed, a model to derive CSCs from murine iPSC by mimicking a carcinoma environment exists [242] and premature termination of reprogramming leads to cancer development [243].

A relationship between claudins and CSC was proposed earlier by others. In breast cancer, an inverse correlation of claudin expression and stem-cell

characteristics are anticipated since claudin-low breast tumors are enriched with stem cell markers [231–233,244]. However, a positive correlation between CSCs and claudins is also suggested as CLDN4 silencing in ovarian cancer results in delayed spheroid formation [245] and CLDN1 is overexpressed in ovarian CSCs compared to differentiated cells [246]. In line with this idea, the data presented here demonstrate a significant positive correlation of *CLDN6* transcript in human ovarian cancer with the (cancer) stem cell markers *BORIS/CTCFL*, *MSI1*, *LIN28B*, *SALL4*, *CD24*, *GNL3*, *ERBB2*, *POU2F1/OCT1*, *EPCAM*, *L1CAM* and *TERT* while a negative correlation was detected for *CLDN6* and *CD44*. While all of these factors show a high expression in ovarian cancer, only *LIN28B*, *CD24*, *GNL3* and *EPCAM* have been described as markers for ovarian CSCs so far [247–251]. However, BORIS/CTCFL, MSI1, SALL4, POU2F1/OCT1, ERBB2, L1CAM and TERT are known to be associated with CSCs of other entities [58,172,252–255]. The positive correlation of CLDN6 with these known (cancer) stem cell markers further supports the idea that CLDN6 could be associated with CSCs. The correlation of CLDN6 with LIN28B and SALL4 found in this work is of particular interest because CLDN6, SALL4 and LIN28 are co-expressed also in other cancer types [172] indicating a broader relevance of this association. The pluripotency factor LIN28 is highly expressed in ESC and iPSC and was found to be expressed in a stem-cell like sub-population of epithelial ovarian cancer (EOC) together with OCT4, co-expression of LIN28 and OCT4 correlates with advanced tumor grade and silencing of both factors results in decreased cell growth and survival suggesting that LIN28 and OCT4 are important for initiation and/or progression of EOC [249]. Moreover, LIN28B is suggested to be an oncogenic driver in CSC [250]. The correlation between CLDN6 and EpCAM is highly interesting because EpCAM is overexpressed in most carcinomas. Depending on the cancer tissue and microenvironment, EpCAM can exert oncogenic or tumor suppressive effects [256]. However, EpCAM is significantly higher expressed in recurrent tumors compared to primary tumors and was recently disclosed as a marker for CSCs [257–259]. CD24 is one of the most established markers of ovarian CSCs [260]. CD24-positive cells from ovarian tumors are enriched in expression of stemness genes, more chemoresistant and tumorigenic compared to CD24-negative cells [261].

Interestingly, the present work displays an up-regulation of CLDN6 throughout the course of reprogramming comparable to known embryonic stem cell markers. Among these, LIN28B, SALL4, EPCAM, TERT, CD24, MSI1 were found matching to the observed correlation with CLDN6 in ovarian cancer. Strikingly, an ESC-like gene expression signature can be found in ovarian epithelial carcinomas as well as germ-cell tumors including embryonic carcinomas and various cancer types with histologically poorly differentiated phenotype indicating that ESC-like programs are commonly activated in cancer that allow cancer stem cells to evolve [249,250,256,262–265]. Intriguingly, all of these cancer types display a high overexpression of CLDN6 as well as SALL4, LIN28B, EPCAM and TERT and other ESC markers [172,266–268] suggesting that a correlation between CLDN6 and these genes may be present in other cancer types as ovarian cancer as well.

The negative correlation of CLDN6 with CD44 found here was surprising as CD44 is described as one of the earliest marker for ovarian CSCs [247,269]. Noteworthy, it has been shown that expression of different CD44 variants are independent prognostic markers for ovarian cancer [270]. For example CD44 variant 5 (CD44v5) has been shown to be higher expressed in late stage ovarian carcinomas compared to other variants [271] and CD44v6 correlates with ovarian cancer progression and recurrence [272]. As the TaqMan® Gene Expression assay used in this work detects also CD44S, the standard isoform which is ubiquitously expressed in most tissues but does not detect all CD44 variants; it is possible that the results are biased. Moreover, CD44 was found in this work to be highly expressed in most of the 42 ovarian cancer samples used. Thus, the impact of the inverse relation between CD44 and CLDN6 will be clarified in further studies by analyzing the correlation of CLDN6 with all known CD44 variants. However, it is not clear which markers really define CSCs in ovarian cancer or other types of cancer. In the literature, a plethora of marker combinations are used to isolate CSCs from tumors [273–275]. Moreover, accumulation of studies regarding ovarian CSCs suggests that not a single marker clearly identifies the ovarian CSC rather distinct marker combinations may represent different ovarian CSC subpopulations [260]. Of course, this is also true for other cancer types [276]. This could explain why CLDN6 did not correlate with other established markers for ovarian CSCs like CD117 or CD133 in the present study. Maybe CLDN6 is present in a distinct subtype of CSCs identified by a specific combination of

markers. In the present work, the correlation analysis of CLDN6 was performed in ovarian cancer only. To increase the impact regarding the role of CLDN6 in CSCs, the correlation will be analyzed in other cancer types as well, for example lung cancer.

In summary, the findings presented here suggest that CLDN6 is associated with ovarian CSC and could serve as a specific marker for CSC. However, involvement of CLDN6 in CSCs can only be speculated so far. The role of CLDN6 in CSCs has to be clarified in further studies including sphere formation assays of CLDN6-positive and CLDN6-negative tumor cells to analyze anchorage-independent growth. The current gold standard to provide evidence that a certain gene is important for CSCs is to examine *in vivo* tumorigenicity by injecting low cell numbers (< 100) of cells positive or negative for the gene of interest in mice. This assay will be included in further studies with CLDN6-positive and CLDN6-negative cells as well.

5.3.4 *CLDN6* is regulated by methylation in combination with tumor-specific transcription factors

5.3.4.1 DNA-methylation of the *CLDN6* promoter is important in regulation of its expression in cancer

The regulation of *CLDN6* in cancer was largely unknown at the beginning of this study. Epigenetic mechanisms were considered to be involved in the regulation of *CLDN6* in cancer because it is known that DNA methylation participates in regulation of claudins in general [194] and *CLDN6* in particular [134–136]. Furthermore, the fact that two independent CpG islands lie within the *CLDN6* promoter region has led to studies of transcriptional regulation by DNA methylation.

In this thesis, it could be shown that tumor cell lines overexpressing CLDN6 display a hypomethylated *CLDN6* promoter and treatment with a demethylating agent induced CLDN6 expression in *CLDN6*-negative tumor cell lines. Accordingly, CLDN6 non-expressing tumor cell lines displayed a hypermethylated *CLDN6* promoter region. Hypermethylation of promoters is a mechanism in cancer cells to repress the expression of tumor suppressor genes whereas oncogenes

can be up-regulated by promoter hypomethylation in cancer [11]. The observed findings are in accordance with reports describing *CLDN6* promoter hypermethylation in breast and esophageal cell lines which do not express CLDN6 [135,136]. Osanai *et al.* state in their report that CLDN6 is expressed in mammary epithelia by referring to a paper analyzing Claudin 6 in Copenhagen rat [277] thus suggesting that human CLDN6 serves as a tumor suppressor in breast cancer because of epigenetic silencing in the human breast cancer cell line MCF-7 [135]. It is questionable to draw conclusions if the corresponding normal tissue of the same species was not analyzed. In contrast, expression of *CLDN6* in human normal breast could not be confirmed in our lab (Figure 13). However, the here presented thesis is the first report showing an association between CLDN6 expression and hypomethylation of the *CLDN6* promoter in ovarian and testicular cancer cell lines. Some reports demonstrated similar results in ovarian cancer cell lines for CLDN3 and CLDN4 [196,197,278].

Intriguingly, the here presented data display nearly a black-white picture of the methylation status of the *CLDN6* promoter region in tumor cell lines. As tumor cell lines may display an altered methylation pattern compared to their tumor tissue counterparts [279], in this study ovarian and lung tumor tissues were also analyzed on *CLDN6* promoter methylation. Differential methylation of the *CLDN6* promoter in ovarian and lung tumor tissues could be demonstrated here whereas the corresponding normal lung and ovary appeared unmethylated. Moreover, MsqPCR performed in this study revealed that normal colon, liver, lung, kidney, ovary, pancreas and testis with the only exception of placenta exhibited a hypomethylated promoter region as well. This is consistent with reports describing increased *CLDN6* promoter methylation in esophageal squamous cell carcinoma tissues that are CLDN6-negative compared to adjacent normal tissues [134,136]. Of note, it was surprising that the *CLDN6* promoter was found to be unmethylated because promoter hypermethylation was assumed to be the main repressive factor of CLDN6 in normal tissues. Many genes that are active in embryonic development are silenced in adult tissues by hypermethylation [6]. Thus, the absent expression of CLDN6 in normal tissues is not entirely dependent on DNA methylation of the promoter region suggesting that rather specific transcription factors are involved in the repression of CLDN6 in normal tissues and its re-activation in cancer.

One of the most important findings presented in this study is that CLDN6-positive ovarian and lung tumor tissues displayed a lower methylation frequency compared to CLDN6-negative tumor tissues indicating that promoter methylation is associated with CLDN6 expression levels in certain tumors. Of course, the difference observed between CLDN6-positive and negative samples is not that impressive as in tumor cell lines. Possibly, remaining normal adjacent tissues, stromal or immune cells from the tumor microenvironment that pervaded the tumor samples could lead to a biased picture of promoter methylation in tumor tissues. These cell types are suggested to be unmethylated and thus tampering DNA methylation frequency of tumor tissues. Alternatively, the *CLDN6* promoter could be partially methylated in tumors. The latter suggestion is supported by studies regarding CLDN4 regulation by DNA methylation which found both methylated and unmethylated CLDN4 promoter in ovarian tumor tissues [196,278].

The fact that CLDN6 is absent in all adult normal tissues and the possibility that the *CLDN6* promoter is only partially methylated further supports the idea that specific transcription factors are responsible for up-regulation of CLDN6 in cancer. Indeed, it has been shown for other claudins, that a combination of DNA methylation and transcription factors such as SP1 or CREB are critical for claudin up-regulation in cancer [196,197,199]. Many studies indicate histone modifications as additional epigenetic regulator of claudin expression [280]. Moreover, it is known that differential methylation of regions distant from promoter-associated CpG islands (“CpG island shores”) are related with gene expression [281]. In which extend histone modifications or CpG island shores are involved in *CLDN6* regulation has to be analyzed in future studies. DNA methylation is an important mechanism in conjunction with transcription factors to regulate gene expression during embryogenesis and to maintain pluripotency of ESC [282,283]. As mentioned in the last chapter, stem cells and cancer cells share many features, thus it is likely that CLDN6 is up-regulated in cancer by deregulaton of embryonic and stem cell signaling pathways which function in concerted action with epigenetic mechanisms.

Collectively, the data presented here implicate that DNA-methylation of the *CLDN6* promoter is associated but not sufficient for regulation of CLDN6 expression in tumors and normal tissues. The next chapter will discuss the search of transcription factors involved in regulation of CLDN6 in cancer.

5.3.4.2 Transcription factors BORIS and CTCF are likely involved in regulation of *CLDN6*

This study provides evidence that BORIS and CTCF are involved in the regulation of *CLDN6* in cancer. This is supported by the following findings: First, RNAi-mediated silencing of *BORIS* results in down-regulation of *CLDN6* expression whereas silencing of *CTCF* results in up-regulation of *CLDN6*. Second, by sequential deletion of the *CLDN6* promoter, BORIS/CTCF, p53 and SP1 binding sites were revealed to be located in a region essential for *CLDN6* transcription. Third, ChIP analysis displayed enrichment of both CTCF and BORIS in cell lines with different CLDN6 expression status, indicating that CTCF and BORIS compete for binding at the promoter which in turn is responsible for *CLDN6* expression level. This is further supported by increased enrichment of CTCF found at the *CLDN6* promoter when BORIS is silenced. Fourth, among all analyzed CSC-markers in ovarian cancer in this study, *BORIS* and *CLDN6* showed the highest correlation indicating a relationship between both genes.

The ubiquitous transcription factors CTCF and the CGA BORIS are involved in epigenetic regulation of several genes in normal physiology as well as up-regulation of many CGAs such as *NY-ESO-1*, *MAGE-A-1/A-2/A-3/A-4* [155,156,284,285] but also non-CGAs such as *hTERT* and *suprabasin (SBSN)* in cancer [286,287]. Many studies suggest CTCF as a repressive factor and BORIS as an activating factor of several genes in cancer since it is known that both factors compete for the same DNA binding sites [155,285,287]. For example, Hong *et al.* describe a reciprocal binding of CTCF and BORIS to the *NY-ESO-1* promoter and binding of BORIS coincides with derepression of NY-ESO-1 expression in lung cancer cells [155]. The data presented in this work clearly demonstrate binding of BORIS and CTCF in CLDN6-expressing NIH-OVCAR3 and NEC-8 cells whereas BORIS but not CTCF is bound to the promoter in CLDN6-non expressing SK-BR-3 cells. However, CLDN6-low expressing HEK293 cells showed enrichment of CTCF but not BORIS at the *CLDN6* promoter. This raises the question if binding of BORIS and CTCF to the *CLDN6* promoter correlates with the methylation status. CTCF is suggested to bind methylated DNA and while BORIS can bind to both methylated and unmethylated DNA [161].This is consistent with the findings presented in this thesis as SK-BR-3 cells displayed a

methylated promoter whereas NIH-OVCAR3 and NEC-8 as well as HEK293 cells displayed an unmethylated promoter. However, CTCF binding to the unmethylated *CLDN6* promoter in HEK293 cells is not compatible with this idea. CTCF functions are context dependent and indeed, CTCF also binds to unmethylated DNA [288]. A possible hypothesis for the regulation of *CLDN6* by CTCF and BORIS is that CTCF is bound to the CLDN6 promoter in normal cells resulting in repression of transcription. Global hypomethylation is one of the earliest events in tumorigenesis and suggested to mediate up-regulation of CGAs including BORIS [153,154,156,204,289–294]. Subsequently, BORIS is able to compete with CTCF on DNA binding and replaces CTCF at certain binding sites. This could result in up-regulation of *CLDN6.* Indeed, treatment of tumor cells with 5-aza-dC resulted not only in up-regulation of *CLDN6* but also *BORIS* in our group (data not shown). Of note, it is not excluded that CTCF is still bound in some cells to the *CLDN6* promoter. BORIS binding might counteract the repressive effect of CTCF thus defining the transcriptional outcome. This has been shown for other genes, too [287,295,296]. Accordingly, in the present work, binding of CTCF to the *CLDN6* promoter in BORIS-silenced NIH-OVCAR3 cells was slightly increased and correlated with decreased *CLDN6* expression. In normal testis, BORIS and CTCF expression correlates with the re-setting of methylation marks – it is of question if this is also true for cancer as some reports demonstrate that BORIS binding is correlating with promoter hypomethylation [143,155,156].

However, overexpression of BORIS was not sufficient to induce *CLDN6* in SK-BR-3 or HEK293 cells in the present work. Consistently, BORIS was found to be not sufficient for CGA expression and promoter hypomethylation in ovarian cancer cell lines, as overexpression of BORIS alone did not induce expression of CGAs MAGE-A1, NY-ESO-1 and XAGE-1 in ovarian cancer cell lines OVCAR3, OVCAR429 and A2780 [297] suggesting that other epigenetic mechanisms or transcription factors additionally are necessary. Possibly, more transcription factors are involved in the regulation of *CLDN6*. SP1 is a common transcription factor, recruiting additional regulatory proteins leading to formation of a functional transcriptional complex [298–300]. Several facts argue for an involvement of SP1 in regulation of *CLDN6*: In close proximity to the p53 and BORIS/CTCFL binding site a SP1 binding site is present in the *CLDN6* promoter, p53 commonly interacts with SP1 in target gene activation [301] and BORIS recruits SP1 for example to

the promoter of NY-ESO-1 in lung cancer cells [285]. However, enrichment of p53 was only very low compared to negative control loci in the present work indicating that p53 is not involved in regulation of *CLDN6* in cancer. Interestingly, expression of BORIS itself is repressed in normal human fibroblasts by DNA methylation, CTCF and wild-type p53 while absence of functional p53 and promoter demethylation are likely to be involved in up-regulation of BORIS in cancer [158,289]. Moreover, CTCF is bound to the *BORIS* promoter in NIH-OVCAR3 cells that express BORIS endogenously [158]. In the present work, a significant correlation was observed between *CLDN6* and *BORIS* but not *CTCF* in ovarian cancer. Furthermore, CLDN6 expression in lung and ovarian tumor samples used for NGS analysis correlated not only with promoter hypomethylation but also with BORIS overexpression (data not shown). Moreover, analysis of *BORIS* and *CLDN6* transcript expression in lung cancer in our group revealed also a remarkable correlation (data not shown). These findings open the idea that *CLDN6* and *BORIS* might be coordinately regulated especially in ovarian cancer.

Of note, *CLDN6* could be up-regulated by ESC signaling pathways especially in embryonic carcinomas or tumors with a primitive phenotype. Interestingly, BORIS is expressed during embryonic development and moreover, BORIS expression is suggested in CSCs [58,151,302]. Given the hypothesis that CLDN6 is expressed in CSCs, BORIS could represent a regulator of CLDN6 also in CSCs.

Collectively, the present work introduces BORIS and CTCF as regulators of *CLDN6* in cancer. However, both factors seem to be not sufficient to mediate *CLDN6* expression. Whether these factors contribute to *CLDN6* promoter hypo- or hypermethylation in cancer could not be disclosed here and has to be addressed in further studies. For example, bisulfite sequencing of the *CLDN6* promoter in cells overexpressing BORIS could answer this question. Moreover, ChIP for SP1 or other factors will disclose which other transcription factors are involved in *CLDN6* regulation in cancer.

5.3.5 Conclusion and future outlook - CLDN6 is a potent tumor antigen

In conclusion, this work adds significant results to the relevance of CLDN6 in cancer particularly with regards to CSCs. As CSCs are hypothesized to be responsible for chemoresistance and tumor recurrence, targeting and elimination of CSCs is a central challenge in cancer therapy. A better understanding of the molecular signature of CSCs may help to develop therapies against recurrent cancers. Because of its possible role in CSCs, its outstanding tumor specificity and accessibility for antibodies, CLDN6 is a highly promising target for future therapies addressing CSCs using for example antibody-based therapies. Preclinical as well as clinical studies using claudin-targeting therapeutics hold great promise for treatment of cancer [114]. Indeed, a CLDN6-targeting antibody is currently in clinical phase I for treatment of ovarian cancer (Ganymed Pharmaceuticals; ClinicalTrials.gov identifier: NCT02054351).

Moreover, the involvement of promoter methylation and cancer-specific transcription factors in the regulation of *CLDN6* might open new therapeutic strategies. For example, epigenetic drugs could lead to up-regulation of CLDN6 which now can be efficiently targeted by antibodies. This would represent a therapeutic option for cancers that down-regulate target molecules during tumor progression.

6 References

[1] Breasted JH. The Edwin Smith surgical papyrus, published in facsimile and hieroglyphic transliteration with translation and commentary in two volumes. Oriental Institute publications, v. 3-4. Chicago, Ill: University of Chicago, Oriental Institute; 1930.

[2] Jemal A, Bray F, Center MM, Ferlay J, Ward E, Forman D. Global cancer statistics. CA: A Cancer Journal for Clinicians 2011;61:69–90.

[3] Hanahan D, Weinberg RA. The Hallmarks of Cancer. Cell 2000;100:57–70.

[4] Hanahan D, Weinberg RA. Hallmarks of Cancer: The Next Generation. Cell 2011;144:646–74.

[5] Berger SL, Kouzarides T, Shiekhattar R, Shilatifard A. An operational definition of epigenetics. Genes Dev. 2009;23:781–83.

[6] Deaton AM, Bird A. CpG islands and the regulation of transcription. Genes Dev. 2011;25:1010–22.

[7] Russo, V. E. A, Martienssen RA, Riggs AD. Epigenetic mechanisms of gene regulation. Cold Spring Harbor monograph series, Vol 32. Plainview, N.Y: Cold Spring Harbor Laboratory Press; 1996.

[8] Ioshikhes IP, Zhang MQ. Large-scale human promoter mapping using CpG islands. Nat Genet 2000;26:61–63.

[9] Li B, Carey M, Workman JL. The role of chromatin during transcription. Cell 2007;128:707–19.

[10] Holland JF, Frei E. Cancer medicine 8. Shelton (Conn.): People's medical publishing house-USA; op. 2010.

[11] Esteller M. Epigenetics in cancer. N. Engl. J. Med. 2008;358:1148–59.

[12] Feinberg AP, Tycko B. The history of cancer epigenetics. Nat. Rev. Cancer 2004;4:143–53.

[13] Jones PA, Baylin SB. The epigenomics of cancer. Cell 2007;128:683–92.

[14] Herman JG, Baylin SB. Gene silencing in cancer in association with promoter hypermethylation. N. Engl. J. Med. 2003;349:2042–54.

[15] Meacham CE, Morrison SJ. Tumour heterogeneity and cancer cell plasticity. Nature 2013;501:328–37.

[16] Al-Hajj M, Wicha MS, Benito-Hernandez A, Morrison SJ, Clarke MF. Prospective identification of tumorigenic breast cancer cells. Proc. Natl. Acad. Sci. U.S.A. 2003;100:3983–88.

[17] Lapidot T, Sirard C, Vormoor J, Murdoch B, Hoang T, Caceres-Cortes J, et al. A cell initiating human acute myeloid leukaemia after transplantation into SCID mice. Nature 1994;367:645–48.

[18] Dick JE. Stem cell concepts renew cancer research. Blood 2008;112:4793–807.

[19] Clevers H. The cancer stem cell: premises, promises and challenges. Nat Med 2011:313–19.

[20] Dalerba P, Cho RW, Clarke MF. Cancer stem cells: models and concepts. Annu. Rev. Med. 2007;58:267–84.

[21] Lou H, Dean M. Targeted therapy for cancer stem cells: the patched pathway and ABC transporters. Oncogene 2007;26:1357–60.

[22] Alison MR, Lin W, Lim SM, Nicholson LJ. Cancer stem cells: In the line of fire. Cancer Treatment Reviews 2012;38:589–98.

[23] Ma I, Allan AL. The role of human aldehyde dehydrogenase in normal and cancer stem cells. Stem Cell Rev 2011;7:292–306.

[24] Hajdu SI. A note from history: Landmarks in history of cancer, part 1. Cancer 2011;117:1097–102.

[25] Berenblum I. The modifying influence of dichloro-ethyl sulphide on the induction of tumours in mice by tar. J. Pathol. 1929;32:425–34.

[26] Berenblum I. Experimental inhibition of tumour induction by mustard gas and other compounds. J. Pathol. 1935;40:549–58.

[27] Kelloff GJ, Sigman CC. Cancer biomarkers: selecting the right drug for the right patient. Nat Rev Drug Discov 2012;11:201–14.

[28] Coley WB. The Treatment of Malignant Tumors by Repeated Innoculations of Erysipelas: With a Report of Ten Original Cases. American Journal of the Medical Sciences 1893;10:487–511.

[29] BURNET M. Cancer; a biological approach. I. The processes of control. Br Med J 1957;1:779–86.

[30] Kim R, Emi M, Tanabe K. Cancer immunoediting from immune surveillance to immune escape. Immunology 2007;121:1–14.

[31] Schreiber RD, Old LJ, Smyth MJ. Cancer immunoediting: integrating immunity's roles in cancer suppression and promotion. Science 2011;331:1565–70.

[32] Mellman I, Coukos G, Dranoff G. Cancer immunotherapy comes of age. Nature 2011;480:480–89.

[33] Couzin-Frankel J. Cancer Immunotherapy. Science 2013;342:1432–33.

[34] Ackermann R, Huber C. Krebsimmuntherapien: Standards und Innovationen. Köln: Dt. Ärzte-Verl.; 2008.

[35] Gires O, Seliger B. Tumor-associated antigens: Identification, characterization, and clinical applications. Weinheim: Wiley-VCH; 2009.

[36] Sharma SV, Settleman J. Oncogene addiction: setting the stage for molecularly targeted cancer therapy. Genes & Development 2007;21:3214–31.

[37] Kufe DW, Pollock RE, Weichselbaum RR, Bast RC, Gansler TS, Holland JF, et al. Holland-Frei Cancer medicine. 6th ed. Hamilton, Ont: B C Decker; 2003.

[38] Disis ML. Immunotherapy of cancer. Cancer drug discovery and development. Totowa, N.J: Humana Press; 2006.

[39] Even-Desrumeaux K, Baty D, Chames P. State of the art in tumor antigen and biomarker discovery. Cancers (Basel) 2011;3:2554–96.

[40] Traversari C, van der Bruggen, P, Van den Eynde, B, Hainaut P, Lemoine C, Ohta N, et al. Transfection and expression of a gene coding for a human melanoma antigen recognized by autologous cytolytic T lymphocytes. Immunogenetics 1992;35:145–52.

[41] van der Bruggen, P, Traversari C, Chomez P, Lurquin C, Plaen E de, Van den Eynde, B, et al. A gene encoding an antigen recognized by cytolytic T lymphocytes on a human melanoma. Science 1991;254:1643–47.

[42] Chen YT, Scanlan MJ, Sahin U, Tureci O, Gure AO, Tsang S, et al. A testicular antigen aberrantly expressed in human cancers detected by autologous antibody screening. Proc Natl Acad Sci U S A 1997;94:1914–18.

[43] Sahin U, Tureci O, Schmitt H, Cochlovius B, Johannes T, Schmits R, et al. Human neoplasms elicit multiple specific immune responses in the autologous host. Proc Natl Acad Sci U S A 1995;92:11810–13.

[44] Akers SN, Odunsi K, Karpf AR. Regulation of cancer germline antigen gene expression: implications for cancer immunotherapy. Future Oncol 2010;6:717–32.

[45] Caballero OL, Chen Y. Cancer/testis (CT) antigens: potential targets for immunotherapy. Cancer Sci 2009;100:2014–21.

[46] Simpson, Andrew J G, Caballero OL, Jungbluth A, Chen Y, Old LJ. Cancer/testis antigens, gametogenesis and cancer. Nat Rev Cancer 2005;5:615–25.

[47] Old LJ. Cancer/testis (CT) antigens - a new link between gametogenesis and cancer. Cancer Immun 2001;1:1.

[48] Zendman, Albert J W, Ruiter DJ, Van Muijen, Goos N P. Cancer/testis-associated genes: identification, expression profile, and putative function. J Cell Physiol 2003;194:272–88.

[49] Jungbluth AA, Silva, Wilson A Jr, Iversen K, Frosina D, Zaidi B, Coplan K, et al. Expression of cancer-testis (CT) antigens in placenta. Cancer Immun 2007;7:15.

[50] Nelson PT, Zhang PJ, Spagnoli GC, Tomaszewski JE, Pasha TL, Frosina D, et al. Cancer/testis (CT) antigens are expressed in fetal ovary. Cancer Immun 2007;7:1.

[51] Old LJ. Cancer is a somatic cell pregnancy. Cancer Immun 2007;7:19.

[52] Glazer CA, Smith IM, Ochs MF, Begum S, Westra W, Chang SS, et al. Integrative discovery of epigenetically derepressed cancer testis antigens in NSCLC. PLoS ONE 2009;4:e8189.

[53] Smith IM, Glazer CA, Mithani SK, Ochs MF, Sun W, Bhan S, et al. Coordinated activation of candidate proto-oncogenes and cancer testes antigens via promoter demethylation in head and neck cancer and lung cancer. PLoS ONE 2009;4:e4961.

[54] James SR, Link PA, Karpf AR. Epigenetic regulation of X-linked cancer/germline antigen genes by DNMT1 and DNMT3b. Oncogene 2006;25:6975–85.

[55] Smet C de, Lurquin C, Lethé B, Martelange V, Boon T. DNA methylation is the primary silencing mechanism for a set of germ line- and tumor-specific genes with a CpG-rich promoter. Mol. Cell. Biol. 1999;19:7327–35.

[56] Koslowski M, Bell C, Seitz G, Lehr H, Roemer K, Müntefering H, et al. Frequent nonrandom activation of germ-line genes in human cancer. Cancer Res. 2004;64:5988–93.

[57] Smet C de, Backer O de, Faraoni I, Lurquin C, Brasseur F, Boon T. The activation of human gene MAGE-1 in tumor cells is correlated with genome-wide demethylation. Proc. Natl. Acad. Sci. U.S.A. 1996;93:7149–53.

[58] Yamada R, Takahashi A, Torigoe T, Morita R, Tamura Y, Tsukahara T, et al. Preferential expression of cancer/testis genes in cancer stem-like cells: proposal of a novel sub-category, cancer/testis/stem gene. Tissue Antigens 2013;81:428–34.

[59] Beard J. EMBRYOLOGICAL ASPECTS AND ETIOLOGY OF CARCINOMA. The Lancet 1902;159:1758–61.

[60] Strickland S, Richards WG. Invasion of the trophoblasts. Cell 1992;71:355–57.

[61] Cross JC, Hemberger M, Lu Y, Nozaki T, Whiteley K, Masutani M, et al. Trophoblast functions, angiogenesis and remodeling of the maternal vasculature in the placenta. Mol Cell Endocrinol 2002;187:207–12.

[62] Wilczynski JR. Cancer and pregnancy share similar mechanisms of immunological escape. Chemotherapy 2006;52:107–10.

[63] Rama S, Suresh Y, Rao AJ. Regulation of telomerase during human placental differentiation: a role for TGFbeta1. Mol Cell Endocrinol 2001;182:233–48.

[64] Weier JF, Weier HG, Jung CJ, Gormley M, Zhou Y, Chu LW, et al. Human cytotrophoblasts acquire aneuploidies as they differentiate to an invasive phenotype. Dev Biol 2005;279:420–32.

[65] Chiu, Rossa W K, Chim, Stephen S C, Wong, Ivy H N, Wong, Cesar S C, Lee W, To KF, et al. Hypermethylation of RASSF1A in human and rhesus placentas. Am J Pathol 2007;170:941–50.

[66] Wepsic HT. Overview of oncofetal antigens in cancer. Ann. Clin. Lab. Sci. 1983;13:261–66.

[67] Koslowski M, Sahin U, Mitnacht-Kraus R, Seitz G, Huber C, Türeci O. A placenta-specific gene ectopically activated in many human cancers is essentially involved in malignant cell processes. Cancer Res. 2007;67:9528–34.

[68] Silva WA, Gnjatic S, Ritter E, Chua R, Cohen T, Hsu M, et al. PLAC1, a trophoblast-specific cell surface protein, is expressed in a range of human tumors and elicits spontaneous antibody responses. Cancer Immun. 2007;7:18.

[69] Jackman SM, Kong X, Fant ME. Plac1 (placenta-specific 1) is essential for normal placental and embryonic development. Mol. Reprod. Dev. 2012;79:564–72.

[70] Cocchia M, Huber R, Pantano S, Chen EY, Ma P, Forabosco A, et al. PLAC1, an Xq26 Gene with Placenta-Specific Expression. Genomics 2000;68:305–12.

[71] Kushi A, Edamura K, Noguchi M, Akiyama K, Nishi Y, Sasai H. Generation of mutant mice with large chromosomal deletion by use of irradiated ES cells--analysis of large deletion around hprt locus of ES cell. Mamm. Genome 1998;9:269–73.

[72] Zechner U, Reule M, Orth A, Bonhomme F, Strack B, Guénet, et al. An X-chromosome linked locus contributes to abnormal placental development in mouse interspecific hybrid. Nat. Genet. 1996;12:398–403.

[73] Hemberger MC, Pearsall RS, Zechner U, Orth A, Otto S, Rüschendorf F, et al. Genetic dissection of X-linked interspecific hybrid placental dysplasia in congenic mouse strains. Genetics 1999;153:383–90.

[74] Chen Y, Moradin A, Schlessinger D, Nagaraja R. RXRα and LXR activate two promoters in placenta- and tumor-specific expression of PLAC1. Placenta 2011;32:877–84.

[75] Fant M, Farina A, Nagaraja R, Schlessinger D. PLAC1 (Placenta-specific 1): a novel, X-linked gene with roles in reproductive and cancer biology. Prenat. Diagn. 2010;30:497–502.

[76] Bork P, Sander C. A large domain common to sperm receptors (Zp2 and Zp3) and TGF-beta type III receptor. FEBS Lett. 1992;300:237–40.

[77] Jovine L, Janssen WG, Litscher ES, Wassarman PM. The PLAC1-homology region of the ZP domain is sufficient for protein polymerisation. BMC Biochem 2006;7:11.

[78] Jovine L, Qi H, Williams Z, Litscher E, Wassarman PM. The ZP domain is a conserved module for polymerization of extracellular proteins. Nat. Cell Biol. 2002;4:457–61.

[79] Jovine L, Qi H, Williams Z, Litscher ES, Wassarman PM. A duplicated motif controls assembly of zona pellucida domain proteins. Proc. Natl. Acad. Sci. U.S.A. 2004;101:5922–27.

[80] Fant M, Weisoly DL, Cocchia M, Huber R, Khan S, Lunt T, et al. PLAC1, a trophoblast-specific gene, is expressed throughout pregnancy in the human placenta and modulated by keratinocyte growth factor. Mol. Reprod. Dev. 2002;63:430–36.

[81] Chen Y, Schlessinger D, Nagaraja R. T antigen transformation reveals Tp53/RB-dependent route to PLAC1 transcription activation in primary fibroblasts. Oncogenesis 2013;2:e67.

[82] Yuan H, Lu J, Xiao J, Upadhyay G, Umans R, Kallakury B, et al. PPARδ induces estrogen receptor-positive mammary neoplasia through an inflammatory and metabolic phenotype linked to mTOR activation. Cancer Res. 2013;73:4349–61.

[83] Koslowski M, Türeci O, Biesterfeld S, Seitz G, Huber C, Sahin U. Selective activation of trophoblast-specific PLAC1 in breast cancer by CCAAT/enhancer-binding protein beta (C/EBPbeta) isoform 2. J. Biol. Chem. 2009;284:28607–15.

[84] Oñate SA, Tsai SY, Tsai MJ, O'Malley BW. Sequence and characterization of a coactivator for the steroid hormone receptor superfamily. Science 1995;270:1354–57.

[85] Voegel JJ, Heine MJ, Zechel C, Chambon P, Gronemeyer H. TIF2, a 160 kDa transcriptional mediator for the ligand-dependent activation function AF-2 of nuclear receptors. EMBO J. 1996;15:3667–75.

[86] Torchia J, Rose DW, Inostroza J, Kamei Y, Westin S, Glass CK, et al. The transcriptional co-activator p/CIP binds CBP and mediates nuclear-receptor function. Nature 1997;387:677–84.

[87] Anzick SL, Kononen J, Walker RL, Azorsa DO, Tanner MM, Guan XY, et al. AIB1, a steroid receptor coactivator amplified in breast and ovarian cancer. Science 1997;277:965–68.

[88] Han SJ, DeMayo FJ, Xu J, Tsai SY, Tsai M, O'Malley BW. Steroid receptor coactivator (SRC)-1 and SRC-3 differentially modulate tissue-specific activation functions of the progesterone receptor. Mol. Endocrinol. 2006;20:45–55.

[89] Geng C, He B, Xu L, Barbieri CE, Eedunuri VK, Chew SA, et al. Prostate cancer-associated mutations in speckle-type POZ protein (SPOP) regulate steroid receptor coactivator 3 protein turnover. Proc. Natl. Acad. Sci. U.S.A. 2013;110:6997–7002.

[90] Lee SK, Kim HJ, Na SY, Kim TS, Choi HS, Im SY, et al. Steroid receptor coactivator-1 coactivates activating protein-1-mediated transactivations through interaction with the c-Jun and c-Fos subunits. J. Biol. Chem. 1998;273:16651–54.

[91] Werbajh S, Nojek I, Lanz R, Costas MA. RAC-3 is a NF-kappa B coactivator. FEBS Lett. 2000;485:195–99.

[92] Louie MC, Zou JX, Rabinovich A, Chen H. ACTR/AIB1 functions as an E2F1 coactivator to promote breast cancer cell proliferation and antiestrogen resistance. Mol. Cell. Biol. 2004;24:5157–71.

[93] McKenna NJ, O'Malley BW. Combinatorial control of gene expression by nuclear receptors and coregulators. Cell 2002;108:465–74.

[94] Xu J, Li Q. Review of the in vivo functions of the p160 steroid receptor coactivator family. Mol. Endocrinol. 2003;17:1681–92.

[95] Zhang H, Yi X, Sun X, Yin N, Shi B, Wu H, et al. Differential gene regulation by the SRC family of coactivators. Genes Dev. 2004;18:1753–65.

[96] Chen H, Lin RJ, Schiltz RL, Chakravarti D, Nash A, Nagy L, et al. Nuclear receptor coactivator ACTR is a novel histone acetyltransferase and forms a multimeric activation complex with P/CAF and CBP/p300. Cell 1997;90:569–80.

[97] Spencer TE, Jenster G, Burcin MM, Allis CD, Zhou J, Mizzen CA, et al. Steroid receptor coactivator-1 is a histone acetyltransferase. Nature 1997;389:194–98.

[98] Ogryzko VV, Schiltz RL, Russanova V, Howard BH, Nakatani Y. The transcriptional coactivators p300 and CBP are histone acetyltransferases. Cell 1996;87:953–59.

[99] Gojis O, Rudraraju B, Gudi M, Hogben K, Sousha S, Coombes CR, et al. The role of SRC-3 in human breast cancer. Nat Rev Clin Oncol 2009;7:83–89.

[100] Teyssier C, Chen D, Stallcup MR. Requirement for multiple domains of the protein arginine methyltransferase CARM1 in its transcriptional coactivator function. J. Biol. Chem. 2002;277:46066–72.

[101] Xu J, Wu R, O'Malley BW. Normal and cancer-related functions of the p160 steroid receptor co-activator (SRC) family. Nat Rev Cancer 2009;9:615–30.

[102] Karmakar S, Foster EA, Smith CL. Unique roles of p160 coactivators for regulation of breast cancer cell proliferation and estrogen receptor-alpha transcriptional activity. Endocrinology 2009;150:1588–96.

[103] Qin L, Liu Z, Chen H, Xu J. The steroid receptor coactivator-1 regulates twist expression and promotes breast cancer metastasis. Cancer Res. 2009;69:3819–27.

[104] Wang S, Yuan Y, Liao L, Kuang S, Tien JC, O'Malley BW, et al. Disruption of the SRC-1 gene in mice suppresses breast cancer metastasis without affecting primary tumor formation. Proc. Natl. Acad. Sci. U.S.A. 2009;106:151–56.

[105] Fantozzi A, Christofori G. Mouse models of breast cancer metastasis. Breast Cancer Res. 2006;8:212.

[106] Muller WJ, Sinn E, Pattengale PK, Wallace R, Leder P. Single-step induction of mammary adenocarcinoma in transgenic mice bearing the activated c-neu oncogene. Cell 1988;54:105–15.

[107] Torres-Arzayus MI, Font de Mora, Jaime, Yuan J, Vazquez F, Bronson R, Rue M, et al. High tumor incidence and activation of the PI3K/AKT pathway in transgenic mice define AIB1 as an oncogene. Cancer Cell 2004;6:263–74.

[108] Massabbal E, Parveen S, Weisoly DL, Nelson DM, Smith SD, Fant M. PLAC1 expression increases during trophoblast differentiation: Evidence for regulatory interactions with the fibroblast growth factor-7 (FGF-7) axis. Mol. Reprod. Dev. 2005;71:299–304.

[109] Kong X, Jackman SM, Fant ME. Plac1 (placenta-specific 1) is widely expressed during fetal development and is associated with a lethal form of hydrocephalus. Birth Defects Research Part A: Clinical and Molecular Teratology 2013:n/a.

[110] Mineta K, Yamamoto Y, Yamazaki Y, Tanaka H, Tada Y, Saito K, et al. Predicted expansion of the claudin multigene family. FEBS Lett. 2011;585:606–12.

[111] Shin K, Fogg VC, Margolis B. Tight junctions and cell polarity. Annu. Rev. Cell Dev. Biol. 2006;22:207–35.

[112] Runkle EA, Mu D. Tight junction proteins: From barrier to tumorigenesis. Cancer Letters 2013;337:41–48.

[113] Ikenouchi J. Regulation of tight junctions during the epithelium-mesenchyme transition: direct repression of the gene expression of claudins/occludin by Snail. Journal of Cell Science 2003;116:1959–67.

[114] Kominsky SL. Claudins: emerging targets for cancer therapy. ERM 2006;8.

[115] Lal-Nag M, Morin PJ. The claudins. Genome Biol 2009;10:235.

[116] Hewitt KJ, Agarwal R, Morin PJ. The claudin gene family: expression in normal and neoplastic tissues. BMC Cancer 2006;6:186.

[117] Angelow S, Ahlstrom R, Yu, Alan S L. Biology of claudins. Am J Physiol Renal Physiol 2008;295:F867-76.

[118] Colegio OR, Van Itallie, Christina M, McCrea HJ, Rahner C, Anderson JM. Claudins create charge-selective channels in the paracellular pathway between epithelial cells. Am J Physiol Cell Physiol 2002;283:C142-7.

[119] Piontek J, Winkler L, Wolburg H, Muller SL, Zuleger N, Piehl C, et al. Formation of tight junction: determinants of homophilic interaction between classic claudins. FASEB J 2008;22:146–58.

[120] Nunbhakdi-Craig V, Machleidt T, Ogris E, Bellotto D, White, Charles L 3rd, Sontag E. Protein phosphatase 2A associates with and regulates atypical PKC and the epithelial tight junction complex. J Cell Biol 2002;158:967–78.

[121] D'Souza T, Agarwal R, Morin PJ. Phosphorylation of claudin-3 at threonine 192 by cAMP-dependent protein kinase regulates tight junction barrier function in ovarian cancer cells. J Biol Chem 2005;280:26233–40.

[122] Itoh M, Furuse M, Morita K, Kubota K, Saitou M, Tsukita S. Direct binding of three tight junction-associated MAGUKs, ZO-1, ZO-2, and ZO-3, with the COOH termini of claudins. J Cell Biol 1999;147:1351–63.

[123] Van Itallie, Christina M, Gambling TM, Carson JL, Anderson JM. Palmitoylation of claudins is required for efficient tight-junction localization. J Cell Sci 2005;118:1427–36.

[124] Gupta IR, Ryan AK. Claudins: unlocking the code to tight junction function during embryogenesis and in disease. Clinical Genetics 2010;77:314–25.

[125] Evans MJ, Hahn T von, Tscherne DM, Syder AJ, Panis M, Wolk B, et al. Claudin-1 is a hepatitis C virus co-receptor required for a late step in entry. Nature 2007;446:801–05.

[126] Zheng A, Yuan F, Li Y, Zhu F, Hou P, Li J, et al. Claudin-6 and claudin-9 function as additional coreceptors for hepatitis C virus. J Virol 2007;81:12465–71.

[127] Katahira J, Sugiyama H, Inoue N, Horiguchi Y, Matsuda M, Sugimoto N. Clostridium perfringens enterotoxin utilizes two structurally related membrane proteins as functional receptors in vivo. J Biol Chem 1997;272:26652–58.

[128] Lal-Nag M, Battis M, Santin AD, Morin PJ. Claudin-6: a novel receptor for CPE-mediated cytotoxicity in ovarian cancer. Oncogenesis 2012;1:e33.

[129] Moriwaki K, Tsukita S, Furuse M. Tight junctions containing claudin 4 and 6 are essential for blastocyst formation in preimplantation mouse embryos. Developmental Biology 2007;312:509–22.

[130] Turksen K, Troy TC. Claudin-6: a novel tight junction molecule is developmentally regulated in mouse embryonic epithelium. Dev. Dyn. 2001;222:292–300.

[131] Gratsch TE, De Boer, Lisa S., O'Shea KS. RNA inhibition of BMP-4 gene expression in postimplantation mouse embryos. genesis 2003;37:12–17.

[132] Kubota H. Retinoid X Receptor α and Retinoic Acid Receptor γ Mediate Expression of Genes Encoding Tight-Junction Proteins and Barrier Function in F9 Cells during Visceral Endodermal Differentiation. Experimental Cell Research 2001;263:163–72.

[133] Chiba H, Gotoh T, Kojima T, Satohisa S, Kikuchi K, Osanai M, et al. Hepatocyte nuclear factor (HNF)-4α triggers formation of functional tight junctions and establishment of polarized epithelial morphology in F9 embryonal carcinoma cells. Experimental Cell Research 2003;286:288–97.

[134] Oka D, Yamashita S, Tomioka T, Nakanishi Y, Kato H, Kaminishi M, et al. The presence of aberrant DNA methylation in noncancerous esophageal mucosae in association with smoking history. Cancer 2009;115:3412–26.

[135] Osanai M, Murata M, Chiba H, Kojima T, Sawada N. Epigenetic silencing of claudin-6 promotes anchorage-independent growth of breast carcinoma cells. Cancer Sci. 2007;98:1557–62.

[136] Tsunoda S, Smith E, De Young, Neville J, Wang X, Tian Z, Liu J, et al. Methylation of CLDN6, FBN2, RBP1, RBP4, TFPI2, and TMEFF2 in esophageal squamous cell carcinoma. Oncol. Rep. 2009;21:1067–73.

[137] Yafang L, Qiong W, Yue R, Xiaoming X, Lina Y, Mingzi Z, et al. Role of Estrogen Receptor-α in the Regulation of Claudin-6 Expression in Breast Cancer Cells. J Breast Cancer 2011;14:20.

[138] Li Q, Zhu F, Chen P. miR-7 and miR-218 epigenetically control tumor suppressor genes RASSF1A and Claudin-6 by targeting HoxB3 in breast cancer. Biochemical and Biophysical Research Communications 2012;424:28–33.

[139] Ren Y, Wu Q, Liu Y, Xu X, Quan C. Gene silencing of claudin6 enhances cell proliferation and migration accompanied with increased MMP2 activity via p38 MAPK signaling pathway in human breast epithelium cell line HBL100. Mol Med Rep 2013;8:1505–10.

[140] Wu Q, Liu X, Liu Y, Lu Y, Wang L, Zhang X, et al. Inhibition of p38 activity reverses claudin-6 induced cell apoptosis, invasion, and migration. Chin. Med. J. 2013;126:3539–44.

[141] Fujita-Yoshigaki J, Matsuki-Fukushima M, Sugiya H. Inhibition of Src and p38 MAP kinases suppresses the change of claudin expression induced on dedifferentiation of primary cultured parotid acinar cells. AJP: Cell Physiology 2008;294:C774.

[142] DelloRusso C, Welcsh PL, Wang W, Garcia RL, King M, Swisher EM. Functional Characterization of a Novel BRCA1-Null Ovarian Cancer Cell Line in Response to Ionizing Radiation. Molecular Cancer Research 2007;5:35–45.

[143] Klenova EM, Morse, Herbert C 3rd, Ohlsson R, Lobanenkov VV. The novel BORIS + CTCF gene family is uniquely involved in the epigenetics of normal biology and cancer. Semin Cancer Biol 2002;12:399–414.

[144] Ohlsson R, Renkawitz R, Lobanenkov V. CTCF is a uniquely versatile transcription regulator linked to epigenetics and disease. Trends Genet 2001;17:520–27.

[145] Chao W, Huynh KD, Spencer RJ, Davidow LS, Lee JT. CTCF, a candidate trans-acting factor for X-inactivation choice. Science 2002;295:345–47.

[146] Phillips JE, Corces VG. CTCF: Master Weaver of the Genome. Cell 2009;137:1194–211.

[147] Loukinov DI, Pugacheva E, Vatolin S, Pack SD, Moon H, Chernukhin I, et al. BORIS, a novel male germ-line-specific protein associated with epigenetic reprogramming events, shares the same 11-zinc-finger domain with CTCF, the insulator protein involved in reading imprinting marks in the soma. Proc Natl Acad Sci U S A 2002;99:6806–11.

[148] Hore TA, Deakin JE, Marshall Graves, Jennifer A., Ferguson-Smith AC. The Evolution of Epigenetic Regulators CTCF and BORIS/CTCFL in Amniotes. PLoS Genetics 2008;4:e1000169.

[149] Filippova GN, Lindblom A, Meincke LJ, Klenova EM, Neiman PE, Collins SJ, et al. A widely expressed transcription factor with multiple DNA sequence specificity, CTCF, is localized at chromosome segment 16q22.1 within one of the smallest regions of overlap for common deletions in breast and prostate cancers. Genes Chromosomes Cancer 1998;22:26–36.

[150] Pugacheva EM, Suzuki T, Pack SD, Kosaka-Suzuki N, Yoon J, Vostrov AA, et al. The Structural Complexity of the Human BORIS Gene in Gametogenesis and Cancer. PLoS ONE 2010;5:e13872.

[151] Monk M, Hitchins M, Hawes S. Differential expression of the embryo/cancer gene ECSA(DPPA2), the cancer/testis gene BORIS and the pluripotency structural gene OCT4, in human preimplantation development. Molecular Human Reproduction 2008;14:347–55.

[152] Shi L, Wu J. Epigenetic regulation in mammalian preimplantation embryo development. Reprod Biol Endocrinol 2009;7:59.

[153] Martin-Kleiner I. BORIS in human cancers – A review. European Journal of Cancer 2012;48:929–35.

[154] Necochea-Campion R de, Ghochikyan A, Josephs SF, Zacharias S, Woods E, Karimi-Busheri F, et al. Expression of the Epigenetic factor BORIS (CTCFL) in the Human Genome. J Transl Med 2011;9:213.

[155] Hong JA, Kang Y, Abdullaev Z, Flanagan PT, Pack SD, Fischette MR, et al. Reciprocal binding of CTCF and BORIS to the NY-ESO-1 promoter coincides with derepression of this cancer-testis gene in lung cancer cells. Cancer Res 2005;65:7763–74.

[156] Vatolin S, Abdullaev Z, Pack SD, Flanagan PT, Custer M, Loukinov DI, et al. Conditional expression of the CTCF-paralogous transcriptional factor BORIS in normal cells results in demethylation and derepression of MAGE-A1 and reactivation of other cancer-testis genes. Cancer Res 2005;65:7751–62.

[157] Suzuki T, Kosaka-Suzuki N, Pack S, Shin DM, Yoon J, Abdullaev Z, et al. Expression of a Testis-Specific Form of Gal3st1 (CST), a Gene Essential for Spermatogenesis, Is Regulated by the CTCF Paralogous Gene BORIS. Molecular and Cellular Biology 2010;30:2473–84.

[158] Renaud S, Pugacheva EM, Delgado MD, Braunschweig R, Abdullaev Z, Loukinov D, et al. Expression of the CTCF-paralogous cancer-testis gene, brother of the regulator of imprinted sites (BORIS), is regulated by three alternative promoters modulated by CpG methylation and by CTCF and p53 transcription factors. Nucleic Acids Research 2007;35:7372–88.

[159] van de Nobelen, Suzanne, Rosa-Garrido M, Leers J, Heath H, Soochit W, Joosen L, et al. CTCF regulates the local epigenetic state of ribosomal DNA repeats. Epigenetics Chromatin 2010;3:19.

[160] Majumder P, Boss JM. DNA methylation dysregulates and silences the HLA-DQ locus by altering chromatin architecture. Genes Immun. 2011;12:291–99.

[161] Nguyen P, Cui H, Bisht KS, Sun L, Patel K, Lee RS, et al. CTCFL/BORIS is a methylation-independent DNA-binding protein that preferentially binds to the paternal H19 differentially methylated region. Cancer Res. 2008;68:5546–51.

[162] Morita K, Furuse M, Fujimoto K, Tsukita S. Claudin multigene family encoding four-transmembrane domain protein components of tight junction strands. Proc. Natl. Acad. Sci. U.S.A. 1999;96:511–16.

[163] Anderson WJ, Zhou Q, Alcalde V, Kaneko OF, Blank LJ, Sherwood RI, et al. Genetic targeting of the endoderm with claudin-6CreER. Dev. Dyn. 2008;237:504–12.

[164] Wang L, Xue Y, Shen Y, Li W, Cheng Y, Yan X, et al. Claudin 6: a novel surface marker for characterizing mouse pluripotent stem cells. Cell Res. 2012;22:1082–85.

[165] Assou S, Le Carrour T, Tondeur S, Ström S, Gabelle A, Marty S, et al. A Meta-Analysis of Human Embryonic Stem Cells Transcriptome Integrated into a Web-Based Expression Atlas. Stem Cells 2007;25:961–73.

[166] Ben-David U, Nudel N, Benvenisty N. Immunologic and chemical targeting of the tight-junction protein Claudin-6 eliminates tumorigenic human pluripotent stem cells. Nat Commun 2013;4:1992.

[167] Turksen K, Troy T. Permeability barrier dysfunction in transgenic mice overexpressing claudin 6. Development 2002;129:1775–84.

[168] Enikanolaiye A, Lariviere N, Troy T, Arabzadeh A, Atasoy E, Turksen K. Involucrin-claudin-6 tail deletion mutant (C 206) transgenic mice: a model of delayed epidermal permeability barrier formation and repair. Disease Models & Mechanisms 2010;3:167–80.

[169] Troy T, Rahbar R, Arabzadeh A, Cheung RM, Turksen K. Delayed epidermal permeability barrier formation and hair follicle aberrations in Inv-Cldn6 mice. Mech. Dev. 2005;122:805–19.

[170] Troy T, Li Y, O'Malley L, Turksen K. The temporal and spatial expression of Claudins in epidermal development and the accelerated program of epidermal differentiation in K14-CaSR transgenic mice. Gene Expr. Patterns 2007;7:423–30.

[171] Sullivan LM, Yankovich T, Le P, Martinez D, Santi M, Biegel JA, et al. Claudin-6 is a nonspecific marker for malignant rhabdoid and other pediatric tumors. Am. J. Surg. Pathol. 2012;36:73–80.

[172] Ushiku T, Shinozaki-Ushiku A, Maeda D, Morita S, Fukayama M. Distinct expression pattern of claudin-6, a primitive phenotypic tight junction molecule, in germ cell tumours and visceral carcinomas. Histopathology 2012;61:1043–56.

[173] Abuazza G, Becker A, Williams SS, Chakravarty S, Truong H, Lin F, et al. Claudins 6, 9, and 13 are developmentally expressed renal tight junction proteins. AJP: Renal Physiology 2006;291:F1132.

[174] VÄRE P, SOINI Y. Twist is inversely associated with claudins in germ cell tumors of the testis. APMIS 2010;118:640–47.

[175] Rendón-Huerta E, Teresa F, Teresa GM, Xochitl G, Georgina A, Veronica Z, et al. Distribution and Expression Pattern of Claudins 6, 7, and 9 in Diffuse- and Intestinal-Type Gastric Adenocarcinomas. J Gastrointest Canc 2010;41:52–59.

[176] Birks DK, Kleinschmidt-DeMasters BK, Donson AM, Barton VN, McNatt SA, Foreman NK, et al. Claudin 6 Is a Positive Marker for Atypical Teratoid/Rhabdoid Tumors. Brain Pathology 2010;20:140–50.

[177] Zavala-Zendejas VE, Torres-Martinez AC, Salas-Morales B, Fortoul TI, Montaño LF, Rendon-Huerta EP. Claudin-6, 7, or 9 Overexpression in the Human Gastric Adenocarcinoma Cell Line AGS Increases Its Invasiveness, Migration, and Proliferation Rate. Cancer Invest 2011;29:1–11.

[178] Wu Q, Liu Y, Ren Y, Xu X, Yu L, Li Y, et al. Tight junction protein, claudin-6, downregulates the malignant phenotype of breast carcinoma. Eur J Cancer Prev 2010;19:186–94.

[179] Xu X, Jin H, Liu Y, Liu L, Wu Q, Guo Y, et al. The expression patterns and correlations of claudin-6, methy-CpG binding protein 2, DNA methyltransferase 1, histone deacetylase 1, acetyl-histone H3 and acetyl-histone H4 and their clinicopathological significance in breast invasive ductal carcinomas. Diagn Pathol 2012;7:33.

[180] Hong Y, Hishikawa D, Miyahara H, Nishimura Y, Tsuzuki H, Gotoh C, et al. Up-regulation of the claudin-6 gene in adipogenesis. Biosci Biotechnol Biochem 2005;69:2117–21.

[181] Fofana I, Zona L, Thumann C, Heydmann L, Durand SC, Lupberger J, et al. Functional Analysis of Claudin-6 and Claudin-9 as Entry Factors for Hepatitis C Virus Infection of Human Hepatocytes by Using Monoclonal Antibodies. Journal of Virology 2013;87:10405–10.

[182] Meertens L, Bertaux C, Cukierman L, Cormier E, Lavillette D, Cosset F, et al. The Tight Junction Proteins Claudin-1, -6, and -9 Are Entry Cofactors for Hepatitis C Virus. Journal of Virology 2008;82:3555–60.

[183] Burnette WN. "Western blotting": electrophoretic transfer of proteins from sodium dodecyl sulfate--polyacrylamide gels to unmodified nitrocellulose and radiographic detection with antibody and radioiodinated protein A. Anal. Biochem. 1981;112:195–203.

[184] Towbin H, Staehelin T, Gordon J. Electrophoretic transfer of proteins from polyacrylamide gels to nitrocellulose sheets: procedure and some applications. Proc. Natl. Acad. Sci. U.S.A. 1979;76:4350–54.

[185] Wagner M, Koslowski M, Paret C, Schmidt M, Türeci O, Sahin U. NCOA3 is a selective co-activator of estrogen receptor α-mediated transactivation of PLAC1 in MCF-7 breast cancer cells. BMC Cancer 2013;13:570.

[186] Neve RM, Chin K, Fridlyand J, Yeh J, Baehner FL, Fevr T, et al. A collection of breast cancer cell lines for the study of functionally distinct cancer subtypes. Cancer Cell 2006;10:515–27.

[187] Bouras T, Southey MC, Venter DJ. Overexpression of the steroid receptor coactivator AIB1 in breast cancer correlates with the absence of estrogen and progesterone receptors and positivity for p53 and HER2/neu. Cancer Res. 2001;61:903–07.

[188] Heck S, Rom J, Thewes V, Becker N, Blume B, Sinn HP, et al. Estrogen-related receptor alpha expression and function is associated with the transcriptional coregulator AIB1 in breast carcinoma. Cancer Res. 2009;69:5186–93.

[189] Lahusen T, Henke RT, Kagan BL, Wellstein A, Riegel AT. The role and regulation of the nuclear receptor co-activator AIB1 in breast cancer. Breast Cancer Res. Treat. 2009;116:225–37.

[190] Colognato H, Yurchenco PD. Form and function: the laminin family of heterotrimers. Dev. Dyn. 2000;218:213–34.

[191] Durbeej M. Laminins. Cell Tissue Res. 2010;339:259–68.

[192] Ekblom M, Falk M, Salmivirta K, Durbeej M, Ekblom P. Laminin isoforms and epithelial development. Ann. N. Y. Acad. Sci. 1998;857:194–211.

[193] Felding-Habermann B, Cheresh DA. Vitronectin and its receptors. Curr. Opin. Cell Biol. 1993;5:864–68.

[194] Kwon MJ, Kim S, Choi Y, Jung HS, Balch C, Kim S, et al. Derepression of CLDN3 and CLDN4 during ovarian tumorigenesis is associated with loss of repressive histone modifications. Carcinogenesis 2010;31:974–83.

[195] Herman JG, Graff JR, Myöhänen S, Nelkin BD, Baylin SB. Methylation-specific PCR: a novel PCR assay for methylation status of CpG islands. Proc. Natl. Acad. Sci. U.S.A. 1996;93:9821–26.

[196] Honda H, Pazin MJ, Ji H, Wernyj RP, Morin PJ. Crucial roles of Sp1 and epigenetic modifications in the regulation of the CLDN4 promoter in ovarian cancer cells. J. Biol. Chem. 2006;281:21433–44.

[197] Honda H, Pazin MJ, D'Souza T, Ji H, Morin PJ. Regulation of the CLDN3 gene in ovarian cancer cells. Cancer Biol. Ther. 2007;6:1733–42.

[198] Ogawa M, Kojima T, Someya M, Nomura K, Takasawa A, Murata M, et al. Epidermal growth factor modulates claudins and tight junctional functions in ovarian cancer cell lines. Histochem. Cell Biol. 2012;138:323–38.

[199] Sahin U, Koslowski M, Dhaene K, Usener D, Brandenburg G, Seitz G, et al. Claudin-18 splice variant 2 is a pan-cancer target suitable for therapeutic antibody development. Clin. Cancer Res. 2008;14:7624–34.

[200] Kovach JS, McGovern RM, Cassady JD, Swanson SK, Wold LE, Vogelstein B, et al. Direct sequencing from touch preparations of human carcinomas: analysis of p53 mutations in breast carcinomas. J. Natl. Cancer Inst. 1991;83:1004–09.

[201] Yaginuma Y, Westphal H. Abnormal structure and expression of the p53 gene in human ovarian carcinoma cell lines. Cancer Res. 1992;52:4196–99.

[202] Botcheva K, McCorkle SR, McCombie WR, Dunn JJ, Anderson CW. Distinct p53 genomic binding patterns in normal and cancer-derived human cells. Cell Cycle 2011;10:4237–49.

[203] Smeenk L, van Heeringen, Simon J, Koeppel M, Gilbert B, Janssen-Megens E, Stunnenberg HG, et al. Role of p53 serine 46 in p53 target gene regulation. PLoS ONE 2011;6:e17574.

[204] Jones TA, Ogunkolade BW, Szary J, Aarum J, Mumin MA, Patel S, et al. Widespread expression of BORIS/CTCFL in normal and cancer cells. PLoS ONE 2011;6:e22399.

[205] Best DJ, Roberts DE. Algorithm AS 89: The Upper Tail Probabilities of Spearman's Rho. Applied Statistics 1975;24:377.

[206] Benjamini Y, Hochberg Y. Controlling the false discovery rate: A practical and powerful approach to multiple testing. Journal of the Royal Statistical Society Series B 1995;57:289–300.

[207] Maloney DG, Grillo-López AJ, White CA, Bodkin D, Schilder RJ, Neidhart JA, et al. IDEC-C2B8 (Rituximab) anti-CD20 monoclonal antibody therapy in patients with relapsed low-grade non-Hodgkin's lymphoma. Blood 1997;90:2188–95.

[208] Hudis CA. Trastuzumab--mechanism of action and use in clinical practice. N. Engl. J. Med. 2007;357:39–51.

[209] Osborne CK, Bardou V, Hopp TA, Chamness GC, Hilsenbeck SG, Fuqua, Suzanne A W, et al. Role of the estrogen receptor coactivator AIB1 (SRC-3) and HER-2/neu in tamoxifen resistance in breast cancer. J. Natl. Cancer Inst. 2003;95:353–61.

[210] Kirkegaard T, McGlynn LM, Campbell FM, Müller S, Tovey SM, Dunne B, et al. Amplified in breast cancer 1 in human epidermal growth factor receptor - positive tumors of tamoxifen-treated breast cancer patients. Clin. Cancer Res. 2007;13:1405–11.

[211] Tien JC, Xu J. Steroid receptor coactivator-3 as a potential molecular target for cancer therapy. Expert Opin. Ther. Targets 2012;16:1085–96.

[212] Azorsa DO, Cunliffe HE, Meltzer PS. Association of steroid receptor coactivator AIB1 with estrogen receptor-alpha in breast cancer cells. Breast Cancer Res. Treat. 2001;70:89–101.

[213] List HJ, Lauritsen KJ, Reiter R, Powers C, Wellstein A, Riegel AT. Ribozyme targeting demonstrates that the nuclear receptor coactivator AIB1 is a rate-limiting factor for estrogen-dependent growth of human MCF-7 breast cancer cells. J. Biol. Chem. 2001;276:23763–68.

[214] Yan J, Erdem H, Li R, Cai Y, Ayala G, Ittmann M, et al. Steroid receptor coactivator-3/AIB1 promotes cell migration and invasiveness through focal adhesion turnover and matrix metalloproteinase expression. Cancer Res. 2008;68:5460–68.

[215] Shao D, Berrodin TJ, Manas E, Hauze D, Powers R, Bapat A, et al. Identification of novel estrogen receptor alpha antagonists. J. Steroid Biochem. Mol. Biol. 2004;88:351–60.

[216] Planas-Silva MD, Shang Y, Donaher JL, Brown M, Weinberg RA. AIB1 enhances estrogen-dependent induction of cyclin D1 expression. Cancer Res. 2001;61:3858–62.

[217] Yu S, Reddy JK. Transcription coactivators for peroxisome proliferator-activated receptors. Biochim. Biophys. Acta 2007;1771:936–51.

[218] Yi P, Xia W, Wu R, Lonard DM, Hung M, O'Malley BW. SRC-3 coactivator regulates cell resistance to cytotoxic stress via TRAF4-mediated p53 destabilization. Genes Dev. 2013;27:274–87.

[219] Cheever MA, Allison JP, Ferris AS, Finn OJ, Hastings BM, Hecht TT, et al. The prioritization of cancer antigens: a national cancer institute pilot project for the acceleration of translational research. Clin. Cancer Res. 2009;15:5323–37.

[220] Micke P, Mattsson, Johanna Sofia Margareta, Edlund K, Lohr M, Jirström K, Berglund A, et al. Aberrantly activated claudin 6 and 18.2 as potential therapy targets in non-small-cell lung cancer. Int. J. Cancer 2014.

[221] Lin Z, Zhang X, Liu Z, Liu Q, Wang L, Lu Y, et al. The distinct expression patterns of claudin-2, -6, and −11 between human gastric neoplasms and adjacent non-neoplastic tissues. Diagn Pathol 2013;8:133.

[222] Morin PJ. Claudin proteins in human cancer: promising new targets for diagnosis and therapy. Cancer Res. 2005;65:9603–06.

[223] Martin TA, Jiang WG. Tight junctions and their role in cancer metastasis. Histol. Histopathol. 2001;16:1183–95.

[224] Boireau S, Buchert M, Samuel MS, Pannequin J, Ryan JL, Choquet A, et al. DNA-methylation-dependent alterations of claudin-4 expression in human bladder carcinoma. Carcinogenesis 2006;28:246–58.

[225] Lioni M, Brafford P, Andl C, Rustgi A, El-Deiry W, Herlyn M, et al. Dysregulation of claudin-7 leads to loss of E-cadherin expression and the increased invasion of esophageal squamous cell carcinoma cells. Am. J. Pathol. 2007;170:709–21.

[226] Dhawan P, Singh AB, Deane NG, No Y, Shiou S, Schmidt C, et al. Claudin-1 regulates cellular transformation and metastatic behavior in colon cancer. J. Clin. Invest. 2005;115:1765–76.

[227] Dahiya N, Becker KG, Wood WH, Zhang Y, Morin PJ. Claudin-7 is frequently overexpressed in ovarian cancer and promotes invasion. PLoS ONE 2011;6:e22119.

[228] Harrell JC, Pfefferle AD, Zalles N, Prat A, Fan C, Khramtsov A, et al. Endothelial-like properties of claudin-low breast cancer cells promote tumor vascular permeability and metastasis. Clin Exp Metastasis 2014;31:33–45.

[229] Huang Y, Bao Y, Peng W, Goldberg M, Love K, Bumcrot DA, et al. Claudin-3 gene silencing with siRNA suppresses ovarian tumor growth and metastasis. Proc. Natl. Acad. Sci. U.S.A. 2009;106:3426–30.

[230] Kominsky SL, Argani P, Korz D, Evron E, Raman V, Garrett E, et al. Loss of the tight junction protein claudin-7 correlates with histological grade in both ductal carcinoma in situ and invasive ductal carcinoma of the breast. Oncogene 2003;22:2021–33.

[231] Perou CM. Molecular stratification of triple-negative breast cancers. Oncologist 2011;16 Suppl 1:61–70.

[232] Prat A, Parker JS, Karginova O, Fan C, Livasy C, Herschkowitz JI, et al. Phenotypic and molecular characterization of the claudin-low intrinsic subtype of breast cancer. Breast Cancer Res 2010;12:R68.

[233] Hennessy BT, Gonzalez-Angulo A, Stemke-Hale K, Gilcrease MZ, Krishnamurthy S, Lee J, et al. Characterization of a naturally occurring breast cancer subset enriched in epithelial-to-mesenchymal transition and stem cell characteristics. Cancer Res. 2009;69:4116–24.

[234] Hough CD, Sherman-Baust CA, Pizer ES, Montz FJ, Im DD, Rosenshein NB, et al. Large-scale serial analysis of gene expression reveals genes differentially expressed in ovarian cancer. Cancer Res. 2000;60:6281–87.

[235] Rangel, Leticia B A, Agarwal R, D'Souza T, Pizer ES, Alo PL, Lancaster WD, et al. Tight junction proteins claudin-3 and claudin-4 are frequently overexpressed in ovarian cancer but not in ovarian cystadenomas. Clin Cancer Res 2003;9:2567–75.

[236] Tassi RA, Bignotti E, Falchetti M, Ravanini M, Calza S, Ravaggi A, et al. Claudin-7 expression in human epithelial ovarian cancer. Int J Gynecol Cancer 2008;18:1262–71.

[237] Zhu Y, Brannstrom M, Janson P, Sundfeldt K. Differences in expression patterns of the tight junction proteins,claudin 1, 3, 4 and 5, in human ovarian surface epithelium as compared to epithelia in inclusion cysts and epithelial ovarian tumours. Int J Cancer 2006;118:1884–91.

[238] Agarwal R, D'Souza T, Morin PJ. Claudin-3 and claudin-4 expression in ovarian epithelial cells enhances invasion and is associated with increased matrix metalloproteinase-2 activity. Cancer Res. 2005;65:7378–85.

[239] Zhao W, Ji X, Zhang F, Li L, Ma L. Embryonic Stem Cell Markers. Molecules 2012;17:6196–236.

[240] Suva ML, Riggi N, Bernstein BE. Epigenetic Reprogramming in Cancer. Science 2013;339:1567–70.

[241] Friedmann-Morvinski D, Verma IM. Dedifferentiation and reprogramming: origins of cancer stem cells. EMBO Rep. 2014;15:244–53.

[242] Chen L, Kasai T, Li Y, Sugii Y, Jin G, Okada M, et al. A model of cancer stem cells derived from mouse induced pluripotent stem cells. PLoS ONE 2012;7:e33544.

[243] Ohnishi K, Semi K, Yamamoto T, Shimizu M, Tanaka A, Mitsunaga K, et al. Premature Termination of Reprogramming In Vivo Leads to Cancer Development through Altered Epigenetic Regulation. Cell 2014;156:663–77.

[244] Turksen K. Claudins and Cancer Stem Cells. Stem Cell Rev and Rep 2011;7:797–98.

[245] Boylan, Kristin L M, Misemer B, Derycke MS, Andersen JD, Harrington KM, Kalloger SE, et al. Claudin 4 Is Differentially Expressed between Ovarian Cancer Subtypes and Plays a Role in Spheroid Formation. Int J Mol Sci 2011;12:1334–58.

[246] Liu T, Cheng W, Lai D, Huang Y, Guo L. Characterization of primary ovarian cancer cells in different culture systems. Oncol. Rep. 2010;23:1277–84.

[247] Ahmed N, Abubaker K, Findlay J, Quinn M. Cancerous ovarian stem cells: Obscure targets for therapy but relevant to chemoresistance. J. Cell. Biochem. 2013;114:21–34.

[248] Lin S, Yu HS. Clinical significance of nucleostemin expression and its correlation with cyclin D1 expression in malignant ovarian tumors. Int. J. Gynecol. Cancer 2011;21:1166–71.

[249] Peng S, Maihle NJ, Huang Y. Pluripotency factors Lin28 and Oct4 identify a sub-population of stem cell-like cells in ovarian cancer. Oncogene 2010;29:2153–59.

[250] Zhou J, Ng S, Chng W. LIN28/LIN28B: an emerging oncogenic driver in cancer stem cells. Int. J. Biochem. Cell Biol. 2013;45:973–78.

[251] Zhan Q, Wang C, Ngai S. Ovarian cancer stem cells: a new target for cancer therapy. Biomed Res Int 2013;2013:916819.

[252] Bao S, Wu Q, Li Z, Sathornsumetee S, Wang H, McLendon RE, et al. Targeting Cancer Stem Cells through L1CAM Suppresses Glioma Growth. Cancer Research 2008;68:6043–48.

[253] Liu Z, Li Q, Li K, Chen L, Li W, Hou M, et al. Telomerase reverse transcriptase promotes epithelial-mesenchymal transition and stem cell-like traits in cancer cells. Oncogene 2013;32:4203–13.

[254] Wang X, Penalva LO, Yuan H, Linnoila RI, Lu J, Okano H, et al. Musashi1 regulates breast tumor cell proliferation and is a prognostic indicator of poor survival. Mol. Cancer 2010;9:221.

[255] Marian CO, Cho SK, McEllin BM, Maher EA, Hatanpaa KJ, Madden CJ, et al. The telomerase antagonist, imetelstat, efficiently targets glioblastoma tumor-initiating cells leading to decreased proliferation and tumor growth. Clin. Cancer Res. 2010;16:154–63.

[256] van der Gun, B. T. F., Melchers LJ, Ruiters, M. H. J., de Leij, L. F. M. H., McLaughlin, P. M. J., Rots MG. EpCAM in carcinogenesis: the good, the bad or the ugly. Carcinogenesis 2010;31:1913–21.

[257] Bellone S, Siegel ER, Cocco E, Cargnelutti M, Silasi D, Azodi M, et al. Overexpression of epithelial cell adhesion molecule in primary, metastatic, and recurrent/chemotherapy-resistant epithelial ovarian cancer: implications for epithelial cell adhesion molecule-specific immunotherapy. Int. J. Gynecol. Cancer 2009;19:860–66.

[258] Terris B, Cavard C, Perret C. EpCAM, a new marker for cancer stem cells in hepatocellular carcinoma. J. Hepatol. 2010;52:280–81.

[259] Yamashita T, Ji J, Budhu A, Forgues M, Yang W, Wang H, et al. EpCAM-positive hepatocellular carcinoma cells are tumor-initiating cells with stem/progenitor cell features. Gastroenterology 2009;136:1012–24.

[260] Foster R, Buckanovich RJ, Rueda BR. Ovarian cancer stem cells: working towards the root of stemness. Cancer Lett. 2013;338:147–57.

[261] Gao M, Choi Y, Kang S, Youn JH, Cho N. CD24+ cells from hierarchically organized ovarian cancer are enriched in cancer stem cells. Oncogene 2010;29:2672–80.

[262] Alagaratnam S, Lind GE, Kraggerud SM, Lothe RA, Skotheim RI. The testicular germ cell tumour transcriptome. Int. J. Androl. 2011;34:e133-50; discussion e150-1.

[263] Skotheim RI, Lind GE, Monni O, Nesland JM, Abeler VM, Fosså SD, et al. Differentiation of human embryonal carcinomas in vitro and in vivo reveals expression profiles relevant to normal development. Cancer Res. 2005;65:5588–98.

[264] Park JT, Chen X, Tropè CG, Davidson B, Shih I, Wang T. Notch3 overexpression is related to the recurrence of ovarian cancer and confers resistance to carboplatin. Am. J. Pathol. 2010;177:1087–94.

[265] Ben-Porath I, Thomson MW, Carey VJ, Ge R, Bell GW, Regev A, et al. An embryonic stem cell–like gene expression signature in poorly differentiated aggressive human tumors. Nat Genet 2008;40:499–507.

[266] Ushiku T, Shinozaki A, Shibahara J, Iwasaki Y, Tateishi Y, Funata N, et al. SALL4 represents fetal gut differentiation of gastric cancer, and is diagnostically useful in distinguishing hepatoid gastric carcinoma from hepatocellular carcinoma. Am. J. Surg. Pathol. 2010;34:533–40.

[267] Venneti S, Le P, Martinez D, Xie SX, Sullivan LM, Rorke-Adams LB, et al. Malignant rhabdoid tumors express stem cell factors, which relate to the expression of EZH2 and Id proteins. Am. J. Surg. Pathol. 2011;35:1463–72.

[268] Deisch J, Raisanen J, Rakheja D. Immunohistochemical expression of embryonic stem cell markers in malignant rhabdoid tumors. Pediatr. Dev. Pathol. 2011;14:353–59.

[269] He Q, Luo X, Wang K, Zhou Q, Ao H, Yang Y, et al. Isolation and characterization of cancer stem cells from high-grade serous ovarian carcinomas. Cell. Physiol. Biochem. 2014;33:173–84.

[270] Rodríguez-Rodríguez L, Sancho-Torres I, Mesonero C, Gibbon DG, Shih WJ, Zotalis G. The CD44 receptor is a molecular predictor of survival in ovarian cancer. Med. Oncol. 2003;20:255–63.

[271] Afify AM, Ferguson AW, Davila RM, Werness BA. Expression of CD44S and CD44v5 is more common in stage III than in stage I serous ovarian carcinomas. Appl. Immunohistochem. Mol. Morphol. 2001;9:309–14.

[272] Shi J, Zhou Z, Di W, Li N. Correlation of CD44v6 expression with ovarian cancer progression and recurrence. BMC Cancer 2013;13:182.

[273] Jaggupilli A, Elkord E. Significance of CD44 and CD24 as cancer stem cell markers: an enduring ambiguity. Clin. Dev. Immunol. 2012;2012:708036.

[274] Fábián A, Barok M, Vereb G, Szöllosi J. Die hard: are cancer stem cells the Bruce Willises of tumor biology? Cytometry A 2009;75:67–74.

[275] Medema JP. Cancer stem cells: the challenges ahead. Nat. Cell Biol. 2013;15:338–44.

[276] Liu H, Chen C, Yang H, Pan Y, Zhang X. Cancer stem cell subsets and their relationships. J Transl Med 2011;9:50.

[277] Quan C, Lu S. Identification of genes preferentially expressed in mammary epithelial cells of Copenhagen rat using subtractive hybridization and microarrays. Carcinogenesis 2003;24:1593–99.

[278] Litkouhi B, Kwong J, Lo C, Smedley JG, McClane BA, Aponte M, et al. Claudin-4 overexpression in epithelial ovarian cancer is associated with hypomethylation and is a potential target for modulation of tight junction barrier function using a C-terminal fragment of Clostridium perfringens enterotoxin. Neoplasia 2007;9:304–14.

[279] Smiraglia DJ, Rush LJ, Frühwald MC, Dai Z, Held WA, Costello JF, et al. Excessive CpG island hypermethylation in cancer cell lines versus primary human malignancies. Hum. Mol. Genet. 2001;10:1413–19.

[280] Kwon MJ. Emerging roles of claudins in human cancer. Int J Mol Sci 2013;14:18148–80.

[281] Irizarry RA, Ladd-Acosta C, Carvalho B, Wu H, Brandenburg SA, Jeddeloh JA, et al. Comprehensive high-throughput arrays for relative methylation (CHARM). Genome Res. 2008;18:780–90.

[282] Altun G, Loring JF, Laurent LC. DNA methylation in embryonic stem cells. J. Cell. Biochem. 2010;109:1–6.

[283] Bibikova M, Laurent LC, Ren B, Loring JF, Fan J. Unraveling epigenetic regulation in embryonic stem cells. Cell Stem Cell 2008;2:123–34.

[284] Bhan S, Negi SS, Shao C, Glazer CA, Chuang A, Gaykalova DA, et al. BORIS binding to the promoters of cancer testis antigens, MAGEA2, MAGEA3, and MAGEA4, is associated with their transcriptional activation in lung cancer. Clin. Cancer Res. 2011;17:4267–76.

[285] Kang Y, Hong JA, Chen GA, Nguyen DM, Schrump DS. Dynamic transcriptional regulatory complexes including BORIS, CTCF and Sp1 modulate NY-ESO-1 expression in lung cancer cells. Oncogene 2007;26:4394–403.

[286] Gaykalova D, Vatapalli R, Glazer CA, Bhan S, Shao C, Sidransky D, et al. Dose-dependent activation of putative oncogene SBSN by BORIS. PLoS ONE 2012;7:e40389.

[287] Renaud S, Loukinov D, Alberti L, Vostrov A, Kwon Y, Bosman FT, et al. BORIS/CTCFL-mediated transcriptional regulation of the hTERT telomerase gene in testicular and ovarian tumor cells. Nucleic Acids Res. 2011;39:862–73.

[288] Ong C, Corces VG. CTCF: an architectural protein bridging genome topology and function. Nat Rev Genet 2014;15:234–46.

[289] Woloszynska-Read A, James SR, Link PA, Yu J, Odunsi K, Karpf AR. DNA methylation-dependent regulation of BORIS/CTCFL expression in ovarian cancer. Cancer Immun. 2007;7:21.

[290] Risinger JI, Chandramouli, Gadisetti V R, Maxwell GL, Custer M, Pack S, Loukinov D, et al. Global expression analysis of cancer/testis genes in uterine cancers reveals a high incidence of BORIS expression. Clin. Cancer Res. 2007;13:1713–19.

[291] D'Arcy V, Pore N, Docquier F, Abdullaev ZK, Chernukhin I, Kita G, et al. BORIS, a paralogue of the transcription factor, CTCF, is aberrantly expressed in breast tumours. Br. J. Cancer 2008;98:571–79.

[292] Link PA, Zhang W, Odunsi K, Karpf AR. BORIS/CTCFL mRNA isoform expression and epigenetic regulation in epithelial ovarian cancer. Cancer Immun. 2013;13:6.

[293] Okabayashi K, Fujita T, Miyazaki J, Okada T, Iwata T, Hirao N, et al. Cancer-testis antigen BORIS is a novel prognostic marker for patients with esophageal cancer. Cancer Sci. 2012;103:1617–24.

[294] Chen K, Huang W, Huang B, Wei Y, Li B, Ge Y, et al. BORIS, brother of the regulator of imprinted sites, is aberrantly expressed in hepatocellular carcinoma. Genet Test Mol Biomarkers 2013;17:160–65.

[295] Fiorentino FP, Macaluso M, Miranda F, Montanari M, Russo A, Bagella L, et al. CTCF and BORIS regulate Rb2/p130 gene transcription: a novel mechanism and a new paradigm for understanding the biology of lung cancer. Mol. Cancer Res. 2011;9:225–33.

[296] Sleutels F, Soochit W, Bartkuhn M, Heath H, Dienstbach S, Bergmaier P, et al. The male germ cell gene regulator CTCFL is functionally different from CTCF and binds CTCF-like consensus sites in a nucleosome composition-dependent manner. Epigenetics Chromatin 2012;5:8.

[297] Woloszynska-Read A, James SR, Song C, Jin B, Odunsi K, Karpf AR. BORIS/CTCFL expression is insufficient for cancer-germline antigen gene expression and DNA hypomethylation in ovarian cell lines. Cancer Immun. 2010;10:6.

[298] Hung J, Wang Y, Chang W. Sp1 deacetylation induced by phorbol ester recruits p300 to activate 12(S)-lipoxygenase gene transcription. Mol. Cell. Biol. 2006;26:1770–85.

[299] Suzuki T, Kimura A, Nagai R, Horikoshi M. Regulation of interaction of the acetyltransferase region of p300 and the DNA-binding domain of Sp1 on and through DNA binding. Genes Cells 2000;5:29–41.

[300] Safe S, Abdelrahim M. Sp transcription factor family and its role in cancer. Eur. J. Cancer 2005;41:2438–48.

[301] Freed-Pastor WA, Prives C. Mutant p53: one name, many proteins. Genes Dev. 2012;26:1268–86.

[302] Benhattar J, Alberti L. Abstract 3383: Expression and role of BORIS/CTCFL in human cancer stem cells. Cancer Research 2012;72:3383.

7 Appendix

7.1 Vectors

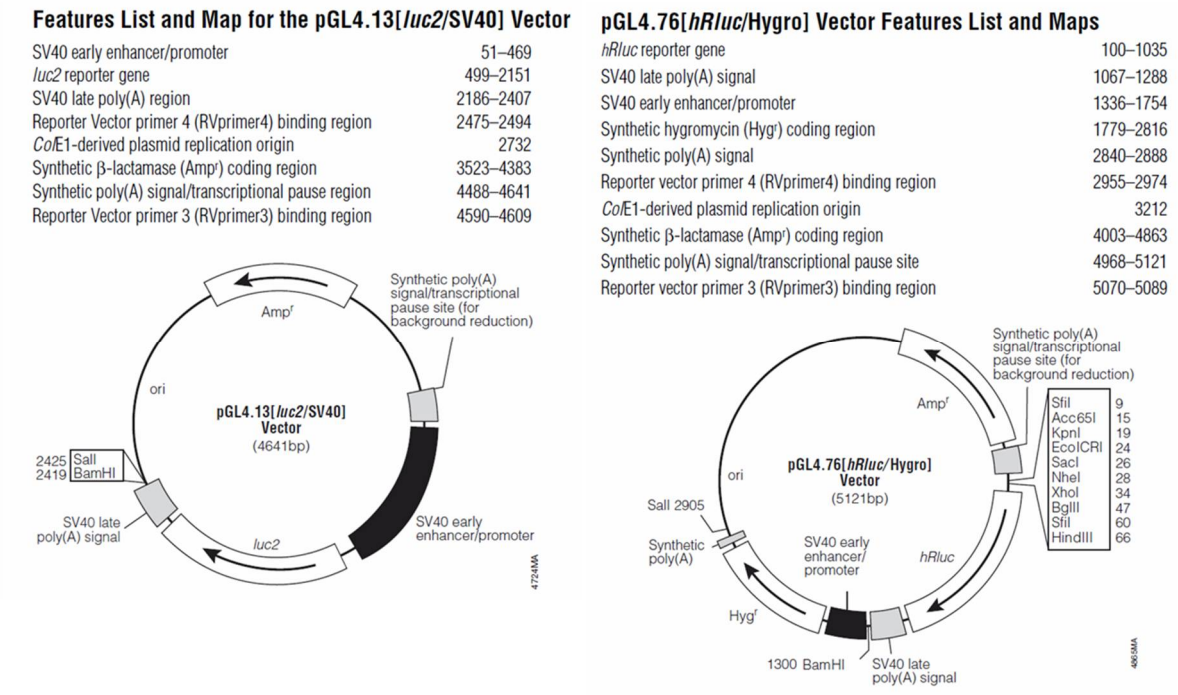

Figure 46 Features and maps of vectors pGL4.13[*luc2*/SV40] and pGL4.76[*hRluc*/Hygro] used for cloning of CLDN6 promoter contructs used in dual luciferase assay. Both vectors were purchased from Promega. pGL4.13[*luc2*/SV40] encodes firefly luciferase under control of SV40 promoter and was used as internal control vector to normalize transfection efficiency. Pictures are adopted from Promega.

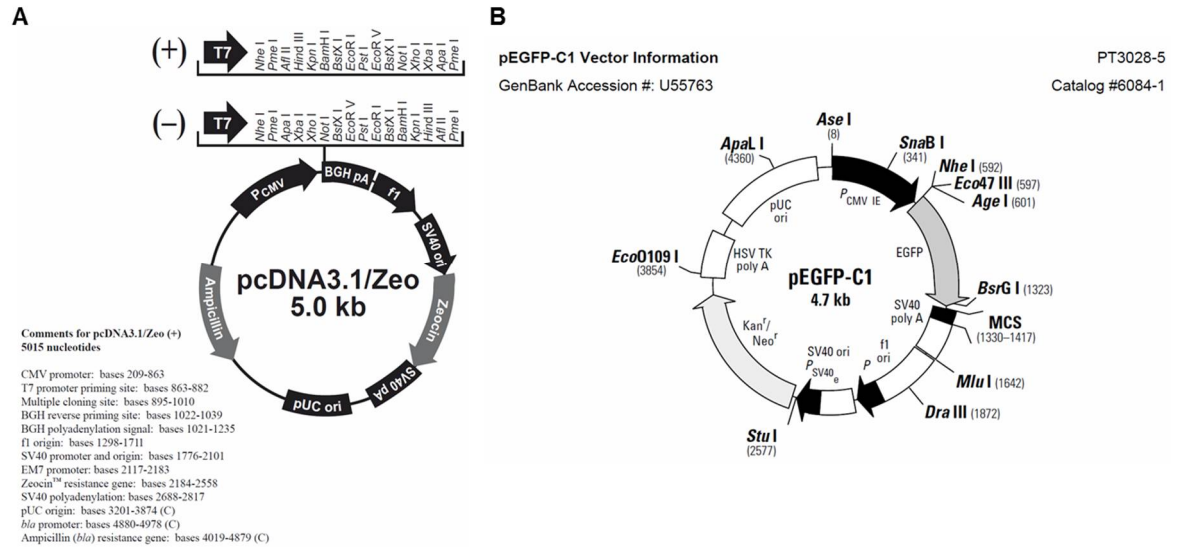

Figure 47 Features and maps of vectors pcDNA3.1/Zeo and pEGFP-C1. (A) pcDNA3.1/Zeo was purchased from Life Technologies and used to overexpress BORIS in tumor cells. (B) pEGFP-C1 was purchased from Clontech and used to analyze transfection efficiency. Pictures are adopted from Life Technologies (A) and Clontech (B).

7.2 siRNA duplexes

Table 10 Sequences of siRNAs and siRNA pools used in this study.

siRNA	Target sequences	Catalog number / Manufacturer
***PLAC1*-siRNA 1; targeting nucleotides 342 to 362**	5'-CUC CAU GAG AGU AGC CAG CAA-3'	SI00685916; Qiagen
***PLAC1*-siRNA 2; targeting nucleotides 670 to 690**	5'-CCG GUU CAG GAC AAA GTC CAA-3'	SI00685895; Qiagen
***SRC-3*-siRNA pool**	siRNA 1 5'-CAC AAU ACC UGC AAU AUA A-3'; siRNA 2 5'-GAA AGG UUG UCA AUA UAG A-3'; siRNA 3 5'-GAA GGU GUA UUC AGA GAU U-3'; siRNA 4 5'-CGG AAA CAU UGU AUU UGU A-3'	M-003759-02-0005; Dharmacon
***CLDN6*-siRNA pool**	siRNA 1 5'-GCG CUA GAG CCA UCC AGA A-3'; siRNA 2 5'-GGG AUG GGU UCG UAC CUU U-3'; siRNA 3 5'-GAU UGU CUU UGU CAU CUC A-3'; siRNA 4 5'-UAC CAA GAA UUA CGU CUG A-3'	M-015883-01-0005; Dharmacon
***BORIS*-siRNA pool**	siRNA 1 5'-GAA AUU GUU CUC ACA GUU U-3'; siRNA 2 5'-GGA AGA AGA ACA AGA AAG A-3'; siRNA 3 5'-GGA AAU ACC ACG AUG CAA A-3'; siRNA 4 5'-UGA AAG AAG UGA CGA AAU U-3'	M-003819-00-0005; Dharmacon
***CTCF*-siRNA pool**	siRNA 1 5'-AAG AAU GAG AAG CGC UUU A-3'; siRNA 2 5'-AAA CAU ACC GAG AAC GAA A-3'; siRNA 3 5'-GAA GAU GCC UGC CAC UUA C-3'; siRNA 4 5'-GAA AGU GGU UGG UAA UAU G-3'	M-020165-02-0005; Dharmacon

7.3 Oligonucleotides

7.3.1 Oligonucleotides for qRT-PCR, cDNA synthesis and cloning

Table 11 Oligonucleotide sequences and annealing temperatures used for quantitative real time RT-PCR analysis.

Gene	Sequence (5'-3')	Annealing temperature (°C)
HPRT1	Sense: TGA CAC TGG CAA AAC AAT GCA Antisense: GGT CCT TTT CAC CAG CAA GCT	62
SRC-1	Sense: GGC ATC AAT ATG AGA TCA GGC ATG Antisense: TTC CTA TCG CTC CTT GCT GCC A	62
SRC-2	Sense: CTG GAG TAC CAA CAC AGG CAC Antisense: CTG TGC ATT TGC CTG GGG AAT CC	62
SRC-3	Sense: GAA AGA GCA TTA TTG GAC CAG C Antisense: TGT CCC TGA AGA TGA AAG CC	60
PLAC1	Sense: AAA TTT GGC AGC TGC CTT CAC Antisense: TGA TGC CAC ATT CAG TAA CAC	60
CLDN6	Sense: CTT ATC TCC TTC GCA GTG CAG Antisense: AAG GAG GGC GAT GAC ACA GAG	58
BORIS	Sense: CAA AGA AAG ACA AAG GGA GCA AAA GG Antisense: TAG GGC CTG GTT CCT GTG TG	62
CTCF	Sense: CAG TGA AAA TGC TGA ACC AGA TC Antisense: GAT AGC TGT TGG CTG GTT CTG	60
Cldn6	Sense: CAG TCT CTT TTG CAG GCT CG Antisense: CAT CTG GCC AGT GCT CTG A	58

Table 12 Oligonucleotides used for cDNA synthesis.

Oligonucleotide name	Sequence (5'-3')
dT18	TTT TTT TTT TTT TTT TTT
dT18-tag	GAG ATC TCG AGA TCT CGA TCG TAC TTT TTT TTT TTT TTT TTT

Table 13 Oligonucleotides used for cloning of CLDN6 promoter and deletion constructs or BORIS.

Oligonucleotide name	Sequence (5'-3')
CL6_HindIII_as	ta tat aaa gct TCG TCT CTC CAA CAC GCA C
CL6_NheI_s	tat atg cta gc CCT TGA GAT TGC GTC TCA CTC
CL6_NheI_del1_s	tat atg cta gc GCC TGT AAT CTC AGC TACTC
CL6_NheI_del2_s	tat atg cta gc CAC CTG TAG TAG TCC CAG
CL6_NheI_del3_s	tat atg cta gc GAC GCC TGG GCA ATA TAA C
CL6_NheI_del4_s	tat atg cta gc GAA GGC TCG GGA AGG TTA G
CL6_NheI_del5_s	tat atg cta gc GCG ACC CCA GCC TCC
CL6_NheI_del5a_s	tat atg cta gc CAA GCC TGG GAT TCG CAC
CL6_NheI_del5b_s	tat atg cta gc GTC AGG GAC AGG GTC TC
CL6_NheI_del5c_s	tat atg cta gc GGG CGG TGG TCC AGT G
CL6_NheI_del6_s	tat atg cta gc GCT TCT TTA AGA CCC CCG C
BORIS-NheI-Koz-HA-s	TA TAT GCT AGC GCC ACC ATG TAC CCA TAC GAT GTT CCA GAT TAC GCT gca gcc act gag atc tct gtc c
BORIS-BamHI-Stop-as	TAT ATA GGA TCC tta tca ctt atc cat cgt gtt gag gag cat

7.3.2 Oligonucleotides for methylation-specific qRT-PCR and bisulfite sequencing

Table 14 Oligonucleotides specific for bisulfite converted DNA used for bisulfite sequencing of the promoter region in front of CLDN6-001 and -201.

Fragment	Amplicon length	Oligonucleotide name	Sequence (5'-3')	Tm (°C)
CLDN6-001-A	284 bp	CLDN6-001_s_1 CLDN6-001_as_1B	caatccatacacttatccaaatcc ggtaggggggttgtggggatt	60
CLDN6-001-B	241 bp	CLDN6-001_s_3 CLDN6-001_as_3	aatccccacaaccccccctacc ggatgtttagtttaggaaggggtac	62
CLDN6-001-C	257 bp	CLDN6-001_s_2 CLDN6-001_as_2B	tacccctttcctaaactaaacatccc ggattgggtgtttggagaatag	62
CLDN6-001-D	345 bp	CLDN6-001_s_4 CLDN6-001_as_4	ctattctccaaacacccaatcc tttgttgaatgaatgattgaattgag	60
CLDN6-001-E	233 bp	CLDN6-001_s_5 CLDN6-001_as_2	ctcaattcaatcattcattcaacaaa tttgttttagatttttaaattgatgggatt	58
CLDN6-201-A02	158 bp	CLDN6_s_A CLDN6_as_A	cctaaacaatataacaaaaccctatct gttatttaggttggagtgtagtgg	56
CLDN6-201-A03	188 bp	CLDN6_s_B CLDN6_as_B	aaactccatctcaaaaacaaacaac gttttgttttgtatagatagggttttg	56
CLDN6-201-B02	193 bp	CLDN6_s_C CLDN6_as_C	tctctactaaaaatacaaaaaaattaatc gttgtttgtttttgagatggagttt	56
CLDN6-201-B03	180 bp	CLDN6_s_D CLDN6_as_D	cctataatcccaacacattaaaaaacc agagtagttgggattattataggtg	60
CLDN6-201-C	345 bp	CLDN6-201_s_2 CLDN6-201_as_2B	Ctacctataatcccaactactcaaa gtttagatttatttagggtgaggg	60
CLDN6-201-D	226 bp	CLDN6-201_s_4 CLDN6-201_as_2	Ccctcaccctaaataaatctaaac aggagataagggaaatttttaggtc	58
CLDN6-201-E	253 bp	CLDN6_s_E CLDN6_as_E	acctaaaaatttcccttatctcctt gagtttttgtttttggggaggg	56

Table 15 Oligonucleotides specific for methylated (M) or unmethylated (U) bisulfite converted DNA used for methylation-specific qPCR.

MSP assay	Region and CpG covered	Oligonucleotide name	Sequence (5'-3')	Tm (°C)
1 U	-170 to -88; 6 CpGs	P1_rev_U P2_for_U	tgtttttgatggtagtgggtgtgtg ctaccaacccaaaacaaacccaaca	60
1 M	-170 to -88; 6 CpGs	P1_rev_M P2_for_M	gtttttgacggtagcgggcg aacgtctaccaacccgaaacg	60
2 U	-288 to -144; 4 CpGs	P5_rev_U P6_for_U	ttgggtttgttttgggttggtagatg catatcaccacactacttaaataataaaaca	62
2 M	-288 to -144; 4 CpGs	P5_rev_M P6_for_M	aggttggggtcgttgggttcg taaataaattccccatatcaccgcg	62
3 U	+118 to +196; 9 CpGs	R1_U	ctcaaaaacttaaacacaaaccaaccaa	60

		F2_U	tgtgtgtgaatttgggttgtggttat	
3 M	+80 to +194; 6 CpGs	R2_M F1_M	cggaggtttgggcgcg taaaaccgaatacaaaataataacgacgta	60

7.3.3 Oligonucleotides and Barcodes for NGS

Six overlapping fragments (N2 to N7) covering region -545 to +230 of the CLDN6-201 promoter were generated. For barcoding of 12 different samples, specific barcodes (6 bp in length) were included at the 5'-end of every oligonucleotide. The barcoded primers were used in PCR to amplify the barcoded sample DNA fragments for ultraplex analysis by NGS.

Table 16 Oligonucleotides specific for bisulfite converted DNA used for NGS.

Fragment	Amplicon length (w/o barcode)	Oligonucleotide name	Sequence (5'-3')
N2	173 bp	CLDN6_s_2 CLDN6_as_N2	ctacctataatcccaactactcaaa gttttaaggtataaattaaagggtatattatt
N3	190 bp	CLDN6_s_N3 CLDN6_as_N3	tctaaaataataccaataatataccctttaa aggtttagggtagaatagagtttg
N4	167 bp	CLDN6_s_N4 CLDN6_as_N4	aatctcaaactctattctaccctaa gaggaggggtagagattttgtt
N5	181 bp	CLDN6_s_N5 CLDN6_as_N5	acaaaatctctaccctcctc tattattttgtattcggttttaagagg
N6	188 bp	CLDN6_s_N6 CLDN6_as_E	cctcttaaaaccgaatacaaaataata gagtttttgtttttggggaggg
N7	151 bp	CLDN6_s_N7 CLDN6_as_N7	acctaaaaatttcccttatctcct gggattcgtttatttaggtggtc

Table 17 Specific Barcodes for the different samples analyzed by NGS.

Sample	Barcode	Sample	Barcode
DAN-G	ACACTA	**743 - lung ca neg**	GATGGT
NEC-8	ATCTTC	**810 - lung ca neg**	GATTCA
426 - ovary	ATGTGC	**779 - ovary ca pos**	GGAGCT
817 - lung	CAGAAG	**1325 - ovary ca pos**	TACAGT
562 - lung ca pos	CGTGAG	**184 - ovary ca neg**	TCGAAG
4404 - lung ca pos	CTGCAC	**1337 - ovary ca neg**	TCTGGA

7.3.4 Oligonucleotides for ChIP-qPCR

Table 18 Oligonucleotides used for qPCR of ChIP samples.

Gene	Sequence (5'-3')	Amplicon length
PLAC1 promoter -348/-198 bp	Sense 5'-CAA CAG CAA GCA CTA CAA GTG-3' Antisense 5'-GAA GCT CAA CTC GGT GCA CTT GTT C-3'	150 bp
PLAC1 upstream negative control -1219/-1064 bp	Sense 5'-AAG CAC TTA GGA CAG CAT CTG-3' Antisense 5'-TGA ATG ATA CCT ACT GTC ATG-3'	155 bp
TSP50	Sense 5'-AGG AGC ATC CCC ACC CAG C-3' Antisense 5'-AGT GCC GCC CCC ACG AC-3'	74 bp
hTERT	Sense 5'-GCG GCG CGA GTT TCA G-3' Antisense 5'-GCA GCA CCT CGC GGT AGT-3'	138 bp
hMYC-G	Sense 5'-GTG CGG GAG CCA GTG AAC T-3' Antisense 5'-AAG ATC CCA GCT CCT CAG CC-3'	55 bp
p21	Sense 5'-CTG GAC TGG GCA CTC TTG TC-3' Antisense 5'-CTC CTA CCA TCC CCT TCC TC-3'	214 bp
CLDN6-promoter 1 -1442/-1277 bp	Sense 5'-TGG TAC GAT CAC GGC TCT CTG-3' Antisense 5'-CAA AGC TGT AGT GGC CAG GC-3'	164 bp
CLDN6-promoter 2	Sense 5'-CTC AAG CTC TGT TCT ACC CTA AG-3'	193 bp

-223/-30 bp	Antisense 5'-CGG TGA CGT CAC TGG ACC A-3'	
CLDN6-promoter 3 +1/+152 bp	Sense 5'-CGA CAC TCG GCC TAG GAA TTT C-3' Antisense 5'-CCA TCC AGG TGG CCG CAG-3'	152 bp
Intergenic control region IgG2	Sense 5'-TGG GAA GAC AAT TTC TGA ACC AAA T-3' Antisense 5'-TCA ACC TGA AAA ATG GGA ATA TGA CA-5'	73 bp
CLDN6 upstream negative control 1 -2510/-2391 bp	Sense 5'-GGA CGG TGG GAG AAA CTG AG-3' Antisense 5'-AGG CGG ATG TGG GGA TCT G-3'	119 bp
CLDN6 upstream negative control 2 -1870/-1762 bp	Sense 5'-CGG TGG CTC ACG CCT TTA ATC-3' Antisense 5'-GTA GAG ACG GCG TTT CAC CAC-3'	108 bp

7.4 TaqMan® Gene Expression Assays

Table 19 TaqMan® Assay ID for target genes analyzed by qRT-PCR on BioMark™ HD (Fluidigm).

Target	*TaqMan® Assay ID*	*Target*	*TaqMan® Assay ID*	*Target*	*TaqMan® Assay ID*
CTCFL	Hs00540744_m1	**EGFR**	Hs01076078_m1	**ABCB1**	Hs00184500_m1
MSI1	Hs01045892_m1	**Endoglin/ CD105**	Hs00923996_m1	**ABCB5**	*Hs02889060_m1*
LIN28B	Hs01013729_m1	**FCGB1A/B/ C**	Hs00417598_m1	**ABCG2**	Hs01053790_m1
SALL4	Hs00360675_m1	**FLT3**	Hs00174690_m1	**AFP**	Hs01040598_m1
CD24	Hs03044178_g1	**FUT4**	Hs01106466_s1	**ALCAM/ CD166**	Hs00977640_m1
GNL3	Hs00205071_m1	**GLI1**	Hs01110766_m1	**ALDH1A1**	Hs00946916_m1
ERBB2	Hs01001580_m1	**GLI2**	Hs01119974_m1	**AMACR**	Hs01091292_m1
POU2F1	Hs00231250_m1	**HIF-2A/ EPAS1**	Hs01026149_m1	**ANPEP/ CD13**	Hs00174265_m1
EPCAM	Hs00901885_m1	**HAVCR2**	Hs00958618_m1	**ATXN1**	Hs00165656_m1
L1CAM	Hs01109748_m1	**IL1A**	Hs00174092_m1	**BMI1**	Hs00180411_m1
TERT	Hs00972656_m1	**IL6RA**	Hs01075666_m1	**BMP4**	Hs00370078_m1
ITGA2	Hs00158127_m1	**ITGA1**	Hs00235006_m1	**BRCA1**	Hs01556193_m1
CD44	*Hs01075863_m1*	**ITGA6**	Hs01041011_m1	**CD151**	Hs00911635_g1
IPO8	Hs00183533_m1	**ITGA9**	Hs00979865_m1	**CD19**	Hs00174333_m1
KIT	Hs00174029_m1	**ITGB1BP1**	Hs00178055_m1	**CD2**	Hs00233515_m1
POU5F1	Hs04260367_gH	**ITGB2**	Hs00164957_m1	**CD27/ TNFRSF7**	Hs00386811_m1
PROM1/ CD133	Hs01009250_m1	**LMO2**	Hs00153473_m1	**CD34**	Hs00990732_m1
PTEN	Hs02621230_s1	**MET**	Hs01565584_m1	**CD38**	Hs01120071_m1
SDC1	Hs00896423_m1	**MS4A1**	Hs00544819_m1	**CD47**	Hs00179953_m1
SHH	Hs00179843_m1	**MYC**	Hs00153408_m1	**CTCF**	Hs00902008_m1
SNAI1	Hs00195591_m1	**MYD88**	Hs01573837_g1	**CX3CR1**	Hs01922583_s1
SOX2	Hs02802330_m1	**NANOG**	Hs02387400_g1	**CXCL1/ Fractalkine**	Hs00605382_gH
SOX4	Hs00268388_s1	**NCAM1**	Hs00941831_m1	**CXCR1**	Hs00174146_m1
ST8SIA1	Hs00268157_m1	**NF2/ Merlin**	Hs00966302_m1	**DLL4**	Hs00184092_m1
STAT3	Hs00374280_m1	**NGFR**	Hs00609977_m1	**DPP4**	Hs00175210_m1
TNFAIP3	Hs00234713_m1	**NOTCH1**	Hs01062014_m1	**THY1**	Hs00174816_m1
TFRC/ CD71	Hs00951083_m1	**PDPN**	Hs00366766_m1	**TRRAP**	Hs01591130_m1
GAPDH	Hs99999905_m1	**PIWIL1**	Hs01041737_m1		
HPRT1	Hs99999909_m1	**PLAUR**	Hs00958880_m1		

8 Affirmation and Publications

Ich versichere, dass ich die von mir vorgelegte Dissertation selbstständig angefertigt, die benutzten Quellen und Hilfsmittel vollständig angegeben und die Stellen der Arbeit - einschließlich Tabellen und Abbildungen -, die anderen Werken im Wortlaut oder dem Sinn nach entnommen sind, in jedem Einzelfall als Entlehnung kenntlich gemacht habe; dass diese Dissertation noch keiner anderen Fakultät oder Universität zur Prüfung vorgelegen habe; dass sie - abgesehen von unten angegebenen Teilpublikationen - noch nicht veröffentlicht worden ist sowie, dass ich eine solche Veröffentlichung vor Abschluss des Promotionsverfahrens nicht vornehmen werde. Die Bestimmungen dieser Promotionsordnung sind mir bekannt. Die von mir vorgelegte Dissertation ist von Prof. Dr. Ugur Sahin in der Abteilung für Experimentelle und Translationale Onkologie der Universitätsmedizin der Johannes Gutenberg-Universität Mainz betreut worden.

Mainz, den 30.06.2014 _____

Meike Wagner

Parts of this study have been published in:

Articles

- **Wagner M**, Koslowski M, Paret C, Schmidt M, Türeci Ö, Sahin U. NCOA3 is a selective co-activator of estrogen receptor α-mediated transactivation of PLAC1 in MCF-7 cells. *BMC Cancer* 2013, **13**:570.
- **Wagner M**, Paret C, Koslowski M, Häcker S, Castle JC, Kneip C, Jung J, VK Tiwari, Löwer M, Bukur T, Türeci Ö, Sahin U. Up-regulation of Claudin 6 in cancer is dependent on hypomethylation and tumor-specific transcription factors. *In preparation.*
- Claudin 6 is a cancer cell selective stem cell marker suitable for antibody therapy. *In preparation.*

Patent

- Sahin U, Türeci Ö, Walter K, **Wagner M**, Kreuzberg M, Häcker S, Jacobs S. Diagnosis and Therapy of Cancer involving Cancer Stem Cells – PCT/EP2013/002272, 31.07.2013.

Oral presentations and posters

- Oral presentation: **Wagner M**. Molecular-functional characterization of tumor-specific antigens. IMB-TRON Symposium, Mainz (2014).
- Poster: **Wagner M**, Häcker S, Paret C, Koslowski M, Kneip C, Castle JC, Türeci Ö, Sahin U. Molecular and functional characterization of the highly specific cancer target T-066. 43. Jahrestagung der deutschen Gesellschaft für Immunologie, Mainz (2013).
- Poster: **Wagner M**, Paret C, Koslowski M, Häcker S, Kneip C, Castle JC, Türeci Ö, Sahin U. Molecular and functional characterization of the highly specific cancer target Claudin 6. 2nd TRON Postersession, Mainz (2012).
- Poster: **Wagner M**, Paret C, Koslowski M, Kneip C, Türeci Ö, Sahin U. A highly specific cancer target, regulated via promoter methylation. 22nd Biennal Congress of the European Association of Cancer Research (EACR), Barcelona, Spain (2012).
- Poster: **Wagner M**, Paret C, Koslowski M, Kneip C, Cagna G, Wöll, S, Türeci Ö, Sahin U. Claudin 6 is a highly specific cancer target regulated via promoter methylation. 1st TRON Postersession, Mainz (2011).
- Invited Talk: **Wagner M**. PLAC1 in cancer – regulation and mechanisms of action. 1st international PLAC1 Symposium – "PLAC1 – A novel gene at the interface of reproduction and cancer", Tampa, Florida, USA (2011).
- Poster and oral presentation: **Wagner M**, Paret C, Koslowski M, Türeci Ö, Sahin U. ERα-mediated transactivation of placental PLAC1 in breast cancer cells is selectively controlled by the transcriptional co-activator SRC-3 (NCOA3). 9th Cancer Immunotherapy (CIMT) Meeting – Targeting Road Maps for Success, Mainz (2011)

Other articles

- Lamy E, Hertrampf A, Herz C, Schüler J, Erlacher M, Bertele D, Bakare A, **Wagner M**, Weiland T, Lauer U, Drognitz O, Huber R, Rohn S, Giesemann T, Mersch-Sundermann V. Preclinical evaluation of 4-Methylthiobutyl-isothiocyanate on liver cancer and cancer stem cells with different p53 status. *PLoS ONE* 2013, 8(8): e70846.
- Löwer M, Renard BY, de Graaf J, **Wagner M**, Paret C, Kneip C, Türeci Ö, Diken M, Britten C, Kreiter S, Koslowski M, Castle JC, Sahin U. Confidence-based somatic mutation evaluation and prioritization. *PLoS Comput Biol* 2012, 8(9): e1002714.

9 Curriculum Vitae

10 Acknowledgements